Università
Ca'Foscari
Venezia

Doctor of Philosophy in

ANALYSIS AND GOVERNANCE OF SUSTAINABLE DEVELOPMENT
22nd Session
(A.A 2006/2007 - 2010/2011)

DEVELOPMENT OF WATER RESOURCES MANAGEMENT STRATEGIES AND HYDROLOGICAL MODELLING FOR UNDERSTANDING WATER AVAILABILITY AND CLIMATIC SCENARIOS IN RIVER BASINS

Code of Scientific Sector: FIS/02

Mohammad KAMRUZZAMAN
Registration: 955279

Coordinator of the PhD programme

Prof. Giovanni Maria ZUPPI

Tutor

Prof. Giovanni Maria ZUPPI

Co-tutor

Prof. Simon BEECHAM

Università
Ca'Foscari
Venezia

Doctor of Philosophy in

ANALYSIS AND GOVERNANCE OF SUSTAINABLE DEVELOPMENT
22nd Session
(A.A 2006/2007 - 2010/2011)

DEVELOPMENT OF WATER RESOURCES MANAGEMENT STRATEGIES AND HYDROLOGICAL MODELLING FOR UNDERSTANDING WATER AVAILABILITY AND CLIMATIC SCENARIOS IN RIVER BASINS

Code of Scientific Sector: FIS/02

Mohammad KAMRUZZAMAN
Registration: 955279

Coordinator of the PhD programme

Prof. Giovanni Maria ZUPPI

Tutor

Prof. Giovanni Maria ZUPPI

Co-tutor

Prof. Simon BEECHAM

ABSTRACT

The aim of this study is clarified water governance, namely the respective roles of government, civil society and the private sector which directly or indirectly impact the development and management of water resources. Water resources-related conflict has been highlighted. Initially, this research study provided recommendations to resolve and minimise water-related conflict. A case study of the Ganges River Basin is then presented, and in particular, the transboundary water sharing issues between Bangladesh and India. It is includes the impact of the Farakka Barrage in the Ganges River Basin area which has led to conflict between the Ganges states since 1951. A Stackelberg leader-follower model was proposed to develop win-win strategies for mitigation of the transboundary water sharing conflict between Bangladesh and India. This can be implemented in any river basin, particularly ones involving upstream – downstream co-riparian states. Secondly, a scenario of relevant climatic drivers was generated by a statistical downscaling technique to develop water resources management strategies for the Murray Darling Basin (MDB). The regression model with either rainfall or temperature is the response and some selections of climatic indicators are considered. A correlation analysis, including a factor analysis of the climatic indicators is presented and is used to guide the choice of climatic indices for the regression models. The recommended strategies were based on a simulation process and superimposed to project the next 100 years water availability in the MDB areas.

Key words: Climatic drivers, management strategies, regression model, statistical downscaling, simulation process and water sharing.

DECLARATION

I am able to state confidently that this thesis work is my own, no materials which has been accepted for the award of any other degree or diploma in any university or other tertiary institution, Also to the best of my knowledge and belief, the thesis contains no materials previously published or written by another person, except where due reference in made in the text

I consent to this copy of my thesis being made available in the School for Advanced Studies and Venice Foundation/Venice International University/Ca Foscari University Library for loan and photocopying.

Mohammad Kamruzzaman
Date:

ACKNOWLEDGEMENT

My sincere thanks go to Professor G M Zuppi, and Professor Simon Beecham, for their enormous support and guidance during their supervision of conduct this research. I would like to express my heartfelt gratitude to them. I am also grateful to Associate Professor Andrew Metcalf for his valuable assistance to learn R programme and his help in my data analysis. I am thankful to Adjunct Professor Dennis Mulcahy of the SA Water Centre for Water Management and Reuse for helpful comments on my chapters.

Completion of this research was possible by the assistance from different organisations and generosity of various individuals in Australia and Italy. I would like to thank the School for Advanced Studies and Venice Foundation (SSAV) the Venice International University, Ca Foscari and IUAV University, Venice, Italy for giving me the opportunity to undertake this doctoral program by offering a scholarship. I am grateful to the SA Water Centre for Water Management and Reuse, the University of South Australia, for giving me an opportunity to undertake a research internship and providing additional scholarship funding from the Australian Research Council (ARC) through grant DP0877707. I am grateful to valuable discussions with ARC Chief Investigators Prof Phil Howlett, and Prof John Bolan from the School of Mathematics and Statistics at UniSA and to Prof Charles Pears, and Prof Nigel Bean from the School of Mathematical Sciences at Adelaide University. I am also grateful to the developers of the R project for open source software and to Jono Tuke, the University of Adelaide, for calculating the Hurst Coefficient for me. I thank Professor G P Nason, the University of Bristol, for access to their efficient R function in simulation code. I am also grateful to Associate Professor David Bruce, UniSA, for helping me to learn the use of the ArcGIS Software. Thanks also to Rosalina Zachariah, Julia Piantadosi and Andrew Plumridge for Matlab programme codes discussions. Also thanks to Peter Cotton for IT and technical support.

Thank are also due to the Bangladesh Water Development Board for providing data and additional materials for the GRB at Farakka and to the Australian Bureau of Meteorology and the MDBC Commission for access to meteorological data and other relevant information.

I thank my family who have been encouraging me all the way through and provided me with all support to complete this task. My parents have been dreaming of this day for a long time. I am grateful to all of you.

Finally, I am grateful to the Almighty for giving me the courage and strength to complete this difficult journey and achieve my goals.

ABREVIATIONS

ACF	Auto correlation function
AR	Autoregressive
ARMA	Autoregressive moving average
BOM	Bureau of Meteorology
CI	Climatic indices
Cr-C/Cr-CF	Cross Correlation/Cross-correlation function
CSIRO	Commonwealth scientific research organisation
CUSUM	Cumulative Sum
ENSO	El Niño - Southern Oscillation
EWMA	Exponentially weighted moving average
FAR	Fourth Assessment report
GARCH	Generalised autoregressive conditional heteroskedasticity
GCM	Global Climate model
GLS	Generalised least square
GRB	Ganges River Basin
IRB	Indus River Basin
IPCC	Intergovernmental Panel on Climate Change
IQR	Inter-quartile range
MDBC	MDB Commission
MRB	Mekong River Basin
PDO	Pacific decadal oscillation
RM	Regression model
RS	Residual series
SAR	Second Assessment Report
SD	Statistical Downscaling
SIM	Semi-arid Integrated Model
SOI	Southern Oscillation Index
SSIPE	Sum of squares one step ahead predictive errors
SSL	Sea level pressure
SST	Sea surface temperature
TAR	Third Assessment report
WRMS	Water Resources Management Strategies

ASSOCIATE PUBLICATIONS IN THIS DISSERTATION

Note: * indicates that publication was peer reviewed

Journal (for peer review)

*Kamruzzaman, M., S. Beecham and A. Metcalfe, 2009: Non-stationarity in Rainfall and Temperature in the MDB, Accepted 11 October 2010, *Journal of Hydrological Process,* Wiley, DOI: 10.1002/hyp.7928 [**ERA ranking A]**

Kamruzzaman, M., S. Beecham and G. M. Zuppi, 2010: A Model for Water Sharing in the GRB(Under review **manuscript WEJ 4690-10**, Water and Environment Journal) .

Beecham,S., Kamruzzaman, M., and A. Metcalfe, 2010: Climatic influence on rainfall and runoff variability in the MDB, (In progress, will be submit to *Journal of Hydrological Process*) [**ERA ranking A]**

Conference papers (*peer reviewed*)

*Kamruzzaman, M., S. Beecham and G. M. Zuppi, 2010: The Water Paradox: Is there a Sharing Crisis? 1st International Conference transboundary aquifers challenges and new directions, UNESCO-IHP, ISARM, and PCCP Programmes 6-8th December 2010, UNESCO, Paris, France

*Kamruzzaman, M., Beecham, S. and Metcalfe, A. (2010): Characteristics of climatic indicators and their influences on rainfall and temperature in the Murray-Darling Basin, 1st International Conference transboundary aquifers challenges and new directions, UNESCO-IHP, ISARM, and PCCP Programmes 6-8th December 2010, UNESCO, Paris, France

*Kamruzzaman, M., Beecham, S. and Metcalfe, A. (2010): Examine the climatic indices and their influences on rainfall in the Murray-Darling Basin, Australian Climate Change Adaptation Research Network for Settlements and Infrastructure Forum and Workshop, 19-21st April 2010, Griffith University, Gold Coast, Australia.

*Kamruzzaman, M., Beecham, S. and Metcalfe, A. (2009), Trends in Rainfall and Temperature in the MDB, 8th International Workshop on Precipitation in Urban Areas, IWA/IAHR, 10-13th December 2009, St. Moritz, Switzerland

*Kamruzzaman, M., S. Beecham and A. Metcalfe, (2009): Climatic Indicators and their Influence on Rainfall and Temperature Time Series in the Murray Darling River Basin, EMAC-2009, 6-9th December 2009, Adelaide University, Adelaide, Australia.

*Kamruzzaman, M., S. Beecham and A. Metcalfe, (2009): Climatic Variation in the MDB Area: A Case Study of Hume Dam. Australian Climate Change Adaptation Research Network for Settlements and Infrastructure Forum and Workshop, 9-11th November 2009, UNSW, Sydney, Australia

*Kamruzzaman, M. and G.M. Zuppi 2008: "The Root cause of the Water Paradox in Bangladesh: A Case Study of the Ganges River Basin": Proceeding of the 13th International Water Technology Conference (IWTC) 2009, 12-15th March Hurgrada, Egypt

CONTEXT OF THE THESIS

LIST OF TABLES

LIST OF FIGURES

LIST OF APPENDICES

CHAPTER 1: INTRODUCTION

This chapter is an overall preface to the research undertaken in this doctoral thesis. It provides a background to the research, an understanding of the water resources management strategies (WRMS) for dealing with climatic drivers and their influence, and the objectives of the study. It then proposes research questions and provides the rationality of the research. The scope of the research being undertaken and the significance of this research to statistical hydrology is also outlined. A summary of how the research achieves its goal is then provided, and this is followed by an overview of the structure and content of remaining chapters in the thesis.

1.1. Background

Water is natural and vital for all forms of life. Its plays a critical role in the functioning of the earth environment through its different forms: liquid, solid and gas. Through complex interactions, the global water cycle integrates the physical, chemical, and biological processes that sustain ecosystems and influence the climate. Inadequate understanding of the water cycle is one of a key source of uncertainty in climate prediction and climate change projections. At the global or regional scale, water is considered a more rigid or critical constraint or limiting factor than temperature. To redress issues, Global Water Cycle research expends considerable effort to improve observations, data assimilation, and modelling/prediction systems that in turn deliver the information necessary for decision-support tools and assessments. These provide a basis for “best practice” in the management of water resources. The integration of research results into models has led to better simulation/prediction capabilities for hydro-climatic variables. Multi-model and ensemble modelling techniques have led to improve seasonal predictions of both the atmospheric and terrestrial hydrological status. Specific techniques have been developed by IPCC, CSIRO, and BOM, among others. This research will develop hydrological systems that use multi-model and empirical tools to “force” hydrological models.

1.2. Understanding of climatic drivers

The climate drivers are potential effects on the water balance and its variability over time. The most dominant climatic drivers for water availability are rainfall, temperature, and evaporative demand (determined by net radiations at ground level, atmospheric humidity, wind speed and temperature, river flow, etc.).

1.2. 1. Rainfall and temperature

Rainfall is the main driver of variability in the water balance over space and time. Geographical variables (mainly high latitude, mid-latitude, equatorial and sub-tropical regions, etc.) bring about change in rainfall and have very important implications for hydrology and water resources at the global scale. The local scale is more equivocal. Hydrological variability over time in a catchment is influenced by variations of rainfall over daily, seasonal, annual, and decadal time scales. Increasing temperature affects the amount of water vapour the air can hold and leads to increased evaporation of water from the earth's surface. Together these effects alter the water cycle and influence the amount, frequency, intensity, duration and type of rainfall. Several studies into trends in rainfall are different parts of the world have been reported. They show a general increase in Northern Hemisphere mid and high latitudes (particularly in autumn and winter) and a decrease in the tropics and subtropics in both hemispheres. Long term trends in regional rainfall have been observed between 1900 and 2008. There is evidence that annual rainfall increased in Central and Eastern North America, North Europe, Northern and Central Asia, and that it decreased in parts of Africa, Southern Asia, And Southern Australia (IPCC 2007a). In particular, the frequency of extreme rainfall has increased in the United States (Karl and Knight, 1998) and in the UK (Osborn *et al*., 2000). However, across large parts of the world the variations associated with global warming are small compared to those resulting from natural multi-decade variability. Furthermore, seasonal rainfall is even more spatially dependent and relate to variations in the climate of a region. Local and regional variability in rainfall is highly dependent on climate phenomena such as the

El Niño - Southern Oscillation (ENSO), change in atmospheric circulation and other large-scale pattern of variability (IPCC, 2007a, pp 316).

1.2.2. ENSO influence

The ENSO relates to the Pacific Ocean. The Pacific Ocean signature, El Niño and La Niña is important measures of temperature fluctuations in surface waters of the Pacific Ocean (Bates *et al*., 2008). Since the Second Assessment Report (SAR) by IPCC, and many studies have explored linkages between patterns of climatic variability, particularly El Niño and the North Atlantic Oscillation, and hydrological characteristics, in an attempt to explain variations in over time. Chiew et al., (1998) found that in Australia, variability is not only just from year to year, but also from a decade to the decade, although patterns of variability vary considerably from the region to a region. ENSO spatial patterns affect the Australian climate system and in particular, its rainfall. The strength and frequency of the El Niño phenomenon is modulated by anomalies in Pacific sea surface temperature (SST), quantified as the Pacific Decadal Oscillation (PDO). Other studies demonstrate a decade variability in patterns of the Pacific SST that is associated with variations in rainfalls (Whiting et al., 2003). The anomalous warming and cooling in the North Pacific SST pattern is termed the Inter Decadal Pacific Oscillation (IPO), and it influences the ENSO phenomenon, particularly in Australia.

1.2.3. River flow and runoff

Due to climate change, significant changes in the volume and timing of rainfall occur, which may affect river flow. A simple link between river flow and runoff is that runoff can be regarded as river flow divided by catchment area, although in dry areas this does not necessarily hold because runoff generated in one part of the catchment may infiltrate before reaching a channel and becoming in river flow. In short period, the amount of water leaving a catchment outlet usually is expressed as river flow. Over the duration of a month or more, it is expressed as runoff. Many studies of the potential effects of climate change on river flows have been published in scientific

journals, and many more studies have been presented in internal reports. These studies use a catchment hydrological model driven by scenarios based on climate model simulations. In general, this research will identify a consistent pattern of influence for rainfall such as an increase in runoff where rainfall has increased and a decrease where it has fallen over the past few years.

1.3. Impact of Climate change on the Hydrological Cycle

1.3.1 Linkage between water and climate change

Water resources are under pressure from increasing demand and competing uses. Over the world, climate change threatens to put further pressure on water resources due to high variability of rainfall and river flow and changes to the geographical distribution of water resources. Water user and management institutions may adapt to this variability. Increasing water demand and the effects of climate change may be significant in the future, which will lead to more uncertainties. In particular, globally the largest water-use factor is food demand, which drives irrigated agriculture. Other factors are a growth rate of population, lifestyle, economy and technology. The Fourth Assessment Report (FAR) by IPCC in 2007, showed a schematic Figure 1.1 of the impact of and response to climate change and their linkage. The information on the linkage clockwise, example for derives to climatic changes and impacts from socio-economic information and emissions.

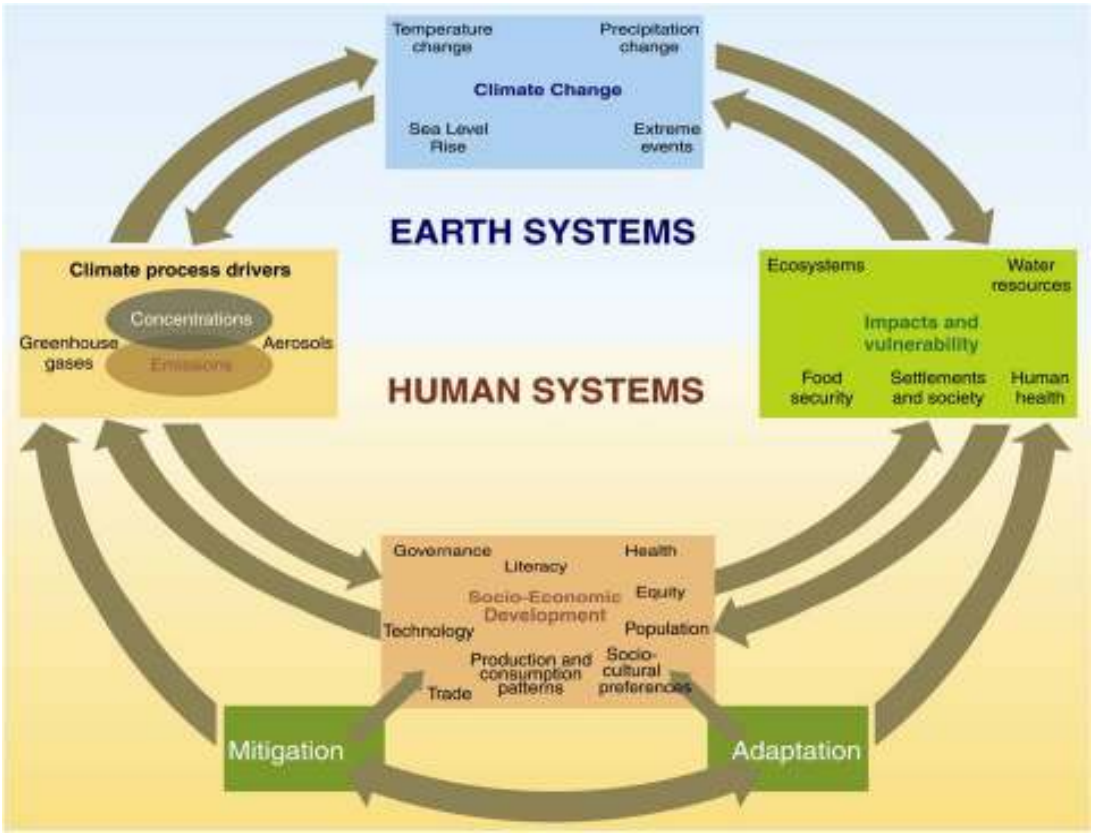

Figure 1. 1: Schematic frame work for indicating impact of and response to climate change and their linkages. Sources IPCC AR4 2007

Since the Second Assessment Report (SAR), linkages between hydrological behaviour and patterns of climatic variability, particularly the El Niño-Southern Oscillation and the North Atlantic Oscillation, have been recognized in many studies, and attempts have been made to explain the resultant variations in hydrological characteristics over time. These studies have covered North America (McCabe, 1996; Piechota et al., 1997; Vogel et al., 1997; Olsen et al., 1999), South America (Marengo, 1995; Compagnucci and Vargas, 1998), Australia (Chiew et al., 1998), Europe (e.g., Shorthouse and Arnell, 1997), and southern Africa (Schulze, 1997). Such research is extremely valuable because it helps in interpretation of observed hydrological changes over time (particularly attribution of change to global warming), provides a context for assessment of future change (e.g., Piechota et al., 1998), and opens up possibilities for seasonal flow prediction that is more efficient in understanding adaptive climate variability. Throughout the world, many aspects of environment, economy and society are dependent upon water resources. It is therefore

difficult to assume a constant hydrological baseline even in the absence of climate change.

The SAR provides examples from the past decades of climate change effects on hydrology and water resources (Arnell et al. 1996). Hydrological behaviour was intensified because of unequal distribution of rainfall around the world (IPCC 2001). Some parts of the world may see significant reductions in rainfall, or major alterations in the timing of wet and dry seasons. The IPCC (2001) warned that global warming would lead to increases in both floods and droughts at the global scale but that climate change in at local scale more equivocal.

1.3.2. Adaptation of water resources to climate change

A wide range of adaptation techniques has been developed and applied in the water sector over the last decade to explore adaptation to climate change. Historically, Integrated Water Resources Management (IWRM) has concentrated on meeting the increasing demand for water. Water management is based on minimisation of risk and exploration the changing conditions in water availability have always been at the core of water management. At present, it requires alterations to methods and procedures, such as standards design and the calculation of climate change allowances. Management of adaptive water resources would be either *autonomous* or *planned* to minimise adverse effects of climate change and maximise effectiveness in coping with climate change. For example, drought related stresses, flood events, water quality problems, and growing water demands are creating the impetus for both infrastructure investment and institutional change in many parts of the world (Wilhite, 2000; Faruqui et al, 2001, Galaz, 2005). In Latin America, some *autonomous* adaptation practices have been put in place, including management of the trans-basin diversions and the optimisation of water use (Bates et al, 2008). *Planned* adaptations are the result of deliberate policy decisions and specifically take climate change and variability into account. Water managers and policy makers in a few countries have begun to address directly the implications of climate change as part of their flood event and water supply management practices. In particular, flood event in The

Netherlands (Klijn et al., 2001) and water supply in the UK (Arnell and Delaney, 2006). They have also been addressed for water planning in general in Bangladesh (Bates et al, 2008). Conceptual challenge has been posed to water managers by introducing uncertainty in future conditions regarding climate change. For several reasons, it is difficult to identify any trend in recorded hydrological data, (Wilby, 2006). Variability over the time is very high, which means adaptation decisions may have to be made before it is clear how hydrological regimes may actually be changing. Therefore, it is required to adopt a scenario-based approach (Beuhler, 2003; Simonovic and Li, 2003). This is put into the practice in the UK (Arnell and Delaney, 2006) and Australia (Dessai et al., 2005).

1.3.3. Linkage between water availability and statistical modelling

For water-related problems, the statistical modelling approach has options to assess how various water-related processes of change generate impact on society. In a more general theoretical framework (Krol, et al., 2005), a conceptual idea (objective or subjective) can be used to explain choices of adaptation strategies. The illustration of adaptive capacity is one of the main challenges in understanding climate change impacts over the world (McCarthy et al., 2001), and it is to be expected that modelling will be increasingly employed to explain behavioural responses of stakeholders to both external driving factors and internal developments (Pahl-Wostl, 2002). Water management issues should be considered to belong to this category, e.g. the degree of risk aversion in strategies dealing with drought or flooding, or the response to uncertain but relevant information like forecasts. The functioning of water management is an essential factor in determining the regional vulnerability to drought and climate change. It is a great challenge to make projections of this vulnerability using modelling approaches. Depending on the research goal, the extent to which water-related behavioural patterns can be represented using modelling is an open question, as is the question to what extent it is desirable. For example, the choices between water management strategies may be an object of discussion between stakeholders and policy-makers, whereas statistical models represent knowledge to support arguments for specific choices rather than attempting to model how the choice is being made. Therefore, a well-balanced modelling and scenario analysis is being

called for. In modelling approaches, realistic representations of the feedback of (water-related) actions were crucially important, as this feedback will be turned to drive the actions dynamically. As a result, integrated modelling will play a central role in filling the gap of understanding adaptive capacity and vulnerability. The degree of detail required in representing the feedback needs to be studied e.g. the MDB in Australia and the GRB in Bangladesh. Many of the relevant climatic indicators can be projected by the statistical model in a consistent way.

1.3.4. Study challenge and rationale

Over the last century, a vast majority of waterways has been heavily modified and regulated to meet the increasingly complex and often conflicting needs for water. The balance between water resources and demand is particularly relevant to the Murray-Darling Basin (MDB) one of Australia's largest drainage divisions, and to the Ganges River Basin (GRB) area. In this research work undertake to explore the adaptive water resources in both the GRB, and the MDB.

1.3.5. The GRB study

The GRB is extends from 70°-88° longitude and 21°-31° latitude (Rahman, 2006). It rises at the ends of the Gangotri glacier in the Uttar Kashi district of Uttar Pradesh province in India, at an elevation of about 3139 m above sea level (Rahman, 2006). It has total length of about 2600 kms and the total drainage area of about 1080000 square km (Rahman, 2006) and is shared by China (3%), Nepal (14%), India (79%) and Bangladesh (4% equivalent to 37% of Bangladesh) (Rahman, 2006).

The river flows through northern India and passes through the state of West Bengal, and then enters Bangladesh and reaches the Farakka barrage about 11 miles below India. About 63 miles later it enters Rajshahi, Bangladesh. Its route is shown in Figure 1.2.

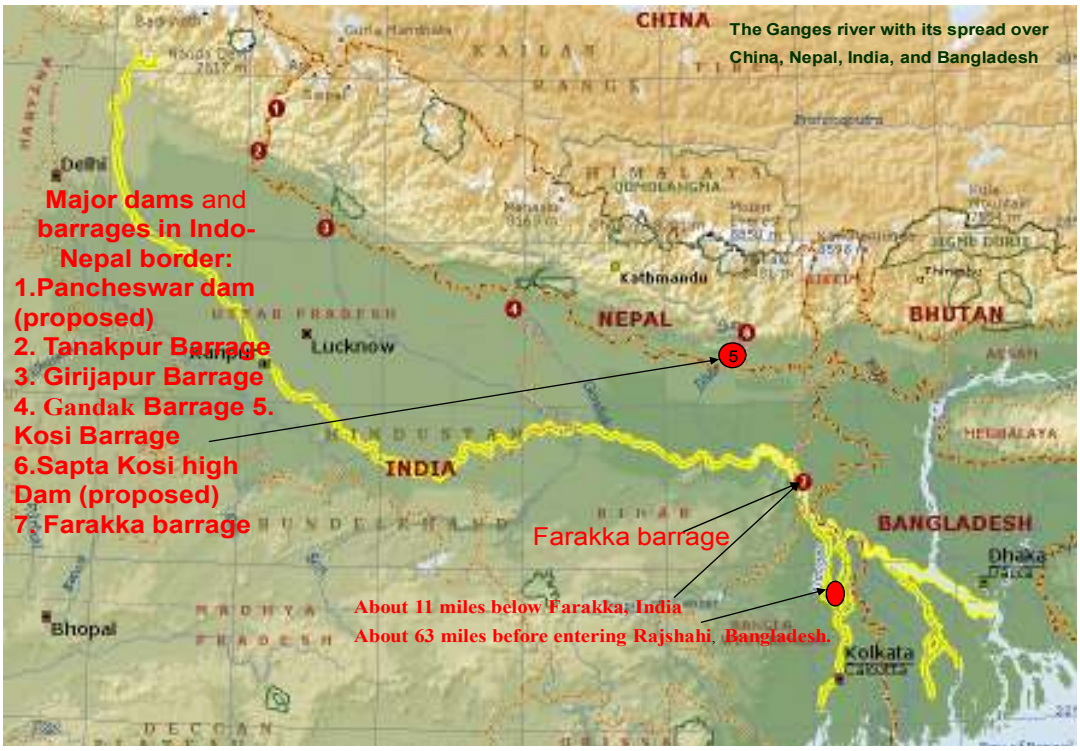

Figure 1. 1: The natural Ganges River flow from the Himalayan plateau to the Bay of Bengal.

The hydrological features have been worked from upstream to the downstream direction. A downstream country, Bangladesh is principally "water resources" controlling the three main rivers - the Ganges, the Brahmaputra and the Meghna Rivers, and their tributaries and distributors. These three river catchments cover more or less 1.75 millions square kilometre areas, only 8% of which lies within Bangladesh (Abbas, 1992). However, these river systems all discharge into the Bay of Bengal through Bangladesh.

In generally, the problems arise from upstream countries. Particularly, in the absence of a treaty, upstream riparian states have a hydrological advantage in a river. In the absence of political constraints, to the contrary, the number of years these upstream states have occasionally abused this advantage. Therefore, India was diverted a disproportionate amount of the Ganges River flow to flush the Port of Calcutta. This has been a violation of the UN conventional principle (ICWE, 1992) shown in Box 1.

Box 1: Water sharing: UN convention principle 1997 (ICWE, 1992)

- the equitable and reasonable use of water resources, obligation not to cause significant harm,
- A commitment to notify affected parties about planned projects.
- All-party participation, transparency of information, and mechanisms for

1.3.6. Objectives of the GRB study

This aims to analyse the Ganges Basin water flow augmentation to match supply and demand. The research has employed a model, "Stackelberg leader-follower game model" to determine the optimal share of water diverted by the upstream country with the opportunity of water flows augmentation from Nepal to resolve the water scarcity. In addition, the study seeks to assess the impacts of water transfer from Nepal to Bangladesh and India. The goals of the study are

i. To present a critical review of the 1996 treaty on the GRB based on water sharing between Bangladesh and India.
ii. To develop a model for optimal water allocation in the GRB between Bangladesh and India.

It is assuming that the existing treaties for water allocation and the potential role of water transfer from Nepal could reduce the water scarcity and mitigate the political water conflict between Bangladesh and India.

Research question have been developed from a holistic point of view, as given below

i. What does water resources sustainability mean? How can it be measured and implemented?

ii. What is the concept of "Paradox" and how is this concept relevant to water resources?

iii. How can the value of a water sharing treaty on between upstream and downstream countries be demonstrated?

iv. Why would a water sharing treaty be violated? Are there any political constraints?

v. Why did India reject a proposal to augment the flow of the Ganges River?

vi. How could the flow of water in the GRB be augmented?

vii. How would it be possible to deter India from unilateral decision making on the Ganges river basin?

1.3.7. Importance of the GRB study

Agriculture is the main economic activity of the basin, Most of it is dependent on the water from the Ganges River and thus around 410 million people directly or indirectly is dependent on this river (Mirza, 2006). During the monsoon period (June-October) there is an abundance of water, whereas during the dry period (November-May) the riparian countries become water stressed (Rahman, 2006). Flooding during the monsoon times and drought in non-monsoon times is a common natural phenomenon in this basin (Rahman, 2006). Therefore, it is a rational and national benefit to understand how to augment the flow availability at Farakka in the Ganges river basin. This research will describe a strategy to develop the water sharing capabilities between Bangladesh and India. In addition, this research will run a long-term win-win solution by modelling the augmentation of dry season flow of the Ganges River.

1.3.8. The MDB study

The MDB is located in south-eastern Australia. It covers over a million square km of the continent, 14% of the land area and includes more than three million residents. It drains one seventh of the continent through twenty major rivers (Newman, 2003). The basin is predominantly flat and dry and transverses a range of climatic conditions. It receives a long term average rainfall of 500,000 GL per annum, but the vast majority

of this evaporates. The average annual runoff is 24,300 GL with 11,400 GL average annual diversion (Craik, and Cleaver, 2008). The basin covers four states and a territory as shown in the map (Figure 1.3).

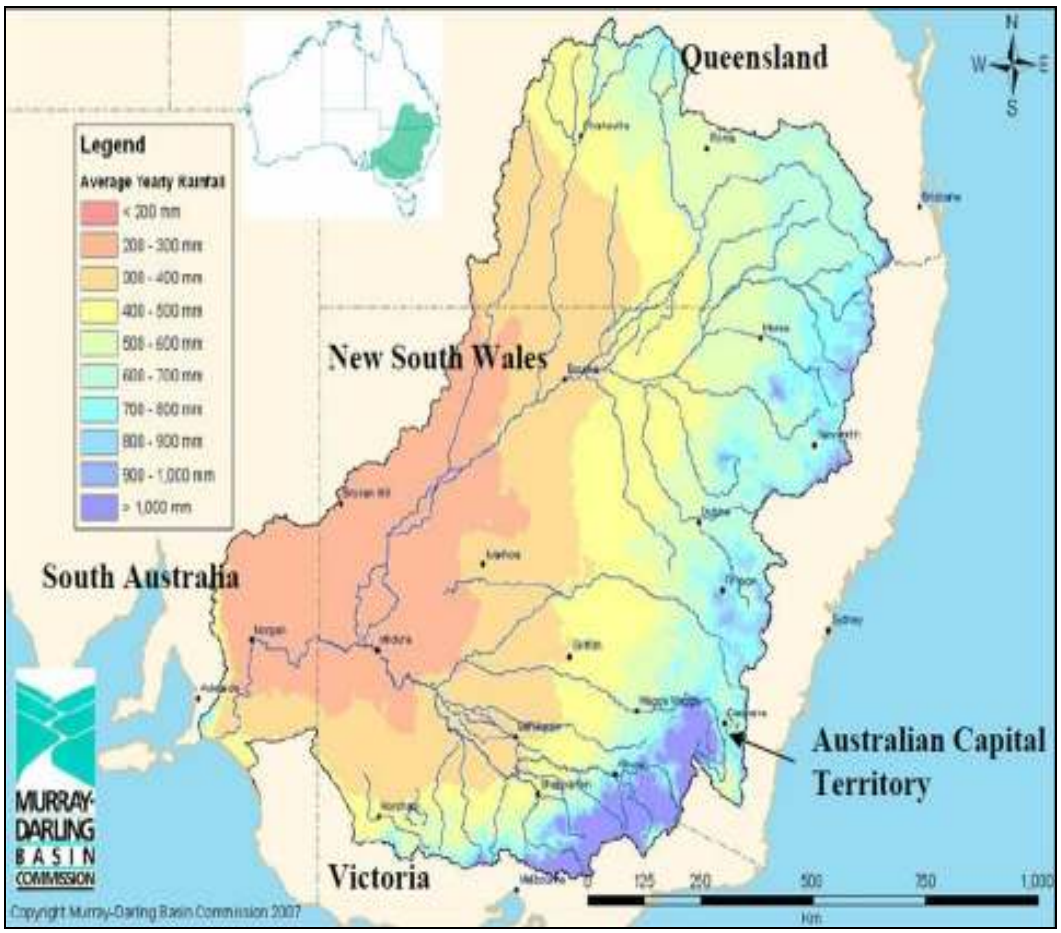

Figure 1. 2: The rainfall distribution in the MDB area (sources: MDB commission, Canberra)

The basin is critical in delivering water supply and supporting agricultural activities, rural communities and the nation's economy. It generates greater than ten billion dollars annually (Mercer et al., 2007). The Murray River, in particular, also has cultural, recreational and ecological significance and flows through several RAMSAR listed wetlands (Albert et al, 2007). Over the last one hundred and twenty years, there have been three particularly notable droughts affecting the MDB: the Federation drought which began in the mid-1890s and reached its devastating climax in 1902; the World War II drought which started in 1937 and lasted until 1945; and the current drought which began in 2002 and is now in its seventh year.

1.3.9. Objectives of the MDB study

The usefulness of time series has been recognized in many studies for WRMS. The statistical evidence of climate change is not straightforward because of several reasons on recorded climatic data. One option might be better to assess the climatic indices (CI) to understand the past and to predict the future, based on a scenario approach.

The particular goals of this study is

i. To examine the relevant CIs and their influence on rainfall and temperature in the MDB area.

ii. To investigate the possible systematic change in rainfall and temperature patterns in the MDB areas and eastern Australia.

Research question has been developed as given below.

i. Is there any trend in CIs?

ii. Is there any seasonal effect on CIs?

iii. Are there any strength or interaction effects between the CIs?

iv. How do CIs influence the rainfall and temperature in the MDB areas?

v. Is there any evidence of trends in rainfall and temperature patterns in the MDB areas?

vi. Is there any seasonal effect on rainfall and temperature in the MDB areas?

vii. How and why have rainfall and temperature been changed in the MDB areas?

viii. Why has water been disappearing during last 50 years in the MDB areas?

ix. Are the rainfall and temperature patterns in the MDB area's distance dependent?

x. Is there any evidence of persistence of rainfall and temperature pattern in the MDB areas?

1.3.10. Importance of MDB study

The effect of changing climatic conditions in the MDB is of particular concern because the MDB produces one third of Australia's food supply and supports over a third of Australia's total gross value of agricultural production, including export (Craik, and Cleaver, 2008). Moreover, it is under utilised, currently the MDB area has become a dry regime where demand has consistently exceeded the supply, such substantially imbalance has occurred in the MDB. The scenario assessment in the basin seems to be reasonable and will be a national benefit for long term process. In this research will analyse the scenario in past and develop a climatic model for understanding the future water availability in the MDB areas.

1.3.11. Limitations of the study

The time-frame of the research work was limited. It is also rational to narrow down to the research study in order to achieve some specific goals. There is some limitation of this research work.

i. Time series data: It was expected that CIs data might have some gaps. The lengths of the various data series might not be equal. Missing data will be replaced by the interpolation of mean method using the software package SPSS 17.
ii. Data availability: Because of the political constraints, water flow data in the GRB maybe even more limited.
iii. Decimal point: In the sensitivity analysis of the climatic drivers, more decimal points would be desirable, but in the table context 4 decimal points will be used.

This research study will make some assumption and use some biased values, which may not absolutely correct in the real world.

1.3.12. Context of the research

Chapter 1: Introduction - This chapter will provide an overall preface to the research undertaken in this doctoral thesis work. It will give a background to the research, an understanding of climatic drivers and their influence, and the objective of this study. It will pose research questions and provide the rationale of research. It will also describe the scope of the research being undertaken and its significance to statistical hydrology. A summary of how the research achieves its goal will then be provided, and this will be followed by an overview of the structure and content of the remaining chapters in this thesis.

Chapter 2: Methodology- In this chapter, methodology will be developed for the conduct of the research in the discipline of statistical hydrology. This chapter will discuss the study areas using statistical tools and methods assessing the climatic influence. Then advanced statistical techniques will be applied to time series data, using the statistical package SPSS, R code and Matlab software application.

Chapter 3: Leverage of water resources management: This chapter will discuss the leverage of water resources in a holistic approach. It will highlight how to manage water resources, and how this can contribute to resolve water related social conflict in the world. Two case studies will be presented in this chapter.

Chapter 4: A case study: Water paradox in Bangladesh: A transboundary water sharing crisis in the GRB will be discussed in this chapter. Mainly, the institutional framework of a water sharing treaty will be critically evaluated. Finally, a model will be developed for a win-win solution to the sharing of water resources in the GRB.

Chapter 5: Characteristics of climatic pattern- This chapter will initiate my core research to characterise the relevant climatic behaviour, applying statistical tools. It

will highlight both the long term and short term rainfall and temperature behaviour in the MDB area, including four capital cities in eastern Australia. Temporal and spatial variability will be categories based on rainfall and temperature data in the MDB area using a clustering method. A non-parametric statistical significance at 5% level will be applied by the Mann-Kendal test.

Chapter 6: Climatic influence- This chapter is a core part of the thesis. It will discuss the climatic phenomena, mainly ENSO indices, and investigate the influence on rainfall and temperature variability. Finally study will highlight the climatic elements. Regression based analysis, including periodic function will investigate the residuals series (RS) after making allowance for ENSO, having first ascertained whether there is evidence of trends in these climatic indicators. The analysis will be realised with p order auto regressive process.

Chapter 7: Hydrological model and its effects- this chapter is the main part of the thesis. Initially sinusoidal model will be applied for testing the amplitude of effects on the rainfall and temperature patterns in the MDB areas and four capital cities in eastern Australia. Allowing for seasonal effects, the RM will be applied to yield evidence of changing climatic condition in the MDB areas.

Chapter 8: Persistence of the hydrological model- This chapter will analyse the stochastic process using RSs from the RM. A distance dependent climatic variability model will be described based on location in the MDB areas. Advanced statistical tools will be applied for developing of long range memory of climatic pattern in the MDB areas and to investigate the evidence of non-stationarity.

Chapter 9: Discussion and conclusions- This chapter will provide a summary of this research work based on the research questions established in Chapter 1 and discuss in detail the relevance to hydrological modelling of climatic and rainfall pattern in the MDB areas. It will also make recommendations for further research work.

1.4. Conclusion

This research study will learn the water governance in the developed and developing countries. A lesson to be learns an IWRM by a holistic approach and adapts to develop strategies on the GRB and the MDB. A hydrological model study will be applied by the statistical downscaling technique using relevant climatic drivers, in particularly. A hydrological model will develop for understanding the future water availability in the MDB areas.

CHAPTER 2: DEVELOPMENT OF METHODOLOGY

2.1. Introduction

The purpose of this chapter is the development of methodology to conduct research in the discipline of statistical hydrology. This research work was conducted for the two fold purpose of developing WRMS for the GRB and for the MDB. The topographical features of river basins can vary greatly around the world. Consequently, the sustainable WRMS may involve a variety of approaches by the local or regional water manager and policy maker. In water resources management in the Ganges River Basin, the transboundary and sharing issues are vital. Recent variability and the influence of major climatic factors upon Australian rainfall have been imposing a challenge for the sustainable management of water resources in that country. The issue of climate change has been directly related to the classic decision analysis of water resources management planning applications. Examples have included evaluation of climate change projections (PMSEIC, 2007; Raisanen and Palmer, 2001) and water management related to climate change (Chowdury and Rahman, 2008); floodplain management strategies (Tkatch and Simonovic, 2006; Stainforth et al, 2007a and 2007b; de Kort et al., 2007); urban water supply system management and reservoir management (Kodikara, 2008); and watershed management practices (Arabi et al., 2007). Furthermore, observed global warming and climatic model projections now call into question the stability of future water quantity and quality estimates. There are several promising new developments to assist to facilitate the water manager and policy maker. This research undertakes the task to develop water resources management strategies in the GRB using a modelling study. In particularly this study focus how to resolve the water sharing crisis with regards to transboundary sharing issues on the GRB.

Traditionally, water resources management is based on use of recorded weather and information to predict future water supply conditions. There are many sophisticated methods, used for reconstruction, re-sampling, and analysis of hydrological parameters, and weather related conditions. It was assumed that the hydrologic determinates of future water resources depend on – temperature, precipitation/ rainfall, stream flow; groundwater, evaporation and other weather dependent factors- would be the same as they had been in the past. There may have been large variation

in the observed weather. It might be assumed that, weather statistics would stay the same and variability would not increase in the future. In stage, the water manager and policy maker imposes one of the core assumptions referred to as "climatic stationarity". *Stationarity means* that statistical properties of climatic variables in the future periods will be similar to past periods.

Today, WRMS progressing with projections of future climate adaptation are faced with the dilemma of how to develop short –and-long range plan that incorporated the uncertainties surrounding climatic scenarios. There are many studies of how the strategies adapted under the paradigm of climatic change include the range of climate scenario, great variability in supply projections, temperature-driven increases in water demand, and many other sources of uncertainty (Waage, 2009 cited in Edward, *at al*. 2010). The issues of climate changes are inherent and modelling of future climate change is in the development phase. It may be many years before the range and uncertainties surrounding the climatic scenario are substantially narrowed (Barsugli, et al., 2009). To address these new uncertainties, this research will incorporate hydrological modelling for understanding future water availability in the MDB using statistical downscaling of climate modelling. Furthermore, this research will assist to readers to understand the options for improving climate modelling. This can be useful not only in the planning for climate uncertainty but also in planning for uncertainty about regularity, environmental, economic, social and other conditions affecting water resources.

2.2. Conceptual models and characteristics of the climate risk

2.2.1. Climate Model study

Over time, many frameworks have been developed to provide an understanding of climate variability in order to manage water resources. There are many conventional approaches to impact assessment of water availability has been constructing the scenario of climate change. The most basic elements are a model (a mental, or

conceptual, model), and a basic knowledge of the hazards and vulnerabilities in order to priorities risk. Both qualitative and quantitative methods can be used to assess risk.

It is important to establish an understanding of the climate may influences water resources within a system being investigated. Suitable approaches have been established (IPCC, 2001, CSIRO 2010) and the nature of climate influence within the system and the sensitivity of the system response is key aspects. The climate sensitivity is defined as the degree of magnitude to which a system is affected, either beneficially or adversely by climate influences. The effect may be direct (e.g. A change in mean range or variability of temperature is the response to crop yield) or indirect (e.g. Damages caused by an increase in the frequency of coastal flooding due to sea level rise; IPCC, 2001). Furthermore, the vulnerability is the partiality of the system towards damage in response to climate sensitivity.

The list of analyse, diagrams, tables, flow charts, will create a body of information that can be further analysed using statistical tools. In the early stage, a conceptual model can help the understanding of the climate – water relationship based on the scientific modelling. The coping range method (Yohe and Tol, 2002) as introduced in Figure 2.1 can be used to assess how climate or the ability to cope, or both changeover time. The coping range is valuable because of its utility as a template for understanding and analysing climate risks, but it is not the only such method that can be used.

If a cropping system response is due to one single variable, e.g. rainfall or temperature, the greatest yields will be in the range to which that system is adapted. If the conditions become a too dry (hot) or wet (cool), then outcome become negative. The response curve in Figure 2.1 on the upper right shows a schematic relationship between climate and levels of profit and loss. Under normal circumstances, outcomes are positive but become negative in response to large extremes in variance. Using that response relationship, the CIs/indicators can be select, for the purposes of assessing risk.

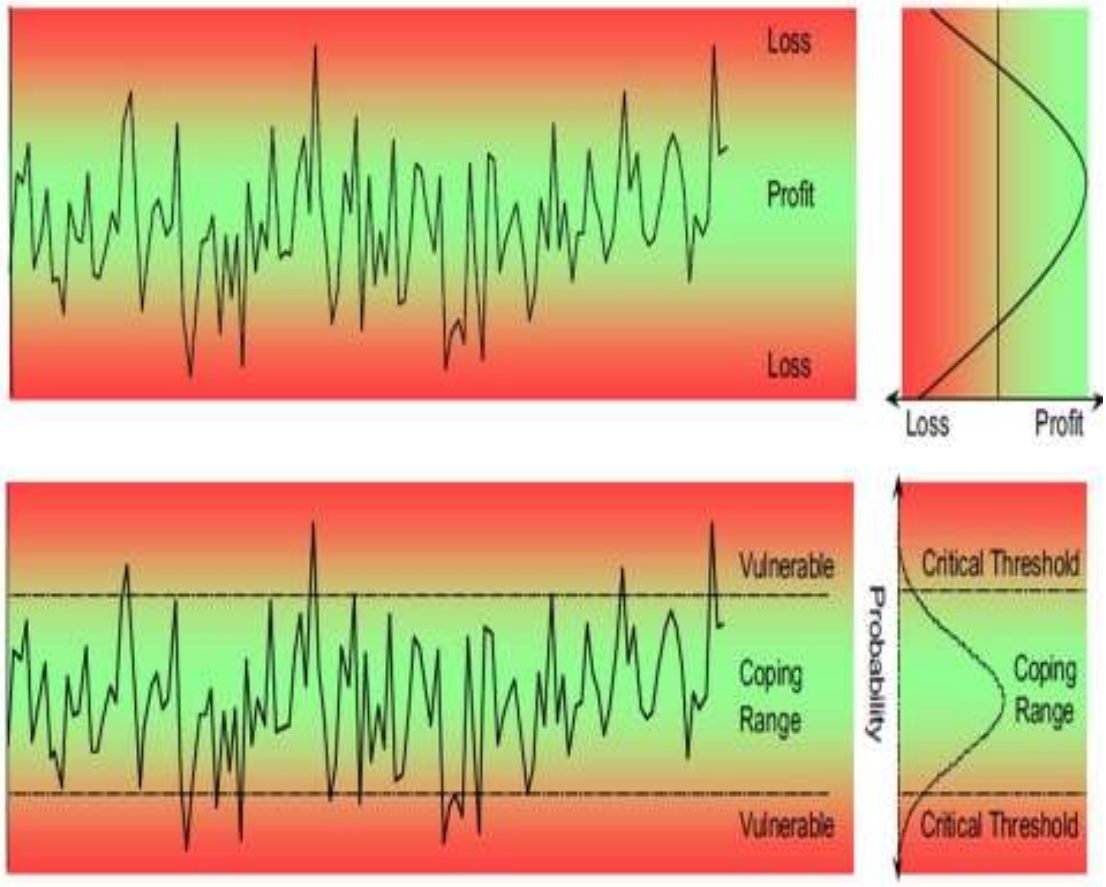

Figure 2. 1: Simple schematic of a coping range under stationarity of climate drivers such as rainfall or temperature and an output such as water yield.

When CIs within a system can be quantified, a response relationship, and one or more criteria representing different levels of performance, can be constructed. This is shown in the Figure 2.1 (lower left). For example, a yield relationship can be divided into good, poor or disastrous outcomes, or in terms of water, provide sufficient demand for a season. While the water user tries to maximise their benefit, from experience, they also know the consequences of not meeting such criteria. One way of deciding how the coping range is separated from the area of vulnerability, is to determine the critical threshold, which is defined as the *tolerable limit of harm*. Knowledge of the level of performance within a system allows us to set criteria, such as critical thresholds, and therefore, to assess risk as in Figure 2.1 (lower right).

2.2.2. Downscaling model study

The Downscaling is a process that transforms output from the Global Climate Model (GCM) into regional and local projections, which perform on identical time scales (e.g., daily, monthly and yearly). In recent years, different downscaling methods have been proposed in many studies around the world. Of particular importance for WRMS are those dealing with linkage of the large-scale climate variability to the historical observations of the hydrological parameters (e.g., rainfall and temperature). If this linkage can be established, then the projected change of climate conditions given by a GCM could be used to predict the resulting change of the selected parameters.

Two broad categories of these downscaling procedures currently exist (Hughes and Guttorp 1994; Wilks and Wilby, 1999; Xu, 1999; Yarnal et al., 2001; Wilby et al., 2002b): dynamical downscaling (DD) techniques, involving the extraction of regional scale information from large-scale GCM data based on the modelling of regional climate dynamical processes, and statistical (or empirical) downscaling (SD) procedures that rely on the empirical relationships between observed (or analysed) large-scale atmospheric variables and observed (or analysed) surface hydrological parameters. Some recent comparisons of DD and SD techniques for climate impact studies (Mearns et al., 1999; Gutowski et al., 2000; Yarnal et al., 2001) suggest that neither technique is consistently better than the other. However, it has been widely recognized that SD methods have several practical advantages over DD procedures, especially in terms of flexible adaptation to specific study purposes, and inexpensive computing resource requirements (Xu, 1999; Prudhomme et al., 2002).

SD technique can be classified into three categories according to the computational techniques used (Xu, 1999; Wilby et al., 2002a): weather typing approaches; regression methods; and stochastic weather generators. In general, these SD methods require three common assumptions.

1. That the large-scale climate variables are being modelled realistically by the GCM.
2. That the empirical mathematical relationships are unchanged when the climate changes.

3. That the global climate variables are capable of representing the entire climate change signal.

Assumption 1 for SD method: The weather typing procedures includes a limited number of classes simulating weather types using stochastic models, establishing the link of rainfall occurrence to whether a type using conditional probabilities, and simulating the rainfall process (or another hydro meteorological processes) using weather types (Murphy, 1999; Yarnal et al., 2001). Moreover, the main limitations of such procedures are that precipitation changes produced by changes in the frequency of weather patterns could be inconsistent with the changes produced by the host GCM (Wilby et al., 2002a).

Assumption 2 for SD method: The regression-based downscaling methods reliant up on the empirical statistical relationships between large-scale predictors and local-scale parameters (Yarnal et al., 2001; Wilby et al., 2002a; Prudhomme et al., 2002). Different computational techniques can be used regarding the choice of the mathematical function for describing the predictor-predicted relationship (Wilby et al., 2002b). In general, the main advantage of the regression downscaling procedures is that these methods are simple and less computationally demanding in comparison to other downscaling methods. However, the application of regression-based procedures is limited to the locations where good predictor-predicted relationships can be found. Furthermore, similar to the regression-based techniques assume validity of the estimated model parameters under future climate conditions.

Assumption 3 for SD method: The stochastic weather generators have been used to simulate the weather information and extensively used in the planning, design, and management of water resources (Wilks, 1998; Wilks and Wilby, 1999). These methods are followed in the WGEN (Richardson, 1981) and LARS-WG (Semenov and Barrow, 1997) stochastic models. These models involve typically the modelling of the daily rainfall occurrences, the point describe the distribution of the rainfall amount on a wet day, and the conditioning of other weather variables (e.g. temperature, runoff,) on the wet/dry status of the day. The climate change scenarios are then stochastically generated based on the linkage between the stochastic model parameters with the corresponding variable changes in the GCM. The main difference

between these models is in the choice of the probability distributions. For example WGEN uses standard distributions (e.g., two-parameter Gamma), whereas LARS-WG employs semi-empirical distributions. One advantage of using a standard distribution is that it will have a smoothing effect on the empirical frequency of the observed data and will only require the estimation of a few parameters. However, such a distribution may not provide a very good fit to the observed data. A semi empirical distribution, with a larger number of parameters, is more flexible and should be able to describe accurately any shape of empirical frequency distribution. The comparative performance of the WGEN and LARS-WG models has been tested using data from a range of diverse climates (Semenov et al., 1998). The LARS-WG generator was found to be able to describe the observed weather characteristics more accurately than that of the WGEN. In general, the principal advantage of the stochastic weather generator procedures is that they are able to reproduce many observed statistical characteristics of daily weather variables at a particular site. The main criticism of these procedures is related to the arbitrary manner of determining the model parameters for future climate conditions (Wilby et al., 2002b)

Finally, because of various practical advantages of SD methods over DD procedures, SD techniques based on the Statistical Downscaling Model (SDSM) (Wilby et al., 2002a) have been selected for testing to establish their feasibility in the simulation of rainfall and extreme temperature processes for the MDB area and four capital cities in Australia.

2.2.3. Dealing with climatic uncertainty

Uncertainty regarding climate change has been recognised (CSIRO, 2010, IPCC 2001, FGCC), and a set of techniques formalised for managing this uncertainty. The IPCC Third assessment report (IPCC, 2001) recommended using a specialised method such as a development and use scenario. Furthermore, assessment of CIs can manage uncertainties (Morgan and Henrion, 1990). Sensitivity modelling under climate variability also helps to identify uncertainties, which, in terms, need to be represented in scenarios (McInnes et al. 2003). Furthermore, there is a guideline on farming and communicating uncertainty (Moss and Schneider 2000, cited in IPCC 2001).

A scenario is a logical, internally consistent description of a possible future condition of the system (e.g. river basin or catchment area). A scenario is not a prediction, and has no likelihood attached beyond being plausible. However, it is the basic building block of risk assessment approaches under climate change that use scenarios, ranges of uncertainty and probability distribution functions.

To understand the extreme climate variability in river basin or catchment areas, it is necessary to characterise all the CIs and analyse how much they are affected, and to develop WRMS. It is also necessary to assess the uncertainty or their sensitivity on the river basin or catchment areas, addressing following questions:

• Which climate variables and criteria should be used in managing climate-affected activities?

• Which climate variables most influence the ability to cope?

• Which variables should be used in modelling and scenario construction?

2.2.4. Selection of CIs

Strong spatial and temporal variations of climate are caused by the influences of synoptic systems (e.g. those at the river basin or catchment scale) that come into effect during different seasons and by the topography of the land. The synoptic systems are influenced by sea surface temperature (SST) and the associated Ocean currents and pressure difference between points on the earth. There is a number of climatic indices based on SST and pressure differences. Such relationship can be used for short-term forecasting (Reference) and also may be useful for investigating the effects of climatic change. Many studies have identified the relationship between Australian rainfall and the El Niño Southern Oscillation (ENSO) (Kane, 1997; Suppiah and Hennessy, 1996; Nicholls and Kariko, 1993; Opoku-Ankomah and Cordery, 1993; Drosdowsky, 1993; Zhang and Casey, 1992; Stone and Auliciems, 1992, McBride and Nicholls, 1983, Simmonds and Hope, 1997; Beecham and

Chowdhury, 2009, Chowdhury and Beecham, 2010). Chiew and McMahon (2003) demonstrated a link between ENSO and Australian rainfall and stream flow for 284 catchments throughout Australia. Furthermore, changes in the Sea Surface Temperatures (SST) caused by Australian rainfall were examined by Latif *et al.* (1997) and Zhang *et al.* (1997). The SST anomalous warming and cooling phases in the Pacific Ocean, termed the Inter-decadal Pacific Oscillation (IPO) influences the ENSO phenomenon in Australia (Franks, 2002). Mantua *et al.* (1997) identified a multi-decade persistence in the north Pacific sea surface temperatures, termed the Pacific Decadal Oscillation (PDO). The PDO index has been used in place of the IPO, as stronger relationships have been found when using this index (Franks, 2002). In the Southern Hemisphere, the Southern Annular Mode (SAM) can be used to describe the variability in atmospheric circulation in the extra-tropics on inter annual timescales (Visbeck and Hall, 2004). These studies, however, have not been linked to trends in runoff time series. The hydrological changes in both rainfall and discharge series have been investigated (Smith, 1995), and provide evidence that the hydrological change in discharge is not a direct result of increased rainfall but is due to a change in the rainfall–runoff relationship. It is therefore, particularly important in analysing time series such as rainfall – temperature in the MDB that exhibit their characteristics across eastern Australia.

The recent variability of SST data has seen the development of indices based on more direct measures of temperature itself. The SST gradients have been indicating some uncertainty also to where exactly the ENSO process should be measured. More recently, another ENSO monitor called the multivariate ENSO index (MEI) has been developed (Wolter and Timlin, 1993, 1998). In this research several CIs are considered, for example 4 CIs from the Pacific Ocean and 3 CIs from the Atlantic Ocean, Indian Ocean, Southern Annular mode (SAM) SOI and PDO these are summarised in Table 2.1.

Table 2. 1: Definition of Climatic indicators (CI).

Region	*CI*	*Descriptions*
Pacific Ocean	Niño1+2, Niño3, Niño4, and Niño3.4	ENSO is composed of an oceanic component and is characterized by warming or cooling of surface waters in the tropical eastern Pacific Ocean. The variation measured in SST in the Pacific Ocean region from 0-10^{o}S and 90^{o}W-80^{o}W indicates Niño1+2, the region 5°N-5°S and 150°W-90°W indicates Niño3, the region 5^{o}N-5^{o}S and 160^{o}E-150^{o}W indicates Niño4 and 5^{o}N-5^{o}S and 170^{o}W-120^{o}W indicates Niño3.4 (Wolter and Timlin 1998).
	Southern Oscillation Index (SOI)	The El Niño Southern Oscillation is characterized by a change in sea surface pressure in the tropical western Pacific. There are two phases, the warm oceanic one of El Niño, in which surface pressures are high, and the cooling phase of La Niña, in which surface pressures are low. Mechanisms that cause the oscillation of sea level pressures are still being studied (BoM, 2008, Troup, 1965, McBride and Nicholls, 1983).
	Pacific Decadal Oscillation (PDO)	The Pacific Decadal Oscillation (PDO) refers to climate phenomena over the Pacific region related to a substantial climatic shift, which is accompanied by major changes in climate variability on the inter-annual time scale. It is associated with changes in the frequency and intensity of the El Nino Southern Oscillation (ENSO) warm and cold events (BoM, 2008).
Atlantic Ocean	North and South Atlantic (NATL), (SATL), Global tropics (TROP)	The tropical Atlantic SST is defined as the difference between north (5^{o}N-25^{o}N) and south (5^{o}S-25^{o}S) Atlantic gradients and the region 0-20^{o}S and 30^{0}W-10^{0}E indicate South Atlantic respectively. Also the region 10°S-10°N, 0-360^{0}C indicates the tropical Atlantic Ocean (Barnston and Livezey, 1987 and Kaplan et al., 1998).
Ant-arctic	Southern Annular Mode (SAM)	The Southern Annular Mode (SAM) explains the percentage of the variability in atmospheric circulation in the Southern Hemisphere extra-tropics on inter-annual timescales. In general, between 15^{o}S-30°S and 45^{o}S-60°S the zonal wind is stronger and between 30^{o}S and 45°S the zonal wind is weaker (stronger) during the positive phase of the SAM (Visbeck and Hall, 2004).
Indian Ocean	Dipole Mode Index (DMI)	This is the SST difference between the tropical western equatorial Indian Ocean (50^{o}E-70^{o}E and 10^{o}S-10^{o}N) and the tropical south eastern equatorial Indian Ocean (90^{o}E-110^{o}E and 10^{o}S-10^{o}N) (Kaplan et al., 1998, Saji, et al, 1999).

2.3. Method and data materials

2.3.1. Data materials

The rainfall and temperature data used in this research were obtained from the Australian BOM (BOM, 2008). They were extracted from a 0.25° × 0.25° grid (Jones and Beard, 1998) for monthly rainfall and temperature from January 1900–December 2008. Sea-level pressure anomalies were derived from records over the Australian continent bounded by 110-160°E and 10-45°S over the period from 1900 to 2008 for each season and other pressure anomalies (e.g. monthly PDO, SOI) values were collected from the National Climate Centre of the Australian BOM over the period 1900-2008. The weather station locations were selected because they recorded both temperature and rainfall data and had the highest BOM quality designation for both data series. The majority of the stations also had less than 1% missing data see Table 2.2.

The MEI in the Pacific Ocean, Atlantic Ocean, and Indian Ocean are defined in Table 2.1. The SST anomalies were derived from data available from Climate Prediction Centre (CPC) of the National Weather Service over the period 1950 to 2008. For the Dipole Mode Index (DMI) in the Indian Ocean, the SST anomalies were collected from the Japan Agency for Marine Earth Science and Technology (JAMSTEC) as derive by Kaplan et al. (1998) over the period from 1950 to 2008. The SAM data were collected from the Natural Environment Research Council, based on the British Antarctic Survey pressure anomalies derived by Marshall (2003) over the period 1957 to 2008. To facilitate time series analysis, the missing values were replaced by series' means, using SPSS version 17. Water flow availability data were collected from the Joint River Commission, Dhaka, Bangladesh. Because of political constraints, data span is only from 1997 to 2007.

2.4. Statistical analysis in water resources

Time series analysis is recognized as an advanced tool for water resources management. One definition of a time series is a collection of quantitative observations that are evenly spaced in time and measured successively. Examples of time series include hourly readings of air temperature, monthly rainfall, runoff, inflow and outflow, etc.

The goals of time series analysis are:

i. Descriptive: Identify patterns in seasonal variation, correlated data and trends
ii. Explanation: understanding and modelling the data
iii. Forecasting: prediction of short-term trends from previous patterns
iv. Intervention analysis: how does a single event change the time series?

Time series are analyses in order to understand structure and functions that produced the observations. Understanding the underlying mechanisms of a time series allows a mathematical model to be developed that explains the data in such a way that scenario assessment, prediction/ forecasting and informed monitoring can occur.

The hydrological data include hourly air temperature, rainfall, runoff, inflow and outflow, etc. about which a statement or summary is to be made. These are called the ***population*** at a particular site. Instead, a short term subset of the observed data called the ***sample*** is selected and measured in such a way that conclusions about the sample may be extended to the entire population. Statistics computed from the sample are only inferences or estimates about characteristics of the population, such as location, spread, and skewness. Measures at a location are usually the sample mean and sample median. Measures of spread include the sample standard deviation and sample Inter-quartile ranges (IQR). Use of the term "sample" before each statistic explicitly demonstrates that these only estimate the population value, the population mean or median, etc. As sample estimates are far more common than measures based on the entire population, the term "mean" should be interpreted as the "sample mean", and similarly for other statistics used in this research. The statistical analysis will be either.

i. Non- parametric statistical analysis

ii. Parametric statistical analysis

2.4.1. Nonparametric statistical analysis

2.4.1.1. Measure of Locations

i. Mean: First Movement

Measures of mean and median are the most commonly used to understand the average of rainfall or temperature or other climatic indicators per day, or month and so on in this study. The observed climatic indicators are saying $X_{i,}$ where i= 1,2,3 4,5……. n, the mean $(\overline{X})$ are of observations (values X_i) divided by number of observation, is given by

$$\overline{X} = \sum_{i=1}^{n} X_i / n \quad \text{…… eq. (1)}$$

For observed data which are in one of k groups, Equation (1) can be rewritten to show that the overall mean depends on the mean for each group, weighted by the number of observations n_i in each group:

$$\overline{X} = \sum_{i=1}^{k} \overline{X}_i * \frac{n_i}{n} \quad \text{……..…….. eq. (2)}$$

where $\overline{X}_i$ is the mean for group i. The influence of any one observation Xj on the mean can be seen by placing all but that one observation in one "group", or

$$\overline{X} = \overline{X}_{(j)} * \frac{(n-1)}{n} + X_j * \frac{1}{n}$$

$$= \overline{X}_{(j)} + (X_{(j)} - \overline{X}_{(j)}) * \frac{1}{n} \quad \text{…… eq. (3)}$$

Where $X_{(j)}$ is the mean of all observations excluding X_j. Influence $\overline{X}$ is $(X_j - \overline{X}_{(j)})$, the distance between those observations. These of all observations have the same influence on the mean. An 'outlier' observation, either high or low, has a much greater

influence on the overall mean $(\overline{X})$ than does a more 'typical' observation, one closer to its $X(j)$.

ii. Median

The median, or 50th percentile $P_{0.50}$, is the central value of the distribution when the observed data are ranked in order of magnitude. To compute the median, the observations first ranked from smallest to largest. So that X_1 is the smallest observation, up to X_n, the largest observation. Then

Median $P_{0.50} = X_{(n+1)} / 2$ when n is odd, and

Median $P_{0.50} = (X_{(n/2)} + X_{(n/2)+1})$ when n is even……..……eq. (4)

The geometric mean (GM) is frequently used for positively skewed data sets. It is the mean of the logarithms, transformed back to their original units.

$$\text{Geometric mean}(X_i) = \exp(Y_i), \text{ where } Y_i = \ln(X_i) \text{ ……..…….. eq. (5)}$$

For positively skewed data the geometric mean is usually quite close to the median.
In fact, when the logarithms of the observed data are symmetric, the geometric mean is an unbiased estimate of the median. This is because the median and mean logarithms are equal. When transformed back to original units, the geometric mean continues to be an estimate of the median, but is not an estimate of the mean.

2.4.1.2. Measures of Dispersion

Variability of observed rainfall or temperatures and other indicators is quantified by measures of spread like variance and Standard deviation. Spread provides knowledge of how CIs are fluctuating from the centre or location. The variance, and its square root, the standard deviation, are the classical measures of spread. Like the mean, they are strongly influenced by outlying values.

Sample Variance $S^2 = \sum_{i=1}^{n} \frac{(X_i - \overline{X})^2}{n-1}$ ……..……eq. (6)

and Standard Deviations $S = \sqrt{S^2}$ ……..……..…eq. (7)

Using the squares of deviations of observed data from the mean computed from the equation (6) outlier's influence their magnitudes even more than for the mean. When outliers are present these measures are unstable and inflated. They may give the impression of much greater dispersion.

In probability theory and statistics, the index of dispersion is the coefficient of variation (CV). It is a measure used to quantify whether a set of observed occurrences are clustered or dispersed compared to a standard statistical model. It is defined as the ratio of the standard deviation (σ) and mean μ.

Coefficient of Variation $CV = \frac{\sigma}{\mu} * 100$

2.4.1.3. Resistant Measure

The IQR is a resistant measure of dispersion. It measures the range of the central 50 percent of the data, and is not influenced at all by the 25 percent on either end. The IQR is defined as the 75th percentile minus the 25th percentile, which means IQR is the range of the middle 50% of values.

Mathematically, as defined $IQR = Q_3 - Q_1$ …….eq. (8)

The 75th, 50th (median) and 25th percentiles split the observed data into four equal sized quarters. The 75th percentile $(P_{0.75})$, a value which exceeds no more than 75 percent of the observed data and is exceeded by no more than 25 percent of the data. The 25th percentile (P.25) or lower quartile is a value which exceeds no more than 25 percent of the data and is exceeded by no more than 75 percent.

Consider a data set ordered from smallest to largest: (X_j), i =1 ... n. Percentiles (P_j) are computed using

$$P_j = X_{(n+1)*j} \text{ ..... eq. (9)}$$

where n is the sample size of X_i, and j is the fraction of data less than or equal to the percentile value (for the 25th, 50th and 75th percentiles, j= .25, .50, and .75). Non-integer values of $(n+1)*j$, imply linear interpolation between adjacent values of X.

For analysis of hydrological data like rainfall, temperature, and other CIs whether the simple summarization method has been applied for common characteristics in this section.

2.4.1.4. Box plot analysis

Time series analysis is generally used when there are 50 or more data points in a series. If the time series exhibits seasonality, there should be 4 to 5 cycles of observations in order to fit a seasonal model to the data.

A box and whisker plot is a way of summarizing hydrological data like an observed rainfall and temperature pattern measured on an interval scale. It is a type of graph, which can be used to show the location and shape of the underlying distributions, their central value, and variability. The graph produced to consist of the most extreme values in the observed data set (maximum and minimum values), lower and upper quartile and the median. The line across the box represents the median, whereas the bottom and top of the box show the location of the first and third quartiles (Q_1 and Q_3). The whiskers are the lines that link bottom and top of the boxes to the lowest and highest observations inside the region defined by

$$Q_1\text{-}1.5\ (Q_3 - Q_1) \text{ and } Q_3 + 1.5\ (Q_3 - Q_1)$$

Box plots (also called box and whisker plots) of individual variables of the sampling station (River) were examined. They are useful for revealing whether a distribution is skewed and whether there are any unusual observations (outliers) in the data set.
Box plots provide visual summaries of

i. The centre of the observed data (the median--the centre line of the box)
ii. The variation or spread (inter quartile range--the box height)
iii. The skewness (quartile skew--the relative size of box halves)
iv. The presence or absence of unusual values ("outside" and "far outside" values)

2.4.1.5. Hierarchical clustering method

Hierarchical clustering techniques represent an alternative set of classification tools. These techniques do not make any assumptions, but pave the way for successive divisions of the climatic pattern of the different sites by agglomerative hierarchical methods.

Agglomerative hierarchical methods: Initially there are as many clusters as stations. The most similar stations are first grouped, and these initial groups are merged according to their similarities of climatic pattern. Eventually, all subgroups are fused into a single cluster.

Divisive hierarchical methods: An initial single group of stations is divided into two subgroups such that the stations of one group are "far from" the ones in the other. We will focus on agglomerative methods. The input to hierarchical clustering methods is also a similarity or Dissimilarity matrix.

The decision of the classification depends on:
1) The choice of the dissimilarity (distance) measure;
2) The choice of the clustering procedure.

Distance methods are based on the definition of dissimilarity between clusters and focus on linkage methods.

A) Single linkage (minimum distance or nearest neighbour): dissimilarity between two clusters = minimum dissimilarity among the stations of each cluster

B) Complete linkage (maximum distance or furthest neighbour): Dissimilarity between two clusters = maximum dissimilarity among the objects of each cluster.

2.4.1.6. Non parametric test

Statistical techniques will be applying to check whether the climate variables like rainfall, temperature, stream flow pattern, change or not due to seasonality effect. First, the relationships between the climatic indicators will be preceding using Pearson's correlation test.

i. Pearson's Correlation test

Pearson's correlations (r) are the most common. r is also called the linear correlation coefficient. If the observed rainfall or temperature data lie exactly along a straight line with positive slope, then r = 1. This assumption of linearity makes inspection of a plot even more important for *r* than for *rho* (ρ) or *tau* (τ), because a non significant value of r may be due either to curvature or outliers as well as to independence.

Pearson's r is invariant to scale changes; the original data is to transformed to standardized form, dividing the distance from the mean by the sample standard deviation, as shown in the formula for r, below.

$$r = \frac{1}{n-1}\sum_{i=1}^{n}\left(\frac{Xi - \bar{x}}{S_x}\right)\left(\frac{Yi - \bar{y}}{S_y}\right) \quad \text{.....eq. (10)}$$

To test the significance of r, where r differs from zero, the test statistic t_r will be computed by equation (11) and compare to a table of the t distribution with n−2 degrees of freedom.

$$t_r = \frac{r\sqrt{(n-2)}}{\sqrt{(1-r^2)}} \quad \text{..... eq. (11)}$$

The same procedure will be applied to check the relationship between rainfall series and others climatic indicators.

ii. Tests for trend detection

Rainfall series may show a significant change over time due to temperature changes, and MEI. Trend analysis of climatic series like rainfall or temperature is practically important because, it is related to future water availability. Statistical procedures are best practice for detection of the gradual trends over time.

Trend may constitute a general examination of increase or decrease over the period (Helsel, and Hirsch, 1992). The purpose of the trend is determining, for example, the amount of rainfall, the number of rainfall events per annum, the average rainfall intensity, storm duration, and dry period duration. Tests will be applied to decide where there is any evidence of significant trend or not. A null hypothesis (H_0): that there is no trend is tested against the alternative hypothesis (H_1) that there is a trend. Parametric or non-parametric tests can be used for this purpose.

a. Mann-Kendall test

The Mann-Kendall test is the most general non-parametric test; it assesses whether Y values (e.g. rainfall or temperature series) tend to increase or decrease overtime T (monotonic change). Assumption of normality is not required. The test is to determine whether the central value or median changes over time. The statistical significance of change will be tested through the confidence interval of the considered variable with the significance level of $\alpha = 5\%$. The Mann Kendall test to perform on S statistics, Kendall's S is calculated by subtracting the number of "discordant pairs", M (the number of (x, y) pairs where y decreases as x increases) from the number of "concordant pairs" P (the number of (x, y) pairs where y increasing with increasing x):

$$S = P - M \quad \text{.....eq. (12)}$$

P is the known as the "number of pluses" the number of times the y's increase as the x's increase, or the number of $y_i < y_j$ for all $i < j$, M is also known as the "number of minuses," the number of times the y's decrease as the x's increase, or the number of $y_i > y_j$ for $i > j$. This applies for all i = 1…….. (n − 1), and j = (i+1),.....n.

Note that there are $n(n-1)/2$ possible comparisons to be made among the n data pairs. If all y values increase along with the x values, $S = n(n-1)/2$. In this situation, the correlation coefficient τ should equal +1. When all y values decrease with increasing x. $S = -n(n-1)/2$ and τ should equal −1. Therefore, dividing S by n (n−1)/2 will give a value between −1 and +1. This then is the definition of τ a measure the strength of the monotonic association between two variables:

Kendall's tau correlation coefficient is

$$\tau = S/\left(n(n-1)/2\right) \ldots\ldots\ldots\ldots\ldots \text{eq. (13)}$$

Considering sample variable Y (y_j, j= 1,2, 3,……..m) length m. Kendall's S statistics denote S_i is the number of sample elements with $y_i < y_j$ for all i < j. The overall statistic S_k is given by,

$$S_k = \sum_{i=1}^{m} Si \quad \ldots\ldots\ldots\ldots\ldots\ldots\ldots\ldots\ldots\ldots\ldots\ldots \text{eq. (14)}$$

The distribution of S_k can be approximated quite well by a normal distribution. S_k is standardized (eq.14) by subtracting its expectation $\mu_k = 0$ and dividing by its standard deviation σ_{s_k}. For m > 10, the distribution S_k follows a normal distribution.

$$Z_{Sk} = \begin{cases} \dfrac{S_k - 1}{\sigma_{Sk}} & \text{if } S > 0 \\ 0 & \text{if } S = 0 \\ \dfrac{S_k + 1}{\sigma_{Sk}} & \text{if } S < 0 \end{cases} \quad \ldots\ldots\ldots\ldots\ldots\ldots\ldots\ldots\ldots\ldots\ldots\ldots \text{eq. (15)}$$

Where $\mu_{Sk} = 0$ and $\sigma_{Sk} = \sqrt{\sum_{i=1}^{m} \frac{n_i}{18} * (n_i - 1) * (2n_i + 5)}$

n_i = number of data in the ith season.

The null hypothesis is rejected at significance level α if $|Z_{Sk}| > Z_{crit}$, where Z_{crit} is the value of the standard normal distribution with a probability exceeding of $\alpha/2$.

2.4.2. Parametric statistical analysis

The rainfall and temperature series are observations measured sequentially in time. Seasonal effects are often present, especially annual cycles caused directly or indirectly by the earth's movement around the sun. This is the rationale for looking

seasonal effects on the rainfall and temperature series for the MDB areas. Furthermore, qualitatively, the rainfall and temperature have been observed to change due to change in SST in Australian continental boundaries. Statistical procedures are best practice for detection of gradual trends over time. The null hypothesis (H_0) that there is no trend is to be tested against the alternative hypothesis (H_1) that there is a trend. Parametric tests can be used for this purpose.

2.4.2.1. Simple regression model (RM)

A simple RM is used to analyze change in the rainfall or temperature pattern due to change in climatic phenomena over a period. The RM is given as follows.

$$Y_i = \beta_0 + \beta_1 * (t_i - \bar{t}) + \beta_2 * (t_i - \bar{t})^2 + \varepsilon \text{ .....eq. (16)}$$

Where Y_i is the rainfall or temperature series in the observed areas, i=1,2,3,……..n, linear and polynomial terms in time (t) are used whether there is a evidence for a trend or not. The trend test is conducted by determining if the slope coefficients on β_1 and β_2 in eq (16) are significantly different from zero at least at 5% level. The RM would be extended by higher order polynomial term

$$y_i = \beta_0 + \beta_1 * (t_i - \bar{t}) + \beta_2 * (t_i - \bar{t})^2 + \beta_3 * (t_i - \bar{t})^3 + \varepsilon \text{ ..... eq. (17)}$$

The fitted RM will be realized by generalized least square (GLS) by an auto regressive (AR) process in order to AR (1). For making a decision on water resources management, it is necessary to make a statistical test for evidence of water availability due to changing rainfall or temperature over the relevant period in the observed areas. As rainfall is qualitatively related to primary resources of water across the MDB area, use of the RM in equation (16 and 17), will provide significance evidence of increasing or decreasing trend in rainfall and temperature in the MDB areas. It is assuming that higher order polynomial term (time (t) in the mean adjusted) may be strongly correlated. Simulation procedures will be adopted for better understanding of future water availability for the policy maker.

2.4.2.2. RM with seasonal effect

The RM in eq (16) will be sinusoidal over a period of one year. However, seasonal effects often vary smoothly over the season. It may be therefore, more efficient to use a sinusoidal function instead of separate indices. Sine and cosine function can be used to build smooth variation into a seasonal RM. A sine wave with frequency *(f)* (cycle per observed interval), amplitude (***A)***, and phase shift ϕ

$$Y_i = A\sin(\omega t_i + \phi) + C \text{ ..... eq. (18)}$$

Equation (18) is non-linear because ϕ is within the sine function. Modelling the phase of a sinusoidal function is tricky because it involves non-linear regression analysis. So, the non-linear model in equation (18) is transformed into a simpler linear model in terms of sine and cosine functions.

$$A\sin(2\pi ft + \phi) = \beta_1 * \text{Sin}(2\pi ft_i) + \beta_2 * \text{Cos}(2\pi ft_i) \text{ ..... eq. (19)}$$

Where,

$A\sin(\phi) = \beta_1, A\cos(\phi) = \beta_2$ and amplitude $A = \sqrt{\beta_1^2 + \beta_2^2}$ ..... eq. (20)

The sine and cosine term, can be re-expressed as the amplitude A of the cycle (half distance from the peak to trough), and the transformation part will be used in the RM. Therefore, an ordinary least square (OLS) method can be estimate the parameter. The model is then defined as

$$Y_i = \beta_0 + \beta_1 \text{Sin}(2\pi ft_i) + \beta_2 \text{Cos}(2\pi ft_i) + \beta_3 (t_i - \bar{t}) + \beta_4 (t_i - \bar{t})^2 \text{ ..... eq. (21)}$$

Here, f=1/T, and T is the period (usually 1 year) of fitted sinusoidal waves. $\beta_o, \beta_1, \beta_3 \text{and} \beta_4$, are the unknown's to be determined. The outcomes of the sinusoidal model are helpful to understand the evidence of

i. Amplitude of sine wave effects
ii. The need for an extended polynomial term for evidence of model improvement (or not).

Extended to include polynomial terms up to the third order, in this case model then becomes

$$y_i = \beta_0 + \beta_1 \mathrm{Sin}(2\pi f t_i) + \beta_2 \mathrm{Cos}(2\pi f t_i) + \beta_3 (t_i - \bar{t}) + \beta_4 (t_i - \bar{t})^2 + \beta_5 (t_i - \bar{t})^3 \ldots \text{ eq. (22)}$$

Applying a regression technique, to determine patterns of rainfall and temperature change in recorded data may not be straightforward. According to Stevenson Screen reports, at the beginning of 20th century, weather stations in Australia may not have been up to modern standards. Therefore, a fitted RM with a linear or more the data itself will show the change the general polynomial trend may not provide the trends of rainfall and temperature patterns. Furthermore, seasonal effects and non-stationarity are being presented via other influential CIs. It is therefore, required to furthermore study on regression techniques using MEI.

2.4.2.3. RM with multi-climatic indices and seasonal indicators

In this section, the focus will be on RMs for climatic variables like rainfall, runoff, temperature and stream flow that allows for seasonal variations and underlying CIs. It is plausible that there may be same abrupt changes in climate, perhaps change in an ocean SST on over the period, rather than some more systematic trends. One of the objectives of this study is to suggest statistical analyses by RMs that are sensitive to small, but highly influential, climatic change. To investigate the possible systematic changes in rainfall and temperature series in the MDB areas and four capital cities in Australia, different RMs will be developed for rainfall and temperature series. The RSs from these regressions represent stochastic components, which give random variation about the fitted values.

A multivariate RM with a sinusoidal period of a year is given as

$$Y_t = \beta_0 + \beta_1 * C + \beta_2 * S + \beta_3 * (t - \bar{t}) + \beta_4 * (t - \bar{t})^2 + \beta_{i+4} * \mathrm{MEI} + \varepsilon_t \ \ldots. \text{ eq. (23)}$$

Where $C = \cos(2\pi * t/12)$, $S = \mathrm{Sin}(2\pi * t/12)$, and t is time (i.e. in the month of rainfall or temperature series,) and $\bar{t}$ is the average of observed time series. Y_t is defined as a rainfall or temperature series and MEI stands for multivariate CIs as defined in Table 2.1. β_i (i= 1,2,…11) defines the coefficients of the MEI.

The multivariate RM with seasonal indicators is given as

$$Y_t = \beta_0 + \beta_1 * (t - \bar{t}) + \beta_2 * (t - \bar{t})^2 + \beta_{i+2} * \mathrm{MEI} + \beta_{j+13} * \mathrm{SI} + \varepsilon_t \quad \ldots\ldots\ldots \text{eq. (24)}$$

SI stands for seasonal indicators from January up to December, β_j (j= 1,2.3…….12) are the coefficients of the SI. The indicator variables January up to December will be denoted $X_1, X_2, \ldots X_{12}$ respectively.

$$\mathrm{Jan}=\begin{cases}1 & \text{if January}\\ 0 & \text{Otherwise}\end{cases} \qquad \mathrm{Feb}=\begin{cases}1 & \text{if February}\\ 0 & \text{otherwise}\end{cases} \qquad \ldots\mathrm{Nov}=\begin{cases}1 & \text{if November}\\ 0 & \text{otherwise}\end{cases}$$

Furthermore, interaction effects of the CIs on rainfall and temperature series are often highly influencing. For example, Australian rainfall has been highlighted (Bates, at el., 2008, and BOM, 2008). It is rational to extend the RM in eq 23 and eq. 24 by the main effects and the interaction effects of CIs. The fitted RM wills statistical tests for evidence of trends in rainfall and temperature series in the MDB area and the eastern Australia.

2.4.2.4. Model selection

To support the planner, or decision maker, statistical inference of the fitted RM will be applied for better understating of past water availability, and could also be facilitating the future water resources management strategies.

i. Assessing normality of the RSs

The RSs are used to assess whether the error terms in the model are normally distributed or not. Although, a histogram can be used to investigate normality,

quantile-normal plot would provide clearer an understanding of difference from normality. Deviation from the straight line will be indicating normality.

ii. Significant test of RM.

The fitted RM will explain the variation of Y (e.g. rainfall and temperature series) which are dependent on x_i (one or more CIs). Total variation can be measure as follows

Sum of Square Total (SST) $= \sum_{i=1}^{n}(Y_i - \bar{y})^2$ …… eq. (25)

The sum of squares can be separated into two parts. One is the sum of square error (SSE) measures of within the group variability and the other is the treatment sum of squares (SSTr). The word treatment comes from the medical applications where the population means models the effects of some treatment.

Total effect = regression (model) effect + error effects

Algebraically,

$$Y_i - \overline{Y} = \hat{Y}_i - \overline{Y} + \hat{Y}_i - Y_i$$

$$(Y_i - \overline{Y})^2 = (\hat{Y}_i - \overline{Y})^2 + (\hat{Y}_i - Y_i)^2$$

$$\sum_{i=1}^{n}(Y_i - \overline{Y})^2 = \sum_{i=1}^{n}(\hat{Y}_i - \overline{Y})^2 + \sum_{i=1}^{n}(\hat{Y}_i - Y_i)^2$$

Total Sum of square (TSS) = Model SS + error SS,

Also, total separation by degree of freedom is as follows

$$\frac{\sum_{i=1}^{n}(Y_i - \overline{Y})^2}{n-1} = \frac{\sum_{i=1}^{n}(\hat{Y}_i - \overline{Y})^2}{n-k} + \frac{\sum_{i=1}^{n}(\hat{Y}_i - Y_i)^2}{k-1} \quad \text{..... eq.(26)}$$

This yields variance decomposition: the total variance = model variance + error variance

iii. R^2 – coefficient of determination

The decomposition of the total sum of squares into the RS sum of squares and the regression sum of square in eq. (27), this allows us to interpretation of how well the RM fits the data. If the RM fits the data well, the RSs sum of squares (RSS), (the

denominator in eq. 27) will be small. If there is a scatter about the RM, then RSS will be big. Equation 27, quantify the definition of R^2 coefficient determinations,

$$R^2 = \frac{\sum_{i=1}^{n}(\hat{Y}_i - \overline{Y})^2 / k - 1}{\sum_{i=1}^{n}(\hat{Y}_i - Y_i)^2 / n - k} \text{.....eq.(27)}$$

When the simple linear RM is appropriate, the value of R^2 is interpreted as the proportion of the total response variation explained by the regression. If the value of R^2 is then close to 1, most of the variation is explained by the regression line, and when R^2 is close to 0, very little (Verzani, 2005).

$$R^2_{adjusted} = 1 - (1 - R^2) * \left(\frac{(n-1)}{(n-k)} \right) \text{.....eq.(28)}$$

The adjusted R^2 value is to moderate the models that get better values of R^2 by using multivariate RM.

iv. Significance tests

a. T-test

In the RM, the RSs are assumed to be normally distributed. Then T has the t-distribution with $n - 2$ degrees of freedom:

$$\frac{\hat{\beta}_0 - \beta_0}{SE(\hat{\beta}_0)}, \qquad \frac{\hat{\beta}_1 - \beta_1}{SE(\hat{\beta}_1)} \text{ …….. eq. (29)}$$

The standard error can be calculated using the known formulae for the variance of the $\hat{\beta}_i$.

$$SE(\hat{\beta}_0) = \hat{\sigma}(\sum \frac{x_i^2}{\sum (x_i - \overline{x})^2} \qquad SE(\hat{\beta}_1) = \frac{\hat{\sigma}}{\sqrt{\sum (x_i - \overline{x})^2}} \text{ ……eq. (30)}$$

$$\text{and } \hat{\sigma}_k^2 = RSS/(n-2). \text{……eq. (31)}$$

b. Marginal t-test

To calculate the confidence interval and construct a significance test, The null hypothesis is: $H_0 : \beta_1 = b$, and The alternative hypothesis is $H_A : \beta_1 \neq b$

Then the test statistics T is given by

$$T = \frac{\hat{\beta}_1 - b}{SE(\hat{\beta}_1)} \quad \text{…….. eq.(32)}$$

A similar test would be used for β_0,

$$T = \frac{\hat{\beta}_0 - b}{SE(\hat{\beta}_0)}$$

A student's t test distribution follows with degrees of freedom n-2, where n is the sample size, s is the standard deviation, and SSx is the sum of squares of the independent variable. When T value computed from the eq. (32) is greater than the critical value α/2 that means a hypothesis is rejected, there is a trend. When the null hypothesis is $\beta_0 = 0$, $\beta_1 = 0$, the term marginal t-test applies (Verzani, 2005).

c. Significance of the F test

The importance of this test is to analyse the variation to decide whether the difference in the CIs means is an analytical difference in the rainfall or temperature pattern. In a generalized multivariate regression problem, the total variation can be partitioned into two parts, as shown in eq. (26). The significance test for hypothesis, $H_0 : \beta_i = 0$, against the alternative hypothesis $H_1 : \beta_i \neq 0$, would be to compare the two values SSTr and SSE. It is expected on the climate data that the SSE would be smaller than the SSTr, but if the climate data have a common mean, then SSE and SSTr would be expected to be roughly the same. If SSE and SSTr are much different, it would be evidence against the null hypothesis.

The F statistic is $$F = \frac{SST_r /(k-1)}{SSE/(n-k)} \quad \text{……. eq. (33)}$$

To get proper scale, each term is divided by its respective degree of freedom (DF) to yield the mean sum of squares. The DF for the sum of squares is n-1, for SSE n-k and for SSTr k-1 (Verzani, 2005).

v. Akaika Criteria Information (AIC)

Given that

$$AIC = \ln(\hat{\sigma}_k^2) + \frac{n + 2k}{n} \quad \text{..... Eq. (34)}$$

Where $\hat{\sigma}_k^2$ is given by eq (31), and k in the number of parameters in the model. The value of k yielding the minimum AIC specifies the best model (Verzani, 2005). The idea is roughly that minimizing $\hat{\sigma}_k^2$, would be reasonable. Therefore policy makers ought to reduce the error variation by a term proportional to the number of parameters.

2.4.2.5. Model accuracy

i. Influential point

The regression line can be influenced by a single or multiple observations that are far from the trend by the data. The difference in slopes between the regression line with all data and the regression line with i^{th} point missing will be mostly small, except for the influential point. The Cook distance will be applied to check the differences of the predicted values of y_i for a given x_i when the point (x_i, y_i) is and isn't included in the calculation of the regression coefficients (Cook and Weisberg, 1982). The predicted values are used for comparison. Moreover, comparison of slopes isn't applicable to the multivariate RM. An R routine will be performed to compute the Cook distance.

ii. Diagnostic plot

To better understand the hydrological model, a policy maker or planner could run diagnostic on the plot for checking on the accuracy of the RM. This can be accomplished by fitted index plot of the Cook distances for each observation. The statistics are defined as

$$D_k = \frac{1}{(q+1)\hat{\sigma}^2} \sum_{i=1}^{n} (\hat{y}_{i(k)} - y_i)^2 \quad \text{..... eq.(35)}$$

Where $\hat{y}_{i(k)}$ is the fitted value of the i^{th} observation, when the k^{th} observation will be omitted from the RMs. The value D_k assesses the impact of the k^{th} observation on the estimated regression coefficients. The values of D_k greater than one are suggestive that the corresponding observation has undue influence on the estimated regression coefficients (Cook and Weisberg, 1982).

The same procedure will be applied to check relationship between climatic variables versus PDO and SOI with seasonal indicators from January to December.

2.4.2.6. Factor analysis

An initial objective of factor analysis is to identify the underlying factors that explain the correlation pattern within a set of observed CIs. This study used the Kaiser-Myer-Olkin (KMO) measure of sampling adequacy and Bartlett's sphericity test (Field, 2005, Chapter 11 and 12). The value of the KMO statistic should be greater than 0.5 if the sample is adequate, then factor analysis will be applied for the data reduction to identify a small number of factors that explain most of the variance observed in a number of manifest variables. The main drawback of the factor analysis is it bring associated with multicollinearity (when correlation (r) is greater than 0.8) and singularity if the determinate value is less than 0.00001, and data is not adequate.

2.4.2.7. Check the adequacy of factor analysis

The KMO statistics vary between 0 and 1. The value of 0 indicates that the sum of the partial correlations is large relative to the sum of correlations, indicating diffusion in the pattern of correlation. Therefore, factor analysis is likely to be inappropriate. A value of r will be indicated that patterns of correlations and so factor analysis should yield distinct and reliable factors. Kaiser (1974) suggested that accepting values greater than 0.5 was acceptable. Values between 0.5 and 0.7 are regarded as mediocre, values between 0.7 and 0.8 good, values between 0.8 and 0.9 excellent, and values

above 0.9 superb. Applying this criterion, this study checked the adequacy for factor analysis.

2.4.3. Alternative time series modelling

In this section, the time series modelling has been considered by two approaches. Firstly, a model is tried based on the assumption that there is a fixed term seasonal pattern about the trend. The trend is estimated by local averaging of the deseasonalized data, which is implemented by R function decomposition. The second approach allows for the seasonal variation trend, described in terms of a slope and level, to change over the time and estimates these features by exponentially weighted averages. This approach will be demonstrated by the Holt-Winters method.

2.4.3.1. Smoothing analysis

a. Local weighted smooth

The smoothing procedure will applied retrospectively to the time series with the objective of identifying an underlying signal or trend. It is usually applied from before and after a point in the time series appropriate for a long term trend or, seasonal components. In particular, if x_t represents the time series, Then

$$m_t = \sum_{j=-k}^{k} a_j x_{t-j} \quad \text{..... eq. (36)}$$

where, $a_j = a_{-j} \geq 0$ and $\sum_{j=-k}^{k} a_j = 1$ is a symmetric moving average of the data.

A second approach to smoothing a time plot is nearest neighbor regression. The regression, which can be linear or polynomial, is referred to as local because it uses only a small number of points on either side of the point at which the smoothing is required. A local weight technique known as lowess is used. First, a certain proportion

of nearest neighbors to x_t is included in a weighted scheme. The values closer to x_t in time get more weight, then a robust regression technique is used to predict x_t, estimate of $_t$. The larger the factors included the smoother the estimate of $\hat{f}_t$.

b. Kernel Smoothing

Kernel smoothing is a moving average smoother that uses a weight function or kernel to average observations. The Kernel smoothing can be define by

$$\hat{f}_t = \sum_{i=1}^{n} \omega_t(i) x_t \quad \text{..... eq. (37)}$$

where $\omega_t(i) = K(\frac{t-i}{b}) / \sum_{j=1}^{n} K(\frac{t-j}{b})$, ... eq.(38)

Where, b is the bandwidth. This estimator is called the Naradaya-Watson estimator (Watson, 1966). The K (.) is the function of the kernel, typically, the normal kernel defined as,

$$K(z) = \frac{1}{\sqrt{2\pi}} \exp(-z^2/2) \quad \text{..... eq.(39)}$$

The equation 39 is used. This formula will be implemented by R routine.

2.4.3.2. Single exponential smoothing

A simple model may be defined by

$$x_t = \mu_t + \omega_t \quad \text{..... eq.(40)}$$

Where μ_t is the non-stationary mean of the process at a t and ω_t is independent random variation with mean 0 and standard deviation i.e. $\omega_t(0,\sigma)$

Let us suppose that the estimate level of μ_t is defined as a_t and subject to the condition that there is no trend, and no seasonal effect. It is a reasonable to estimate the mean at time t by a weighted average of the observation at time t and an estimate of the mean at time t-1.

The first step model will be

$$a_t = \alpha x_t + (1-\alpha) * a_{t-1} \qquad 0 < \alpha < 1 \quad \text{.....eq. (41)}$$

and the step ahead forecast error will be $x_t - a_{t-1}$, where a_t is the exponentially weighted moving average (EWMA) at time t. the value of α is referred to as a smoothing parameter. If it smoothing parameter α is close to 1 little smoothing is needed and it seems that the estimated level a_t is approximately x_t and if the value of α is near 0, a highly smoothed estimate of the mean level which takes little account the recent observation.

Secondly, by repeated back substitution,

$$a_t = \alpha x_t + \alpha(1-\alpha) * x_{t-1} + \alpha(1-\alpha)^2 * x_{t-2} + \alpha(1-\alpha)^3 * x_{t-3} \text{.....eq.(42)}$$

In this form a_t can be seen as a linear combination of the current and past observation. The restriction, $0 < \alpha < 1$ ensure that the weight $\sum_{i=0}^{\infty} \alpha * (1-\alpha)^i$ becomes smaller as i increases. Note that these weights form a geometric series, and the sum of the finite series is unity.

2.4.3.3. Holt-Winters Method

The Holt-Winter method, (Holt, 1957 and Winters 1960), provides an alternative to a regression followed by an analysis of RSs. In its standard form, at least, it does not allow the incorporation of climatic indicators. The Holt-Winters model assumes an underlying level with a possible trend and seasonal effects, and its strength is that the level, trend and seasonal effects are assumed to change over time. Thus it is a non-stationary model and is useful for tracking changes in time series. The level, trend and seasonal effects are updated as data become available by exponential smoothing. The updating equations for a series x_t with period p is

$$a_t = \alpha * (x_t - s_{t-p}) + (1-\alpha) * (a_{t-1} + b_{t-1}) \qquad 0<\alpha<1 \ldots\ldots\ldots\ldots \text{ eq.(43)}$$

$$b_t = \beta * (a_t - a_{t-1}) + (1-\beta) * b_{t-1} \qquad 0<\beta<1 \ldots\ldots\ldots\ldots \text{ eq.(44)}$$

$$s_t = \gamma (x_t - a_t) + (1-\gamma) * s_{t-p} \qquad 0<\gamma<1 \ldots\ldots\ldots\ldots\ldots \text{ eq.(45)}$$

where a_t, b_t and s_t are the estimated level, trend (slope) and seasonal effect at time t, and α, β and γ are smoothing parameters respectively. Equation (43) takes a weighted average of the latest observation, with our existing equation appropriately seasonally adjusted. Equation (44) takes a weighted average of the previous estimate and the latest estimate of slope which is the difference between the estimated level at time t and the estimated level at time t-1. Note that Equation 45 can only be applied after Equation 10.5 has been applied to determine a_t. Finally, the seasonal effect is estimated from the difference between the observation and the estimated level. A weighted average is taken of the last smoothed estimate of the seasonal effect and the latest estimate of the seasonal effect which is made at time t-p. In principle the smoothing parameters can be estimated by minimising the sum of squared one step ahead predictions, but for the purpose of tracking the underlying level, trend and seasonal effects, a choice of 0.2 for α, β, and γ works well.

2.4.4. Stochastic model analysis

In the mathematical model for the time series data will use the discrepancies between the fitted values, calculated from the model, and the data as "RSs error" will be used. If the model encapsulates most of the deterministic features of the time series, then RS error should be appeared as the realization of independent random variables from some probability distribution. Moreover, the RSs usually correlated, which could be used to improve the forecast and make the simulation for more realistic.

2.4.4.1. Spatial correlation model

The spatial correlation coefficients provide evidence of the strength of association between locations. The RS at different stations are correlated when they are, or are

nearly, synchronous. In particular the cross-correlation (Cr-C), rho (ρ), at lag 0 can be estimated by r:

$$r_{ij} = \frac{\sum_{t=1}^{n} x_{i,t} x_{j,t}}{\sqrt{\sum_{t=1}^{n} x_{i,t}^2 \sum_{t=1}^{n} x_{j,t}^2}} \quad \ldots\ldots\ldots\ldots\ldots\ldots\ldots\ldots (46)$$

where $\{x_{it}\}$ and $\{x_{jt}\}$ are the RS at stations *i* and *j* respectively. Since the RS have mean of 0, the formula for r is given without explicit means. There are 45 pairs of stations, the number of choice of 2 stations from 10. The distance dependence correlation models are based on the strength of rainfall association between the stations,

The correlation model is

$$Model_{cor.rainfall} = e^{-k*distance} \quad \ldots\ldots\ldots\ldots\ldots \text{ eq. (47)}$$

Where k is the distance coefficient, the model is fitted to the data using the following RM:

$$y = \log((r_{rain} - |r_{rain}|)/2 + 0.001) \text{ or } y = \log((r_{temp} - |r_{temp}|)/2 + 0.001) \quad \ldots\ldots. \text{ eq. (48)}$$

on distance.

Therefore the model will be designed as,

$$y = \log(Model_{cor.rainfall}) = -k * distance \quad \ldots\ldots\ldots\ldots\ldots \text{ eq. (49)}$$

Including the north-south (NS) and east-west (EW) distances the correlation model will be extended to

$$Model_{cor} = e^{-K_1*NSdistance \quad -K_2*EWdistance} \quad \ldots\ldots\ldots\ldots\ldots (50)$$

2.4.4.2. Autocorrelations function (ACF)

In the statistical analysis, the mean and variance play an important key role, two keys distributional properties were played a central location and the spreads. Similarly, in the time series' models, a key role plays by the *second order properties*, which include mean, variance and serial correlation.

Consider a time series model that is stationary in the mean and the variance. A variable, for example, SOI, may be correlated and the model is *the second order stationary*, if the correlations between the variables of SOI depend only on the number of time steps. The number of time steps between the variables is called the *lag (*a lag is defined as an event occurring at a time t + k (k > 0). A correlation of a variable with itself at different times is known as an *autocorrelation or serial correlation*. A time series model which is second-order stationary known as an autocovariance function (ACVF), it is possible to define γ_k as a function of lag *k:*.

$$\gamma_k = E\left[(x_t - \mu)(x_{t+k} - \mu)\right] \text{..... eq.(51)}$$

Where, $\mu = \sum_{i=1}^{N} x_t / N \quad t = 1,2.....N$, and $k = 1,2.....t-1$.

and N=size of series. The function γ_k does not depend on time t because of the expectation, which is across the ensemble, is the same at all times t. More specifically, the autocorrelation at lag k is defined as

$$\rho_k = \frac{\gamma_k}{\sigma^2} \text{.....eq.(52)}$$

It follows from the definitions that $\rho_0 = 1$. The ACVF and ACF will be estimate from a time series by their sample equivalents. The sample ACVF defines c_k, as follows

$$c_k = \frac{1}{n}\sum_{t=1}^{n-k}(x_t - \bar{x})(x_{t+k} - \bar{x}) \text{.....eq.(53)}$$

Note that the covariance at lag 0, c_0, is the variance with denominator n. The denominator is also n used to calculate c_k. Only n-k term added to form the numerator. The constraints of sample autocorrelations lie between -1 to 1. And the sample ACF defined r_k as follows.

$$r_k = \frac{c_k}{c_0} \text{.....eq.(54)}$$

The lag zero auto correlations is always 1 and is shown in the relevant plot. In addition, it helps to compare values of the other auto correlations relative to the theoretical maximum of 1. This is useful because for a long time series, small values of r_k that are of no practical consequence may be statistically significant. In that

situation, from a practical point of view, some discernment is required to decide the noteworthy auto correlations. Squaring the autocorrelation can help in understating the percentage of variability explained by a linear relationship between the variables. For example, a lag one autocorrelation of 0.1 implies that a linear dependency of x_t and x_{t-1} would only explain 1% of the variability of x_t.

2.4.4.3. Cross correlation function (Cr-CF)

The interaction effect of CIs has been highlighted in this study. This idea will be demonstrated by the Cr-CF. supposed to two time series models have been variable defined x_t and y_t that are stationary in the mean and variance. The variables may be serially correlated, and correlated with each other at a different time lags. The combined model exhibits second order stationarity, if all these correlations depend only on the lag. Then the cross covariance function (CCVF) can be defined $\gamma_k(x,y)$ as g k.

$$\gamma_k(x,y) = E\left[(x_{t+k} - \mu_x)(y_{t+k} - \mu_y)\right] \text{.....eq.(55)}$$

This is not a symmetric relationship, and the variable x is lagging variable y by k. from a practical point of view, y will be responsive to by the input of x. The CCVF will be 0 for positive k, and there will be spikes in the CCVF at negative lag. The definition of CCVF is given in many textbooks, like the variable y lagging when k is positive. In this study the definition.

$$\gamma_k(x,y) = \gamma_{-k}(y,x) \text{.....eq.(56)}$$

is used, which is consistent in R routine. For multivariate stationarity it is possible to refer to an autocovariance function (ACVF) of one rather than the CCVF of a pair, for example $\gamma_k(x,x)$. The lag k Cr-CF is defined by

The CCVF and Cr-CF will be estimated from the time series by the sample equivalent. The CCVF is defined as

$$c_k(x,y) = \frac{1}{n}\sum_{t=1}^{n-k}(x_{t+k} - \bar{x})(y_t - \bar{y}).....eq.(58)$$

and the Cr-CF is defined as

$$r_k(x,y) = \frac{c_k(x,y)}{\sqrt{c_0(x,x)(c_0(y,y)}}.....eq.(59)$$

2.4.4.4. Correlogram analysis

In order to detect seasonality, plots of the ACF r_k against k are made such plots is called the correlogram. In general, the correlograms have some properties as follows

i. The x-axis gives the lag (k) and the y-axis gives the autocorrelations (r_k) at each lag. The unit of the lag is the sampling interval, e.g. second, hour, day and month and so on. The correlation is dimensionless, so there are no units for the y-axis.

ii. If $\rho_k = 0$, the sampling distribution of r_k is approximately normal, with a mean of $-1/n$ and a variance of $1/n$, and the dotted lines on the correlogram are down at

$$-\frac{1}{n} \pm \frac{2}{\sqrt{n}}.....eq.(60)$$

If r_k falls outside these lines, then the evidence against the null hypothesis that $\rho_k = 0$ at the 5% level. But in the multiple hypothesis tests, firstly if $\rho_k = 0$ at all lags k, we expect 5% of the estimates r_k to fall outside of the lines. Secondly, r_k are correlated, so if one falls outside of the lines the neighboring ones are more likely to be statistically significant. This will become clear when the time series is simulated. In the meantime, for specific lags corresponding to the seasonal period, for example monthly series, a significant autocorrelation at lag 12 might indicate that the seasonal adjustment is not adequate.

2.4.4.5. ARMA model

The previous section, introduces ACFs and Cr-CFs as tools for clarifying relations that may occur within and between CIs time series at different lag. In addition, this study explained how to build linear models based on classical regression theory for exploiting associations indicated by large values of ACF or Cr-CF. In the time domain. The emphasis is on forecasting future values, and the classical RM is often insufficient for explaining the dynamic time series. For example, in the static case, the policy maker or planner could assume the rainfall or temperature to be influenced by the SST. However, over the time, it is desirable to allow the rainfall or temperature to be influenced by the past values of the SST and its own past phenomena. If the present can be plausibly modelled in terms of only the past values, the SST input, and then policy would benefit from the enticing prospect that forecasting would be possible.

Instead, the idea of correlation as a phenomenon that may be generated though lagged linear relations leads to the proposal of the AR and autoregressive moving average (ARMA) models.

In mathematical modelling, the series $\{x_t\}$ is an auto regressive process of order 1 given by

$$x_t = \alpha x_{t-1} + \omega_t \quad \text{..... eq. (61)}$$

Where w_t is the white noise series with mean zero and variance σ^2 and α_i is the model parameter. Therefore, for an AR process of order p, the model AR (p) is given as

$$x_t = \alpha_1 x_{t-1} + \alpha_2 x_{t-2} + \text{.....} \alpha_p x_{t-p} + \omega_t \text{.....eq(61a)}$$

Adding a moving average process of order q defined as MA (q), the ARMA (p,q) model is given by,

$$x_t = \alpha_1 x_{t-1} + \alpha_2 x_{t-2} + \text{.....} \alpha_p x_{t-p} + \omega_t + \beta_1 \omega_{t-1} + \beta_2 \omega_{t-2} + \text{.....} + \beta_q \omega_{t-q} \text{.....eq.(62)}$$

In MA (q) models, the ACF will be zero for lags greater that q; moreover, the ACF will not be zero at lag q. Thus the ACF provides a considerable amount of information about the order dependence when the process is a moving average process. If however the process, is a ARMA or MA, the ACF alone tell us little about the orders of the dependence. Hence, it is worthwhile pursuing a function that will behave like an ACF of MA, namely one known as a partial autocorrelation function (PACF). To motivate this idea, consider a casual AR (1) model in equation (61).

In equation (61), the autocorrelations are non-zero for all lags even through in the underlying model the x_t only depend on the previous value x_{t-1}. The partial autocorrelation at lag k is the correlation that results after removing the effects of any correlations due to terms at shorter lags. For example, the PACF of an AR (1) process will be zero for all lags greater than 1. Moreover, the PACF at lag k is the kth coefficient of a fitted AR (k) model. If the underlying process is AR (p), then the coefficient α_k will be zero for all $k > p$. Thus an AR (p) process has a correlogram of PACF that is zero after lag p. Hence a plot of the partial autocorrelation can be useful when determining the order of a suitable AR process for a time series.

2.4.4.6. GARCH model

Recently, there have been several studies on volatility in climate series (e.g. Romilly, 2005), for example, for time series, from which any trend, seasonal and linear effects have been removed. In such cases, the questions are about volatility alone. In order to account for this, a model is required that allows for conditional change in the variance. One approach to this is to use an AR model for this variance process, and the standard tools have become the ARCH / GARCH models, defines as a series ε_i. This is a first order auto regressive conditional heteroskedastic if

$$\varepsilon_t = \omega_t \sqrt{\alpha_0 + \sum_{i=1}^{p} \alpha_1 \varepsilon_{t-i}^2} \quad \ldots\ldots\ldots\ldots \text{ eq. (63)}$$

Where $\{\omega_t\}$ is defined as white noise with mean zero and unit variance. Also α_0, α_1 are model parameter. To introduce the volatility, eq.(63) is squared first to calculate the variance

$$\text{Var}(\varepsilon_t) = E(\varepsilon_t^2) = E(\omega_t^2)E(\alpha_0 + \alpha_1\varepsilon_{t-1}^2)$$

$$= E(\alpha_0 + \alpha_1\varepsilon_{t-1}^2)$$

$$= \alpha_0 + \alpha_1 \text{Var}(\varepsilon_{t-1}) \text{.....eq(64)}$$

Since ω_t has unit variance and ε_t has zero mean. Compare equation (63) with the AR (1) process,

$$x_t = \alpha_0 + \alpha_1 x_{t-1} + \omega_t \text{.....eq(64a)},$$

The result is that the variance of an ARCH (1) process behaves just like an AR (1) model. Hence in the model fitting, decay in the autocorrelations of squared RSs should indicate whether an ARCH is appropriate or not.

The first order ARCH model can be extended to a p^{th}-order process by including higher lags. An ARCH (p) process is given by

$$\varepsilon_t = \omega_t \sqrt{\alpha_0 + \sum_{i=1}^{p} \alpha_p \varepsilon_{t-i}^2} \quad \text{..... eq.(65)}$$

A further extension is the generalised ARCH (or GARCH) model for order (p,q). Then the series $\{\varepsilon_t\}$ is GARCH (p,q) given by

$$\varepsilon_t = \omega_t \sqrt{h_t} \text{.....eq.(66)}$$

Where $h_t = \alpha_0 + \sum_{i=1}^{p} \alpha_i \varepsilon_{t-i}^2 + \sum_{j=1}^{q} \beta_j h_{t-j}$

and α_i and β_j $(i = 0,1,\text{.....p}; j = 1,2,\text{.....q})$ are the model parameters. If the GARCH model is suitable, the RS should appear to be a realisation of white noise with zero mean and unit variance. In this case of a GARCH (1,1) model,

$$\hat{h}_t = \hat{\alpha}_0 + \hat{\alpha}_1 \varepsilon_{t-1}^2 + \hat{\beta}_1 \hat{h}_{t-1} \text{.....eq.(67)}$$

with $\alpha_1 + \beta_1 < 1$ to ensure stability (Trapletti and Hornik, 2008)

2.4.4.7. Hurst phenomena

Hurst found (Koutsoyiannis, 2003) that certain long hydrological time series with no apparent trend displayed a long range dependence phenomenon that is now often referred to as long-memory (Beran, 1994). The mathematical definition of this phenomenon is that auto correlations decay in proportion to the reciprocal of the lag, rather than exponentially with the lag as they do for AR processes. The practical importance of this is that long-memory processes are best modelled by fractional difference before fitting auto-regressive moving average models. The Hurst coefficient H is a measure of dependence that always lies between 0 and 1, and equals 0.5 for a process that consists of independent random variation. In theory, for a stationary process H > 0.5 corresponds to long range dependence, and H is equal to 0.5 if correlations decay exponentially, but in realisations of time series, which are necessarily finite, sample estimates of H are biased above 0.5. One method of estimating H for a time series (Stainforth 2007a) is to regress to the logarithm of the rescaled adjusted range R_m, calculated from a sub series of length $m \leq n$ against the logarithm of m. The rescaled adjusted range is itself calculated from adjusted partial sums (S_k) which are given by:

$$S_k = \sum_{t=1}^{k} x_t - k\bar{x}_k \text{.....eq.(68)}$$

for k from 1 to m where $\bar{x} = \sum_{t=1}^{m} x_t / m$.

Then $$R_m = \{\max(S_1,.....S_m) - \min(S_1,.....S_m)\}/S\text{.....eq.(69)}$$

Where $$S = \sqrt{\sum_{t=1}^{m} (x_t - \bar{x})^2 /(m-1)}\text{.....eq.(70)}$$

The R_m, which is the average of the n+1-m values, can be calculated for block sizes, m, from 2 up to the length of the original time series n, and for each value of m. There are n+1-m different values corresponding to the different starting points for the sub-series. Although straightforward in principle, the calculation is considerable for large

values of n and an efficient computer program is required. The theoretical relationship (Beran, 1994) between R_m, H and m is $R_m \propto m^H$. In logarithmic terms:

$$\ln(R_m) = a + H\ln(m).....eq(71)$$

where a is an intercept. H is thus estimated as the slope of a regression of the values of computed (R_m) against ln (m), where the ln (R_m) is the average of the n+1-m values.

Hurst estimated a value of H=0.91 for the River Nile (Sakalauskienė, 2003) which is high enough to be considered evidence of long-memory. The Hurst phenomenon is the final aspect of monthly scale persistence to be investigated in hydrologic time series, in particular in rainfall and temperature series for all 10 stations. Persistence can be characterised by a rescaled adjusted range behaving as a function of m^H. H>0.5 of the sample size m, rather than the $m^{1/2}$ that is characteristic of the short memory process (Koutsoyiannis, 2003). The sequence of the independent Gaussian variables (sequence with an absence of long term memory) will have a value of H of approximately 0.5 and higher values of H are directly related to higher intensity of persistence.

2.4.4.8. CUSUM method

The Cumulative sum (CUSUM) method can be used to test whether there is evidence that the RSs is non-stationary. Let $\{x_t\}$ represent a RS. Then the CUSUM at time t is given by $C_t = \sum_{i=1}^{t}(x_i - \bar{x})$, where $\bar{x}$ is the mean of the time series of length n. If the mean remains below average then C_t will have a negative slope and if the mean remain above the Ct if will have a positive slope. Locally, if a climatic record can be categorised into a few periods of above and below average values the corresponding plot of C_t will be characterised by substantial excursions from the centre line. Such features are apparent in the CUSUM of the RSs in this study and were quantified using standardised CUSUM range statistic referred to as *Q*, defined by:

$$Q = \frac{\max_{1\le t\le n}(C_t) - \min_{1\le t\le n}(C_t)}{\tilde{\sigma}} \text{.....eq.(72)},$$

where $\tilde{\sigma}$ is a median range estimate of the standard deviation that is relatively insensitive to occasional shifts in the process. The usual method for testing for a shift in the mean level is to use V-mask or an equivalent algebraic algorithm (Cowpertwait and Metcalf, 2009). However this assumes the process standard deviation during periods when the mean is stationary (σ) is known. The algorithm is to first calculate K= σ/2, and H=5 σ, then, calculate σ for t=1,2,3,…..n. the confidence interval is given by

$$SH_t = \max\left[0, (x_t - \bar{x}) - K + SH_{t-1}\right]$$

$$\text{And } SL_t = \max\left[0. - (x_t - \bar{x}) - K + SL_{t-1}\right] \text{.....eq.(73)}$$

A significant shift is the mean is declared if either SL_t or SH_t exceeds H. If the variable is normally distributed with a standard deviation σ and the successive values are independent then the false alarm rate is about 1 in 440. In this investigation σ should be estimated by a moving range technique that is insensitive to occasional shift in the process mean. In the simulation process, a Gumbel distribution was applied and calculated the factor. It was assumed that observed lags were independent and the median of the absolute values of the difference for a normal distribution was calculated. The σ is estimated by the product of 1.047 and this median moving range, a result that has an easy theoretical justification. Calculated factors are applied for the temperature and rainfall RS. It was supposed that data were from Gumbel distribution and a factor of 1.17 was used based on simulations (1000 white noise series of length 1290).

The extreme values distribution

$$F(x) = e^{-e^{-(\frac{x-\xi}{\theta})}} \quad \text{…… eq (73)} \quad \text{for } -\infty < x < \infty$$

Without loss of simplification, it can be assumed that $\xi = 0,$ and $\theta = 1,$

then $$F(x) = e^{-e^{-x}} \text{ …….. eq (74)}$$

To obtain a random number

$$F(x) = e^{-e^{-x}} = r$$

where r is $U[0,1],$ and $x = -\ln(-\ln(r))$

The CUSUM was derived about $\bar{x}$ and therefore founds at 0. However for climatic data in general there appear to be a few underlying changes in the mean, typically attributed to some changes in climate state with long sojourns between them. Therefore, the statistic that highlighted this feature was tested, as was its significance, the latter with a Monte Carlo simulations procedure. The null hypothesis was that the data are the realisation of an AR (p) process with Gumbel random variations. In particular, the mean of the AR (1) is constant. The standard deviation of the process was estimated as $\tilde{\sigma}$ because it was evident by insensitive to shifts in the mean.

2.5. Conclusion

Climate change and their future projected scenario by TAR (IPCC, 2001) share deep uncertainties. IPCC has suggested that portfolio planning method could be used to embrace the uncertainties of planning for multiple possible future scenarios irrespective of their probability. One of the most suitable statistical techniques will be demonstrated in this study for development WRMS in the GRBand the MDB areas respectively. Parametric and non parametric test will be applied for better understanding of climatic variability and influence on rainfall and temperature patterns in the MDB areas and eastern Australia. Various RMs will be applied for analysis of time series data that will be capable of assessing the deterministic trends and seasonal changes. The evidence of climate change in recorded data is not straightforward. Presenting correct statistical evidence is important, and in this study generalized least squares methods will be used, which could improve estimates of the standard error to account for autocorrelation in the RSs. To assist the policy maker, evidence of distance dependence and statistically persistency for the long term and short term will be taken into account.

To develop the strategies, most fitted time series model will be used to simulate the data. The most standard statistical distribution will be simulated, and it will be applied to generate plausible future scenarios and construct confidence intervals for model parameters.

CHAPTER 3: LEVERAGE OF WATER RESOURCES

3.1. Introduction

Water is the hub of life and an indispensable part of all terrestrial ecosystems (Vo, 2007) The distribution of these water resources throughout the earth is as follows: Surface water is 0.017%, subsurface water is 0.619%, icecaps and glaciers are 2.147%, and Oceans is 97.217% (Bras, 1990). This indicates the limited availability of fresh water. It is no longer a substance that people can take for granted. The increase in water demand, which is a result of rapid population and economic growth, has dramatically reduced the volumetric water availability per-capita. Moreover, fresh water is unevenly distributed over the earth both spatially and temporally. This fresh water system is being changed naturally in terms of quality, quantity and morphology, and these changes are being further accelerated due to human interventions and exploitation. This competition has to be led to numerous conflicts within the society. These conflicts, as predicted by Gleick (1998), will be even more frequent and serious in the future as populations continue to grow. As a result, conflict around water is not confined within specific the countries, but it has become a transboundary issue as well. Conflicts between riparian nations may arise regarding economic development, infra structural capacity, or political orientation. Water resources issues heavily aggravate the tension. Indeed, there is already clear evidence of escalating conflicts in different parts of the world concentrated on water quantity and quality issues. Examples of some international water disputes around the world are depicted in Figure 3.1. There is one fortunate consequence of water induced conflict. It provides an incentive for hostile co-riparians to cooperate, even as disputes are waged over other issues. The historical evidence of cooperation between co-riparians can be found from many different studies. To mitigate conflicts over shared water 157 treaties have been negotiated and signed in last five decades (Wolf, et al. 2003). Researchers have proposed different approaches to conflict. Unfortunately, it is evident that the contemporary approach to water management not only in developing countries but also in developed countries is not sustainable (Rahman, et al. 1998). It is noteworthy that the situations are worse in developing countries. Solution is not straightforward; rather than depends on willing to resolution among riparian countries by political

cooperation, geographical, socio-economical aspects, even the third party involvement.

3.2. Objective of Study

Water is a necessity for sustaining the population, not only for direct household consumption, but also for everything from food production to electricity generation. Thus, it becomes a resource not only critical for sustaining life, but also for achieving and maintaining an acceptable standard of living. Given its importance to life, this study highlights how water resources became the source of conflict? It also explains how these conflicts can develop, especially in the context of developing nations. Furthermore, the literature reviewed on the Mekong River Basin (MRB), and the Indus River Basin (IRB) was a lesson in learn into integrated water resources management (IWRM) via a holistic approach. This study also explored details of the Manyara region in Tanzania to understand the governance of water resources, and how stakeholder wraps up on conflict over water resources. In addition, how the conflicts over water resources tend to be exacerbated in both developed and developing nations, as a consequence of political, institutional, and environmental problems.

The following sections will also briefly examine the causes of social conflict over water resources, the types of conflicts that may arise, and the methods that may be used to resolve.

3.3. A causes of water conflict

3.3.1. Ovation of water conflicts

The potentials for water conflicts exist everywhere around the world, in developing countries and also in developed countries. In developing countries, there is a higher potential for these conflicts, because of the poverty of the people, water scarcity, high

and rising populations and mostly no or less than adequate fresh water purification. Furthermore, international river basins lead to a lot of conflicts, and it is important to identify their nature in order solve the problems through cooperation and to prevent escalation. Figure 3.1 below is a map of international basins at risk.

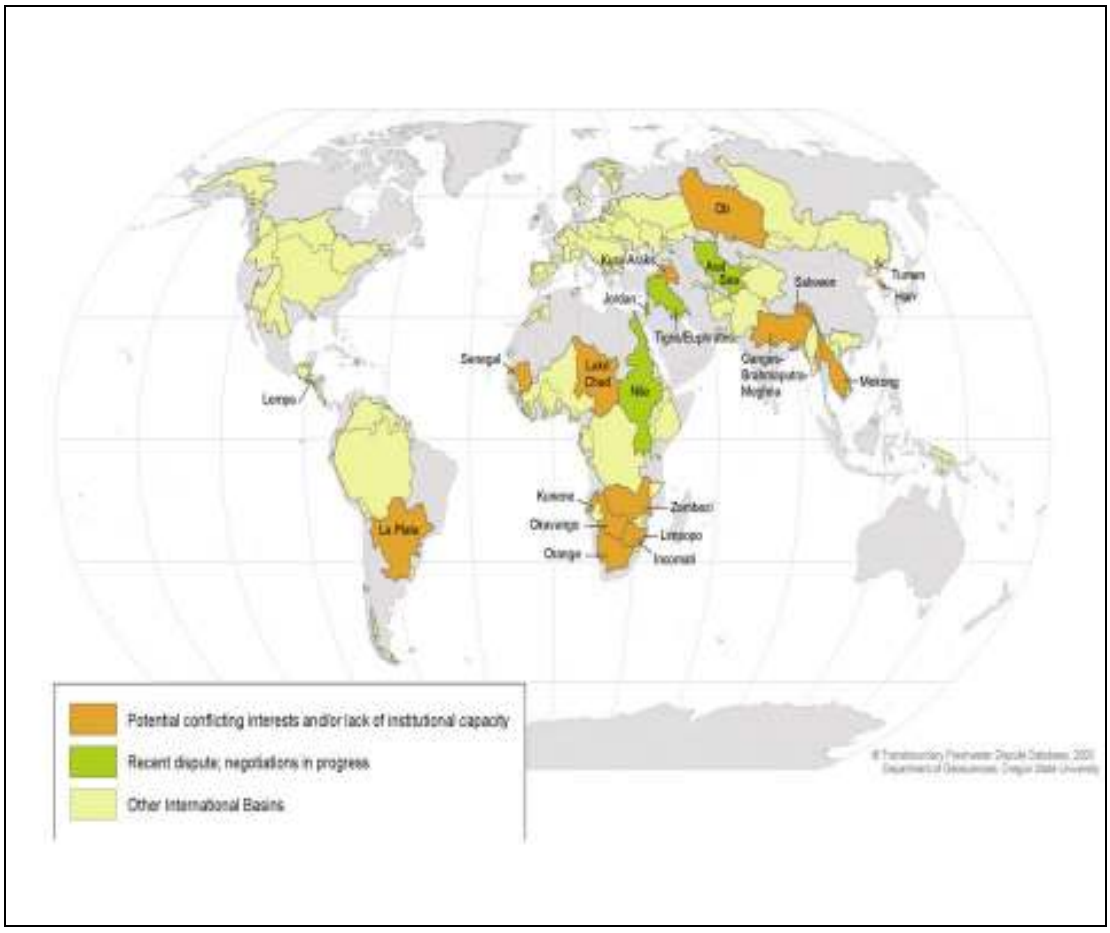

Figure 3. 1: International Basins at Risk (sources: Yoffe, et al. 2002)

The Figure 3.1 divides the basins at risk in three categories on the basis of Potential conflicting interests and/or lack of institutional capacity. The orange colour category is the one with the highest risks. The basins included in this category are also known as the 'hot spots', because of the high potential of disputes between the different countries user. To this category of risk belong to the Ganges-Brahmaputra-Meghna, Mekong, Lake Chad, Incomti, Okavango, Kuneno, Senegal, La Plata, and Salween basins. The dispute and negotiation light green colour category indicates a potential of future conflicts. In this category are the Nile, Jordan, Aral Sea, and Tigris-Euphrates. The risk is not at high as in the basins mentioned above. There have been several protests because of the water and also stresses upon the water system management. The last category has the same indicators as the light green one, but it represents an

even a lower risk. Most of the countries with risk of conflicts about water are based in Asia and Africa, where the developing countries are situated. After defining where the conflict areas are, it is necessary to find ways to solve the conflicts through cooperation. A good example of this is the Nile basin. There are 10 countries sharing the River Nile: Burundi, Egypt, Eritrea, Ethiopia, Kenya, Rwanda, Sudan, Tanzania, Uganda, and the Democratic Republic of the Congo. Whereas Egypt and Sudan reserve the right of using 100 percent of the river water, and except of Egypt and Kenya, the other countries are some of the poorest 50 countries in the world. Every country wants to use as much water from the Nile as possible, for agricultural irrigation, for energy production, and also for producing drinking water. Consequently, conflict has arisen across the Nile river basin.

3.3.2. The Developing world dilemma

The disparity in living standards between developed and developing countries have expanded rapidly in recent history. Management of water resources has played a pivotal role in the advancement of living standards in developed countries, and efforts have been made to afford the developing countries the benefits of better water management strategies. At the dawn of the 21st Century, the United Nations declared its intent to close the gap between the developed and the developing countries, through the achievement of the key Millennium Development Goals (MDG). These goals seek to improve the livelihood and living standards of people in some of the poorest regions of the world (UNDP, 2009). The most recent World Water Development Report, published in April 2009, suggests that although the environment and water resources are identified as one of these goals, the management of this most precious resource permeates all eight MDG independently (UNESCO, 2009).

As virtuous as the United Nation's development goals may be, the challenges associated with implementing the necessary changes present contradiction concerns. As discussed by UNESCO (2009), population growth merely presents a baseline for the stresses imposed upon water resources. The process of improving living standards within the developing world will exacerbate problems – particularly with the changing diets of burgeoning populations in water-stressed regions. Seemingly simple

improvement to living standards, such as an increase from one meal to two meals per day, will incur a massive increase in water consumption through demand for agricultural irrigation.

The developing world will be responsible for 90% of the predicted 3 thousand million increases in global population by the year 2050 (UNESCO, 2009). This massive increase in the number of mouths requiring feeding, plus other pressures such as ongoing trends towards urbanisation, will further stress water resources that are already severely limited. Of concern is the fact that much of this population growth is expected to occur in regions challenged by extremely dry climates, such as sub-Saharan Africa and many Arab states. It is therefore, important to understand the causes of these conflicts, especially in the context of developing nations.

3.3.3. Relation of water resources and social conflicts

Water has a closely relationship with societies because of its roles in food security and rural development, health and sanitation. Societies need water for their basic needs, including agriculture, industry, sewage treatment, recreation, etc. Conflicts over water can develop between competing. Competition can occur over both quantity and quality of water (Wolf 2007), and can develop between drinking and agriculture uses, rural and urban uses, and between head-reach and tail-end reach farms as suggested by Iyer (2003). Competitions can also develop between riparian states/countries sharing the same river basin (OECD 2005). The stress upon global water resources in the 21st Century presents a growing management dilemma. Countless publications and media articles have drawn attention to the current water woes of the world. One of the major causal agents of conflict over water resources is the concept of scarcity. Scarcity arises because water is a finite resource, such that an increase in the population of a particular basin results in a decrease in the per capita water supply. Ohlsson (2000) suggests that scarcity of water resources can be divided into two categories: first-order scarcity of the water resource itself and second-order scarcity of the social resources required to adapt to the first-order scarcity. First-order scarcity creates conflicts related to the direct use of the resource (i.e. first-order conflict),

while second-order scarcity causes conflicts related to the difficulties faced in adapting to the challenges created by the limitations to the resource (i.e. second-order conflict).

3.3.4. Conflicts over water shortage

There are plenty of reasons for conflicts a rising through water. The key aspects of water conflicts are quantity, exponentially growth of population, climate change, and quality of life improvement (Malkina-pykh, 2003). According to Conca (2006) point out that change in community access to water supplies can generate social conflict. The water conflict is not a new problem. It has occurred since at least 3000BC *(Gleick, 2008)*. Nowadays, it is occurring especially in developing countries. Israel vs. Palestine, India vs. Bangladesh and all ten riparian states of the Nile River are examples *(Wolf, 1999)*. Some regions will build some large dams, irrigation schemes and transportation canals, which can enlarge their water supplies. As *Nilsson, et al. (2005)* pointed out, over 5% of world's rivers/water bodies have been damaged by dam construction, which cause water pollution by resulting in relatively low flows. For example, the world largest dam (Three Gorges Dam, China), up to 1.4 million residents have been relocated without sufficient compensation and with no right to object to government (WSJ. 2008). Moreover, there must be also other influential factors such as socio-economic factors, institutional or political factors, and environmental factors. The socioeconomic factors include the increase of affluence and the associated demand for water, but also the poverty of the people, and at least the social inequity between the different water users. The institutional or political factors are more about governance failure, and lack of transparency, to handle the water scarcity problem. Furthermore, included in this factor are damming projects, which result in the millions of people, or other water development projects.

In developing country contexts, conflicts arising over water resources may be amplified due to a number of factors. One of the most significant factors is poverty, which leads to a lack of maintenance practices, poor irrigation services, and little

research and development activity for enhancing the supply and use of water resources (Maxwell and Reuveny, 2000; Easter, 2000; Hooper, 2006). Transaction costs, such as these for monitoring and fee collection, are also higher in developing countries. This is in part because developing countries typically possess large numbers of small-scale stakeholders in the water resources (Hooper, 2006). This complicates control over water usage, particularly as many developing countries may possess inadequate institutional structures relating to property rights (Maxwell and Reuveny, 2000; Easter, 2000; Hooper, 2006). In addition to these factors, there is another environment and societal-related factors that may enhance scarcity issues in developing nations, some key points are:

- Climates of developing countries are generally more extreme, with lower and more irregular rainfall in comparison to developed countries (Hooper, 2006). This frequently promotes a higher usage of groundwater in developing nations (Hooper, 2006).
- Water is commonly the source from rain or private storages in developing countries, whereas developed nations commonly derive water from service providers (Hooper, 2006).
- The population distributions of developed nations tend to be concentrated in downstream areas of rivers, while greater densities exist in both upstream and downstream areas in developing countries (Hooper, 2006).

All of these factors lead to poor water resource management practices, which can induce second-order conflict. However, it is acknowledged that conflict is more likely to arise due to the institutional and political issues within developing countries rather than simple water shortage issues (Easter, 2000; Mehta, 2007).

3.3.5. Types of conflict over river basin management

There are many examples in the history of conflict caused by disagreements over the river basin management (Gleick, 2008), and the schematic diagram of conflict on river basin management Figure 3.2 arises from visual impression of how water resources become a basis for conflict at the user versus stakeholder, state versus state

levels. Moreover, at the national and international level, conflict may result from many different factors. Domestic conflict Case 1 in Figure 3.2 can exist either within states or across state borders.

Conflict between states shown as Case 2 in Figure 3.2, is often an upstream-downstream conflict, but may also involve "states" that are bordered by a river. The upstream-downstream conflict situation is more likely to result in conflict (Toset et al., 2000), given that the downstream entity is more likely to feel disadvantaged over the available resources than the upstream one. A relevant and topical example of water resource conflict between states exists in the Murray-Darling basin of Australia, where disputes between the states of South Australia, Victoria and New South Wales over management of the basin are ongoing with regard to state-by-state allocations, particularly with the current drought experienced in the basin. Another example may be found in Kiteto, in North-Eastern Tanzania. They are the water resources are primarily shared by three main groups of people co-existing in the area, which include hunter-gatherers, pastoralists, and farmers (Water Aid, 2003). Competition exists between all these groups for access to land and water resources, while other conflicts are also present. For instance, pastoralists are criticised for increasing herd numbers, while farmers receive criticism for degrading land through unsustainable land use (Water Aid, 2003). Each issue puts pressure on the available water resources, which is exacerbated by the semi-arid nature of the environment, this has characteristically irregular rainfall patterns and associated scarcity problems (Water Aid, 2003). Due to these issues, violent conflict has intermittently emerged in the region, resulting in deaths in some cases (Water Aid, 2003).

In other cases in Figure 3.2, an aquifer that is entirely in one country is hydrological linked with another aquifer in a neighbouring country, or is recharged in a foreign state (Cases 3 and 4). Moreover, a river basin hydrological relationship may be with one more river and across one more geographical boundary as in Case 5. In that situation, the sharing issues over water resources may raise a conflict between countries, known as riparians, who share a river basin or even between competing stakeholders for the resources where there is a scarcity. The shared water resources between countries are an ever-present source of potential conflict, particularly in

developing countries where populations are high and water supply irregular, leading to scarcity. Evidence suggests that international disagreement over water resources is often born from attempts to avert domestic conflict caused by second-order scarcity (Ohlsson, 2000). Examples of conflicts over water resources can be found in many parts of the world, such as between Iraq, Syria and Turkey over the Tigris-Euphrates basin; between Jordan, Syria and Israel over the Jordan River basin; and between India and Bangladesh over the Ganges-Brahmaputra-Megna basin (Wolf and Newton, 2008).

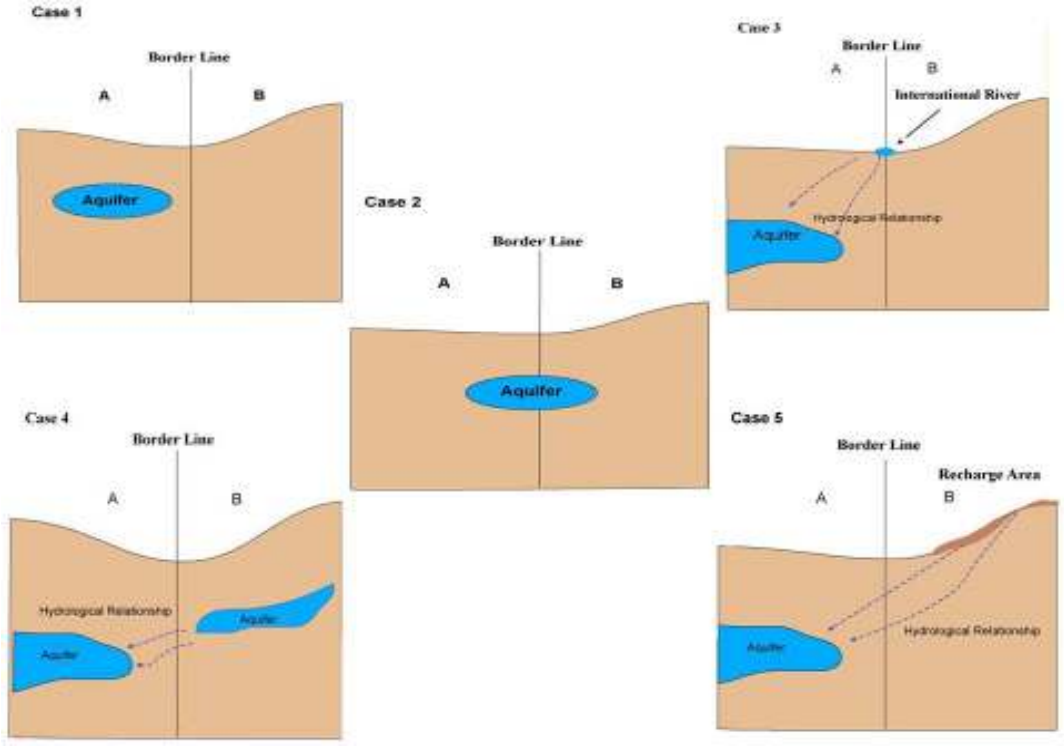

Figure 3. 2: Schematic diagram of conflict over river basin management

Transboundary water resources are those that cross one or more international borders. The stronger countries in a region frequently manage water for their own benefit, at the expense of the weaker countries, and to the detriment of the river basin as a whole. Across the world, there are many river basins that cross international boundaries as illustrated in Table 3.1. The river basins that cover two or more nations are very difficult to manage. It is noted that poor management of such basins will result in political and social conflict.

Table 3. 1: The World's International Rivers

World Region	Number of International river basins	Percentage of land area in international river basins	Number of countries in one or more international basins
Africa	59	62%	47
Asia	57	39%	34
Europe	69	54%	42
North America	40	35%	12
South America	38	60%	13
WORLD TOTAL	263	45%	145

(Source: Reproduced from Ken Conca, Fengshi Wu and Joanne Neukirchen (2003, p2)

There is no international law which prescribes the rights of each riparian country to a particular water resource. Issues associated with management of international river basins, and the potential for conflict are described in the following section.

3.4. Case study: Disputes over Water in Developing Countries

3.4.1. Case study: the MRB,

The MRB is a shared catchment between the countries of Tibet, Burma, Laos, Thailand, Cambodia and Vietnam. Water resources in the wet season are more than adequate to meet the basin needs; however, there are regional shortages during the dry season, when only 1-2% of the annual flow reaches the Mekong Delta. Recent rapid agricultural and economic development in the basin has led to increasing competition for Mekong waters. A structured approach to the management of the basin is required to achieve efficient, equitable, and environmentally sustainable water allocation

mechanisms that support the socioeconomic development of the region. The MRB is highly valuable as it:

- supports diverse and lucrative fisheries;
- provides water supply to communities;
- supports agriculture and
- otherwise supports communities within its flood plain

The Mekong River Commission (MRC) Agreement was formed in 1995. The Mekong River Commission (MRC) fosters inter-governmental cooperation among the four lower Mekong countries of Cambodia, Laos, Thailand and Vietnam.

A significant shortcoming of the MRC has been the refusal of China to become a member of the Commission. China takes the view that it has no obligation to submit its actions for discussion or consideration by the other countries. However, in 1996, China did join as a dialogue partner (Milton, 2004).

In addition to China's dam construction projects for generation of hydropower, the Chinese is undertaking a major programme of blasting and dredging along the river's course to significantly expand its use for commercial navigation. This work along the river has brought substantial changes to the Mekong River, the effects of which are experienced by the downstream countries. The Governments of the riparian states downstream from China have vehemently opposed the actions of the Chinese; however, they have continued to act in the interests of their country alone.

3.4.1.1 Transboundary Conflict in MRB

The Mekong River is one of the world's major water systems with its source in the Tibetan Plateau flowing through to the Mekong Delta. It plays a major role in the livelihoods of people in China, Myanmar (Burma), Laos, Thailand, Cambodia and Vietnam, with millions of people relying on the river for drinking water, fish stocks, irrigation, hydro-power, transportation and commerce. More than a third of the population of Cambodia, Laos, Thailand and Vietnam live in the Lower Mekong Basin (Popplestone, 2008). A map of the Mekong River is presented in Figure 3.4.

Figure 3. 3: the MRB Map, Source: http://hereticdhammasangha.files.wordpress.com /2008/03/mekong-map1.jpg.

Approximately, one fifth of the Mekong Basin lies within China. This represents only 2% of China's territory. More than 80% of Laos and 90% of Cambodia lie within the basin. It is upper reaches of the Mekong River that are in China, and the upstream water management activities have a significant impact on the downstream. To date, China has acted unilaterally, and without consultation or consideration of the downstream nations. China maintains it is within its sovereign rights to do what it wants on its portion of the river (Salidjanova, 2007).

As noted in Section 4.1, the Mekong River Commission came together in 1995 and represents the four lower Mekong countries of Cambodia, Laos, Thailand and Vietnam. The Mekong River Commission has a mission to preserve the natural resources and environmental quality of the river basin while promoting the inter-dependent and economic growth of the Mekong Region (Popplestone, 2008).

There is a significant lack of parity between countries along the Mekong River. The conflicts in the Mekong area are aggravated because neither China nor Burma belongs to the negotiating Mekong River Commission. This absence of these two powerful nations from the Commission seriously hinders the Commission's ability to negotiate effectively between the parties concerned.

The absence of China, and in particular its ongoing behaviour of acting independently and without consultation with the other countries, has caused massive problems in the region. China's construction of dams and a navigation channel along the upper reaches of the Mekong threatens the complex ecosystem of the Mekong. Development of an 8-dam cascade is already well underway. The schedule for completion of the dam locations all in China is shown in Table 3.2 and a site location map for others dams is shown in Figure 3.6.

Table3. 2: Scheduled dam construction along the MRB

Dams	Scheduled Completion Date	Hydropower Megawatts (MW)
Manwan Dam	1996	1500
Dachaoshan Dam	2003	1350
Gonfhoqiao Dam	2008	750
Jinghong Dam	2010	1750
Ziaowan Dam	2013	4200
Nuozhadu Dam	2017	5850
Ganlanba Dam	n/a	150
Mengsong Dam	n/a	600

Source: Probe International, (http://www. probeinternational. org/catalog/ content fullstory.php)

The scheme will drastically change the river's natural flood-drought cycle and block the transport of sediment, affecting ecosystems and the livelihoods of millions living downstream in Burma, Thailand, Laos, Cambodia and Vietnam.

The construction of the dams has resulted in scenarios such as people being forced off their small holdings (without adequate compensation), downstream fishing stocks dwindling so much that fishermen can no longer make a living, changes in seasonal flooding regimes, and impacts on agricultural activities (e.g. rice growing). All of these scenarios present a significant threat to the countries in the lower basin region that utilise the river both as a source of water and of sustenance, as well as economic growth.

Figure 3. 4: Dams along MRB marked in red circle,

Source: http://www.dams.org/images/maps/map_mekong.htm.

3.4.2. Case study: Manyara region in Tanzania

3.4.2.1. Access and Ownership of Land and Water

Kiteto is one of the five districts of the Manyara Region in the north-east of Tanzania. Figure 3.3 shows a map of Tanzania, and the location of Kiteto. Access to water, and its allocation and use, are critical concerns that drive conflict. Access to water is becoming a critical problem that may have significant impacts on social stability In Kiteto. The state owns all land, and given water and land are closely interconnected, water is generally available to the occupier of the land. Tanzanian law allows all citizens to be free to move anywhere on the land.

Figure 3. 5: Location Map for Kiteto, Tanzania, Source: Water Aid, 2003

There are three main groupings of livelihoods in Tanzania; (1) hunter-gatherers, (2) pastoralists and (3) farmers.

The *hunter-gatherers* are people who live off the land by hunting wild animals and collecting roots, wild berries and honey (Water Aid, 2003). The Hunter-gatherers are the most vulnerable and marginalized group of people in Kiteto. The *pastoralists* are people who manage livestock including sheep, cattle, camels and/or goats. They are often nomadic, and move throughout the year with their families and herds. *Farmers* obtain most of their income from farming the land. Typical crops grown include maize, beans and sorghum. The high nutrient levels in the soil make the land high-yield farming land.

As the *pastoralists* migrate, they move over large areas of grazing land, utilising the local water resources. It is not uncommon for a pastoralist to return to a piece of land utilised the previous year, only to find that a farmer has taken over the land. Similarly, *hunter-gatherers* may have to relinquish occupancy of land they have lived on and utilised for hundred of years to allow pastoralists to utilise the land and water source.

The lack of knowledge of land laws by local villagers can result in inequitable distribution of land and water, and illegal land take over. There is an increasing trend towards rich farmers and pastoralists taking over large areas of land and water resources for farming. A change to water supply arrangements in a local village in Kiteto is likely to result in a significant change in the community's dynamics. It is reported that one village that implemented a borehole scheme had a three-fold increase in population over a five year period (Water Aid, 2003). Borehole schemes are common in Kiteto, and can lead to a migration of pastoralists and farmers into the district.

The poorest people and in particular, women living in Kiteto have limited control over land and water resources and therefore, limited power. Although the intended strategy of most community water related projects are to provide domestic water for free to these minority groups, they are often excluded from equitable access to community resources. There are reported cases of women being refused access to water sources until owners of large cattle herds have watered their animals (Water Aid, 2003). In Kiteto, water resources are limited; control issues have led to conflicts, which have resulted in fatality (Water Aid, 2003).

3.4.3. Case study: the IRB

The IRB is shared by a number of riparian states, which include India, Pakistan, Afghanistan, China, and Nepal, with Pakistan as the main one (Giordano et al., 2002). The basin has a size of approximately 1.14×10^6 km^2, with an average annual flow of approximately 240 km^3/yr (Wolf and Newton, 2008), The semi-arid climate of the region, the irregular rainfall and the alternating wet and dry periods exert pressure on the limited resource, and create an environment of scarcity. The disputes over the IRB have arisen due to a number of interrelated factors. The major factors are detailed as follows:

3.4.3.1. Heavy reliance on the IRB

The semi-arid nature of the climate means that rainfall is highly variable in the area, making irrigation from the river system the primary means of crop production (Alam, 2002). During British occupation of the region, irrigation was extended along the Sutlej and Indus Rivers, the Sutlej being a major source of inflows into the Indus (Alam, 2002; Wolf and Newton, 2008). These works involved extensive construction of irrigation canals and supporting infrastructure (Alam, 2002), and as results, Pakistan developed a high dependence of the river system for its food production.

The basin was partitioned into separate countries – namely India and Pakistan – by the British in 1947, under the Indian Independence Act of August 15, 1947 (Wolf and Newton, 2008). This partitioning was primarily based on a religious difference, and little structure was put in place to account for management arrangements of the river system following the split (Alam, 2002; Wolf and Newton, 2008).

Partitioning led to a number of disputes and disagreements between the two countries, heightening political tensions (Wolf and Newton, 2008). Among the disputes, was the conflict over territory, in particular over the ownership of Kashmir (Alam, 2002). Escalating violence also created a refugee problem in the area, which disrupted food production, making the issue of water resources even more crucial (Alam, 2002).

There was also the issue of religious differences between the nations, which is a separate issue altogether.

Irrigation and municipal water in Pakistan are wholly dependent on the Indus River. However, the Sutlej River is located in India, along with the infrastructure for flow control (Alam, 2002). This situation learns Pakistan with a diminished sense of control over their critical resources, and as such increase anxiety in the country with respect to these resources.

3.4.3.2. Pre-existing conflict over the Indus water resources

Conflict existed over irrigation and ownership of the river's resources prior to the partitioning of the region into separate countries. However, such conflicts could be dealt with by existing structures implemented by British India (Wolf and Newton, 2008). This situation began to change when the Government of India Act of 1935 was introduced, which placed ownership of the water resources under the rule of the provinces (Wolf and Newton, 2008). Conflict was then enhanced between upstream and downstream users, particularly between the upstream Punjab and downstream Sindh provinces, which possessed the most extensive irrigation works of the region (Wolf and Newton, 2008). Conflict was further deepened upon partitioning of the countries, which turned the disputes into international conflict (Alam, 2002). This partitioning also split the province of Punjab into east and west entities, where East Punjab held the flow-controlling infrastructure on which the canals downstream were dependent (Alam, 2002). Note also that conflict was maintained between the Punjab and Sindhu provinces following partitioning of the countries, creating internal as well as international conflict in Pakistan (Alam, 2002).

The poverty of the region made it extremely difficult for Pakistan to construct the necessary infrastructure to compensate for reducing of the Sutlej River inflows from the Indus River (Alam, 2002). Infrastructure projects including additional storage capacity and additional canals were seen by Pakistan as an absolute necessity if access to the upstream flows was removed.

It is clear from the factors described above Section 4.2.1 and 4.2.2, that conflict between the countries was a result of a combination of factors. Firstly, the upstream-downstream relationship of the countries, with the major riparian country located downstream, exacerbated the nature of the tensions between Pakistan and India. Domestic water conflict existing between neighbouring provinces in Pakistan was as much an issue as the conflict occurring between the countries, and may have raised political tensions generally. Poverty was also a major factor in driving conflict, with Pakistan in particular unable to deliver funds for improving its own water infrastructure. It might also be inferred that over-development of irrigation in the basin had occurred, which in turn resulted in a major water scarcity issue in the basin. Also, conflict between the countries was present over more than simply water resources following the partitioning of the countries, with other issues such as territorial ownership creating political violence. Having said that, there is no doubt that debate over division of the water resources was a major cause of the conflict.

3.5. How conflict can be resolved

As identified in the previous sections above, social conflict in developing countries typically raised pursuant to second-order conflicts resulting from poor water resource management techniques. Irrigation is a particularly important aspect of food production in many developing countries, such as Bangladesh, Pakistan, India, China, Tanzania and Indonesia (Easter, 2000), and, as such, is one of the main sources of second-order scarcity that creates conflict in these countries. Thus, water resources management techniques that improve the efficiency of water use for irrigation are most important in reducing conflict in developing countries.

3.5.1. Understanding the human element

History has shown that the critical value of water is often as a powerful incentive to develop mutually agreeable solutions to the use of the resource (Cosgrove, 2003). This suggests that cooperation and communication are key components of any solution to resolve water disputes, as they are key components in the resolution of any

dispute. However, to enable cooperation and communication to occur an understanding of the reasons for the conflict is needed.

Rummel (1979) suggests that conflicts can occur due to:

i. opposing interests and capabilities;

ii. contact and salience (awareness);

iii. significant changes in the balance of power;

iv. a disrupted structure of expectations;

v. individual perceptions and expectations;

Rummel (1979) also suggests that conflict can be triggered by surprise or a perception of opportunity, threat or injustice. The first step in the resolution of disputes, including those over water is to understand the ethical and cultural values of those involved in the dispute (Cosgrove, 2003). This will then enable the reasons for the conflict to be understood and solutions to be developed to address the concerns of each party.

The UNESCO under its Potential Conflict to Co-operation Potential (PCCP) programme has developed resources to encourage conflict prevention and resolution regarding water disputes. The PCCP programme is designed to facilitate dialogue to foster peace, cooperation and development related to the management of shared water resources. For example, it runs training courses in participation, consensus building and conflict management specifically targeted at water dispute prevention, and also runs a conflict resolution support system. Much of this information is targeted at enabling individuals by providing them with the skills necessary to assess potential and existing disputes over water independently and impartially to enable an equitable, effective solution to be developed.

This type of consultative approach was used in the mid 1950s to help resolve conflict in the Jordan River Basin. Water use in the area was seen to be a trigger point to escalate tensions between the new state of Israel and the Arab League. The United States was concerned about the possibilities of hostilities in the area and dispatched Ambassador Johnstone as a presidential envoy to diffuse the situation and put forward

a plan to manage the water resources in the area. The final plan that Johnstone negotiated with Israel and the Arab League was known as the "Unified Plan for the Development of the Jordan Valley" (Haddadin and Shamir, 2003) and included areas such as water allocation, storage and supervision.

3.5.2. Development a framework

To enable cooperation and consultation to occur a framework needs to exist to outline the principles and process that should be used by those involved in the dispute (or potential dispute). The Dublin Principles and World Bank approach are two examples of attempts to develop frameworks to guide the prevention and resolution of disputes relating to watering.

3.5.2.1. The Dublin Principles

The key outcome of the International Conference on Water and the Environment in Dunlin, Ireland, 1992 was 4 key principles that the attendees at the conference, which included government designated experts from more than 100 countries and representatives from over 80 international, inter-governmental and non-government organizations, agreed to should be used to develop programs for water and sustainable development (Cosgrove, 2003). The 4 key principles were:

1. Fresh water is a finite and vulnerable resource, essential to sustain life, development and the environment;
2. Water development and management should be based on a participatory approach, involving users, planners and policy-makers at all levels;
3. Women play a central part in the provision, management and safeguarding of water; and

4. Water has an economic value in all its competing uses and should be recognized as an economic good.

These principles were then used to underpin an Action Agenda from the conference, with one specific action relating to resolving water conflicts, suggesting that a priority should be the development and implementation of integrated management plans supported by all affected governments and backed by international agreements.

3.5.2.2. Integrated water resources management

The modern day paradigm of sustainable water management is Integrated Water Resources Management (IWRM). This philosophy of managing water resources features a shift from the previous paradigm of increasing supply through expansion of physical solutions, such as dams and canals, to managing demand, increasing the efficiency of water usage, and generating sustainable means for water use (Gleick, 2000). In essence, it is about managing second-order scarcity issues rather than dealing with supply-side, first-order scarcity. The trend of IWRM is becoming a framework, based on the Dublin Principles (1992). It seeks to promote the 'coordinated development and management of water, land and related resources, in order to maximize the resultant economic and social welfare in an equitable manner without compromising the sustainability of vital ecosystems' (World Health Organization). Because water underpins society, a holistic approach to its management linking social and economic development with the protection of the environment ensures that all factors that affect water are taken into consideration and managed.

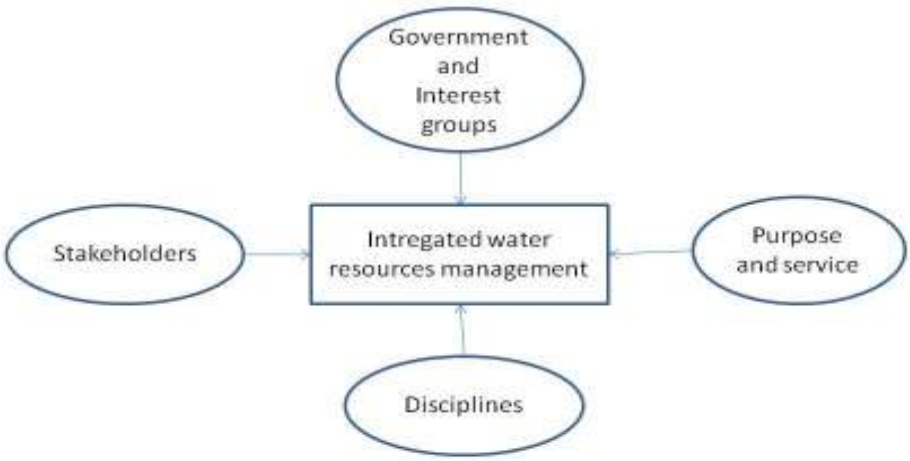

Figure 3. 6: The schematic flow of integrated water resources management

Technological advances and innovations in water management practices are also drivers of IWRM (Gleick, 2000). The IWRM promotes the attainment of sustainable water use and water security, which involves a number of challenges, including (Savenije and Van der Zaag, 2008):

- Ensuring that critical requirements are met, via the provision of safe and reliable water sources, and engaging the entire population for participation in the water management process;
- Improving allocation and efficiency of water usage for food production, thereby improving "food security";
- Protecting ecosystems through sustainable practices;
- Promoting cooperation of stakeholders over managing of shared resources;
- Managing risks from drought, flood, and water quality issues;
- Ensuring an adequate valuation of the water resources such that management of the resources to reflect its true value;
- Promoting fair and equitable governance of the resources, involving all stakeholders in the management process, regardless of gender.

3.5.3. The holistic Approach to IWRM in the MRB

An effective river basin management must consider the impact of water management activities on others within the basin. In turn, this requires consideration of the diverse values associated with water resources.

Historically, water management focused on water quantity and its allocation. Issues such as ecosystem health and water quality were not seen as important issues. These issues are inherently linked to the supporting of societies. Therefore, implementation of water management with multiple objectives is required. A holistic assessment of water resources and related decisions is necessary to account for linkages between:

- Water quality and quantity;
- Land and water resources; and
- Upstream and downstream entities.

The following sections point out the possible solutions for resolving water disputes, with particular reference to conflict in the MRB.

3.5.3.1. Objectives and Targets in the MRB

Traditional approaches to water management have been piecemeal and fragmented because of a lack of coordination among stakeholders, management agencies and political entities sharing a river basin.

In order to achieve an integrated solution to water resources management, all stakeholders must engage in the task of determining appropriate basin-wide solutions. The success of integrated water resource management will depend on strong relationships being developed between all stakeholders. This will be achieved over time, through open and honest communication, knowledge sharing and demonstration of commitment to achieving agreed goals. Furthermore, each country should commit the appropriate resources (including financial resources) to support an integrated development in the basin.

The first essential step towards integrated management of the Mekong Basin must be convincing China and Burma to become members of the Mekong Basin Commission, as active participants in holistic basin management. This will only be achieved if China can be convincing of the benefits of a basin-wide approach, or if appropriate penalties can be applied to China for the impact its actions are causing on the lower reaches of the Mekong River.

The next step is for the members of the Mekong Basin Commission to define basin-wide targets for water quantity and quality throughout the Basin and then develop a joint action plan and strategy to achieve the agreed targets. Resolving the conflicting goals of each individual MRC member is likely to prove a highly difficult task. The parties may agree on certain effects of different actions, but disagree on the desirability of these effects, and therefore, disagree on the desirability of an action itself (Water Encyclopaedia, 2008). Regular meetings among riparian countries of the Mekong should be set up to help strengthen relationships between the countries, and to promote information sharing.

3.5.3.2. Sharing of Information amongst Stakeholders

By sharing information and promoting holistic understanding of Basin-wide water problems, stakeholders will gain an overall appreciation of the issues within the Basin, and the potential impact of their actions on other stakeholders.

Sharing of information should extend to education of the public on issues such as water management, sustainable use, pollution control, the value of bio diversity and ecosystems, etc. This should be achieved through training programs, workshops, seminars and school education. It is noted that the four current member countries of the Mekong River Commission (MRC) have signed a formal agreement to implement procedures for data and information collection, exchange, sharing and management.

The objectives of the undertakings of the procedures are to:

- Implement the data and information exchange among the four MRC member countries;

- Make available, upon request, basic data and information for public access; and
- Promote understanding and cooperation among MRC member countries in a constructive and mutually beneficial manner to ensure the sustainable development of the MRB (Mekong River Commission, 2001).

The Agreement requires the MRC members to cooperate with one another in providing critical data and information to the MRC information system. Typical information (current and historical) that must be provided by the individual countries includes:

- water resources;
- topography;
- natural resources;
- agriculture;
- navigation and transport;
- flood management and mitigation;
- infrastructure;
- urbanisation/industrialisation;
- environment/ecology;
- administrative boundaries;
- Socio-economic data and tourism.

In practices, education and involvement of the public in the planning process, decision making processes and strategy development will also assist in achieving the sustainable use of water resources across the basin.

3.5.3.3. Implementation of Effective Governance

The Institutional mechanisms such as upstream-downstream partnerships and river basin commissions are critical for coordinated water-related research and management, avoiding and mitigating water conflicts and achieving an integrated approach to managing water resources. The broad function of such institutions is

capacity building, facilitating communication among various stakeholders and establishing procedures for managing conflicts.

International treaties and other agreements are also important mechanisms for promoting the IWRM. Water agreements typically address:

- Procedures for water allocation;
- Information exchange;
- Conflict resolution mechanisms;
- Principles of equitable and reasonable use of water resources;
- Obligation not to cause significant harm; and
- Transparency in planned activities and information in general.

Moreover, there is no government with a clear set of rules for managing international rivers, even across the MRB. In order to manage an international river, a regulatory institution that provides all states with a common framework, a clear set of rule, and provisions for the utilisation and conservation of waters, is paramount. Concerning the MRB, there are currently six multilateral frameworks through which various projects in the Mekong Region are planned and carried out (Tsering, 2008). This is the Mekong Committee, the Mekong River Commission, Golden Quadrangles, and the Forum for Comprehensive Development in Indo-China, Mekong Basin Development Programme and the ASEAN-Mekong Basin Development Cooperation. These international frameworks for the Mekong Region are not coordinated, and are driven mostly by economic and political interests rather than environmental ones.

The establishment of the Mekong River Commission has been a significant step forward in overall integrated management of the Mekong Basin. The MRC provides a framework for all development work related to the Mekong River, with an emphasis on the protection of the environment, based on the principles of sovereign equality and reasonable and equitable utilisation of the basin. The agreement includes provisions for resolving possible riparian disputes, and is open to all the riparian states. This framework is considered a reasonable one to manage the Mekong across the boundaries of the participating countries. The major shortcoming of the agreement

is its failure to attract the participation of China and Burma, thus precluding a whole of basin management approach to the Mekong River.

The agreement largely remains ineffective in delivery of the best management outcomes for the Mekong Basin. It is imperative that China and Burma become willing partners in the MRC. At this point in time, there is no incentive for China to join the agreement. There are no apparent environmental or strategic threats of non-cooperation to China. China is the uppermost riparian state, and the most powerful, and stands to achieve lower relative gains by joining the lower riparians.

3.5.4. Expedient approach

Lankford et al. (2007) suggest that the ideals promoted by IWRM have some shortcomings in the case of developing countries, which lack financial resources and capacity required to implement IWRM policy. Even those countries with significant financial resources, including Australia, find difficulty in implementing a full water management policy using the IWRM framework (Lankford et al., 2007). They identify that "Expedient" IWRM should instead be promoted, which involves a more fundamental approach for effectively managing water resources, beginning by analysing the baseline and determining local problems framed against regional and national priorities and being informed by those. The approach taken is four fold but provides an alternative to the widely accepted broad IWRM approach. It is shown in Figure 3.7.

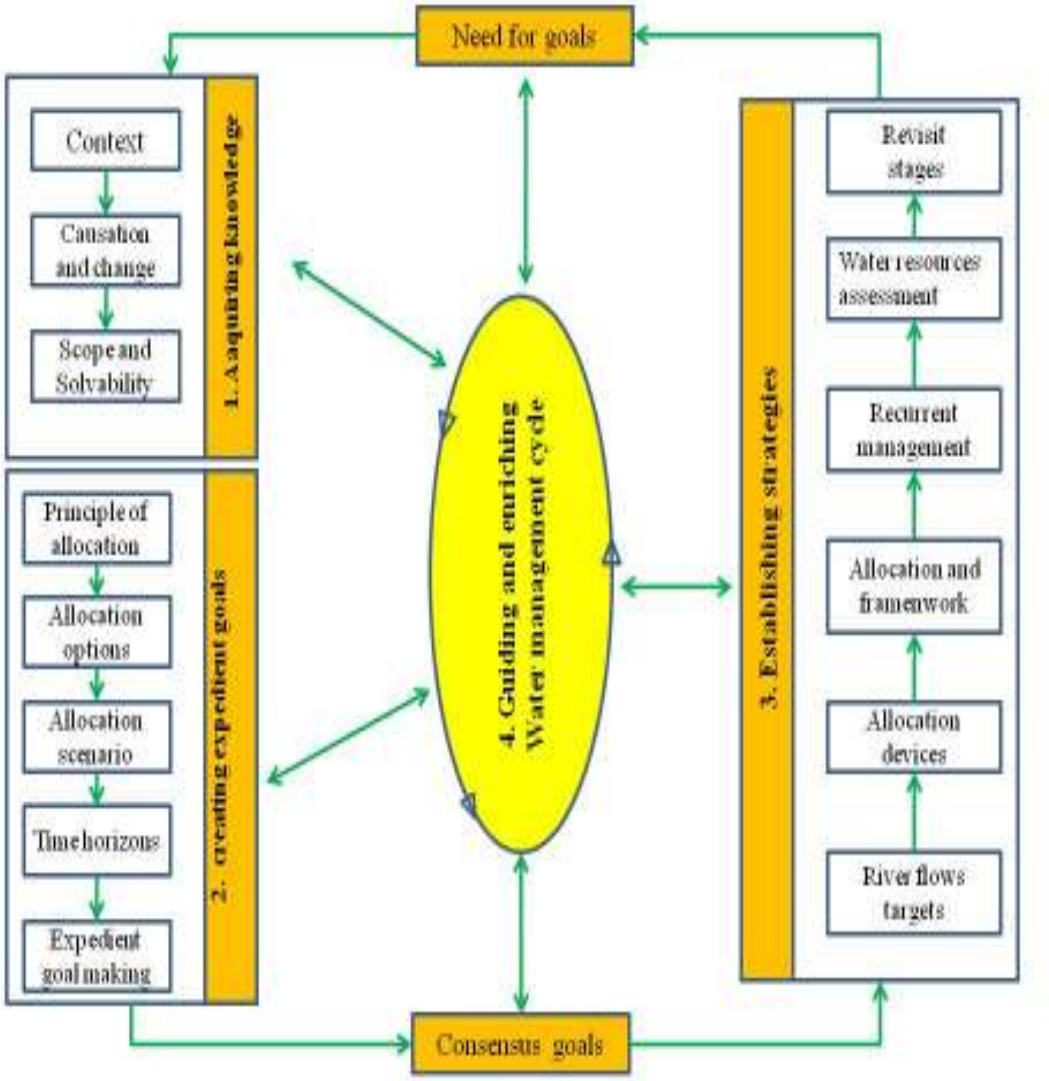

Figure 3. 7: A modified adaptive cycle of expedient water management (sources: Lankford et al, 2007)

Expedient IWRM (shown in Figure 3.7) involves a focus on understanding the unique features of the resource management environment, creating realistic and practical goals for overcoming identified problems with water usage, and adapting policies that will be most effective in achieving these goals, all the while involving the stakeholders in the developments in an iterative approach. The framework that Lankford et al. (2007) promote for expedient IWRM involves the following steps:

1. *Acquiring knowledge* – attaining a specific understanding of the nature of the basin with regard to people and their behaviours, land, water and ecosystems.
2. *Creating goals* – developing specific aims for resource management based on the knowledge-acquiring step.

3. *Establishing strategies* – developing strategies to achieve the goals in a practical sense.
4. *Guiding and enriching the WRM cycle* – "social learning", which involves activities designed to promote the drive for achieving the first three steps.

Essentially, these guidelines help to target water management policy towards solutions that will work in the context of the basin dynamics, rather than relying on policy that may be unsuited to the region.

3.5.4.1. An Example of expedient IWRM

How expedient IWRM guidelines can be beneficial for management of conflict is highlighted in a case study by Thebaud and Batterbury (2001): In eastern Niger, pastoralists on a significant part of the economy. Due to the arid climate, rainfall is irregular, and this has caused the pastorals to develop a nomadic-type management of their herds over the centuries to make best use of the dispersed resources. The nature of this nomadic behaviour makes governance over the pastoral with regard to their water usage a complicated matter under normal guidelines. Traditionally, pastoralists would gain access to water in the dry season by constructing their own wells, which would be negotiated with local residents. However, the state introduced public bores in fixed locations in order to gain more control over the water usage of the pastoralists. Their introduction was implemented "in the absence of any thorough analysis of pastoralists" needs or perceptions" (Thebaud and Batterbury, 2001), and created a number of problems, including:

- The water recharge in the public boreholes was significantly greater than that of the traditional bores, allowing for an increase in the size of herds;
- Regulations set to control access to the bores were soon found to be extremely difficult to enforce, which encouraged free access to the bores, and in turn gave the pastoralists a perception of having fundamental rights to the water;

- The bores eliminated the need for negotiation to be used for access to the water, thereby having a detrimental effect on the community dynamics that were formed through the traditional way of accessing water.
- Over-access of the public bores exacerbated disputes, causing violent conflict.

Thebaud and Batterbury (2001) conclude that the traditional method of water resource allocation, which is settled on a local, rather than the state, level, is the most effective way of reducing conflict, while also providing a method of managing the resource. Thus, by attempting to institutionalise the distribution of water without acquiring a good understanding of the dynamics of the pastoralist's community, conflict was exacerbated, while a sustainable use of the resources in the basin was substantially reduced. By implementing an Expedient IWRM Framework, these factors could be identified, and water resources could be more effectively managed in the Basin.

The case of water management in eastern Nigeria above highlights that water management at the user-level can be more effective than centralising control over water allocations. In fact, experience around the world has shown that decentralised, user-managed systems involving local communities generally outperform central, government-managed systems (Easter, 2000; Madulu, 2003). The reason for this is related to factors such as fee collection enforcement and institutional factors, which present a substantial challenge for one central authority to manage. However, by encouraging participation of users and communities in the management process, measures to control the allocation and management of irrigation licences have the potential to be much simplified, while there is also the benefit of reducing the costs for management of these systems (Easter, 2000). By the same token, it allows demand-side management of the resources by the local communities, who can tailor their service requirements to their needs (Madulu, 2003). For instance, the formation of Water User Associations (WUA) in many Asian countries has been implemented in recent times to decentralise management of the resources (Easter, 2000).

Solutions to social conflicts over water resources cannot be addressed peacefully without some degree of cooperation between the relevant stakeholders. The effect of cooperation on resolving conflict can be seen most clearly in many of the

international conflicts over water resources that have occurred in the past, where agreement over management of the water resources has been reached to some functional degree. An example of cooperation providing effective solutions for water resources management is based in the Senegal River Basin, of which Wolf and Newton (2008) provide case study material: The countries of Guinea, Mali, Mauritania and Senegal all share the basin, with the major economic activities of the region, including cattle, agriculture, and fishing, all dependent on the health of the water resources. Severe drought in the region, experienced from the 1960s to the 1980s, disrupted these economies and caused a degradation of the water resources and ecosystems of the basin. However, rather than conflict erupting over the competition for the dwindling resources, the countries decided that working together, and sharing costs in water resource developments, was the most effective method of achieving an increase in living standards for all. The Organisation for the Development of the Senegal River was formed between Mali, Mauritania and Senegal, and it implemented many reforms, which were designed to promote sustainability in the region, and safeguard and increase in economic development for all the partner countries.

3.5.4.2. World Bank policy adaptation

The Dublin Principles laid the groundwork for an integrated approach to water management and prompted the World Bank to develop its water resources management approach.

In its 2003 Water Resources Strategy Paper, the Bank outlined 7 key messages for its involvement with water resources management, including:

1. water resources management and development are central to sustainable growth and poverty reduction and therefore, of central importance to the World Bank;
2. most developing countries need to be active in both management and development of water resource infrastructure;

The World Bank identified that a key component of their involvement with the management and development of water resources was focussing on water resources

management, not services. The scope of their strategy is shown in Figure 3.8 (World Bank, 2003).

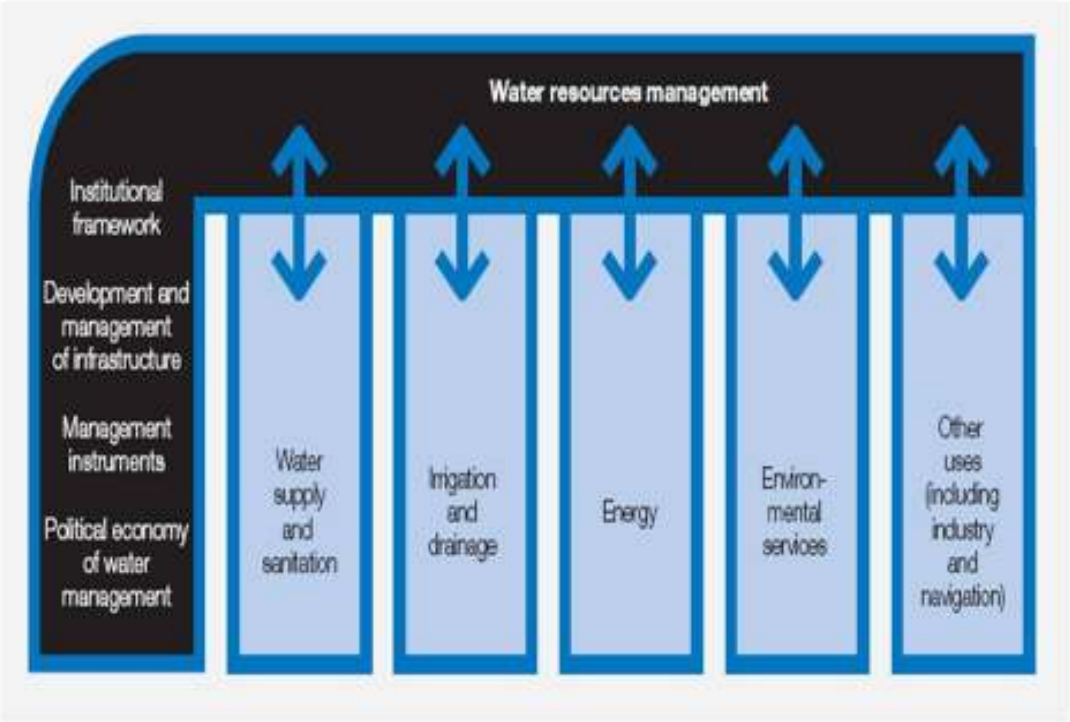

Figure 3. 8: Schematic diagram of the World Bank Water Resource Management (sources: water resources strategy development 2003)

The World Bank's portfolio for Water Resource Management is US $3.1 billion, so they have a significant ability to influence the management of water resources and prevention of disputes. They also do this by developing country water resource assistance strategies detailing specific integrated water resource management approaches for a particular country. The following section describes how World Bank strategies were adopted in the IRB to resolve the dispute over WRM (World Bank, 2003).

3.5.4.3. Adoptive strategies for the IRB

Following a "flash point"" event, a more formal agreement was attempted via cooperation between the two governments. Protestations by the Pakistan government

resulted in the Indian government ordering a resumption of supply to Pakistan shortly after the stoppage of flow. The following agreement that was developed, known as the Delhi Agreement, ensured that Pakistan would not divert water flows until it could develop alternative sources (Wolf and Newton, 2008). Once again, this agreement soon failed, this time due to conflicting interpretations of the agreement between the countries, in particular with Pakistan unhappy with the inference in the agreement that it held fewer rights to the water than upstream India (Alam, 2002).

Given the pre-existing hostilities between the countries, greater success was achieved with the introduction of an independent body, namely the World Bank, to the dispute discussions. The Bank invited both sides to negotiate a treaty over the water resources of the Indus under the following principles (Alam, 2002; Wolf and Newton, 2008):

- The waters of the basin were sufficient for the supplies of both countries;
- Management of the basin was to be considered in an integrated, whole basin perspective, with discussions involving all rivers and tributaries in the system; and
- The talks would focus on management of the system from a technical, rather than political, perspective.

In these talks, each side submitted their own plans for desired allocation of the resources, at the request of the World Bank. When these plans, and the following revised plans, were not close enough to each other to derive an acceptable resolution, the focus of water resource management was changed to one of separation, with each country managing their own resources. This entailed allocating the entire flow of the eastern rivers to India, and the entire western flow to Pakistan (Alam, 2002; Wolf and Newton, 2008).

The following points describe the basic structure of the Indus Basin Treaty (Wolf and Newton, 2008; Alam, 2002):

- Pakistan would receive unimpeded flow of the western river;

- To account for the loss of flow from giving up eastern river flow, Pakistan would be afforded a transition period of 10 years, in which time India would continue to allow flow into Pakistan while construction of infrastructure (i.e. dams, canals, barrages and wells) took place within Pakistan.
- India would contribute a fixed amount to construction of the infrastructure for Pakistan during the transition phase.
- Communication between the countries would be mandatory in relation to any works intended to proceed upstream or downstream of the system, including the provision of all data relating to the works to the other party.
- The Permanent Indus Commission would be established, which would be comprised of one commissioner from each country. The Commission would be responsible for promoting cooperation over the basin between the countries, and facilitate information transfer.
- Conflicts and disputes would be resolved by an independent expert, or failing that, elevated conflicts could eventually be referred to in a Court of Arbitration.

Part of the success of the IRB treaty in encouraging cooperation between India and Pakistan was due to the financial assistance that the treaty raised, allowing Pakistan to compensate for removal of their rights to the eastern river flows (Alam, 2002). This assistance proved vital for overcoming the poverty issue faced by Pakistan in developing new infrastructure. Additionally, the treaty provided the conduit for securing long-term water supplies for each country. Other measures such as war would clearly have been detrimental to this (Alam, 2002). Financial assistance from the World Bank has also changed over time since the inception of the treaty, with a focus shifting from development of new irrigation projects to the improvement of existing projects (Easter, 2000). In other words, the initial aim of the funding was to address first-order scarcity, but this has shifted to address second-order scarcity issues.

One of the main weaknesses of the treaty was that it was developed with division of the water supplies between the countries, rather than setting up a basin-wide management approach, governed by an IWRM framework. Without this type of

management, issues relating to watershed and environmental impacts were not considered and hence environmental and drainage problems have resulted in both India and Pakistan (Easter, 2000). Note, however, that IWRM was the aim of the initial discussions implemented by the World Bank, but disagreements between the countries were too entrenched at the time to make the option workable. This is reflected in the current day scenario of the treaty, which shows that no projects designed for "future cooperation" have been put forward (Wolf and Newton, 2008). Conflicts over other developments such as hydroelectricity and dam projects are also currently unresolved, (Wolf and Newton, 2008).

Another weakness is that, while the treaty addresses how the water resources will be apportioned between the countries (i.e. first-order scarcity issue), it does not directly encourage changes in management practices associated with irrigation. Addressing this weakness may be one of the best ways of improving management of the basin, and thereby reducing conflict. In fact, WUA's have actually been formed in both India and Pakistan in an attempt to decentralise and improve resource management practices (Easter, 2000). In Pakistan however, many of these WUAs have largely become inactive due to:

- their authority being restricted to improving irrigation waterways under government assistance, so that once the improvements were completed, they had little further value (Easter, 2000);
- larger stakeholders in many of the WUA areas being against their formation, due to these stakeholders perceiving them to be potentially detrimental to their own operations (Easter, 2000); and
- local irrigation agency officials perceiving WUAs as being a threat to their own employment (Easter, 2000).

In the absence of attaining direct cooperation between India and Pakistan for the integrated basin-wide management of the Indus River system, conflict could be managed by regenerating the WUAs in the region. This could be done by extending the powers of the WUAs to become the service providers for irrigators, acting as the point for both water delivery and fee collection for usage (Easter, 2000). This method of water management would have the benefit of reducing transaction costs of managing the water delivery and fee collection practices. These costs would otherwise

be unacceptably high at the government level. This system would allow closer monitoring and control over withdrawals for irrigation, thus improving the health of the river system, and most importantly reducing conflict over usage of the basin.

3.5.5. Water legislation

Legislation is another framework, which can be used to prevent and resolve disputes over water resources. At a national level legislation is used to codify the accepted practices and standards of behaviour in that society. International law offers a series of ways to resolve both diplomatic and legal international disputes (Cosgrove, 2003). There are a number of international laws, treaties and bodies in place such as the 1997 UN International Watercourses Convention, and the Convention on the Protection and Use of Transboundary Watercourse and International Lakes.

These conventions include principles like:

- Equitable and reasonable utilization of water;
- Protection of waters by preventing, controlling and reducing pollution; and
- Exchange of information on existing and planned water uses.

International law, in particular the International Court of Justice, was involved in the Gabčikovo–Nagymaros case (also known as the Danube River Case), which involved Hungary and Czechoslovakia. The dispute in this case arose over the implementation of a bilateral treaty (concluding in 1977) with the aim of constructing a series of dams on a stretch of the Danube River crossing Hungary and Czechoslovakia (Cosgrove, 2003). The case was sent to the International Court of Justice after Hungary did not deliver its part of the treaty and Czechoslovakia then diverted 80-90% of the water from the river at the boundary of the two countries (Cosgrove, 2003). The International Court of Justice was asked to resolve the dispute. It found both parties had acted unlawfully and upheld the legal validity of the 1977 treaty. It ruled that the operational regime of the original project be reinstalled and the parties, unless they

agreed otherwise, would have to compensate each other for the harm caused (Cosgrove, 2003).

Since this time, the International Commission for the Protection of the Danube River has been set up to serve as a platform for coordinating the development of the Danube River Basin Management Plan which is to be developed by 2009. Participation in the development of basin management plans is also compulsory for all European Union countries (UNESCO, 2008).

The management of the Columbia River is another example where the development of a permanent legal and administrative framework helps prevent or at least resolve disputes in the management of the water resource. Canada and the United States have a long history in the development and use of institutional mechanisms to resolve disharmony along their border (Muckelston, 2003). Several years of negotiations led to the development of the Boundary Waters Treaty in 1909, which focuses on equality rather than equity and this has remained as the foundation document for the resolution of disputes since this time. This also led to the formation of the International Joint Commission which serves to implement the requirements of the treaty and has judicial, investigative, and administrative and probably powers. Analysis of the management of the Columbia River identifies several key points for consideration (Muckelston, 2003) including:

- A history of good relations is a foundation for agreements to be built for the international management of shared waters;
- The establishment of a permanent comprehensive legal and administrative framework enables states to address water related issues in an organized manner;
- Following the principle of equality rather than equity provides for more certainty and less subjectivity; and
- International water agreements should have flexibility and provision for periodic review to reflect changing values.
-

3.5.6. Public Participation

The involvement of the public in the prevention and resolution of water disputes is a fundamental requirement to ensure that the potential human benefits associate with the dispute resolution, including, for example, stability and security, are achieved (Cosgrove, 2003).

Non government organizations can help in this process by being the catalysts for local initiatives, and facilitators in foreign alliances, by exchanging information by acting, and as mediators among different sectors of the community (Cosgrove, 2003). They can also encourage public participation. An example of this is the World Wildlife Fund, which is working in the Orinoco River Basin which is shared by Venezuela and Columbia. This river currently threatened by plans to re channel it to provide for transport. The World Wildlife Fund is working with the local community to develop alternative methods for increasing transport capacity whilst not affecting the Orinoco River Basin (Cosgrove, 2003). The Cebu Uniting for the Sustainable Water (CUSW) initiative is an example of the local community participating in the management of its water resources and facilitating cooperation. This initiative began in 1994 when community representatives agreed to take action to integrate and broaden the community's involvement and resolve conflicts in watershed management and planning (Cosgrove, 2003).

3.5.7. Education and training

The PCCP programme beneath UNESCO has a significant component of education targeted at all levels from professionals to decision makers. It has developed courses including postgraduate qualifications focused on conflict prevention and cooperation in the management of international water resources. The rationale for this focus is that enhancing the skills of people involved in the area of water resource management will improve the outcomes delivered in this area.

Priscoli (2003) suggests that today's water professionals need both technical excellence and functional relationships with those that they are serving. Technical skills are required to consider all options and alternatives that in the past may not have been identified. Water professionals also require skills in bringing together stakeholders in the decision making process and working with them to identify and deliver the preferred option. This capacity building in the water industry will help to reduce the ineffective management of water resources and therefore, to reduce the likelihood of conflicts over water resources in the future.

3.6. Conclusions

Scarcity of water resources is a primary cause of conflict between stakeholders of the resource. Financial issues are a particular driver of such conflict, contributing to a greater probability of conflict within developing countries. Just as important are institutional and political factors, which create an atmosphere of second-order scarcity. An upstream-downstream relationship of stakeholders is a significant contributing factor for the creation of conflict, and may involve a number of entities, such as agriculturalists, rural or city populations, the government, and the environment.

Conflicts need to be addressed by improving water resources management policy. IWRM is a set of guidelines, which are designed to drive sustainable development of water resources under conditions of scarcity, and may aid in achieving cooperation by setting unifying goals and policy to achieve these goals. Decentralising water resource management to empower users with control over allocation and fee collection is noted as being particularly effective in reducing water scarcity issues, thereby reducing conflict. This requires cooperation between all stakeholders, such that each side can be satisfied with equitable distribution of the resource. This cooperation may be spontaneous, or may require intervention from an independent mediator where conflict is too ingrained to allow beneficial solutions to be developed.

Case studies over conflicts on the MRB, and the IRB is highlighting many of the issues relating to conflicting over water resources in the cases the Danube River, Orinoco River, and MDB. Disputes over property rights of the IRB arose without a predefined structure for its allocation between the riparians; India felt that as upstream riparian, it held the rights to use the river for its own benefit, while Pakistan argued that it's critical dependence on the resource gave it rights to the majority of the flows from the system. This conflict also existed between provinces inside Pakistan over upstream and downstream usage of the river, helping to raise tensions further. Poverty was an inhibiting factor for Pakistan to develop alternative resources for its extensive irrigation sector, forcing conflict to come to a head. Other pre-existing tensions brought to a head due to the partitioning of the states helped to fuel this conflict.

Direct cooperation was attempted at the start of negotiations; however, the political landscape of the region resulted in failure of the agreements developed. An independent mediator – the World Bank – intervened to facilitate resolution of the conflict, and an agreement was reached with a compromise over allocation of the resources. This agreement involved splitting ownership of the river along the border, rather than managing the river basin as a whole entity as was originally intended. Thus, scarcity issues still persist, causing continued conflicts in the region. To better resolve these conflicts, a shift in water resource management to user-based management through Water User Associations (WUAs) was proposed. While this has actually occurred, to a certain extent, due to a change in emphasis from the World Bank, the progress of WUAs in management of the system has stalled in Pakistan due to a lack of authority afforded to them. By re-empowering the WUAs and enabling them to mange distribution of the available resources and fee collection, management costs can be reduced, and hence conflict in the region may also be reduced. Furthermore, this lesson will be incorporate in the GRB and the MDB. The GRB will be analyzed in Chapter 4, and MBD in Chapters 5, 6, 7 and 8.

CHAPTER 4: WATER PARADOX - A CASE STUDY IN THE GRB

4.1. Introduction

The quantity, quality and timing of water flows in Bangladesh are closely linked (Adel, 2001) as shown in Figure 4.5. The quantity issue arising from water sharing is particularly critical. It depends on bilateral agreements among the co-riparian states and therefore water sharing issues often become controversial in water resources management (Haftendorn, 2000). No more is this so than in Bangladesh where water flow control is a crucial factor to maintenance of the water sharing agreements between Bangladesh and India. In Bangladesh, the natural resources are available but the level of water becomes a "*Paradox*" and defined as resources are available but can't be used. Water flows in the Ganges River impact on human activities at local and regional level in Bangladesh. The flow of the Ganges River in Bangladesh is influenced largely by the actions of its neighbouring countries, India and Nepal. The research work presented in this chapter aims to clarify how and why the sharing of water resources becomes a paradox in Bangladesh. This chapter analyses the sharing of water in the GRB in terms of matching supply and demand. A Stackelberg leader-follower game model is applied to determine the optimal share of water diverted by upstream countries with, in this instance, the opportunity of water flow augmentation from Nepal to resolve the water scarcity. In addition, the impacts of water transfer from Nepal to both Bangladesh and India are assessed.

4.2. Background study

4.2.1. History of the Farakka barrage

The conflict over the Ganges water between Bangladesh and India dates back to 1951 when India decided to construct the Farakka barrage in order to divert water from the Ganges to the Hugli river (in India) by a 38-kilometre long feeder canal with a carrying capacity of 1133 cusec (Crow et al, 2000). The main purpose for constructing the Farakka barrage in 1975 was to provide irrigation for agriculture in West Bengal and to re-start and flush the Hugli River to keep the port of Calcutta navigable (Rudra, 2000). The construction of a barrage across the Ganges and diversion of water towards Bhagirathi was first suggested by Sir Arthur Cotton as far back as in 1853 (Rudra, 2000). Many other British Engineers supported this view, though they were not unanimous about the site of the barrage. The construction of the Farakka barrage was started in 1962 and was completed in 1971 (Rudra, 2000). The project about the 38-km long diversion was started on 21st April, 1975, and took fours years. During the construction of this powerful barrage, there was a revolution in the political scenario of this subcontinent. Bangladesh emerged as a sovereign country from erstwhile East Pakistan and this rendered a new dimension to the dispute over the sharing of Ganges water. There was also large scale expansion of irrigation in the upper Ganges Basin since the introduction high yielding techniques in agriculture. Figure 4.1 shows the feeder channel across the Ganges Basin, located in Bangladesh, and Table 4.1 describes the technical details of the Farakka Barrage Project (Rudra, 2000).

Table 4. 1: Technical details of the Farakka barrage

Important features of Farakka Barrage project	
Length of the barrage over Ganges	2.246 Km
Number of Bays	109
Span of Each Bay	18.30m.
Head Regulator Full Supply Level at Land	1133 cumec.
Feeder Canal Length	38.30 km
Feeder Canal Design Discharge	1133 cumec.

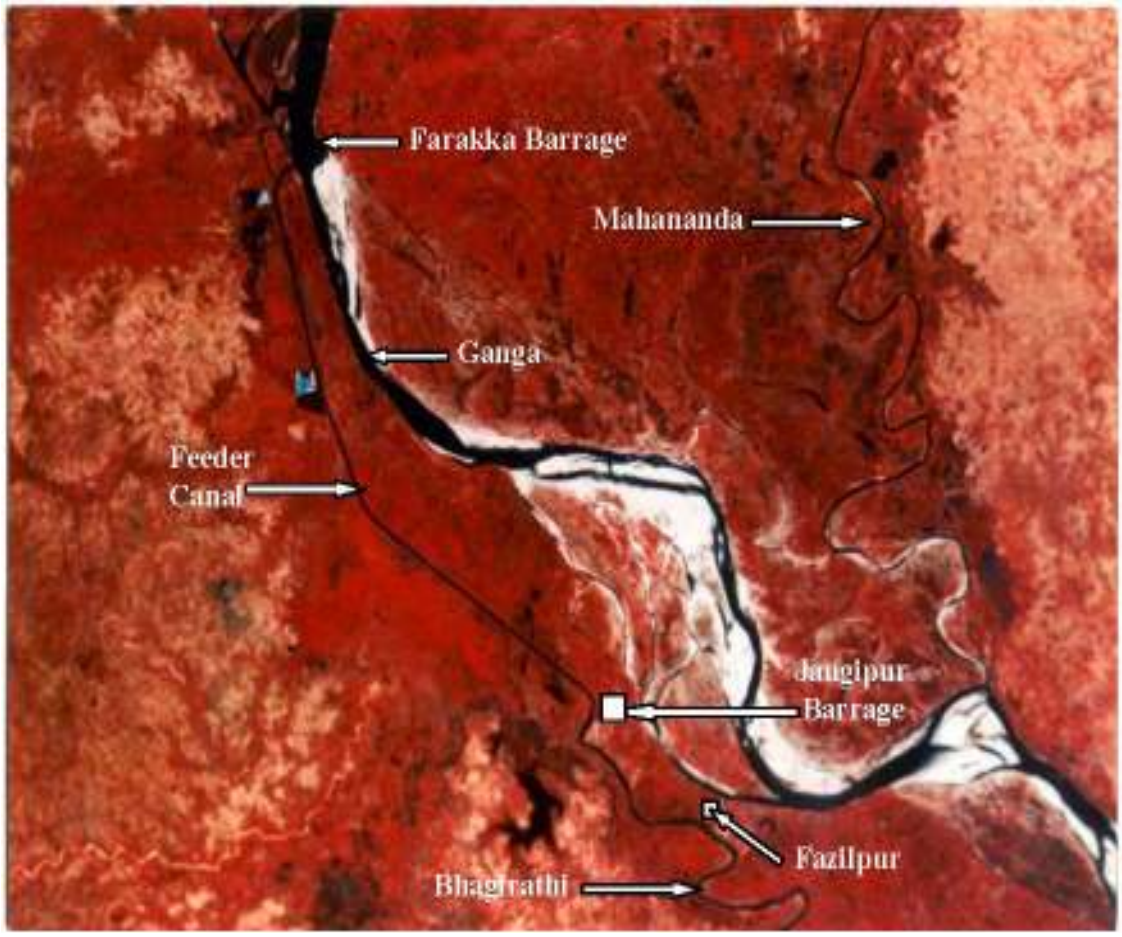

Figure 4. 1: Location of the Farakka Barrage Project.

In 1975 India completed the Farakka Barrage about 11 miles from the borders of Bangladesh to divert 40,000 cumsec of the Ganges water into the Bhagirathi - Hoogly River with the ostensible purpose of flushing the accumulated silts from the bed of the

river and thereby improving the navigability at the Calcutta Port. The unilateral withdrawal of the Ganges water during the low flow months has caused both long-term and short-term effects in Bangladesh.

4.2.2. Water resources management issues for the Ganges Basin

Bangladesh is located at the tail end of the Ganges Basin. After crossing over Bangladesh the Ganges River flows into the Bay of Bengal. The dry season (November-May) in the Bangladesh part of the Basin adequate water supply from the upstream stretch of the river is essential for agriculture, forestry, industry, fisheries, drinking water supplies, navigation, and retarding saline water intrusion from the Bay of Bengal (Mirza,1998). The river flow started declining when India commissioned the barrage in 1975 at Farakka, 18 kms from the western border of Bangladesh (Fig 3.2) in order to divert water (40,000 cumsec) into the Bhagirathi to flush the port of Calcutta, located about 160 kms downstream of the Bhagirathi from the barrage (Adel, 2002). Such diversion has caused several negative impacts on the society, the economy and the environment of Bangladesh directly and indirectly, these are discussed below.

4.2.2.1. Depletion of surface water and hampered ecology

The flow obstruction at Farakka causes water paucity, drying out of the Ganges and its tributaries as shown in Figure 4.2. The river can no longer feed thousands of ponds, ditches and more than 900 km^2 of flood plains (Adel, 2001). For example, the Baral, one of the main distributors of the Ganges, used to discharge, on average, 2000m^3/s for 5 months (July-November) annually, whereas now it can hardly discharge one-fourth of that amount (Adel, 2001). Moreover, weak flushing of the Ganges and consequently, in the Baral, helped to form a shoal over the year (Adel, 2001). The surface water resources had been the breeding and rising grounds of 109 species of Gangetic fishes and people used to fish to supplement their income and dietary intakes for about 10 months (July-April) (Adel, 2001). Some of these species have vanished fronts the Basin (Adel, 2001). In addition to that, all the aquatics and

the amphibian's species that lived in a stretch of about $20000 \times 12 \times 12\ m$ of the watercourse during July through November and in about $20000 \times 100 \times 10\ m$ during November to June, along with sportive Gangetic dolphins, are now extinct (Adel, 2001).

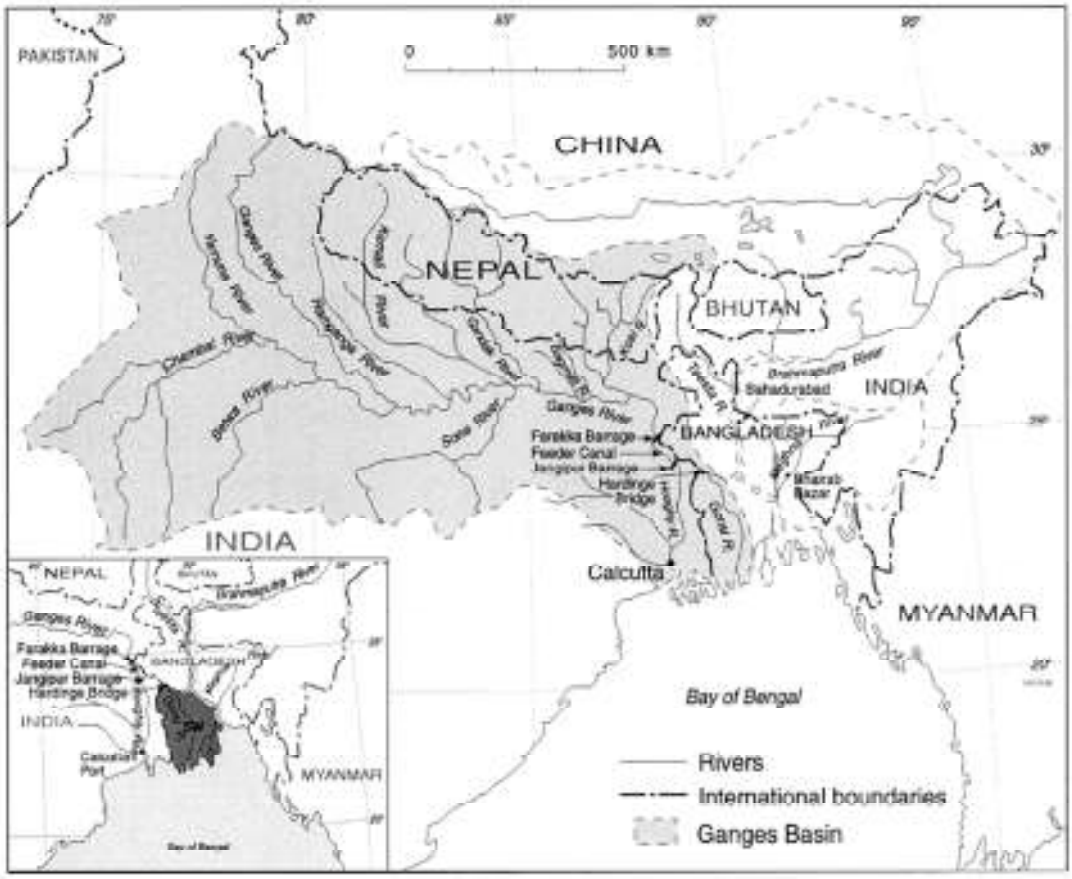

Figure 4. 2: The GRB and Farakka Barrage project. Area (shaded) dependent on the flow of the Ganges River is shown in the inset (Sources, Mirza, 1998)

4.2.2.2. Salinity problems

Substantial changes in Ganges River flow impacts on the Gorai River and the south-west region of Bangladesh. In the dry season, reduced flow in the Gorai River exacerbated the salinity problem in this area, which adversely affected agriculture, forestry, industrial production and drinking water (Mirza, 1998). To provide a clear view of salinity impacts, pre and post-Farakka average monthly salinity at four stations in south-west Bangladesh is shown in the Table 4.2.

Table 4. 2: Pre and post-Farakka average monthly salinity in south-west Bangladesh

Station name	January		February		March		April		May	
	0	1	0	1	0	1	0	1	0	1
Khulna	293	1,254	371	3,396	467	8,305	1,626	12,149	1,508	11,208
Goal Para power Station	340	515	397	1,303	750	4,422	1,320	7,422	786	5,456
Chalna	2,600	6,280	2,625	11,510	8,950	17,310	8,675	21,927	12,000	19,009
Mongla	2,300	5,200	3,900	7,880	7,500	11,075	11,800	17,150	13,500	17,100

Salinity expresses in micro-mhos/cm (m-mhos/cm) and measured at 25°c, 0 = Pre Farakka, 1 = post Farakka (Sources: Mirza, 1998)

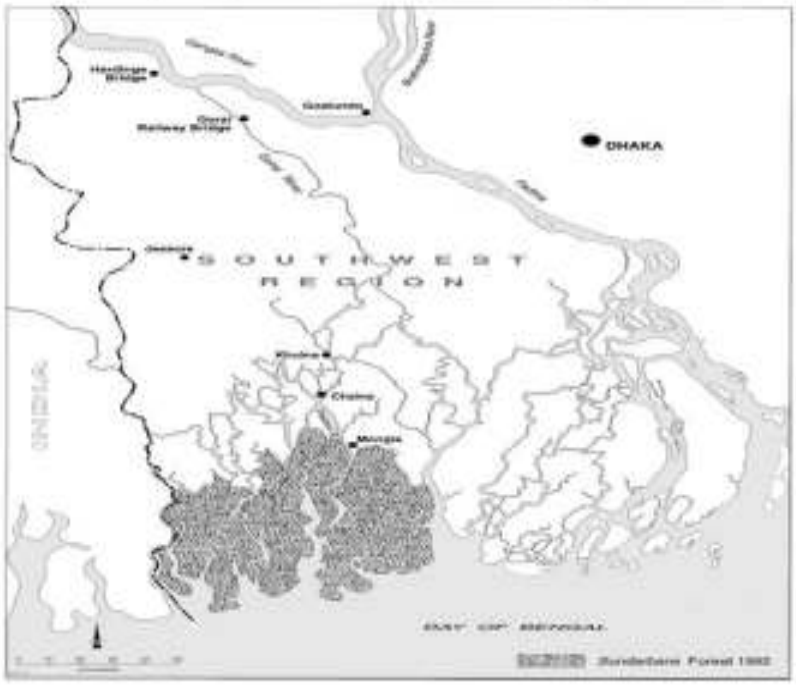

Figure 4. 3: the south-west region of Bangladesh. Areas dark shaded are those affected by salinity problems (Mirza, 1998).

4.2.2.3. Agriculture

Agriculture is the core of the economy of Bangladesh. Its contribution to GDP was 30% in 1998 (Rahman 1998). As a consequence of the water diversion, are summarised shown in Figure 4.4. Agricultural production losses are due to soil moisture depletion, delayed planting and increased salinity. Among many other crops, all rice paddy varieties are very sensitive to increased salinity (Mirza, 1998) and rice is the staple food of Bangladesh. Saline tolerance starts dropping when electrical

conductivity (EC) exceeds 2000 µmho/cm; at 6000 µmho/cm, plant growth expressed in terms of weight declines to below 50% and at 16,000 µmho/cm yields it becomes zero (Mirza, 1998). Agricultural loss was estimated as 647,000 tons in 1976 whereof 21% were due to increased salinity (Hannan 1980 cited in Mirza 1998). Even Bangladesh claimed an annual loss of US$675 million in the agriculture sector as a consequence of the Farakka Barrage (Xinhua 1993 cited in Mirza 1998).

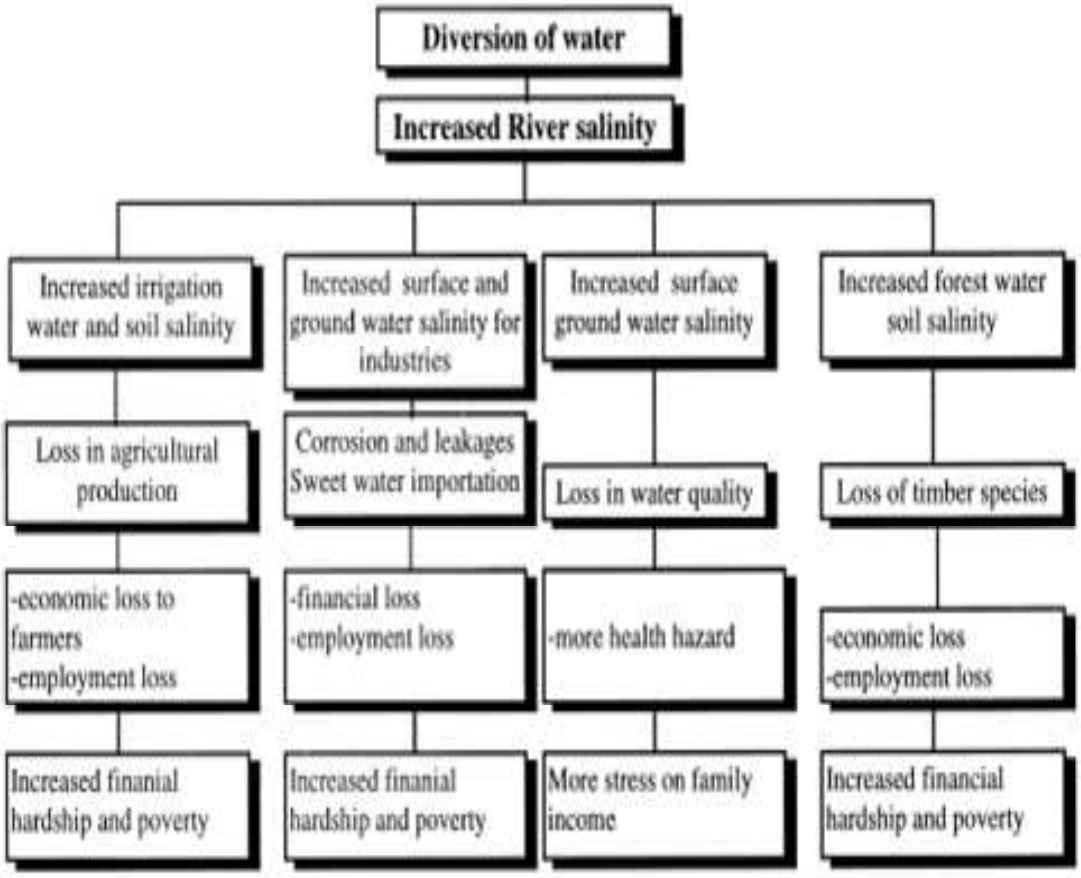

Figure 4. 4: Increased river salinity and its possible effects (Sources: Mirza, 1998)

4.2.2.4. Forestry

The biggest mangrove forest of the world, "The Sundorbans" is located in the south-west portion of Bangladesh. In this forest there is an extensive network of tidal rivers and streams, along with small, local drainage channels (Mirza, 1998). The main mangrove species in The Sundarbans are: Sundoari (*Heriteria fomes*), Gewa (*Excoecaria agallocha*), Keora (*Sonneratia apetala*), and Goran (*Ceriops decandra*)

which requires fresh as well as saline water for their regeneration and growth (Mirza, 1998). After diversion by the Farakka barrage, reduction in fresh water through the Ganges River had the consequences of depletion of soil moisture and increased in salinity. The adverse effect of increased salinity on the ecosystem of this forest can be observed by the dying tops of Sundori trees, retrogression of forest types, slowing of forest growth and reduced productivity of forest sites (Mirza, 1998). The loss of Sundori trees was 1.43 million cubic meters in 1976-1982 (Mirza, 1998). Moreover, a conservative estimate showed a $320 million financial impact from timber loss due to the Farakka effect (Swain 1996 cited in Mirza, 1998).

4.2.2.5. Industry

Khulna is the second largest industrial city in Bangladesh. It is home to a newsprint mill, a 60-mW thermal power plant and a number of jute mills (Mirza, 1998). Even these industries suffered from the salinity problem of post-Farakka period. For instance, Khulna newspaper mill which used to require 300 ton of fresh water daily for its operation had to use saline water for cooling purposes and this resulted in leakage of condensers and a hampering of production (Mirza, 1998). Use of saline water caused disruption of the power generation system in the Goal para power plant. The Paksi paper mill was forced to close in 1993. In the period of 1976-1993, the total financial loss estimated in the industrial sector was US$37 million (Mirza, 1998).

4.2.2.6. Deterioration of water quality

Bangladesh is largely dependent on groundwater for drinking and irrigation uses, and 90% of drinking water is abstracted from aquifers (Rahman, 2000). Hence any natural or man-made contamination to this natural resource will bring a serious disaster to the overall socio-economic environment of Bangladesh. The salinity problem in southwest Bangladesh and the recently identified arsenic problem in groundwater almost over all of Bangladesh have been a matter of deep concern. Depleting groundwater let air get in the ground and Arsenopyrites buried in a deep

layer of sediment formed water-soluble compounds of arsenic which infiltrated into water (Adel, 2001). Iron can purify water of arsenic in the presence of oxygen, but this natural purification of groundwater has not been occurred because of inadequate recharging of water after the water diversion (Adel, 2001). In the case of surface water, patches of stagnant water in rivers, ponds and floodplains contain large amount of suspended materials and algae (2.00-5.00 g/l) for the most of the time (Adel, 2001). Moreover, during the dry period fluctuation of both the groundwater and surface water head influences the groundwater quality in terms of the concentration level of different chemical constituents (Rahman, 2000). Additionally, the salinity of both surface and ground water in the south-western region of Bangladesh exceeds the threshold value of 960 µmho/cm is for potable use (Mirza, 1998). People, who have to municipal water supply, are exposed to and affected by various diarrhoeal diseases (Mirza, 1998). Flourishes grow in water of low salinity and high temperature in the presence of high concentration of organic nutrients in the inland coastal areas in Bangladesh (Colwell 1996 in cited Mirza 1998). The seawater tends to invade upstream fresh water along the bottom of the river in the tidal estuary when the discharge level in the river is low (Rahman, 2000). In order to back seawater out of the estuary or halt its forward at a given point in the estuary there should be a fresh water flow coming down from upstream movement. Minimum flows in the Gorai and Ganges Rivers during the dry period necessary to limit the salinity level are presented in the Table 4.3.

Table 4. 3: Mean monthly discharge requirements for Gorai and Ganges rivers to limit maximum salinity at 750 and 2,000 µmho/cm at Khulna (Mirza, 1998).

	Required discharge (m^3/sec)				
	Gorai River			Ganges River	
Month	Present discharge (m^3/sec)	750 µmho/cm	2,000 µmho/cm	750 µmho/cm	2,000 µmho/cm
February	64	187	78	2,015	1,466
March	46	201	125	1,961	1,573
April	52	240	158	1,844	1,586

4.2.2.7. Increased occurrence of the worst floods and droughts

Bangladesh is prone to flooding due to its geological location at the confluences of the Ganges, Brahmaputra and Meghna (GMB) rivers (Mirza, 1998). About 92.5 percent of the combined Basin area of the three rivers lies outside of the country (Mirza, 1998). Moreover, during the post-Farakka period, floods have been aggravated; floods hit unprecedentedly over almost all the country from time to time (Adel, 2001). Barrages are used as the outlet for flood water when the upstream country cannot withhold the rising flood water. This causes irreparable damages to human life and habitation, crops, livestock. In other words, it further paralyses the weak economy of a developing country, Bangladesh. No warning of potential floods from the neighbouring country leaves Bangladesh to face the flood without preparation (Adel, 2001). On the other hand, an extreme scarcity of water is observed in the dry season. When drought comes at the flowering stage of paddy, it causes the total loss of production. Bangladesh, where most of the people earn their livelihood by agriculture, falls into miserable trouble. Simultaneously, the price of the agricultural production goes up as there is a shortfall in the market. Thus it affects the total economy of the country.

4.2.2.8. Climate change

Climate data pertaining to the GRB in Bangladesh were analysed by (Adel, 2002) to find any climate changes effects relating to the upstream water diversion by the Farakka barrage. The followings are the outcomes during the post-baseline era:

1. Heater degree days and cooler degree days were respectively 1.33 and 1.44 times more frequent than the pre-baseline era.
2. The summertime and wintertime average temperatures were respectively 1°C more and 0.5°C less than the corresponding quantities during the pre-baseline era.
3. The mode 32°C of summertime maximum temperatures was 1°C higher and occurred 414 times more, and the mode 25°C of wintertime temperature was 1°C less and occurred 17 times less than the corresponding values during the pre-baseline era.

4. The average value of maximum relative humidity has increased by more than 2% and that of minimum relative humidity has been dropped by the same amount.
5. The mode 95% and 70% of maximum and minimum relative humidity values have occurred 1322 times and 84 times more respectively than their pre-baseline counterparts.
6. The frequency of 100 mm or more rainfall and the monthly average rainfalls have been declined by about 50% and 30% respectively.

The researcher concluded that these climate change effects are the result of changing the land-cover and land-use upstream water diversion.

4.2.2.9. Environmental destruction and migration to India

The water diversion at Farakka introduced a new ecological system against the usual course of nature. Such man made changes cause severe morphological imbalances in downstream zone, i.e., silting up the river beds, and shifting of channels and consequent the bank line movement. For instance, the Ganges-dependent Basin area is severely affected by river bank erosion, i.e., Kakchira, and Dhulia; the two small townships of the Patuakhali district are on the verge of extinction (Swain, 1996). Moreover, increased numbers of floods, salinity problems, and the river bank erosion have brought misery and hardship to the people of the Ganges-dependent south-western part of Bangladesh. As a result, poor Bangladeshis from the Farakka-affected area have been compelled to migrate into India by crossing the porous border losing their last hope of being absorbed into the urban economy of Bangladesh (Swain, 1996). From a survey, it is revealed that 74% of the migrants directly blamed the Farakka barrage for causing this situation (Swain, 1996). Whenever migrants settle they flood the labour market and exert demand for food and other necessities of life, putting new burdens on the receiving society. On the other hand, scarcities generate strong feelings of nativism among the original inhabitants of the society by claiming more rights upon land, employment, political power and cultural hegemony than the migrants. Hence a chance of conflict between natives and migrants poses insecurity. Some political parties treated the migrant as a “vote bank”. They tended come under the shadow of a political party to save themselves, whereas others opposed them.

Thus the migration became a political issue. For example, in 1983 the political violence between native Assamese and migrant Bangladeshis cost more than 3,000 lives (Swain, 1996). Moreover, most of the migrants were Muslims as Bangladesh is a Muslim populated country whereas India is predominately a Hindu land. These migrants from Bangladesh have spread to different parts of India. The ever-expanding urban centres of Bombay and Delhi have become the major destinations for the fleeing migrants (Swain, 1996). The communal riots in early 1993 in Bombay caused a mass killing of these migrants by fanatical Hindus (Swain, 1996). The increasing violence and growing threats made the Indian government in 1992 to forcibly deport Bangladeshi Muslims back to their country and a refusal to accept them by Bangladesh government caused them to push back (Swain, 1996). Thus disputes over migration between these two countries have become a bilateral agenda similar importance to Farakka itself.

4.2.3. Launched water conflict: past and present

When there was no barrage on the Ganges Basin at Farakka in India, no question arose about the sharing the water. At that time water flowed naturally through the Ganges and its distributor. After the construction of the Farakka Barrage in India, crucial questions arose as to who control the led the gate of the barrage, and for what purposes and how water would be used, and how water would be shared between Pakistan and India (after the1971 independence of Bangladesh, shared between Bangladesh and India). How could the UN convention principles be met? The Farakka Barrage has become regarded as a man-made disaster for Bangladesh. Relevant instance of water tension has arisen between the co riparian states as a result of dam construction are in Table 4.3.

Table 4. 4: Nature of dam on Ganges Basin into the Indo-Nepal and Indo-Bangladesh Border.

Name	River/ tributary	Location	Nature	Remarks
Terhi dam	Bhagirathi	Uttar Pradesh (India)	Unilateral	Nearly in Completion[1]
Tanakpur Barrage	Mahakali or Sarada	Uttar Pradesh (India)	Unilateral	Adoptedin 1996 Mahakali treaty between Nepal and India
Sarada Barrage	Mahakali or Sarada	Uttar Pradesh (India)	Bilateral	Indo-Nepal Agreement 1920
Girijapur Barrage	Ghagra	Uttar Pradesh (India)	Unilateral	Indo-Nepal water tension
Saryu Barrage	Saryu or Babai	Uttar Pradesh (India)	Unilateral	Indo-Nepal Water tension
Laxampur Barrage	Rapti	Uttar Pradesh (India)	Unilateral	Indo-Nepal Water tension
Banganga Barrage	Banganga	Uttar Pradesh (India)	Unilateral	Indo-Nepal Water tension
Gandak Barrage	Gandak	Baisaltan (Nepal-India border)	Bilateral	Indo-Nepal Agreement (1959) (Major source of Indo-Nepal water conflict)
Bagmati Barrage	Bagmati	Nepal	Unilateral	In response to the unilateral construction of Tanakpur and Girijapur barrages by India
Kosi Barrage	Kosi	Bhimnagar, (Nepal)	Bilateral	Indo-Nepal Agreement (1954) (Major source of Indo-Nepal water conflict).
Farakka Barrage	Ganges	(West Bengal) India	Unilateral	Major source of water tension between Bangladesh and India.

[1] Main purpose is drinking water supply to Delhi, 162 Million gallons/day, 3.6 BCM water storage and 2400 MW energy (Pun 2004: 17).

India had to decide to construct a barrage across the Ganges at Farakka in 1951 and then negotiated the sharing of Ganges water at Farakka in 1960 at the time of signing the "Indus Water Treaty" between India and Pakistan (Abbas, 1992). India rejected a later proposal to augment the flow of the Ganges River and violated UN convention principle box 1 (ICWE, 1992). It also violated the norms of any construction for diversion of water on any river. This was the root of the paradox of water sharing between India and Bangladesh.

4.3. The GRB study

The water crisis in Yellow River in China, shortage of water in the Murray-Darling Basin in Australia, water sharing and sedimentation of Ganges-Brahmaputra Basin in South-Asia, salinity of the Aral Sea Basin in Tajikistan, conflict with water sharing of the Mekong river in South-east-Asia, water conflict and crisis in Palestine, and Mercury pollution of the Amazon river in Brazil are some prominent examples of

water related problem in the world. However, it is reasonable to take a case and study the problems in the light of social equity, rationality and justice and thereby to demonstrate some solution that may work for the specific problem. Therefore, the GRB has been chosen to discuss the burning issue in the context of Bangladesh.

4.3.1. Origin of the River flow in Bangladesh

Bangladesh is a very low-lying country situated in the delta of three large rivers, the Ganges, Brahmaputra and Meghna (GBM). The country has a complex network of 230 rivers, including 57 cross-boundary rivers (BWDB, 2008). The Ganges is one of the most important river systems of Bangladesh. Like many other rivers in the world, the Ganges River ignores political boundaries. It rises in the Gangotri glacier in the Himalaya Mountains at an elevation of 7138 m above mean sea level (BWDB, 2008). From source to sea level, the Ganges is about 2510 kms long with a drainage area of about 980,000 sq. km, and only 34,188 square kilometres (3.6%) of this drainage area lies within Bangladesh (BWDB, 2008). The Ganges within the plan of Bangladesh is primarily a meandering river system (Singh et al. 2004 and Islam et al. 1999). About 96% of the total Basin area of the Ganges is beyond the boundary of Bangladesh and located in China (3%), Nepal (14%) and India (79%) (Mirza,1997). Therefore, Bangladesh acts as a drainage outlet for the cross-border runoff (Mirza, 1997). The Ganges Basin is characterized by some unique ecological and socio-political diversities and complexities; accordingly, proper utilization of water resources is dependent upon a number of typical advantages as well as difficulties. Consequently, in Bangladesh, the supply of the fresh water is very poor and still the majority of the population are beyond access of the drinking water. The context of Bangladesh water bodies' contradiction is shown in Figure 4.5 which is closely link quantity, quality and timing issues.

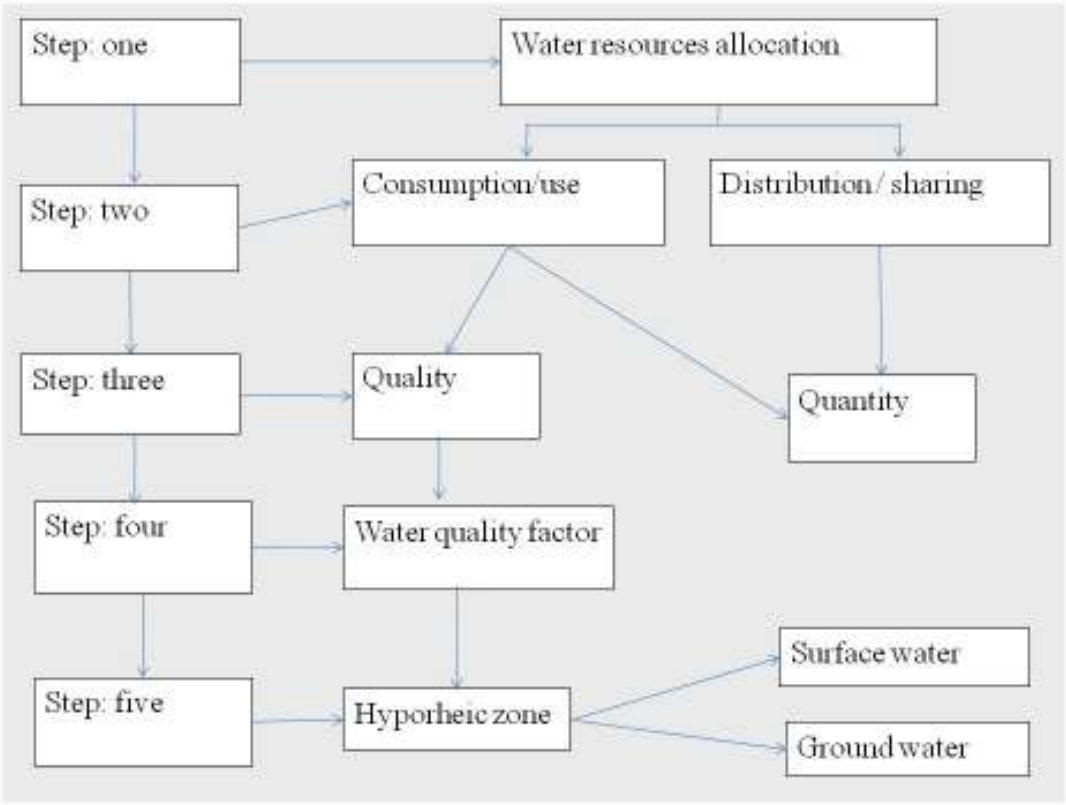

Figure 4. 5: Simple water flow chart in Bangladesh

4.3.2. Overview of the water sharing issue

From 1952 to 1971 the Pakistani government deliberately neglected to solve the water sharing issue at the Farakka Barrage as they were keen on resolving a dispute over the Indus River (Hossain, 1998). In spite of this, there were ten meetings regarding the Farakka Barrage issue between India and Pakistan and the significant outcome was that India agreed to a reorganisation of the Ganges as an international river and accepted the principle of sharing its water (Hossain, 1998). Bangladesh emerged as a country independent from Pakistan in 1971. After that Bangladesh proposed to build storage facilities in the GRB to augment the flow during the dry season (Haftendorn, 2000). As this would involve Nepal, India rejected the plan because of it not being a bilateral issue (Khan, 1996). On the other hand, India's proposal of diverting water from the Brahmaputra River to the Ganges River by a link canal was opposed by Bangladesh (Haftendorn, 2000) because of diversion of water from the Brahmaputra River during the dry period would cause adverse effects on its downstream reaches. In

addition, the excavation of a link canal through Bangladesh would cause other problems (Khan, 1996).

In 1974, the Indo-Bangladesh Joint River Commission estimated that during the dry season the average minimum discharge below the Farakka Barrage was 55,000 cusec (Adel, 2001). Of this, India claimed 40,000 cusec to flush the Hooghly River leaving the rest for Bangladesh, who on the other hand demanded the entire 55,000 m^3/s for the dry season. Hence a deadlock prevailed between these two countries (Hossain, 1998). Bangladesh's Prime Minister Sheikh Mujibur Rahman intervened to break the deadlock by proposing an "interim agreement" which allowed India to commission at the Farakka barrage. The agreement was signed on 18 April 1975 (Hossain, 1998). After the agreement expiry on only 31 May 1975, India unilaterally continued the withdrawal of water at Farakka, adversely affecting a vast area of Bangladesh. Consequently, Bangladesh raised the issue at the thirty-first session of the United Nations General Assembly, in September 1976 (Khan, 1996). But attempts to internationalize the issue failed and a bilateral solution with India had to be sought. This attempt reportedly angered the Indian Prime Minister Indira Gandhi, who took a hard line by arguing that Bangladesh was not adversely affected by the Farakka Barrage (Hossain, 1998). With the defeat of Indira Ghandi's Congress Party in the Indian Parliamentary election in March 1977, the Janata Party government under Morarji Desai came up with a solution to this problem in the form of the 1977 treaty for five years (Rahman, 2006). This treaty contained a guarantee clause under which Bangladesh was promised 80 percent of the water available during the dry period (Rahman, 2006). Each side received some satisfaction from the water treaty. However, it was criticised strongly in India, with the Central Indian Government being accused of sacrificing the interests of the state of West Bengal which uses this water to keep part of the Calcutta port navigable (Hossain, 1998).

As the expiry date of the 1977 treaty was looming Bangladesh urgently needed to find another agreement for the water sharing of GRB? Then two MOUs were signed on 7 October 1982 and 18 October 1985 for the next two dry seasons and three years respectively following the terms of the original 1977 agreement. After expiration of the second MOU there was no further agreement until 12 December 1996 (Rahman, 2006). On this date a thirty year accord was signed by the subsequent Bangladeshi

Prime Minister, Sheikh Hasina, and the Indian Prime Minister, Deve Gowda (Salman *et al*., 1999). This will be referred to in this paper as the 1996 treaty.

4.3.3. Institutional framework

The conflict over the GRB between Bangladesh and India in fact dates back to 1951 when India decided to construct the Farakka Barrage. When the barrage was opened for operation in 1975, the dispute over the sharing and controlling of the Ganges water flow became the key issue of controversy between these two countries. The chronology of water conflicts and cooperation between Bangladesh and India along the GRB is presented in Table 4.5.

Table 4. 5: Chronology of water conflicts in the GRB between Bangladesh and India.

Period	Outcomes
1951	Pakistan (Bangladesh after 1971) officially objected to the plan on 29th October 1951 (Haftendorn, 2000)
1961	India officially agreed to the unilateral construction of the Farakka Barrage on 30th January 1961 (Rahman, 2006)
1972	On 24th November 1972, India and Bangladesh signed statutes of the Indo-Bangladesh Joint River Commission (JRC) (Adel, 2001).
1974	Farakka Barrage construction is completed. In a joint declaration on 16th May 1974, Bangladesh and India acknowledged (that there was) a need to augment the dry season flow of the Ganges River to meet the full requirements of both countries. The Indo-Bangladesh JRC report relating to the augmentation of the dry season Ganges River flows made recommendations to meet the requirements of the both countries (Rahman, 2006).
1975	Through a Ministerial level declaration, on 18th April 1975, India allowed between 310 and 450 cusec of water to be diverted to Bangladesh to test the feeder canal of the Farakka Barrage. The barrage first operated between April and June 1975. Bangladesh suggested augmentation of dry season flow involving the building of a storage reservoir in Nepal. India on the other hand suggested augmentation through diversion of water from the Brahmaputra River to the Ganges River (Abbas, 1992).
1976	India diverted the Ganges River flow beyond the stipulated period in 1975 and Bangladesh raised the issue with the United Nation (UN) on 26th September 1976. The UN General Assembly directed both countries to urgently negotiate a fair and expeditious settlement of the Farakka Barrage problem to promote the well being of the region (Rahman, 2006).
1977	Under the direction of the UN, India and Bangladesh signed the five-year Ganges Water Agreement on 5th November 1977 (Rahman, 2006).
1982	On 7th October 1982, a Memorandum of Understanding (MOU) was signed between the two countries for the Ganges River sharing dry season flow for the years 1983 and 1984. Provisions of this MOU were similar to the 1977 Agreement except that it contained a guarantee clause.

1985	There was no agreement for the 1985 dry season (January to May). On 22nd November 1985 another MOU was signed for three years (1986 to 1988), which expired on 31st May 1988.
1988=1992	The 1988 MOU expired leaving no agreement. Negotiations continued but without success.
1993	Bangladesh take the issue to the Commonwealth Summit held in Cyprus in October 1993.
1995	On 23rd October 1995, Bangladesh again raised the issues to 50th UN General Assembly concerning the welfare of the Bangladeshi people due to the unilateral water diversion at Farakka Barrage (Adel, 2001).
1996	An historical thirty year agreement between Bangladesh and India on dealing with sharing water at Farakka Barrage was signed on 12th December 1996 (Rahman, 2006).

4.4. Analysis and results of the treaty of 1996

For each year, the water sharing treaty of 1996 covered a 10-day period in each of the five from January to May. The water sharing formula presented in Table 4.6 granted at least 35,000 cusec of water to both Bangladesh and India.

Table 4. 6: 1996 Water sharing arrangement for the Ganges River between Bangladesh and India

Availability at Farakka	Share for India	Share for Bangladesh
70,000 cusecs or less	50%	50%
70,000 - 75,000 cusecs	Balance of flow	35,000 cusec
75,000 cusecs or more	40,000 cusecs	Balance of flow

Table 4.6 shows that estimating flow availability at the Farakka Barrage in the Ganges River is essential but is dependent on natural variability. To assess flow variability from 1997-2007, the median range estimator of standard deviation is used because it is relatively insensitive to occasional large shifts in the process. The estimated standard deviation $(\tilde{\sigma})$ is calculated from the median of the range multiplied by 1.047. The factor of 1.047 is based on an assumption of a random sample from a normal distribution, although it is irrelevant for calculating the statistical significance. The average flow availability and shifts in the process are shown in Table 4.7.

Table 4. 7: Assessing the flow variability in the GRB from 1997 to 2007

Statistics	1997	1998	1999	2000	2001	2002	2003	2004	2005	2006	2007
Mean	70911	113630	89821	91393	74128	86646	82290	85524	72699	62225	78675
Median	66449	102022	87236	87201	69837	85233	84627	78569	68749	57618	78015
Standard deviation	15427	37293	21960	20186	16063	14530	7717	20496	11601	12829	9782
Estimated standard deviation	69572	106817	91336	91299	73119	89239	88604	82262	71980	60326	81681
IQR	20488	41705	29505	13541	23798	15644	11600	36838	20602	15393	13046

The values of the median range estimator of standard deviation are substantially larger than the standard deviation s. Therefore, there is reason to suspect occasional shifts in the mean. Moreover, the interquartile range shifts under the mean process. To illustrate the clear variability from 1997 to 2007, box plots for each year are shown in Figure 4.6.

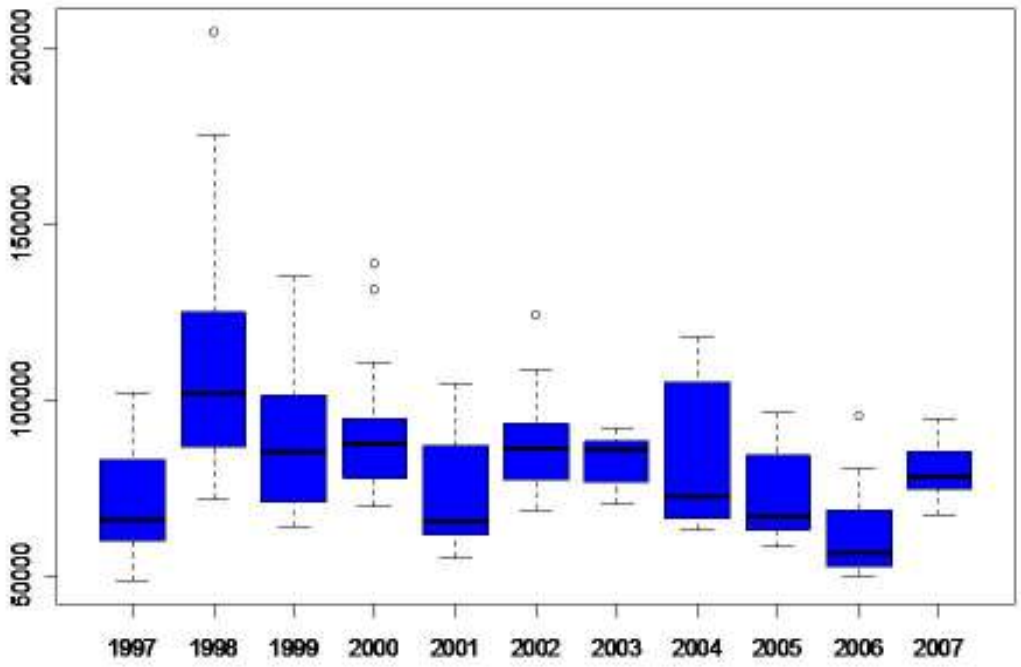

Figure 4. 6: Flow variability (in cusec) at Farakka Barrage in the GRB during the period 1997 to 2007

The effects of the 1996 water sharing treaty compared to the agreement of 1977 and the MOUs of 1982 and 1985 are presented in Appendix 4.1. The water sharing ratios between Bangladesh and India from January 1 to May 31 are approximately 61:39 (1977 Agreement), 60:40 (1982 MOU), 60:40 (1985 MOU) and 55:45 (1996 Treaty). This shows that Bangladesh's share decreased from about 61% under the 1977 Agreement to about 55% under the 1996 Treaty.

The strength of availability of flow was highly correlated ($r > 0.55$) at the 5% significance level ($p < 0.05$) during the period 1997 to 2006, except in 2003. For 2007, the flow availability was negatively correlated with the previous period, 1997 to 2006; moreover, it was positively correlated to the availability in 2003, as shown in Table 4.8.

Table 4. 8: The strength of flow availability at Farakka Barrage from 1997 to 200

	1997	1998	1999	2000	2001	2002	2003	2004	2005	2006	2007
1997	1										
1998	0.86	1									
1999	0.92	0.92	1								
2000	0.62	0.77	0.78	1							
2001	0.75	0.88	0.9	0.92	1						
2002	0.59	0.64	0.72	0.95	0.87	1					
2003	0.41	0.3	0.38	0.53	0.48	0.61	1				
2004	0.89	0.84	0.94	0.75	0.84	0.73	0.31	1			
2005	0.94	0.81	0.91	0.55	0.74	0.53	0.43	0.86	1		
2006	0.78	0.96	0.9	0.88	0.94	0.76	0.38	0.80	0.75	1	
2007	-0.38	-0.3	-0.32	0.12	-0.08	0.23	0.39	-0.39	-0.36	-0.14	1

Appendix 4.2 shows the available flows at Farakka during the period 1997 to 2007. The average availability of flows was more than 10% below the 11-year average in 1997, 2001, 2005 and 2006, with 2006 being the worst year at 25% below the 11-year average. However, the 1998 flow availability increased to 36% above the 11-year average but the average seasonal variation shown in Figure 4.7 indicates that in the critical non-monsoonal period from February 20 to May 31 the decline was in fact most severe in 1998, which is the year with the highest average availability. The seasonal availability of flow at Farakka in the non-monsoonal season continuously declined from 1997 to 2006. Eventually in 2007, seasonal variation was reduced but the average flow availability in 2007 still only remained close to the 11-year average (see Appendix 4.3).

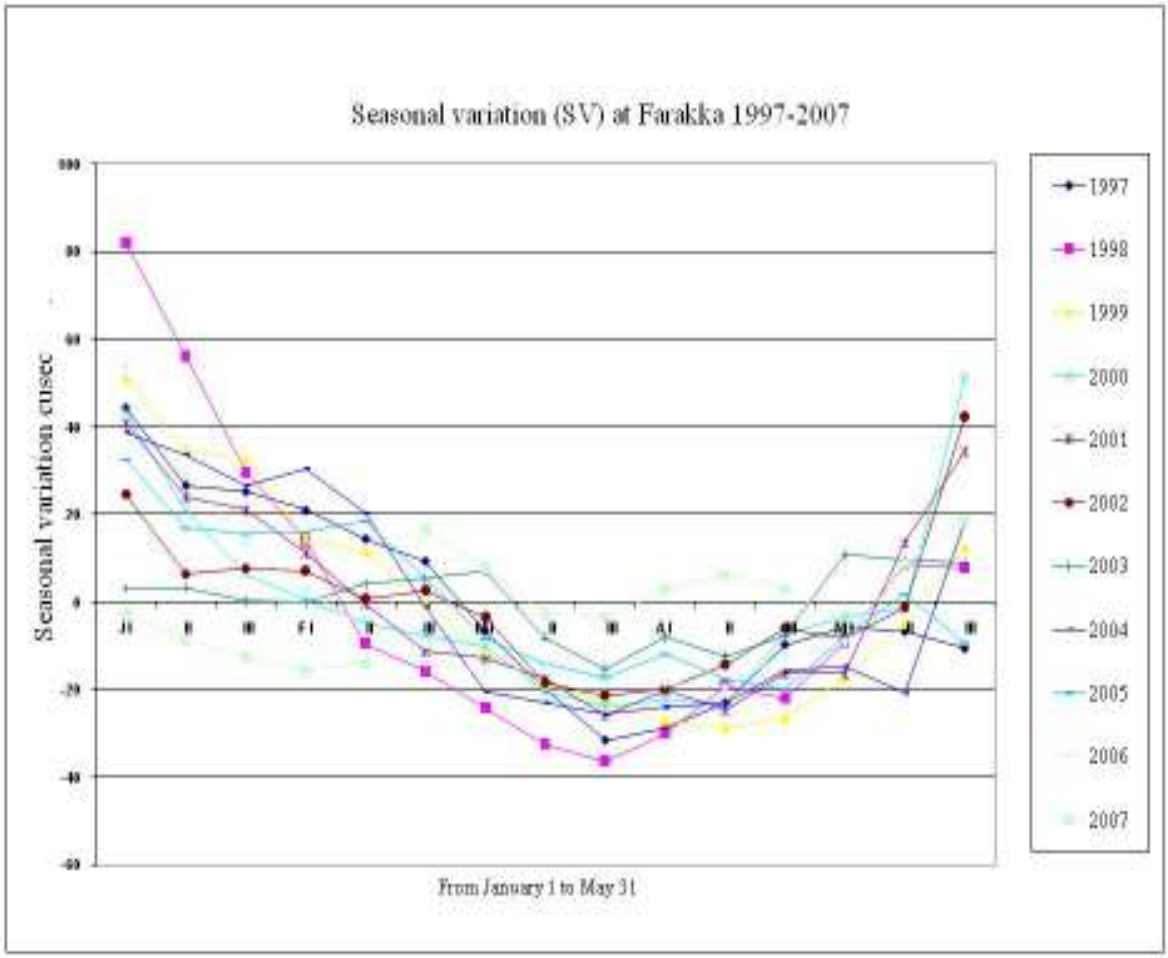

Figure 4. 7: Average seasonal variation (percentage) at Farakka 1997-2007

In a time series analysis, a lag is defined as follows: an event occurring at time t lags behind an event at time t+k (where k>0), with the extent of the lag being k. More specifically, the autocorrelation at lag k in the time series is estimated by:

$$r_k = \sum_{t=1}^{N-k}(x_t - \bar{x})(x_{t+k} - \bar{x}) / \sum_{t=1}^{N}(x_t - \bar{x})^2$$

where x_t is the time series, $\bar{x}$ is the mean of the values in the time series, and N is the number of data points. The null hypothesis for autocorrelations is that the time series observations are not correlated to one another.

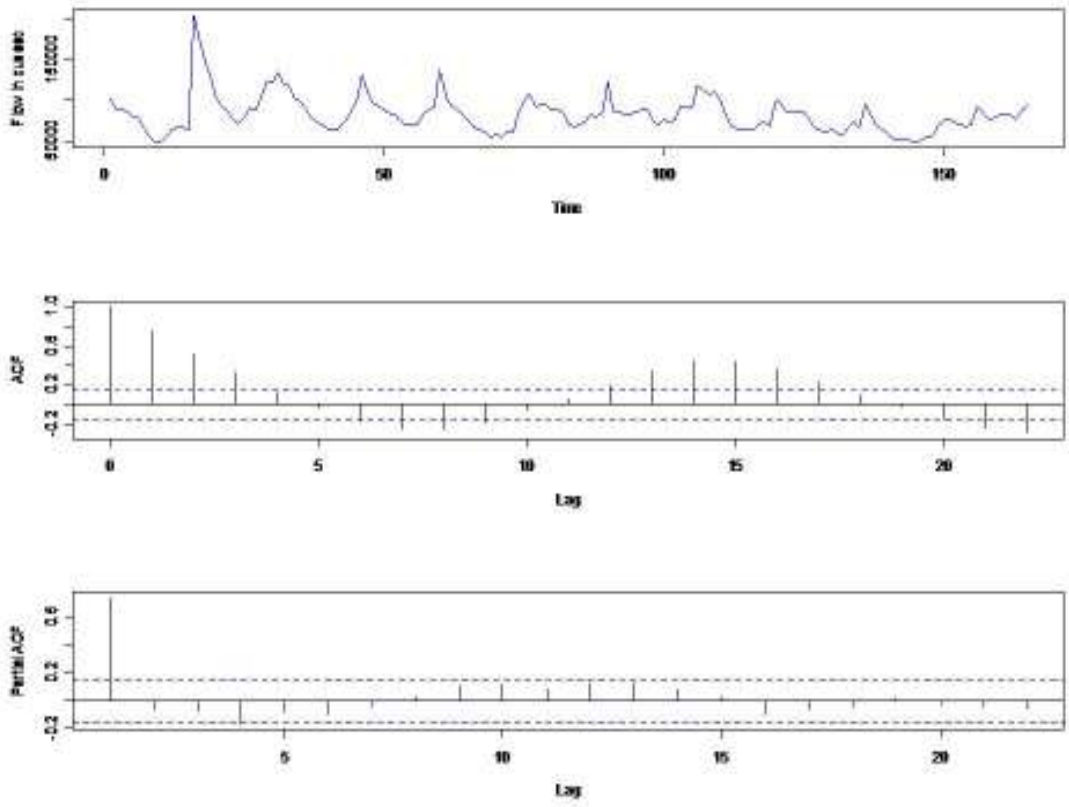

Figure 4. 8: Correlogram of water flow at Farakka from 1997 to 2007

Figure 4.8 shows that the flow variability of the time series is high and even obscures the trend of flow availability in the time series plot. In the correlogram with 5% lines of significances included, correlations lie beyond these lines and there is evidence of persistence when the water flow is aggregated at the monthly level. The autocorrelation lag at 0 is included by default. Our interests are the autocorrelations at other lags. The evidence of the autocorrelation lag 1 ($r_1 = 0.742$) is fairly large and the lag 2 ($r_2 = 0.523$), lag 3 ($r_3 = 0.334$), and lag 4 ($r_4 = 0.13$) autocorrelations are successively smaller and lags 1 to 4 are positively correlated. Following that came a negative correlation pattern. The autocorrelations continue to decrease as the lag becomes larger. Variation is increased indicating that there is no linear association of flow among the observations separated by lags larger than 4.

We may summarise that indeed, flow availability at Farakka is a crucial factor to resolve the water sharing constraints between Bangladesh and India. In order to implement the water sharing formula shown in Table 4.6, there is a need for flow augmentation of the Ganges River by water transfer from a third upstream country. We ran schemes regarding this long-term solution using a model study involving augmenting dry season flow of the Ganges River. We describe a Stackelberg leader-follower game model for the optimal allocation of water diverted from the upstream country.

4.5. Model study

The Stackelberg leader-follower model considers two actors such as an upstream country (as a leader who can make a choice how much or what quantity of water to divert for their own purpose) and a downstream country (as a follower whose usage of water is dependent on the flow of water diverted). Described a model of a two-country river basin water allocation, with the opportunity of water augmentation from a third country, applying a leader-follower game to determine the optimal share of water diverted by the upstream country.

4.5.1. Step one: Water sharing proportion

Assume that:

i. The two countries have proportional rights for water allocation.
ii. The two countries are authorized to buy water from a third country, Nepal
iii. India diverts water at a single location on the Ganges River at the Farakka Barrage

Therefore, we may argue that at Farakka the proportion of water allocated to India is α, and to Bangladesh is $1-\alpha$, with $0< \alpha<1$.

4.5.2. Step two: Flow augmentation

Assume that water flows on the Ganges River can be augmented by additional water transfers or releases from Nepal. So if the storage water volume is S in Nepal, it could release this amount of water to downstream countries for flow augmentation. India is downstream of Nepal, and Bangladesh is even further downstream. The sharing parameter (β) is determined by agreement or treaty. So if the proportion of flow to India downstream is β then flow to Bangladesh further downstream is 1-β, with $0 < \beta < 1$.

The two step argument model key point is α, as India can make its own decision to buy water from Nepal with the option of unilaterally diverting additional water rather than paying a price to buy water from Nepal. One option for Bangladesh to augment water flows is to buy more water from Nepal. However, Nepal will release additional water from their reservoirs only if both downstream countries, Bangladesh and India, pay for their increased share of this released water. In this case, Bangladesh is buying an amount (1-β)*S of water from Nepal. Then India needs to buy the remaining amount β*(S) of water. Otherwise, Nepal will not be fully compensated for the water it releases from its storage and thus will not agree to the water transfer. Indeed, Bangladesh needs to make an agreement with India for water transfer from Nepal and may also force India to buy more water from Nepal to divert more water (i.e. increasing α) at the Farakka Barrage. Bangladesh may impose its own credible threat of buying more water from Nepal (i.e. increasing S). In this situation, the key issues that arise are:

- Initially, how do additional water transfers from Nepal to India and Bangladesh occur?
- What additional water transfers from Nepal to India and then Bangladesh need to occur?
- Would India ever agree to an additional water treaty between the three countries to allow such water transfers to take place?
- Why would India reject the proposal to augment the flow of the Ganges River?

The model at first examines the case of the situation with water transfer treaties existing between Bangladesh, India and Nepal compared to the situation without them. Then examine what happens if India's share of water transfers, β, is increased. Assume that Bangladesh could increase water diversion from India through increased water release by Nepal, which would impose higher transfer costs on India as well.

4.6. Model application

A function can represent by

$$\omega_i = f_i(\alpha, S), \text{ subject to the constraint } f' > 0, f'' < 0 \quad i = 1,2..... \tag{1}$$

Where $f(\alpha,S)=\alpha^a S^b, 0<a,b<1$ for India,

$f(\alpha,S)=\alpha^{-c} S^d, 0<c,d>1$ for Bangladesh

(2)

Assume that:

α = the consumptive usage of water for India and Bangladesh and is a function of the share of water diverted in India.

S = amount of water transferred from Nepal to both countries.

ω_i = the contribution of α and S to the consumptive usage of water.

It is assumed that a country utilizes water to produce some economic output (e.g. agricultural production, industrial production, etc.), such that $P_i = p_i(\omega_i, v_i)$ for i=1, 2, where *v* is the vector of inputs used in the production. The production for India (P_1) and Bangladesh (P_2) respectively are represented by:

$$P_1 = p_1(\omega_1, v_1) = Av_1\alpha^a S^b, \text{ and } P_2 = p_2(\omega_2, v_2) = Bv_2\alpha^c S^d \tag{3}$$

In addition, Nepal will charge a price for supplying water to both countries Bangladesh and India. If r is the total amount of water demanded by both India and Bangladesh from Nepal, then:

$$r = kS^\gamma \qquad -1 < \gamma < 0, k > 0 \tag{4}$$

Therefore the demand r will decrease at an increasing rate of charge (γ). This assumption has bearing as it increases the reliability of the threat to India from

Bangladesh's actions. If India does not provide enough water to Bangladesh then Bangladesh can buy more water from Nepal at a lower price.

The profit functions $\prod_1$, and $\prod_2$ represent the profit to Bangladesh and India

$$\prod_1(\alpha,S) = (p-c)p_1(\omega_1,v_1) - r\beta(S) \quad \text{for India} \tag{5}$$

$$\prod_2(\alpha,S) = (p-c)p_2(\omega_2,v_2) - r(1-\beta)S \quad \text{for Bangladesh} \tag{6}$$

First compute Bangladesh's reaction to an arbitrary share of water diverted upstream by India. So $R_2(\alpha)$ solves the following equation:

$$\underset{S>0}{Max}\prod_2(\alpha,S) = \underset{S>0}{Max}\left[(p-c)Bv_2\alpha^{-c}S^{d} - k(1-\beta)S^{\gamma+1}\right]$$

Maximizing the above expression with respect to S yields the following first order condition

$$(p-c)Bv_2\alpha^{-c}dS^{d-1} - k(1-\beta)(\gamma+1)S^{\gamma} = 0 \tag{7}$$

The expression of Equation 7 proposes that Bangladesh will maximize their profit function if the net marginal benefit $\left[(p-c)Bv_2\alpha^{-c}dS^{(d-1)}\right]$ of buying additional water from Nepal equals the marginal cost of the water $\left[k(1-\beta)(\gamma+1)S^{\gamma}\right]$.

If $R_2(\alpha)$ is Bangladesh's best response function to India's share of water diversion α, then:

$$S = R_2(\alpha) = X\alpha^{-\delta}, \text{ Where } \delta = \frac{c}{\gamma-d+1} \text{ and } X = \left[\frac{(p-c)Bv_2d}{k(1-\beta)(\gamma+1)}\right]^{\frac{1}{\gamma-d+1}} \tag{8}$$

The slope of the reaction function is

$$\frac{\partial S}{\partial \alpha} = 0 \quad if\ \gamma = d-1 \Rightarrow \frac{\partial \ln(MC)_2}{\partial \ln(S)} = \frac{\partial \ln(NMB)_2}{\partial \ln(S)} \tag{9}$$

If water diversion is increased by India, the slope of the reaction curve in Equation 9 will be positive. If the proportional change in the net marginal benefit $(NMB)_2$ to Bangladesh of purchasing water from Nepal exceeds the proportional change in the marginal cost $(MC)_2$, then Bangladesh will gain. So if India decreases the share of water diverted to Bangladesh, then Bangladesh will buy water from Nepal provided the proportional change in net marginal benefits exceeds the proportional change in

the cost. Since India can resolve Bangladesh's problem as well, India should anticipate that the amount of water bought from Nepal will be met with the reaction $R_2(\alpha)$. Thus India could maximize their profit functions if:

$$\underset{\alpha>0}{\text{Max}}\prod_1(\alpha,S) = \underset{\alpha>0}{\text{Max}}\left[(p-c)Av_1\alpha^a S^b - k\beta S^{\gamma+1}\right]$$

subject to constraints $S=R_2(\alpha)=X\alpha^{-\delta}$.

Substituting the above conditions, maximization of the above function with respect to the choice variable α yields in the following objective function for India:

$$(p-c)Av_1X^b(a-\delta b)\alpha^{a-\delta b-1} - k\beta X^{\gamma+1}\left[-\delta(\gamma+1)\right]\alpha^{-\delta(\gamma+1)-1} = 0 \qquad (10)$$

The above equation suggests that India will choose a level of water diversion α, up to the point when the net marginal benefit $\left[(p-c)Av_1X^b(a-\delta b)\alpha^{(a-\delta b-1)}\right]$ of increasing α equals the marginal cost $\left[k(\beta)X^{(\gamma+1)}\left[-\delta(\gamma+1)\right]\alpha^{-\delta(\gamma+1)-1}\right]$. The net marginal benefit is the marginal value to India of a unit increase in the share of upstream water. Therefore Equation 10 will yield India's optimal value of α*

$$\alpha^* = Y^{\frac{1}{\theta}}, \text{ and } \theta = \delta(b-\gamma)-(a+\delta) > 0 \Rightarrow \delta > \frac{a}{(b-\gamma-1)} \Rightarrow \frac{\partial \ln(MC)_1}{\partial \ln\alpha} > \frac{\partial \ln(NMB)_1}{\partial \ln\alpha} \quad (11)$$

At the optimum level, positive values of θ mean that the proportional change in the marginal cost to India due to increased water diversion will exceed the proportional change in net marginal benefits. Equation 11 indicates that the optimal level of water diversion, α*, by India will be affected not only by the marginal costs but also its effect on the share, β, of water transfers from Nepal. This study demonstrate using the data in Appendix 4.3, that if there is an increase in the share of water diverted from Nepal to India, then the optimal level of water diversion by India will decrease i.e. $\frac{\partial\alpha^*}{\partial\beta} < 0$. This result implies that if India's share of water from Nepal as dictated by a water augmentation treaty is in fact increased, then the optimal amount of water diversion α will decrease because Bangladesh will impose more costs on India by buying water from Nepal. In this case, India will actually divert less water to Bangladesh.

4.7. Strategy implementation

The recommended strategy is based on water transfer from Nepal to India followed by water diversion from India to Bangladesh. Initially, India's situation without water augmentation was considered. It was presumed that the additional amount of water transferred by Nepal would affect India's welfare. This situation was compared to that without water flow augmentation.

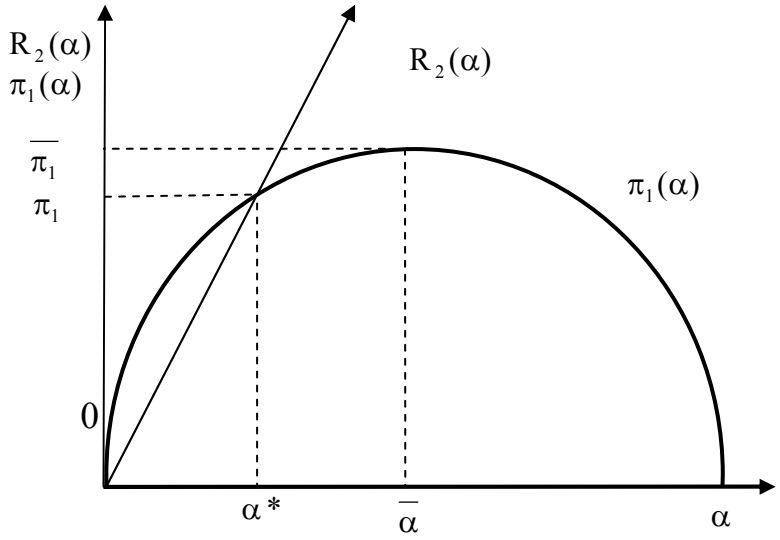

Figure 4. 9: Optimal level of water diversion by India

It was assumed that India's water scarcity is not extreme. Therefore, that India's profit function is concaving in diverting α. It is justified to diminish the marginal productivity of water utilization and to assume a negative second order profit condition as shown in Figure 4.9. From Figure 4.9, the producers in India could maximize their profit up to the net marginal benefit of increasing sharing diversion upstream equal to the marginal cost. Secondly, it was assumed that there is no provision for additional water supply from Nepal and a credible threat from Bangladesh in response to India increasing the diversion proportion of α, then India

has a unilateral option to divert water, and the efficient rate of water utilization corresponds to the optimal level of water diverted, α. So the function, $\omega_1 = f(\alpha)$ to ensure that the net benefit or profit will be at an optimal level $\overline{\pi_1}$ in Figure 4. and profit through choice of α is $\pi_1 = (p - c)p_1(\omega_1, v_1)$. Therefore the first order condition maximizing the profit is $(p - c)\frac{\partial(p_1)}{\partial(\omega_1)}\frac{\partial(\omega_1)}{\partial(\alpha)} = 0$ which shows that the profit to India will be maximized when the marginal benefit of water diversion equals zero. Since the function $\omega_1 = f(\alpha)$ is convex, that means the slope of the profit function with respect to the share of water diversion is positive when $\alpha < \overline{\alpha}$ and conversely is negative when $\alpha > \overline{\alpha}$ in Figure 4.9.

In that situation, it could be assumed that usage of water is a fixed proportion of the availability of water and is a function of α. r utilization would require a lower value of α. This lower value of under-utilization condition generates lower profit for the producer. Similarly, from Figure 4.9, over-utilization of water will ensure a lower profit $\pi < \overline{\pi}$, because of the diminishing marginal pro d a negative second-order profit condition. If there is no credible threat from Bangladesh, India could maximize their profit $\overline{\pi}$ by diverting a share $\overline{\alpha}$ of water upstream and allocating the rest to flow downstream to Bangladesh. In Figure 4.9, it can be compare the results and see that water transfers from Nepal will reduce the profit to India. From Equations 10 and 11, when water transfers from Nepal take place, it forces India to face an additional cost to increase the diversion, α. Therefore, if Bangladesh buys water from Nepal then India's optimal share of water diverted upstream, α*, will be less than the optimal level of water diverted by India in the unconstrained case, α. In such a case, India would be better off without a water augmentation treaty. This perhaps better explains why in the

past India has strongly resisted efforts by Bangladesh to couple any agreement on water sharing with proposals for augmenting the Ganges dry season flow with water transfers from Nepal

8. 4. Conclusion

The GRB water sharing issue between Bangladesh and India is a unique example for developing countries because of its wide variety of impacts. The Farakka Barrage is a matter of controversy between Bangladesh and India. It has introduced a number of negative socio-economic and environmental impacts for Bangladesh. The Ganges water-sharing treaty of 1996 between Bangladesh and India was a step forward that might result in a new era of positive relations and political commitment to solving long-standing disputes. But the important aspect is the insufficient water flows from March to May at Farakka Barrage. Its capacity to meet the future demands of both Bangladesh and India seems questionable.

In this chapter, it recommended a way to augment water flows at Farakka Barrage on he Ganges River Basin. The model studies suggest that water transfer from Nepal would augment the flow of water at Farakka during the dry season and in periods of drought. It was shown that market-based water transfers from Nepal would help to resolve the water sharing conflict between Bangladesh and India. If the water charge by Nepal is demand determined, then water can be used efficiently in the two downstream countries, and thus it can help in mitigating the water scarcity problem. Because water supply from Nepal is non-separable between India and Bangladesh, this means that any water augmentation treaties will most likely require that if Bangladesh buys excess water from Nepal then India will also have to pay for an additional proportion of water from Nepal. If water augmentation treaties exist, then Bangladesh can furthermore use this opportunity to impose a credible threat to India to stop the latter from diverting more water at Farakka. In contrast, if there is no treaty, there would be no credible threat from Bangladesh to India because as shown by Equations 10 and 11, India is likely to be better off without a water treaty. Moreover, without a treaty India can gain from deciding unilaterally on how much

water to divert. Our analyses therefore suggest that India has an incentive to reject any proposal for water transfers from Nepal, as it has done consistently in the past.

Regarding this situation, the analysis suggests several policies. First of all, it is assumed that Bangladesh and India's water sharing conflicts are now resolved by an existing treaty regarding the Farakka Barrage. Analysis suggests that India would be strongly motivated to ignore the provisions of the treaty and to decide how much water to divert, as indicated in Figure 4.9. However, a water augmentation treaty between Bangladesh, India and Nepal not only provides additional water to both downstream countries in times of chronic scarcity but also gives Bangladesh a mechanism for deterring India from violating the Ganges River Treaty and deciding unilaterally to divert more water at the Farakka Barrage. In this regard, a water augmentation treaty is likely to reinforce the existing Ganges River Treaty.

According to Equations 10 and 11, this study suggests that India would not be happy to develop a water augmentation treaty with Bangladesh and Nepal. Without India's cooperation, such as market-based water transfers could not be negotiated and implemented. If a treaty is established, it could be suggested that it may be in the interest of all parties to ensure that their share of any water transfers is relatively large.

International river basin problems are more complex than those of national river basins (Haftendorn, 2000). Therefore, international river basin conflicts should be dealt with at a multi-lateral level, depending on the type of basin (Rahman, 2006). It is wise not to impose solutions but to resolve problems among the nations involved. In the case of the Ganges River Basin, actual implementation of the treaty depends on India, which has the control over other co-riparian countries. For a sustainable solution of water sharing in the Ganges River Basin, integrated water resources management involving all the co-riparian countries is vital and models such as the one presented in this chapter can assist in understanding the key policy drivers. However, further research is needed to develop more sophisticated analytical and policy tools.

CHAPTER 5: CHARACTERISTICS OF CLIMATE VARIABILITY

5. 1. Introduction

The Murray Darling Basin Commission (MDBC) is a natural resources management agency in Australia, which works with six state governments to supply water for irrigators and urban consumers, and to deliver environmental protection. An agriculture production, natural ecosystems and water resources are highly dependent upon local rainfall and there is a great potential for adverse effect if rainfall undergoes to change under greenhouse effect conditions. In 2001, the Working Group 1 of the Intergovernmental Panel on Climate Change (IPCC) released the summary of its TAR on "climate change" (IPCC, 2001). This provides a wide range of projected temperatures. Increase is always indicated. Local precipitation may increase or decrease under enhanced greenhouse conditions. Moreover, greenhouse gas impacts signal are much weaker for rainfall than for temperature because of much higher natural variability of precipitation. The high temporal and spatial variability of rainfall and contemporary temperature patterns in Australia has been recognised by the BOM (BoM) and Commonwealth Scientific Industry and Research Organisation (CSIRO). This imposes a major challenge for the sustainable management of Australian water resources. The projections of future climate change are large uncertainties that must be incorporated into impact assessment. To facilitate the planning, development and prioritisation of water resources management, knowledge and understanding of rainfall variability and the factors influencing this variability are important for not only for the water managers but also for the policy makers.

In this chapter climatic behaviour is analysed using statistical tools. This study highlights both the long term and short term rainfall and temperature behaviour in the MDB area, including four capital cities in Eastern Australia. Temporal and spatial variability will be examined based on rainfall and temperature in the MDB area using a clustering method. A non-parametric Mann-Kendal test was applied to detect the trend at 5% level of significance.

5.2. Study approaches

This research was initiated to assess the monthly rainfall and temperature pattern in the MDB area and for one meteorological station in each of Sydney, Melbourne Canberra and Adelaide of Australia. Many studies have identified the Pacific Decadal Oscillation (PDO) and Southern Oscillation Index (SOI) as influences on Australian rainfall (Chiew, et al, 2000, CSIRO, 2001 and BoM 2008). This study has investigated characteristics of rainfall and temperature patterns, categorized by climatic phenomena for understanding water availability in the MDB. The importance of this study is to analyses climatic variability information beyond the seasonal-to-inter annual timescale, in particular, information regarding the next 10-30 years for purposes such as planning decisions for transportation, infrastructure project, and water reservoir design, this require information both on the mean and the likely characteristics of variability over the next several decades. Understanding and predicting climate on longer time scales constitutes one of the most challenging in climate science today. It must bridge a gap between natural variability on the decade and multi decade time scales and include anthropogenic trends. This study seeks to describe and explain the mechanism of decade variability. More specifically the study has been applied the statistical tools for assessment of change in rainfall and temperature pattern, such as measuring index of dispersion by the coefficient variation and also checking the IQR of the rainfall and temperature pattern in both short term and long term in the MDB area and four capital cities in Australia. A box plot analysis has been employed to summarize the distribution of rainfall and temperature series in observed areas. The variability of rainfall and temperature patterns was assessed in 1971-2006, 1987-2006, and 1997-2006 in comparison to 1901-2006. Agglomerative hierarchical technique is used represents the number of categories of the climatic pattern in the different sites in the MDB and eastern Australia. The statistical significance of change was tested by a non-parametric Mann-Kendall test.

5.3. Data analysis

Statistical summaries for change in monthly annual mean rainfall and temperature for 10 years, 20 years, and 36 years in comparison to the long term means for the six MDB areas and four capital cites in Australia are shown in Table 5.1 and Table 5.2.

Table 5. 1: Rainfall pattern change in the MDB and four capital cities in Australia

Sitename	Observed mean of monthly annual mean rainfall			1971-2006 rainfall			1987-2006 rainfall			1997-2006 rainfall		
	Period (a)	Mean (b)	IQR (c)	mean	Percentage change from column 2(b)	IQR	mean	Percentage change from column 2(b)	IQR	mean	Percentage change from column 2(b)	IQR
Hume dam	1900-2007	58	51	60	3.45%	55	59	1.72%	52	53	-8.62%	45
Adelaide airport	1956-2007	37	30	38	2.47%	30	37	-0.22%	28	36	-2.92%	25
Broken hill	1958-2007	22	26	24	7.06%	27	23	2.60%	24	19	-15.24%	20
Canberra airport	1940-2007	52	46	51	-0.97%	43	51	-0.97%	44	45	-12.62%	33
Loxton met station	1910-2006	23	22	23	0.36%	19	23	0.36%	13	23	0.36%	2
Melbourne airport	1971-2006	45	31	45	0.00%	31	44	-2.22%	31	39	-13.33%	25
Mildura airport	1901-2006	23	24	24	4.35%	25	22	-4.35%	22	19	-17.39%	19
Murray bridge	1901-2006	30	27	30	-0.28%	26	30	-0.28%	24	30	-0.28%	24
Sydney obs. hill	1901-2006	100	94	103	3.26%	93	102	2.26%	92	94	-5.76%	89
Lake Victoria	1923-2006	22	23	21	-2.70%	23	20	-7.34%	20	18	-16.60%	19

The percentage of difference between the mean annual rainfall in the past 10 years (1997-2006) and 20 years (1987-2006) in comparison to 1900-2006 show that the mean annual rainfall at all stations is statistically significantly lower ($\alpha = 0.05$) than in 1901-2006. The contemporary mean annual temperature pattern in 1997-2006 is statistically significantly higher than in 1901-2006. The variability of rainfall and temperature pattern at all observation stations was relatively steeper in 1997-2006 than in 1901-2006 and 1987-2006. The

percentage change in rainfall pattern increased in 1971-2006, due to change in the temperature pattern. Moreover, in a last 20-year rainfall pattern increase in Hume's dam, Broken Hill, Loxton met and Sydney's Observatory Hill area as due to temperature pattern change in less than 1%. The study provided the evidence that if the temperature pattern increased more than 1%, then the rainfall pattern reduced dramatically, in compare 1901-2006 in all observed areas shown in Table 5.1 and Table 5.2.

Table 5. 2: Temperature pattern change in MDB and four capital cities in Australia

Site name	Observed mean of monthly annual mean temperature			1971-2006 Temperature pattern			1987-2006 Temperature pattern			1997-2006 Temperature pattern		
	Period (a)	Mean (b)	IQR (c)	mean	Percentage change from column 2(b)	IQR	mean	Percentage change from column 2(b)	IQR	mean	Percentage change from column 2(b)	IQR
Hume dam	1900-2007	21.50	2.15	21.5	0.00%	2.04	21.7	0.79%	2.02	22.25	3.49%	2.13
Adelaide airport	1956-2007	30.25	3.25	30.5	0.83%	3.42	30.6	1.09%	3.5	30.75	1.65%	2.98
Broken hill	1958-2007	24.00	5.75	24	0.00%	5.38	24.1	0.33%	5.4	24.17	0.71%	5.05
Canberra airport	1940-2007	26.00	3.23	26.33	1.27%	3.25	26.8	2.88%	3.04	27.42	5.46%	2.77
Loxton met station	1910-2006	23.65	1.89	23.58	-0.30%	1.63	23.8	0.76%	1.63	24	1.48%	1.9
Melbourne	1971-2006	28.08	3.42	28.08	0.00%	3.42	28.3	0.89%	3.5	29	3.28%	3.33
Mildura airport	1901-2006	24.00	2.08	23.75	-1.04%	1.81	23.9	-0.33%	1.88	24.25	1.04%	1.83
Murray bridge	1901-2006	22.75	4.34	22.75	0.00%	1.83	22.8	0.35%	2.08	22.92	0.75%	4.1
Sydney obs.Hill	1901-2006	29.33	4.29	29.67	1.16%	3.94	29.7	1.16%	3.5	30.08	2.56%	3.71
Lake Victoria	1923-2006	23.58	2.92	23.75	0.72%	2.58	23.7	0.38%	5.4	23.75	0.72%	2.81

5.3.1. Box plot analysis

A box and whisker plot is a way of summarizing a rainfall and temperature pattern measured on an interval scale. The graphs present the shape of the underlying distribution, its central value, and its variability. The line across the box represents the

median, whereas the bottom and top of the box show the first and third quartiles (Q_1 and Q_3). The whiskers are the dash lines that link the bottom and top of the box respectively to the lowest and highest observations inside the region defined by Q_1-1.5 (Q_3 - Q_1) and Q_3+ 1.5 (Q_3 - Q_1. The graphical representation using box plots is shown in Figure 5. 2. Clear seasonal variability in rainfall and temperature patterns in the observation areas and a detailed visual snapshot of seasonal variability is presented shown in Appendix 5.1.

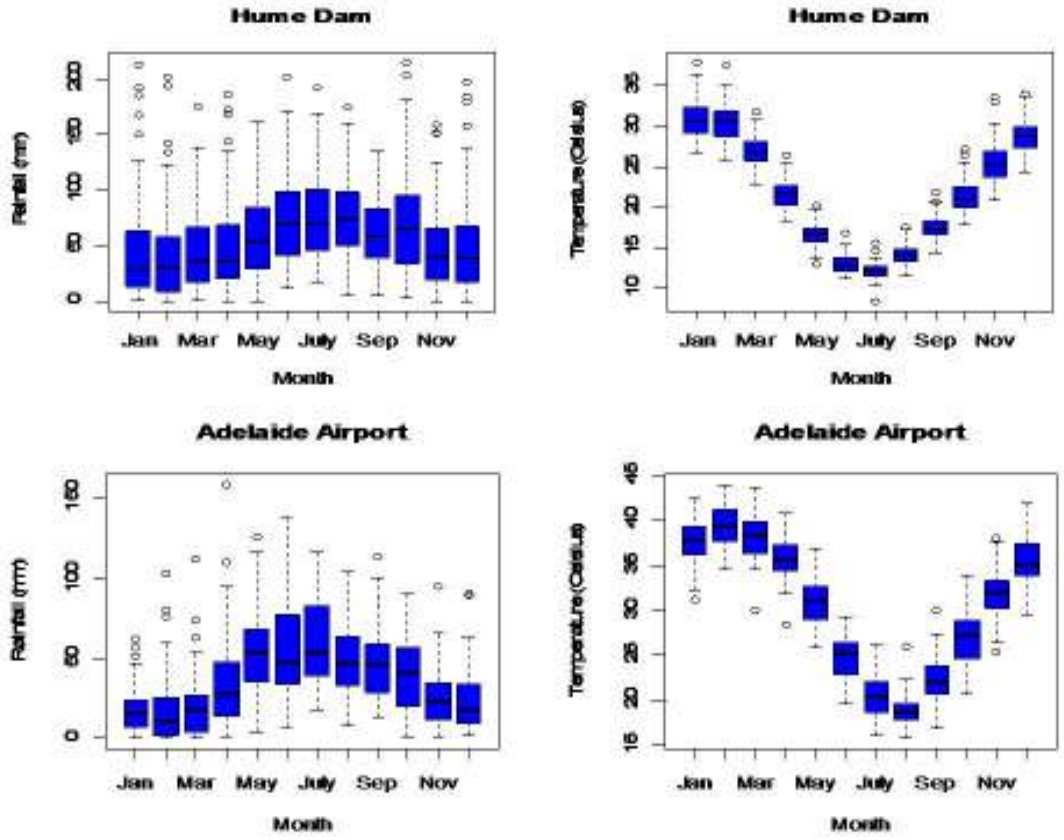

Figure 5. 1: Seasonal variability in the rainfall (left side) and temperature (right side) in Hume dam and Adelaide airport areas using box plot.

In practice, the Figure 5.1 has been shown. The distributions of rainfall and temperature pattern have been positively skewed except that at Adelaide airport, Melbourne Airport and the Sydney Observatory Hill area. The temperature pattern is negatively skewed.

5.3.2. Assessing the rainfall and temperature patterns

In the short term seasonal variability like 1997-2006 years, 19987-2006 years and 1971-2006 rainfall and temperature pattern compared in 1901-2006 shown bellow, particularly Hume Dam and Adelaide Airport areas, and given similar plot are in Appendix 5.2.

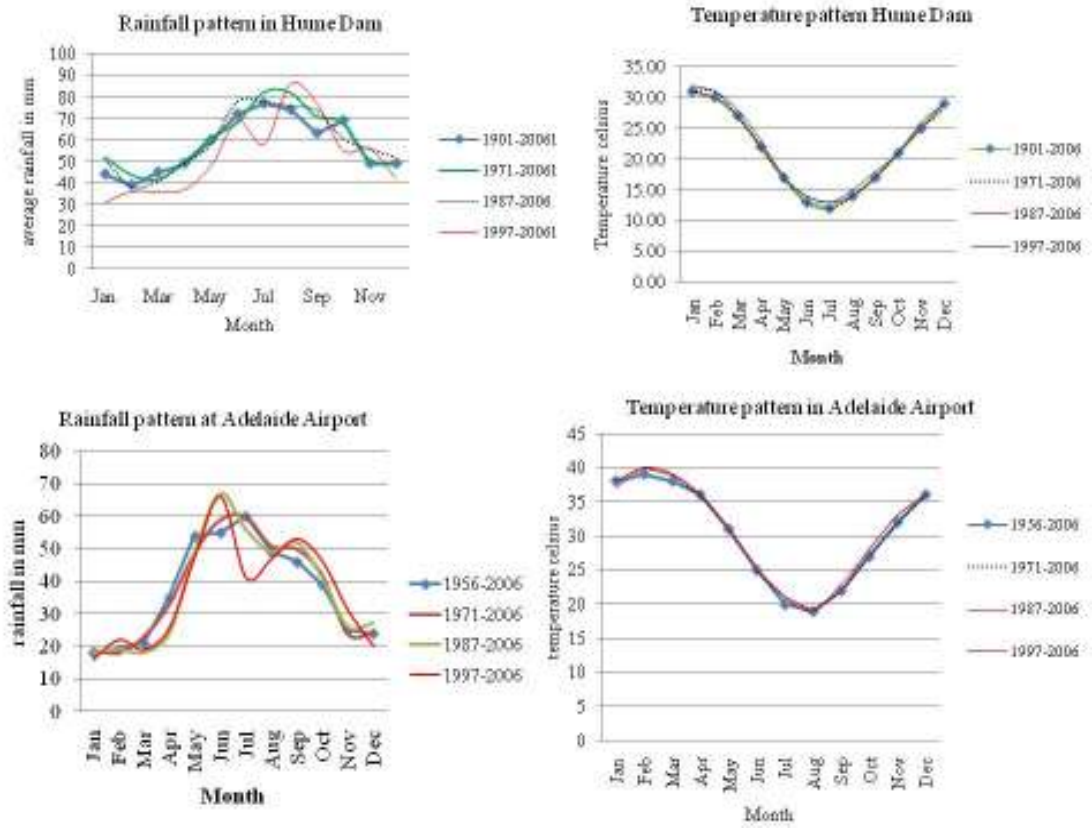

Figure 5. 2: Monthly mean step change in rainfall (left side) and temperature (right side) pattern change in both short term and long term in Hum dam (upper row and) Adelaide airport (bottom row).

Figure 5.2, shows the clear seasonal pattern in the rainfall and temperature time series. The rainfall pattern in 1997-2006 was below the average rainfall in 1901-2006 from January to December. This study revealed that there was no statistically significantly evidence of change in rainfall pattern at $\alpha = 0.05$ due to change in temperature patter in the contemporary period. Moreover, in Sydney Observatory Hill area temperature pattern decreased, and contemporary rainfall pattern also decreased. The variability of

temperature pattern shows January to June was increased and July to December was reduced except Sydney. Contemporary variability of rainfall pattern was abrupt from January to December in both short term and long term. It can be shifting to a lower level.

5.3.3. Clustering method: hierarchical Method

Assessment of rainfall and temperature patterns has been shown by temporal and spatial variation in the MDB and four capital cities in Australia. Using the hierarchical method, hydrological patterns were categorised in order to temporal and spatial weighted values. The issue of climate change was considered and without considering other hydrological parameters, temporal and spatial variability of rainfall and temperature pattern were characterised, as shown in Table 5.3 and Table 5.4.

Table 5. 3: Spatial characteristics of rainfall and temperature variability and distance patterns in the MDB area and eastern Australia.

Standardized data for analysis		
	Rainfall	Temperature
Hume dam	0.685	-1.287625
Adelaide airport	-0.1712	1.6664179
Broken hill	-0.7829	-0.443613
Canberra airport	0.44036	0.231587
Loxton met	-0.7421	-0.561775
Melbourne airport	0.15494	0.9338152
Mildura airport	-0.7421	-0.443613
Murray bridge	-0.4587	-0.866619
Sydney obs. hil	2.39748	1.3568214
Lake victoria	-0.7829	-0.595407
check	0.00	0.00

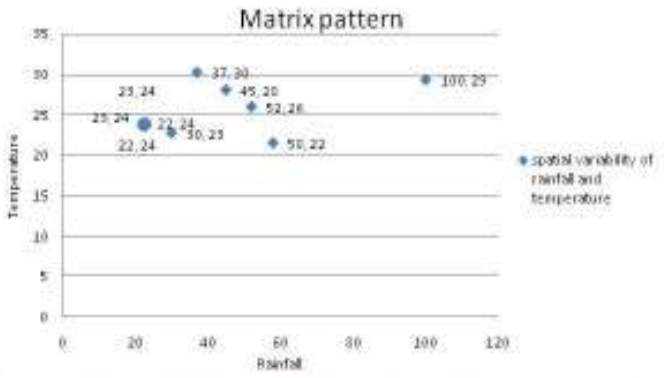

	Hume dam	Adelaide airport	Broken hill	Canberra airport	Loxton met	Melbourne airport	Mildura airport	Murray bridge	Sydney obs. hill	Lake Victoria
Hume dam	0									
Adelaide airport	1.875634	0								
Broken hill	1.693281	2.196881	0							
Canberra airport	1.538793	1.889734	1.397190858	0						
Loxton met	1.681061	2.38015	0.124998691	1.423932537	0					
Melbourne airport	2.283883	0.881939	1.66636128	0.758885257	1.743569346	0				
Mildura airport	1.657979	2.195881	0.848773517	1.361636426	0.118161724	1.64376842	0			
Murray bridge	1.217158	2.548872	0.533374068	1.417223743	0.416872815	1.90693192	0.589461187	0		
Sydney obs. hill	3.14967	2.587441	3.654385912	2.257040915	3.678868743	2.28190486	3.638674573	3.616759315	0	
Lake Victoria	1.427171	2.333484	0.141794869	1.470961291	0.647127141	1.78535367	0.147539953	0.438020365	3.725975548	0

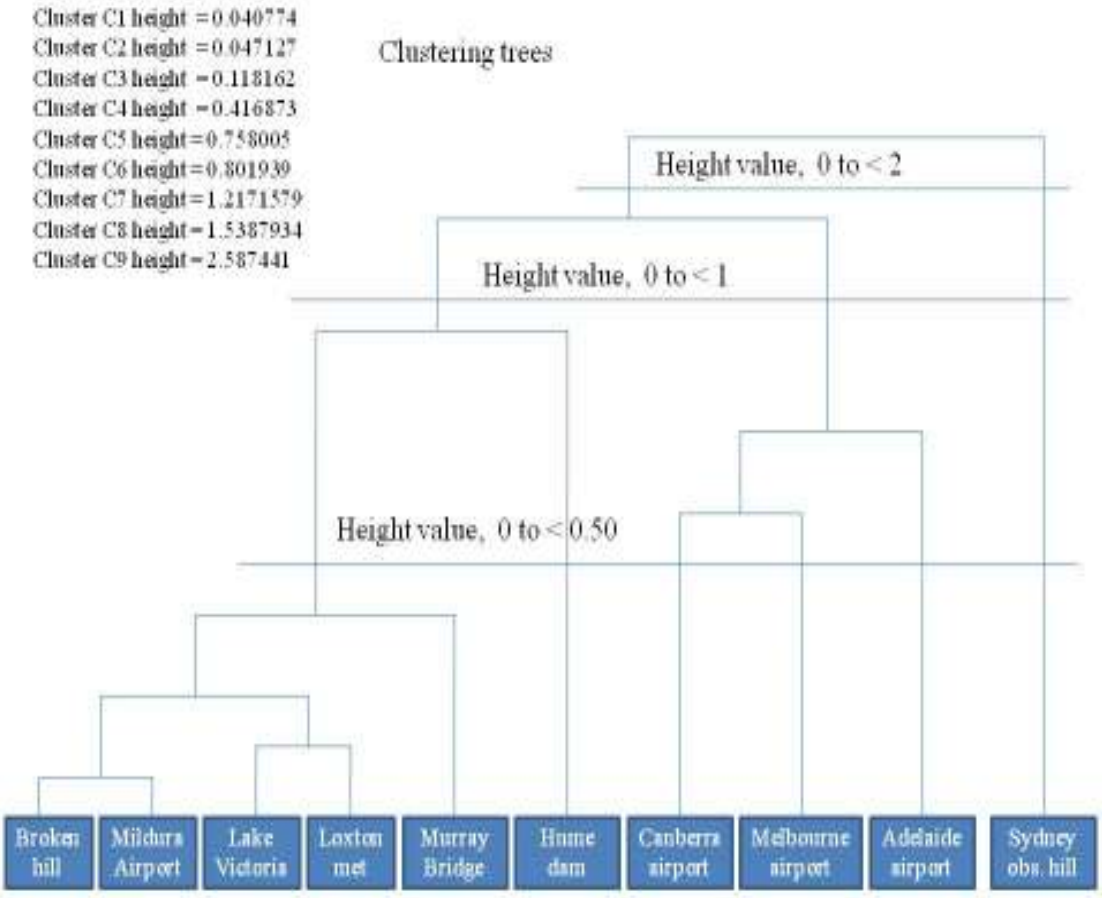

Figure 5. 3: Tree diagram of spatial characteristics of rainfall and temperature in MDB area and eastern Australia.

The tree diagram has been used to assess the characteristics of rainfall and temperature patterns at the different sites. A single linkage was categories based on height values in the below. For the height value 0 to 0.5, the study observed at Broken Hill, Mildura Airport, Lake Victoria, Loxton met, and Murray Bridge was categories similar rainfall and temperature characteristics to MDB areas and other observed areas have particular rainfall and temperature characteristics to eastern Australia. When the height values 0 to 1, the study observed like the Broken Hill, Mildura Airport, Lake Victoria, Loxton met, and Murray Bridge and Hume Dam that have a similar rainfall and temperature pattern, Canberra Airport, Melbourne and Adelaide Airport had the similar pattern and Sydney Observatory Hill had particular rainfall and temperature characteristics in rainfall and temperature pattern. The height values 1 to 2, the study identified 2 groups Sydney Observatory Hill had a particular rainfall

and temperature pattern and other observed areas have similar rainfall and temperature in observed MDB areas. If the height value is more than 2.58, and then this study claims the similar rainfall and temperature characteristics in the MDB and Eastern Australia.

Seasonal pattern was assessing based on monthly rainfall pattern and temperature pattern, in Hume Dam area was selected randomly.

Table 5. 4: Temporal characteristics of rainfall and temperature variability and distance pattern at the Hume dam in the MDB area.

month	Rainfall	Temperature
Jan	43	31
Feb	39	31
Mar	46	27
Apr	49	22
May	60	17
Jun	74	13
Jul	77	12
Aug	75	14
Sep	63	18
Oct	69	21
Nov	49	26
Dec	48	29

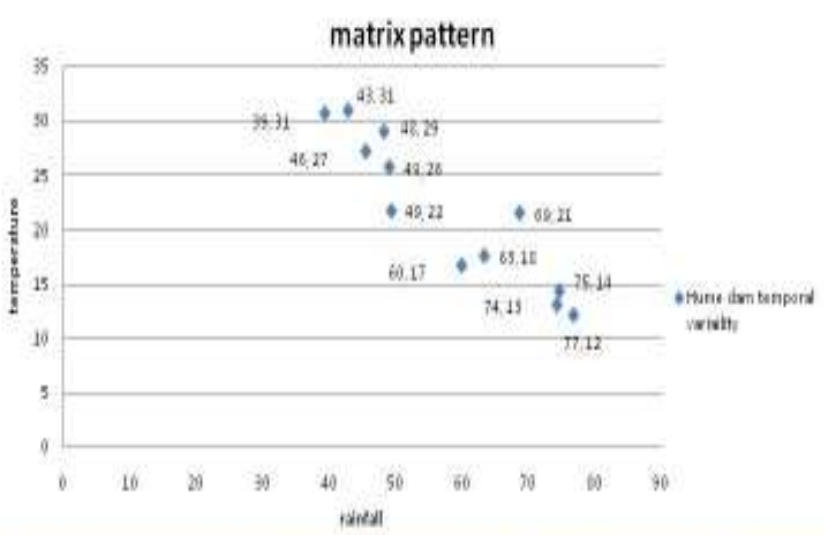

	Jan	Feb	Mar	Apr	May	Jun	Jul	Aug	Sep	Oct	Nov	Dec
Jan	0.00000											
Feb	0.26066	0.00000										
Mar	0.57554	0.67706	0.00000									
Apr	1.41420	1.48734	0.83866	0.00000								
May	2.41169	2.52474	1.85142	1.06570	0.00000							
Jun	3.46829	3.61821	2.94249	2.22234	1.18000	0.00000						
Jul	3.69094	3.84311	3.16781	2.44941	1.40438	0.22719	0.00000					
Aug	3.35332	3.51207	2.83910	2.14783	1.13590	0.18357	0.35302	0.00000				
Sep	2.44867	2.58721	1.91029	1.19133	0.28268	1.03787	1.26484	0.95651	0.00000			
Oct	2.33878	2.53244	1.89279	1.42301	0.94749	1.28905	1.48087	1.12835	0.68866	0.00000		
Nov	0.87725	1.00744	0.33332	0.58178	1.53444	2.61078	2.83577	2.50609	1.58081	1.56972	0.00000	
Dec	0.48580	0.69865	0.33270	1.05615	1.97655	2.99757	3.21849	2.87772	1.98947	1.85304	0.47525	0.00000

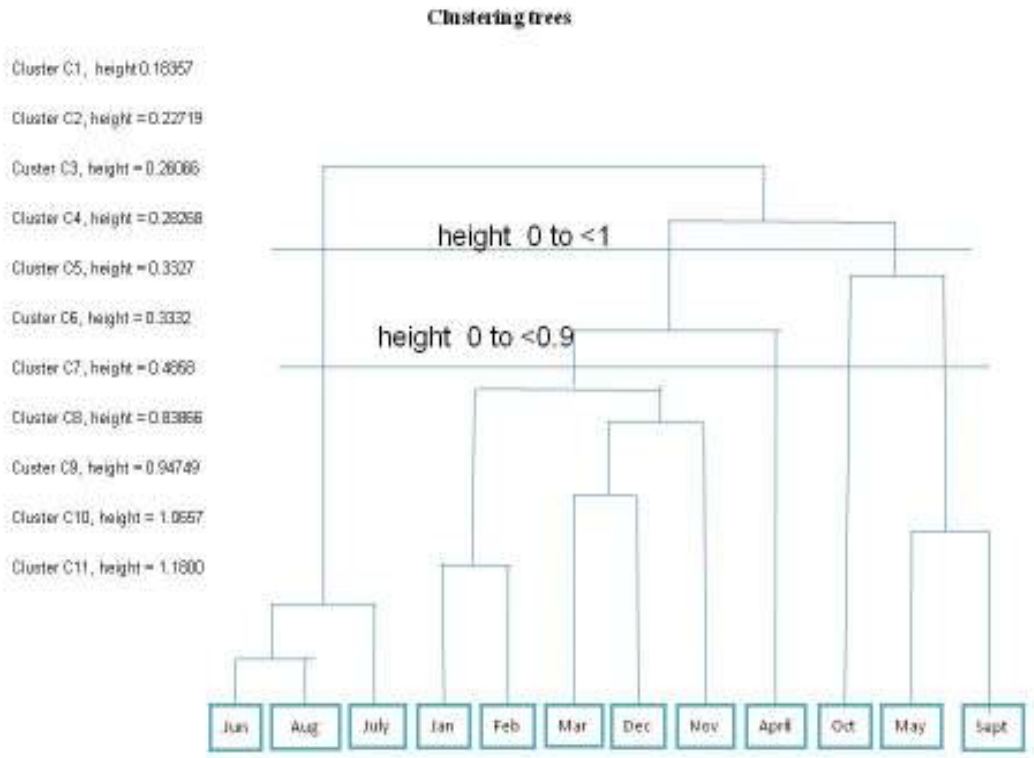

Figure 5. 4: Tree diagram of temporal characteristics of rainfall and temperature at Hume Dam in the MDB area.

Since from 1900 to 2006, the tree's clustering shows the height values 0 to less than 1, the study claims 3 categories of seasonal pattern, one category in November Dec, Jan Feb March, April, have been the similar rainfall and temperature pattern second one is June, July and August, third one is September and October where May is relative to whole month.

5.3.4. Non-parametric Mann Kendal test

A Non parametric Mann- Kendall's test was applied for assessing the strength of association of rainfall and temperature patterns at 30 years, 60 years and 90 years windows with significance at $\alpha = 0.05$ level. The significant evidence of trends has shown in Table 5.5 below.

Table 5. 5: Mann-Kendal test statistics for rainfall and temperature association at 30-years, 60-years and 90-years windows in the MDB areas and the eastern in Australia

	Years	Rainfall pattern			Temperature pattern		
		Mann Kendall tau (t)	Z-values	Decision	Mann Kendall tau (t)	Z-values	Decision
Hume dam	30	-0.04	-0.34	we accept Ho of no trend	0.23	1.77	we accept Ho of no trend
	60	0.04436	-0.497	we accept Ho of no trend	0.242	2.73	we accept Ho of no trend
	90	0.067	0.94	we accept Ho of no trend	0.042	0.5855	we accept Ho of no trend
Adelaide airport	30	-0.13	-1.02	we accept Ho of no trend	0.1	0.75	we accept Ho of no trend
Broken hill	30	-0.04	-0.32	we accept Ho of no trend	-0.01	-0.09	we accept Ho of no trend
Canberra airport	30	-0.12	-0.95	we accept Ho of no trend	0.31	2.37	we reject Ho of no trend
	60	0.18	-2.067	we reject Ho of no trend	-0.3186	3.59	we reject Ho of no trend
Loxton met	30	0.21	1.61	we accept Ho of no trend	0.23	1.78	we accept Ho of no trend
	60	0.058	-0.6569	we accept Ho of no trend	0.2718	3.074	we reject Ho of no trend
	90	0.005	0.0697	we accept Ho of no trend	0.075	-1.0446	we accept Ho of no trend
Melbourne airport	30	-0.14	1.12	we accept Ho of no trend	0.22	1.69	we accept Ho of no trend
Mildura airport	30	-0.13	-1.05	we accept Ho of no trend	0.19	1.48	we accept Ho of no trend
	60	0.1623	-1.83	we accept Ho of no trend	-2294	2.54	we reject Ho of no trend
	90	0.004	0.0523	we accept Ho of no trend	-0.076	1.07	we accept Ho of no trend
Murray bridge	30	0.03	0.25	we accept Ho of no trend	0.24	1.87	we accept Ho of no trend
Sydney obs. Hill	30	-0.06	-0.52	we accept Ho of no trend	0.18	1.41	we accept Ho of no trend
	60	0.101	1.141	we accept Ho of no trend	-0.25	2.9	we reject Ho of no trend
	90	0.697	0.9689	we accept Ho of no trend	-0.014	0.2056	we accept Ho of no trend
Lake Victoria	30	-0.1	-0.82	we accept Ho of no trend	-0.04	-0.32	we accept Ho of no trend
	60	0.205	2.32	we reject Ho of no trend	-0.1972	2.2322	we reject Ho of no trend

The strength of the 30 year, 60 year and 90 year the rainfall and temperature association has been shown to be a very weak even negative one. This study identified that there is no statistically significant evidence of a trend in the MDB areas. Moreover, in Lake Victoria and Canberra Airport station the 60 years rainfall and temperature pattern have a very weak association with statistical evidence of trend. However, the 90-year window shows there is no evidence of trend of rainfall and temperature pattern in the MDB areas and four capital cities in Australia. The strength of association 30 year's rainfall and temperature patterns shown in Figure 5.5.

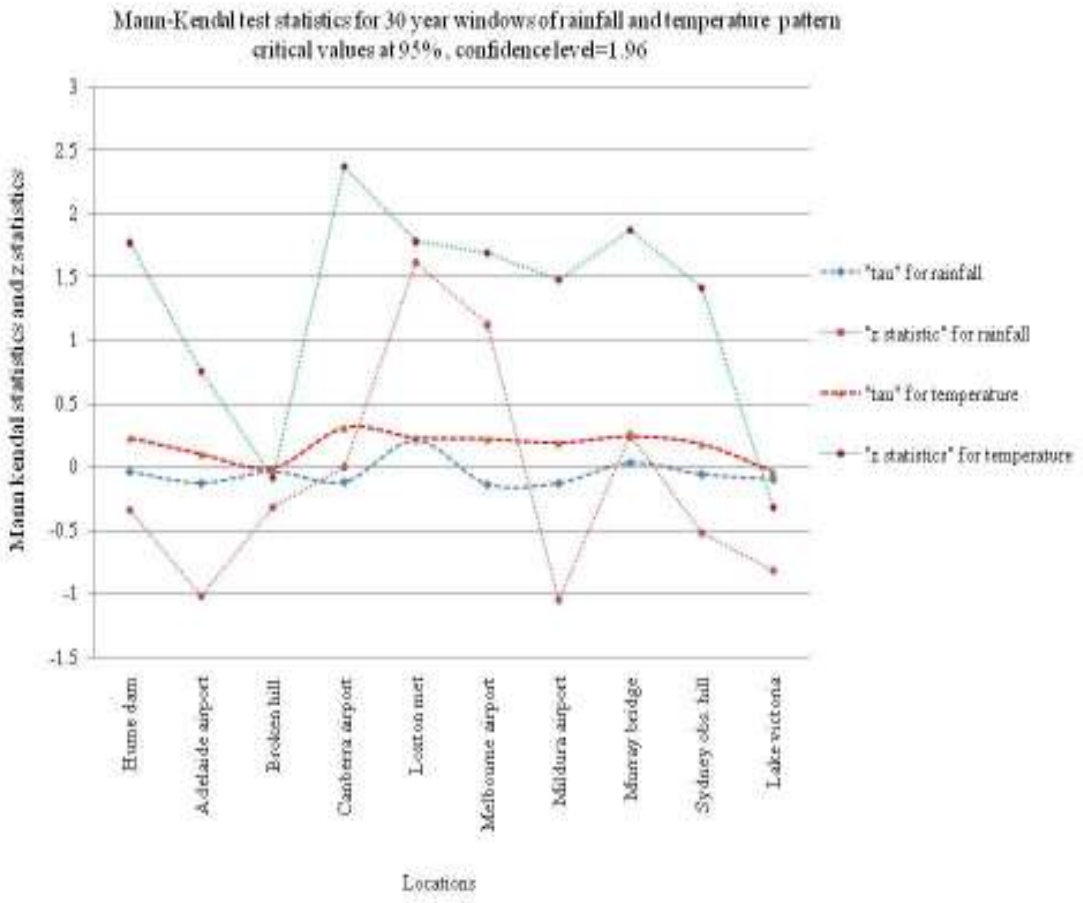

Figure 5. 5: Strength of association rainfall and temperature pattern at 30-years windows in the MDB and the eastern Australia

5.4. Discussion and conclusions

Climatic diversity and consequently, a key aspect of rainfall and temperature variability have been used to assess future water availability across the MDB areas and the eastern of the Australia. There is evidence of shifts in the underlying mean rainfall and temperature over the past hundred years. The analysis has reinforced the claim that the past ten years have been relatively dry and hot, but also highlighted the fact that similar anomalies have occurred in the past century. The rational for this study is that the characteristics of rainfall and temperature patterns must play the key role in the sustainable water resources planning and management. Nevertheless, there are scientific arguments to explain the recent changes, and it would be unwise to

suppose that they will be followed by a period of conditions closer to the long term average. In the short term climatic scenario (from 1997 to 2006), the mean monthly rainfall and temperature pattern over the Murray-Darling Basin (MDB) in particular, in Hume's Dam 53 mm monthly mean rainfall and 22 25^0C monthly mean temperature respectively stands out. This is 8.62 percent of rainfall lower than the 1900 to 2007 and 3.49 percent of temperature higher than the 1900 to 2007. The scenario of the rainfall and temperature pattern is only where the mean monthly rainfall and temperature over the past ten years are statistically significantly different from the long-term mean (significantly at 5% level). The scenario of the rainfall and temperature pattern using box plot shows clear seasonal variability in the MDB area and in the eastern of Australia. The statistical significance depends on the difference between the 10 years, 20 years and 36 years, and 107 years mean monthly rainfalls and temperature. Furthermore, there is an evidence of the inter-annual rainfall and temperature variability. The climate scenario is used to assess the range of possible temporal and spatial variability from 1900 to 2007. The tree diagram has been used to categories the similarities of rainfall and temperature are patterns in terms of temporal and spatial variability using different height values. Non-parametric Mann Kendal tests were used to assess the strength of association between 30-years, 60-years and 90-years windows for rainfall and temperature patterns no statistically significant evidence of trend was found.

This study pointed out the characteristics the rainfall and temperature variability by statistical tools at different temporal scales in the MDB areas and the eastern of Australia. Rainfall followed a decreasing pattern, whereas temperature followed an increasing pattern in both the long term and the short term. Non parametric statistical tests showed that there was no evidence of trend between the rainfall and temperature patterns in the MDB areas. The relationship between rainfall and temperature was negative. The increasing trend of temperature could further reduce rainfall in the MDB areas. Moreover, this study provided evidence of the temporal and spatial variation of rainfall and temperature patterns. Projecting rainfall and temperature patterns for future water availability in the MDB areas, this study provided a recommendation for minimizing temporal and spatial variability.

i. **Minimize spatial variation**: The height values from 0 to 2.587 represent the spatial variation as shown in Figure 5.3. Considering height value 2.587 would be convenient way to minimize the spatial variation and furthermore develop strategies for future water availability in the MDB areas.

ii. **Minimize temporal variation**: the height values from 0 to 1.18 represent temporal variation as shown in Figure 5.4. Considering the height value 1.18 could minimize the temporal variation in rainfall and temperature pattern in the MDB areas.

It is recommended to assess rainfall and temperature patterns and in addition examine how the rainfall and temperature patterns are influenced by relevant CIs across the MDB areas. In the next phase of this research will identify CIs and their interaction effect on rainfall and temperature pattern across the MDB area and the eastern of Australia. Furthermore, the research will identify the statistical evidence of distance dependency and the evidence of mathematical persistency.

CHAPTER 6: CLIMATIC INFLUENCE ON RAINFALL AND TEMPERATURE

6.1. Introduction

The El Niño-Southern Oscillation (ENSO) phenomenon is the primary global mode of climate variability in the 2 to 7-year time bands (IPCC, 2007, Ropelewski, and Halpert, 1987, 1996, Kiladis and Diaz, 1989, Chiew *et. al.,* 1998). In particular, the ENSO phenomenon has been linked to climatic variability in Australia (BoM, 2008). ENSO occurs as a result of large scale change or fluctuations in an atmospheric and ocean circulation process in equatorial regions of the Pacific Ocean. Such circulation changes are the main cause of variations in both sea surface temperatures (SST) in the equatorial Pacific and in sea level pressure (SLPs) in the southern Pacific. The Pacific Ocean signatures, El Niño and La Niña, follow temperature fluctuations in surface waters of the tropical Eastern Pacific Ocean (Bates *et al*., 2008). In Australia, the Southern Oscillation Index (SOI), which is the normalized difference between monthly sea level pressures in Tahiti and Darwin, is generally used to define El Niño and La Niña conditions (Troup, 1965). Values of SOI below -1 correspond to El Niño conditions, which are known to be associated with reduced rainfall in the east of Australia, and values above +1 correspond to La Niña conditions, which are associated with increased rainfall. Furthermore, there is evidence that the effects of El Niño in the east of Australia is modulated by the Pacific Decadal Oscillation (PDO), which is based on anomalies in the sea surface temperature throughout the Pacific, and that rainfall tends to be further reduced if an El Niño coincides with negative PDO (Whiting *et al.* 2003).

It is important to examine relationships between climate indices and their impacts on weather patterns in major agricultural production areas such as the MDB in Australia. These impacts can be analyzed using a number of hydrological methods. One objective is to use regression based analysis of climatic indices and to investigate their influence on rainfall and temperature patterns in the MDB areas. In this chapter, this study will identifies relevant CIs and highlights their influence on rainfall and temperature phenomena in the MDB areas and eastern Australia will be highlighted.

6.2. Study approach

The Southern Oscillation Index (SOI) and various indices of SST are the most widely used as ENSO indicators. The monthly SST indices to be used in this study were summarized in the Chapter 2. The association between CIs calculated on a monthly basis, including the El Niño Southern Oscillation (ENSO), and monthly rainfall and temperature pattern in the MDB during the period 1957 to 2007 is investigated. The indices considered are El Niño 1+2, Niño 3, Niño 4, and Niño 3.4, the Dipole Mode Index (DMI), Northern and Southern Atlantic Oscillation, Global tropics, Southern Annular Mode (SAM), Southern Oscillation Index (SOI), and PDO. As previously noted definitions of these indices, in terms of ocean temperatures and pressures are provided in the Chapter 2. A RM representing CIs with periodic functions is used to allow for seasonal variation, and the RS are examined for evidence of non-stationarity over the study period. The GLS are used to allow for the effect of autocorrelation when estimating the standard error of the regression parameters. Any estimated trend is removed from the RS which are then analysed as a multivariate time series to highlight the dependence structure between indices. The Correlograms and Cr-C are used to determine whether there is an autocorrelation in the series. This would require a further model. A variety of regression techniques will be compared for assessing the influence of CIs on monthly rainfall and on monthly temperature pattern in the MDB areas and the eastern Australia. Possible interaction effects of the CIs will be included. The PCA will be employed to reduce the number of climatic predictors. The statistical tools are displayed in R routine version 2.10.0. To facilitate the time series analysis, the missing values are replaced by series means, using SPSS Version 17.

6.3. Results analysis

6.3.1. Time series analysis of CI

The 11 CIs from the Pacific, Atlantic and Indian Ocean, are plotted for the period 1960-2007 as time series, they clearly show seasonality in Figure 6. 1.

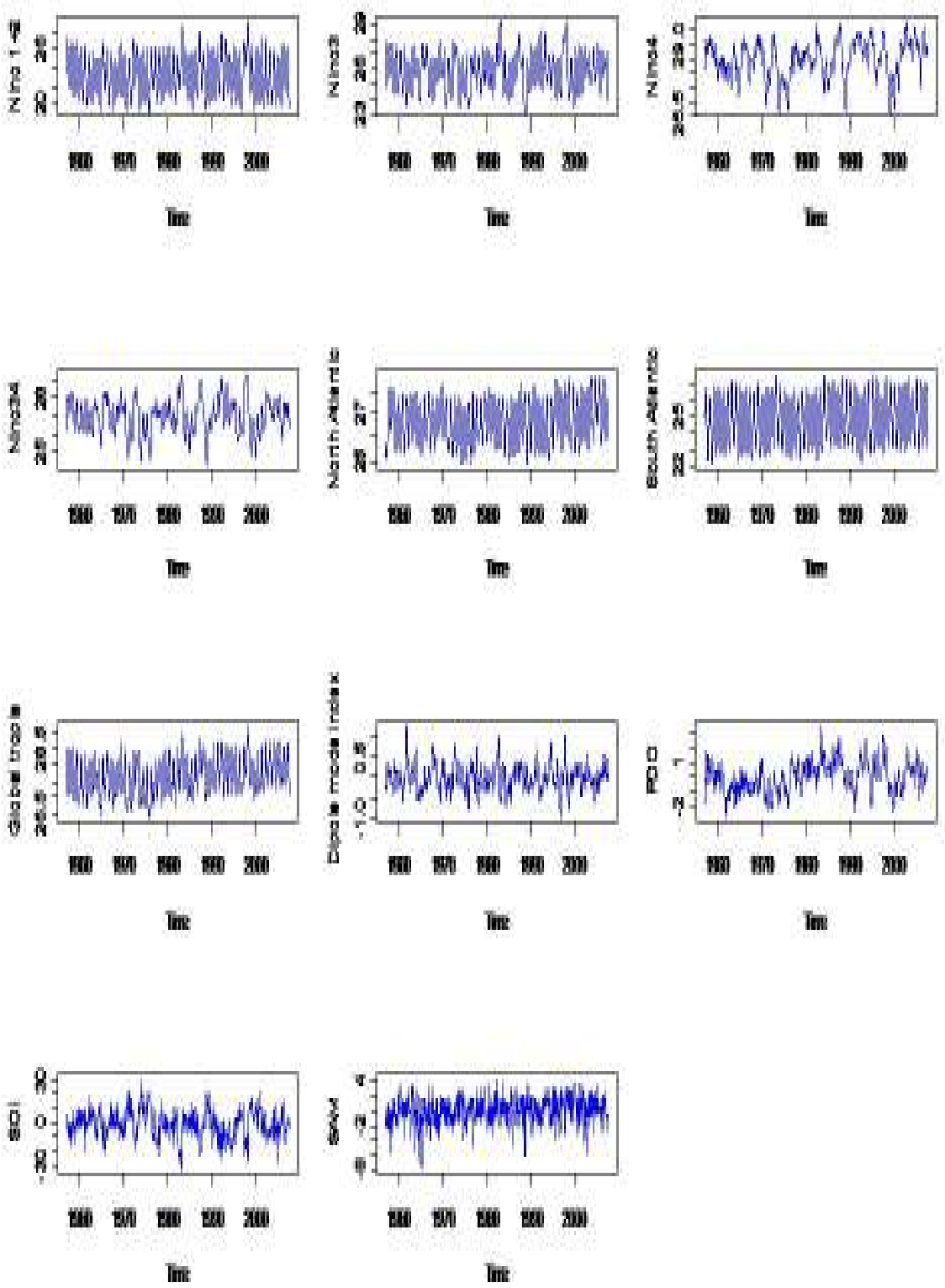

Figure 6. 1: Climatic indicators times series plots from 1960-2009.

6.3.2. Correlation pattern of ENSO in the Pacific Ocean

The correlations (lag 0 cross-correlations) and their statistical significances between the CIs are shown in Table 6.1.

Table 6. 1: Correlation between CIs with statistical significance test results

	NINO12	NINO3	NINO4	NINO3.4	NATL	SATL	TROP	DMI	PDO	SOI	SAM
NINO12	1										
NINO3	.801**	1									
NINO4	.031	.446**	1								
NINO3.4	.426**	.851**	.797**	1							
NATL	-.767**	-.481**	.297**	-.082*	1						
SATL	.835**	.626**	-.151**	.221**	-.839**	1					
TROP	.744**	.864**	.396**	.682**	-.454**	.759**	1				
DMI	.111**	.179**	.179**	.194**	-.036	.037	.134**	1			
PDO	.241**	.371**	.331**	.393**	.024	.084*	.332**	-.011	1		
SOI	-.247**	-.479**	-.651**	-.649**	-.040	-.010	-.352**	-.187**	-.342**	1	
SAM	-.049	-.064	-.048	-.087*	.063	-.025	-.004	.078	-.004	.031	1

*coefficients are statistically significant at the 5% level
**coefficients are statistically significant at the 1% level
***coefficients are statistically significant at the 0.1% level

The strength of the relationship in the Pacific Ocean indices, and Atlantic and Indian Ocean indices, showing significant evidence are starred marked in Table 6.1. There are reasonably high correlations $(r = 0.8)$ between Niño1+2 and Niño3, Niño3 and Niño3.4 and Niño4 and Niño3.4. The correlations between Niño1+2 and Niño3.4 are moderate $(r = 0.4)$ but the most surprising finding is the low correlation $(\mathrm{r} = 0.03)$ between Niño1+2 and Niño4. The Atlantic Ocean group including the North and South Atlantic and Global tropics indices, are substantially correlated (e.g. r = 0.76 for the Global Tropics with the South Atlantic index. The Pacific Ocean group indices including Niño1+2, Niño3, Niño4 and Niño3.4 indices area moderately correlated with the Global Tropics index. The DMI in the Indian Ocean shows only a

weak correlation $(r < 0.20)$ with the Pacific Ocean indices and weak correlation $(r < 0.13)$ with the Atlantic indices. The correlation between the PDO and SOI are negative $(r = -0.342)$ and significantly correlated $(r > 0.23)$ between the PDO and Pacific indices. Moreover, there is a weak correlation between PDO, SOI and the Atlantic indices. There is no evidence that SAM is correlated with any of the other indices. Scatter plots of Niño1+2 against all the other indices expect SAM are shown in Figure 6.2 and a similar snapshot is given in Appendix 6.1 for all climatic indicators.

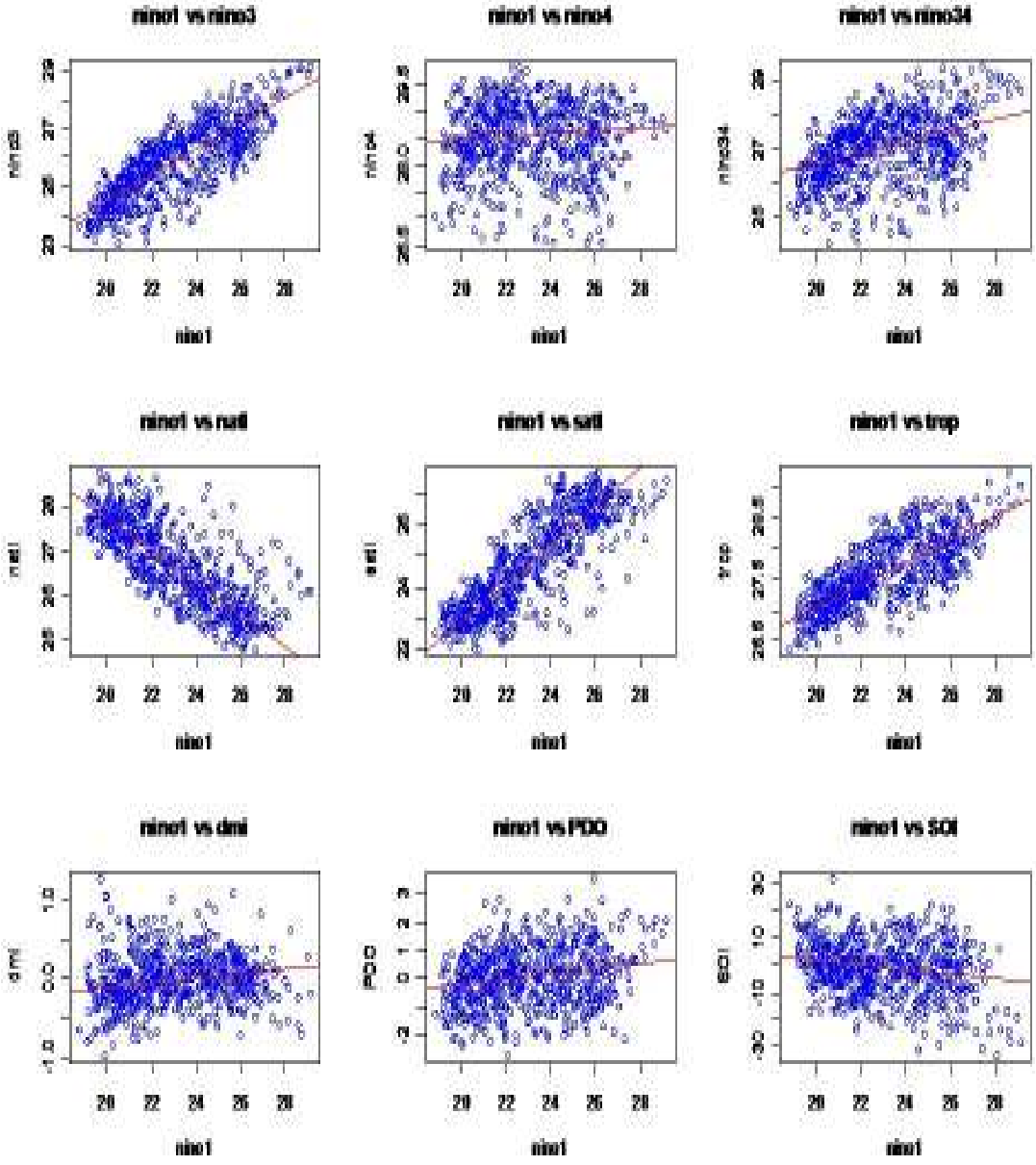

Figure 6. 2: Correlation plots between the selected CIs

6.3.3. Detected trends in CI with periodic function with one year

The time series plots suggest a slight negative trend in monthly SOI over the period, but if a RM is fitted this is not found to be statistically significant. For example, fitting a regression including linear and quadratic terms and a sinusoid of period one year gives:

$$\text{SOI} = -1.337 - 0.00724 * (t - 304.5) + 0.00000006 * (t - 304.5)^2 - 0.05808 * \cos(2\pi t/12) + 0.0735 * \sin(2\pi t/12)$$

where t is time in months from January 1957 and runs from 1 up to 608 with mean value 304.5. Details are shown in Appendix 6.2. It is important to allow for autocorrelation in RS when estimating standard deviations of estimations of coefficients. Otherwise, in the case of positive autocorrelations, statistical significance will be exaggerated. So the estimated standard deviations of the estimations of the coefficients are calculated using generalised least squares (Cowpertwait and Metcalfe, 2009) with the errors modelled as AR(1) with auto regression coefficient equal to 0.63 for SOI as shown in Table 6.2. The value of $\alpha = .644$ is estimated from the correlogram of the RSs from the regression. The estimated standard deviations of the coefficients in the regression for SOI are: 0.005064, 0.000032, 0.57158, 0.824328, and 0.822379 respectively. It follows that none of the estimated coefficients is significantly different from 0 at even the 10% significance level. For example, the t-ratio for the coefficient of (t-304.5) is -0.0071809 divided by .0.0050638 which equals -.1418547. A similar analysis of the PDO, using generalised least squares with the errors modelled as AR (1) with auto regression equal to 0.803, gives:

$$PDO = 0.226553 + 0.001658 * (t - 304.5) - 0.000005 * (t - 304.5)^2 + 0.219726 * \cos(2\pi t / 12) + 0.067282 * \sin(2\pi t / 12)$$

The estimated standard deviations of the estimators of the three coefficients in the regression PDO is: 0.000710, 0.000004, 0.066001, and 0.065966 respectively, so there is no evidence of a linear trend even at the 10% significance level. All other indices are shown in Appendix 6.2. A generalised linear least square method with first order auto regressive order AR [1], was applied to realise the RM with one periodic function. The statistically significant evidence of any trend at 5% level is shown in the Table 6.2 for 11 climatic indicators.

Table 6. 2: GLS model of CIs by linear quadratic term fitted with one year periodic function

i.) Coefficient of regression

GLS	coefficient	Niño1+2	Niño3	Niño4	Niño3.4	N Atl	S Atl	G Tropic	DMI	PDO	SOI	SAM
estimated	Alpha	0.891214	0.916531	0.933504	0.931771	0.816713	0.788156	0.786393	0.795027	0.815861	0.644710	0.216527
	AR(1)	0.879000	0.903000	0.924000	0.920000	0.800000	0.777000	0.772000	0.786000	0.806000	0.636000	0.208000
Intercept	β_0	23.173460	25.866906	28.390873	26.997586	26.572880	24.802912	27.592730	-0.002527	0.226553	-1.379905	-0.121606
(t-304.5)	β_1	0.000194	0.000334	0.000605	0.000163	0.000594	0.000885	0.000908	0.000051	0.001658	-0.007181	0.001753
$(t-304.5)^2$	β_2	-0.000004	-0.000003	0.000003	0.000000	0.000004	-0.000001	0.000001	0.000000	-0.000005	0.000009	0.000000
Cosine	β_3	1.976310	1.201999	0.005634	0.556214	-0.851841	1.510362	0.514886	-0.005797	0.219726	-0.749904	-0.057412
Sine	β_4	-2.093577	-0.376963	0.234816	0.160222	0.825054	-1.368877	-0.254708	-0.021954	0.067282	-0.288513	0.073172
Est. Std. error	coefficient	Niño1+2	Niño3	Niño4	Niño3.4	N Atl	S Atl	G Tropic	DMI	PDO	SOI	SAM
Intercept	β_0	0.292036	0.278579	0.215667	0.295897	0.071708	0.070145	0.061216	0.061034	0.189575	1.340858	0.135925
(t-304.5)	β_1	0.001082	0.001024	0.000786	0.001079	0.000269	0.000263	0.000230	0.000229	0.000710	0.005064	0.000516
$(t-304.5)^2$	β_2	0.000007	0.000006	0.000005	0.000007	0.000002	0.000002	0.000001	0.000001	0.000004	0.000032	0.000003
Cosine	β_3	0.060704	0.044497	0.027499	0.038700	0.024855	0.027866	0.024507	0.023514	0.066001	0.824328	0.122718
Sine	β_4	0.060731	0.044531	0.027526	0.038737	0.024842	0.027842	0.024485	0.023495	0.065966	0.822379	0.122316

ii) Significant test of regression model

t-value	Coefficient	Niño1+2	Niño3	Niño4	Niño3.4	N.Atl	S.Atl	G.Tropic	DMI	PDO	SOI	SAM
Intercept	β_0	79.351310	92.852930	131.64196	91.239680	370.56880	353.5970	450.7433	-0.041411	1.195056	-1.029121	-0.894653
(t-304.5)	β_1	0.179550	0.326320	0.770240	0.150780	2.211800	3.361800	3.948600	0.224056	2.334655	-1.418088	3.398916
$(t-304.5)^2$	β_2	-0.648480	-0.440020	0.525340	-0.059110	2.538400	-0.615100	0.774300	0.083962	-1.152028	0.269706	0.006735
Cosine	β_3	32.556520	27.013270	0.204890	14.372440	-34.2721	54.200300	21.009900	-0.246542	3.329113	-0.909716	-0.467839
Sine	β_4	-34.472880	-8.465180	8.530770	4.136130	33.211800	-49.1666	-10.40280	-0.934423	1.019958	-0.350827	0.598225
p-value	coefficient	Niño1+2	Niño3	Niño4	Niño3.4	N.Atl	S.Atl	G.Tropic	DMI	PDO	SOI	SAM
Intercept	β_0	0.000***	0.000***	0.000***	0.000***	0.000***	0.000***	0.000***	0.967	0.232	0.303	0.371
(t-304.5)	β_1	0.857	0.744	0.442	0.880	0.027*	0.000***	0.000***	0.823	0.01**	0.157	0.000***
$(t-304.5)^2$	β_2	0.517	0.660	0.600	0.953	0.011**	0.539	0.439	0.933	0.250	0.788	0.995
Cosine	β_3	0.000***	0.000***	0.838	0.000***	0.000***	0.000***	0.000***	0.805	0.001	0.363	0.640
Sine	β_4	0.000***	0.000***	0.000***	0.000***	0.000***	0.000***	0.000***	0.351	0.308	0.726	0.550

*coefficients are statistically significant at the 5% level
**coefficients are statistically significant at the 1% level
***coefficients are statistically significant at the 0.1% level

From Table 6.2, the climatic indicators show strong correlation $(r \geq 0.636)$ under AR [1] process except the Southern Annular mode $(r = 0.208)$. an, it has been shown that there is a statistically significant evidence of a linear trend at 0.01% level. Moreover, the RM is well fitted $(R^2_{adj} \geq 0.6)$ as shown in Appendix 6.2. There is no evidence of second order polynomial trend, except the North Atlantic Ocean during 1957-2007. There is statistical evidence of seasonality in all 11 CIs.

6.3.4. Deseasonalized and Assessment of trend

The 11 time series are plotted in Figure 6.1 and correlations between indices are shown in Table 6.1. There is a clear seasonal variation for at least some of the indices and in order to assess evidence of a trend, RMs are fitted with three periodic functions to allow for seasonal variation and linear and quadratic terms to allow for any trend.

The general formula is given by.

$$Y_t = \beta_0 + \beta_1 * C_1 + \beta_2 * S_1 * \beta_3 * C_2 + \beta_4 * S_2 + \beta_5 * C_3 + \beta_6 * S_3 + \beta_7 * (t - \bar{t}) + \beta_8 * (t - \bar{t})^2 + \varepsilon_t \ldots \text{(A)}$$

Where t runs from 1 up to 608 and $\bar{t}$ is 304.5. Y_t is a rainfall or temperature series and

$$C_1 = \cos(2\pi * t/12), S_1 = \text{Sin}(2\pi * t/12), C_2 = \cos(2 * 2\pi * t/12), S_2 = \text{Sin}(2 * 2\pi * t/12),$$
$$C_3 = \cos(3 * 2\pi * t/12), S_3 = (3 * 2\pi * t/12),$$

An example of the fitted model is that for Nino1+2 shown below

$$\text{Ninol} + 2 = 23.0677 + 0.0924945 * C_1 + 2.8665 * S_1 - 0.2841 * C_2 + 0.09471 * S_2$$
$$- 0.1189237 * C_3 - 0.094301 * S_3 + 0.0002215 * (t - \bar{t})$$

In this case, the time series plot gives no indication of any trend, and neither of the trend terms are statistically significant. The results of fitting the RM (equation A) to the 11 CIs are summarized in Table 6.3. The intercept is the mean value, and the next rows give the standard deviation of the natural time series and the standard deviation of the RS. The RS is obtained by removing the seasonal effect and the linear and quadratic trends and is henceforth referred to as the deseasonalized – detrended time series. The standard deviations are followed by the coefficients of the linear and quadratic trends and their standard errors. The standard errors and associated P-values are given after allowing for the correlations of the error which have been modelled by the first order auto-regressive AR [1]. The coefficients of the AR [1] fitted to the RS are given in the final row of Table 6.3.

Table 6. 3: Standard deviations of natural and deseasonalized climatic indicators.

ENSO indices	NINO1.2	NINO3	NINO4	NINO3.4	NATL	SATL	TROP	DMI	PDO	SOI	SAM
Intercept	23.120	25.800	28.370	26.940	26.560	24.300	27.580	-0.004	0.218	-1.337	-0.122
Natural series Standard dev.	2.318	1.273	0.673	0.967	0.933	1.499	0.553	0.334	1.034	10.238	1.812
Deseasonalized Standard dev.	1.092	0.895	0.631	0.862	0.361	0.349	0.269	0.331	0.984	10.144	1.781
Co eff linear t	0.00022	0.00041	0.00070	0.00025	0.00058	0.00087	0.00091	0.00003	0.00157	-0.00724	0.00176
Est Standard error	0.00025	0.00021	0.00015	0.00020	0.00008	0.00008	0.00006	0.00008	0.00023	0.00236	0.00041
P-values	0.383	0.0484*	0.000***	0.2180	0.000***	0.000***	0.000***	0.679	0.000***	0.002**	0.000***
Co eff quadratic t	-0.0000019	0.0000005	0.0000036	0.0000023	0.0000051	-0.0000006	0.0000017	0.0000002	-0.0000047	0.0000064	0.0000001
Est Standard error	0.0000016	0.0000013	0.0000009	0.0000013	0.0000005	0.0000005	0.0000004	0.0000005	0.0000014	0.0000150	0.0000026
P-values	0.253	0.720	0.000***	0.068	0.000***	0.237	0.000***	0.723	0.001***	0.672	0.982
AR(1) coeff of residuals	0.902	0.922	0.937	0.936	0.88	0.849	0.936	0.736	0.807	0.636	0.208

*coefficients are statistically significant at the 5% level
**coefficients are statistically significant at the 1% level
***coefficients are statistically significant at the 0.1% level

Table 6.3, shows that the estimated standard deviations ($\tilde{\sigma}$) for the deseasonalized climatic series are substantially smaller than the standard deviation (s) of corresponding climatic series, So there is no reason to suspect occasional shifts in the mean process. From the RM under three period functions, there is strongly significant evidence of linear trend at 0.1% level in CIs in the Atlantic Ocean region, the El Nino Southern Oscillation (SOI) between Darwin, Australia and Tahiti and the PDO. There is also significant evidence of linear trend at 5% level in the Niño3 indices in the Pacific Ocean. Moreover, there is a linear even higher order polynomial trend in Niño4 indices in the Pacific Ocean, North Atlantic and Global Tropic indices in the Atlantic Ocean, and PDO in Darwin, Australia at 0.1% level.

6.3.5. Pre whitening with ARMA model and Cr-C model

The substantial correlations between CIs described. Indicators may be due, partially at least, to common trends and seasonal variation. In this section, investigate the Cr-C between climatic indicators after removing trend and seasonal variation and allowing for correlation structure. This process is known as pre-whitening. In principle, the pre-whitening climatic indicator series are the realisation of the independent random variation and can therefore be Cr-C at just one lag.

6.3.5.1. Fitting the ARMA model

The best fit Auto regressive moving average (ARMA) RM deseasonalized by the higher order sinusoid of one year period is defined in Equation (62). The RS from a RM was used to fit the ARMA model, and the RS appears to be a realisation of a stationary process and series being cointegrated. The best ARMA model chooses smallest Akaika information and the estimated square root of sigma. AIC is defined as

AIC = -2*Log likelihood + 2* number of parameter

Comparison of the AIC for the ARMA (1,0,1), ARMA (2,0,2) and ARMA (3,0,3) models are shown Table 6.4 and Appendix 6.3. It is clear there is a little difference and that the ARMA (3, 0, 3) model would be satisfactory except for the fact that Nino1+2 and the Southern Oscillation index (SOI) would be best fitted with the ARMA(2,0,2) model, and the best fitted model marked bold in Table 6.4.

Table 6. 4: Best fit ARMA model for climatic indicators.

Model	(p,d,q)	AR(1)	AR(2)	AR(3)	MA(1)	MA(2)	MA(3)	Intercept	Estimated σ^2	Loglikehood	AIC
Nino1+2	(1,0,1)	0.874			0.1653			-0.032	0.2159	-397.57	803.14
	(2,0,2)	1.847	-0.866		-0.819	-0.099		-0.0238	**0.2108**	**-390.46**	**792.92**
	(3,0,3)	1.3538	0.0443	-0.426	-0.3251	-0.497	-0.057	-0.0241	0.2108	-390.44	796.88
Nino3	(1,0,1)	0.8643			0.3205			-0.0277	0.129	-241.13	490.25
	(2,0,2)	0.2592	0.4902		0.9711	0.3273		-0.025	0.1263	-234.67	481.34
	(3,0,3)	1.1468	0.4048	-0.582	0.0679	-0.669	-0.291	-0.0187	**0.1234**	**-227.69**	**471.39**
Nino4	(1,0,1)	0.9252			0.0757			-0.0007	0.05166	37	-66.01
	(2,0,2)	1.8202	-0.84		-0.8266	0.0119		-0.0089	0.05061	43.19	-74.37
	(3,0,3)	-0.256	0.1353	0.892	1.2736	1.0412	0.0485	-0.005	**0.05051**	**43.39**	**-70.79**
Nino3.4	(1,0,1)	0.8895			0.2797			-0.0191	0.1014	-168.06	344.13
	(2,0,2)	0.7212	0.1178		0.4889	0.2023		-0.0165	0.09913	-161.16	334.32
	(3,0,3)	0.8638	0.9755	-0.876	0.3245	-0.897	-0.25	-0.0182	**0.0958**	**-151.24**	**318.47**
North Atlantic	(1,0,1)	0.7697			0.2755			-0.0037	0.04391	86.76	-165.5
	(2,0,2)	0.5473	0.0663		0.5515	0.3165		-0.0025	0.04227	93.28	-184.6
	(3,0,3)	1.9144	-1.914	0.914	-1.0151	0.9979	0.0011	-0.0064	**0.02896**	**208.97**	**-402**
South Atlantic	(1,0,1)	0.7359			0.3131			-0.0048	0.04982	48.42	-88.85
	(2,0,2)	0.6764	-0.097		0.4246	0.3271		-0.0036	0.04747	61.05	-114.1
	(3,0,3)	1.8595	-1.86	0.86	-0.9357	0.9437	0.0563	0.009	**0.03427**	**157.25**	**-298.5**
Global Tropic	(1,0,1)	0.7222			0.6503			-0.0044	0.02917	210.82	-413.6
	(2,0,2)	0.9003	-0.365		0.6993	0.397		-0.0021	0.02259	288.07	-564.1
	(3,0,3)	1.9425	-1.943	0.942	-0.8409	0.8465	0.1458	-0.0046	**0.00865**	**574.56**	**-1133**
DMI	(1,0,1)	0.6804			0.9706			-0.0001	0.01812	354.38	-700.8
	(2,0,2)	0.4746	-0.123		1.7952	0.8739		0.0001	0.01118	499.73	-987.5
	(3,0,3)	0.1664	-0.318	0.557	2.3702	2.2315	0.8117	-0.0007	**0.00667**	**654.40**	**-1295**
SAM	(1,0,1)	0.5677			-0.3696			-0.0021	3.076	-1204.3	2416.6
	(2,0,2)	0.2116	0.3948		0.0206	-0.404		-0.0036	3.038	-1200.6	2413.2
	(3,0,3)	1.3368	-0.667	-0.078	-1.1199	0.3934	0.2978	-0.0028	**2.993**	**-1196.2**	**2408.4**
PDO	(1,0,1)	0.821			0.0134			-0.0096	0.334	-529.94	1067.9
	(2,0,2)	1.5944	-0.612		-0.7664	-0.09		-0.0107	0.3301	-526.38	1064.8
	(3,0,3)	0.464	-0.704	0.821	0.3714	1.0067	0.0194	0.0064	**0.3279**	**-526.23**	**1068.5**
SOI	(1,0,1)	0.8741			-0.4275			0.0346	56.2	-2087.9	4183.8
	(2,0,2)	1.7938	-0.825		-1.3937	0.4947		0.0533	**55.42**	**-2083.7**	**4179.3**
	(3,0,3)	-0.302	0.039	0.862	0.747	0.4888	-0.41	-0.0257	56.00	-2086.9	4189.7

6.3.5.2. Correlogram and Cr-C analysis

The correlograms in Figure 6.3 suggest that the RS of the fitted ARMA model have significantly small autocorrelation in Niño3 and Niño4 indices with the ARMA(3,0,3) and partial autocorrelation in a Niño3 and Niño4 indices with ARMA(3,0,3) model do not constitute a significant improvement. This is consistent with a realisation of white noise and supports the use of the ARMA (3,0,3) model except for the Nino1+2 indices and SOI, where for ARMA (2,0,2) is preferable.

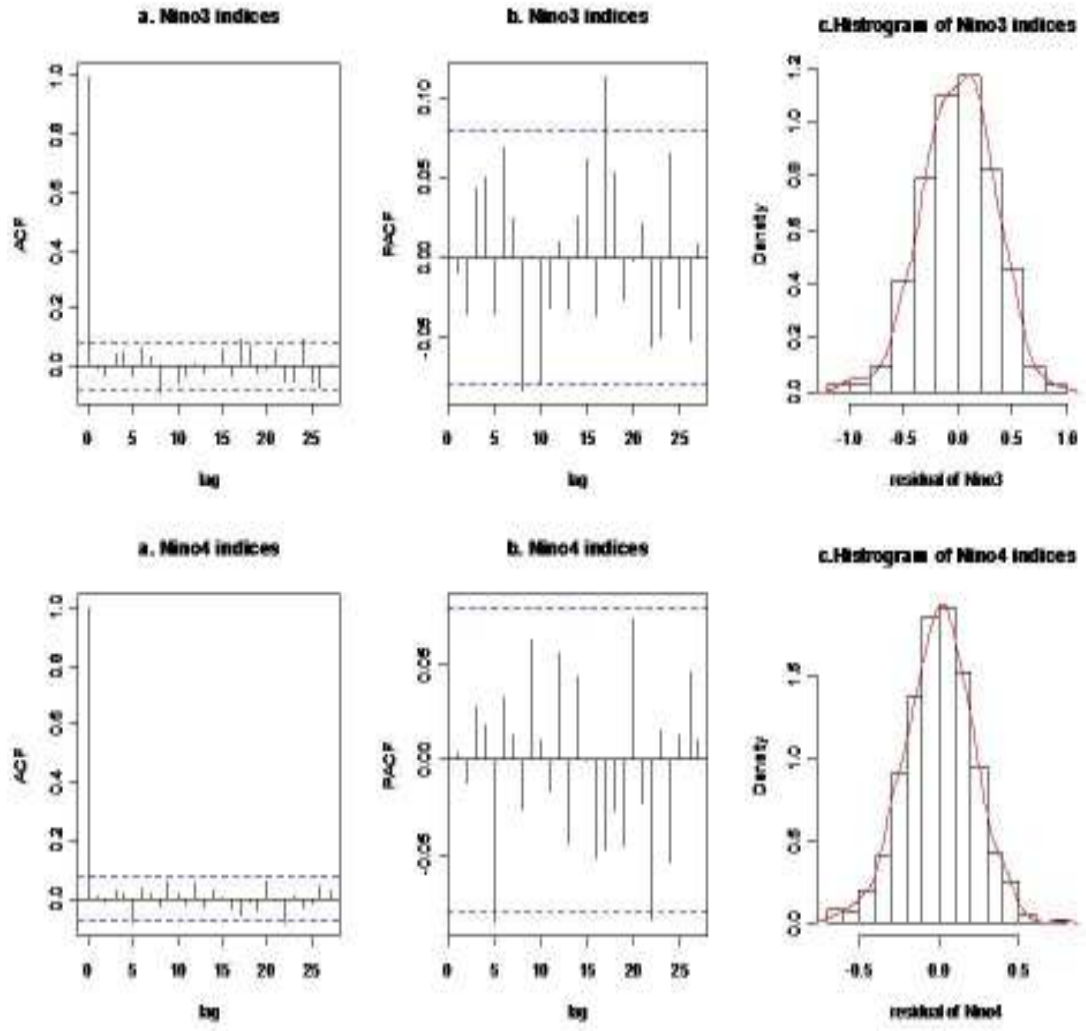

Figure 6. 3: The correlogram of the RS for the ARMA (3, 0, 3) model fitted to the Nino 1+2(upper row) and Nino3 (bottom rows) indices a) Autocorrelation b) partial autocorrelation and c) Histogram from 1957-2007

It is verified that the Cr-C for white noise series (11 CIs $^{11}C_2 = 55$) is approximately zero for all non zero lags shown in Appendix 6.5 and CCF lag 0 shown in Table 6.5. Separated ARMA models were fitted to multiple time series variables so that the RS of fitted model appear to be a realisation of multivariate white noise. The method worked well suggesting that multiple time series have no common stochastic trends and the Cr-C structure is restricted to the error process.

Table 6. 5: Cr-C pre-whitening climatic indicator series and lag (bracket)

	NINO1.2	NINO3	NINO4	NINO3.4	NATL	SATL	G. TROP	DMI	PDO	SOI	SAM
NINO1.2	1.000										
NINO3	0.395 (0)	1.00									
NINO4	0.031(0)	0.201 (0)	1.00								
NINO3.4	0.088 (0)	0.766 (0)	0.510 (0)	1.00							
NATL	-0.024 (0)	0.003 (0)	0.049 (0)	0.025 (0)	1.00						
SATL	0.010 (0)	0.103 (0)	0.075 (0)	0.082 (0)	0.036 (0)	1.00					
G. TROP	0.365 (0)	0.673 (0)	0.532 (0)	0.673 (0)	0.127 (0)	0.301(0)	1.00				
DMI	0.098 (0)	0.71 (0)	-0.032 (0)	0.030 (0)	0.055 (0)	0.059 (0)	0.060 (0)	1.00			
PDO	0.092 (0)	0.040 (0)	-0.058 (0)	0.014 (0)	0.115 (0)	0.010 (0)	0.039 (0)	0.040 (0)	1.00		
SOI	-0.078 (0)	-0.035 (0)	-0.098 (0)	-0.084 (0)	-0.106 (0)	-0.003 (0)	-0.091 (0)	-0.081 (0)	-0.021 (0)	1.00	
SAM	-0.019 (0)	-0.027 (0)	-0.026 (0)	-0.043 (0)	-0.002 (0)	-0.079 (0)	-0.094 (0)	0.084 (0)	-0.021 (0)	-0.043 (0)	1.00

6.3.6. Factor analysis

The inter-correlations between the climatic indicators were calculated by the Pearson correlation coefficient and shown in Table 6.1. Table 6.1, provides the evidence that El Nino3 indices in the Pacific Ocean are significantly correlated ($r > 0.8$ with $\alpha < 0.001$) with Niño1+2, and Niño3.4 indices in the Pacific Ocean and the Global Tropic index in the Atlantic Ocean. Furthermore, there is evidence of strong correlation ($r = 0.84$ with $\alpha < 0.001$) between the Northern and Southern Atlantic indices in the Atlantic Ocean, shown in Table 6.1. The deterministic value is 0.00000508, which is significantly lower than 0.00001. This study indicates a multicollinearity and singularity problem in the factor analysis. To avoid this problem, the extreme multicollinearity of Niño1+2, Niño3.4, and the Global Tropics and Northern Atlantic indices has been eliminated for factor analysis and modified correlation matrix is shown in Table 6.6.

Table 6. 6: Modified Climatic indicators for assessing the correlation pattern.

Climatic Indicators	NINO3	NINO4	SATL	DMI	PDO	SOI	SAM
NINO3	1.000						
NINO4	.446	1.000					
SATL	.626	-.151	1.000				
DMI	.179	.179	.037	1.000			
PDO	.371	.331	.084	-.011	1.000		
SOI	-.479	-.651	-.010	-.187	-.342	1.000	
SAM	-.064	-.048	-.025	.078	-.004	.031	1.000
Sig. test							
NINO3							
NINO4	.000***						
SATL	.000***	.000***					
dmi	.000***	.000***	.180				
PDO	.000***	.000***	.019**	.391			
SOI	.000***	.000***	.406	.000***	.000***		
SAM	.057*	.120	.269	.028	.457	.220	

*coefficients are statistically significant at the 5% level
**coefficients are statistically significant at the 1% level
***coefficients are statistically significant at the 0.1% level

Table 6.6, presents the modified the correlation patterns between climatic indicators, which are shown significantly correlated ($r < 0.8$ with $\alpha < 0.05$) with climatic indicators included. The determinate value is 0.118 which is significantly greater than 0.00001. This study indicates that modified climatic indicators have no multicollinearity and to singularity. KMO and Bartlett's statistics were used, to check the adequacy of factor analysis. The KMO statistic value is .551, indicating reasonable confidence in factor analysis for these data. Bartlett's test shows high significance ($p < 0.0001$) and therefore factor analysis is appropriate.

6.3.6.1. Factor extraction by the principal component method

The eigenvalue associated with each component (factor) before extraction, after extraction and after rotation is shown in Table 6.7. SPSS identified seven linear components within the data set. The eigenvalue associated with each factor represent the variance exhibited by that particular linear component (factor).

Table 6. 7: The eigenvalues in terms of the percentage variance accounted for factor analysis

Total Variance Explained									
Component (Column 1)	Initial eigenvalues (Column 2)			Extraction Sums of Squared Loadings (Column 3)			Rotation Sums of Squared Loadings (Column 4)		
	Total (a)	% of Variance (b)	Cumulative of % (c)	Total (a)	% of Variance (b)	Cumulative of % (c)	Total (a)	% of Variance (b)	Cumulative of % (c)
1	2.447	34.959	34.959	2.447	34.959	34.959	2.215	31.641	31.641
2	1.377	19.669	54.628	1.377	19.669	54.628	1.587	22.677	54.318
3	1.077	15.381	70.009	1.077	15.381	70.009	1.098	15.691	70.009
4	.942	13.451	83.460						
5	.657	9.379	92.839						
6	.351	5.019	97.858						
7	.150	2.142	100.000						

Extraction Method: Principal Component Analysis.

In Table 6.7, factor 1 account for 34.959% of total variance of the CIs, whereas subsequent factors are account for only small amounts of variance. In this study, the entire factors with eigenvalues greater than 1 were extracted. This revealed three factors of the CIs. The eigenvalues associated with these three factors are displayed in Column 2, by extraction of sums of squared loadings. The values in column 3 are the same as the values before extraction in column 2, except that the values for the

discarded factors are ignored. (Hence, the rows in Column 3 are blank after three factors). In Column 4 of Table 6.7, after rotation of sums of the squared loadings, the new eigenvalues of the factors are displayed. Rotation has the effect of optimizing the factor structure and one consequence for these data is that the relative importance of the three factors is equalized. Before rotation, factor 1 in Column 3(b), accounted for considerably more variance than for the remaining two (34.959% compared to 19.669 and 15.381% respectively). However, after extraction, it accounts for only 31.641% of the variance (compared to 22.677 and 15.691% respectively) in column 4(b).

A Scree plot is shown below with the arrow indicating the point of inflexion on the curve. The curve begins to tail off after three factors but there is still a further drop after the three factors before a stable level is reached. It is safe to assume Kaiser's Criteria.

Figure 6. 4: Scree plot of the principal component analysis

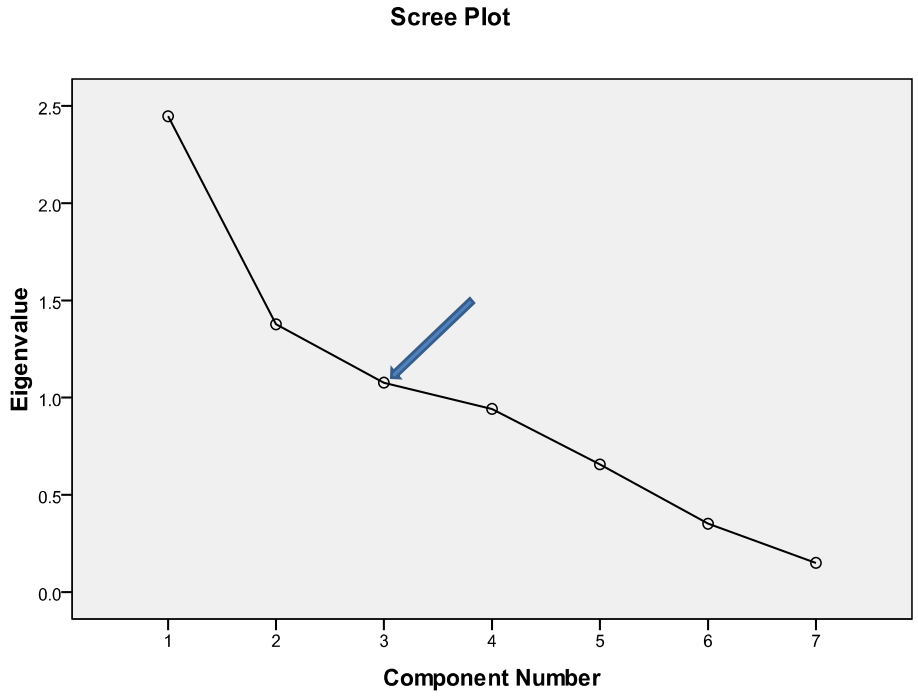

Using the SPSS package Version 17, applied Kaiser Criterion statistics were applied and verifying the factors, which are now explanatory tools,

6.3.7. RM for rainfall and temperature series

A RM was fitted to determine whether the CIs and their interaction effects are significantly influencing the rainfall and temperature patterns in the MDB areas and eastern Australia. A linear, and a quadratic term (mean adjusted) and a sinusoidal of period one a year were included in the RM 1. It was then extended by seasonal indicators from January to November, with December is relative to others, and the sinusoidal of the period one year excluded in RM 2. No evidence of improvement in model 2 is shown is Table 6.8. The influence of CIs is given in detail in Appendix 6.6 and Appendix 6.7. The estimated regression line for rainfall and temperature patterns with the sinusoidal of a period one year are given in Appendix 6.6a and 4 7a. The similar regression line for rainfall and temperature with seasonal indicator from January to November included are shown in Appendix 6.6b and 4.7b. Significant levels are marked by (*).

From RM 1, including the sinusoidal with the period one year, there is a statistically significant evidence of SOI influence on rainfall for all locations in the MDB area and eastern Australia are shown in Appendix 6.6 (a), and slight evidence in the temperature pattern, have shown in Appendix 6.7 (a) at 5% level even 1% level.

Consider now the seasonal indicators from January to November, fitted in RM 2 for rainfall and temperature series. In the case of temperature patterns, there is a significant evidence of a decreasing trend from April to November in six weather stations in the MDB, and four weather stations in the eastern capital cities in Australia. There is a slightly significant evidence of a seasonally increasing trend on rainfall patterns at the Adelaide Airport station from May to October, and some evidence at Hume Dam from May to June, and at Loxton Met station and Murray Bridge from July to October, as shown in Appendices 6.6 (b) and 4.7 (b).

Considering both in terms of the sinusoidal of period one a year and seasonal effects from January to December, this study provided evidence that the rainfall has an increasing trend of SOI influence. Recently, the SOI influence has been decreasing in temperature patterns at 5% significance level. Moreover, there is significant evidence of a decreasing trend of DMI influence on rainfall and temperature patterns at 5% level. There is also weak evidence of Niño1+2, Niño3, Niño4, Niño3.4, South and North Atlantic indices, Global Tropic index and SAM influence on rainfall and temperature pattern in the MDB areas and eastern Australia.

Models 1 and 2 demonstrated variability of rainfall and temperature patterns in the sinusoidal of a period one year, which is close to the seasonal variation of rainfall and temperature in the MDB areas and the eastern Australia. Furthermore, that the CIs were highly influential in temperature patterns rather than the rainfall pattern is provided in Table 6.8.

Table 6. 8: Application of RM for rainfall and temperature series in MDB areas and the eastern Australia

Rainfall	Model 1			Model 2			Model 3			Model 4			Model 5			Model 6		
	DF	std	R^2_{adj}	DF	std	R^2_{adj}	DF	std	R^2_{adj}	DF	std	R^2_{adj}	DF	std	R^2_{adj}	DF	std	R^2_{adj}
Adelaide Airport	590	23.53	0.292	581	23.53	0.292	535	27.89	0.356	578	23.14	0.315	595	23.59	0.289	586	23.44	0.297
Broken Hill	588	28.17	0.074	579	28.11	0.078	533	27.96	0.088	580	28	0.085	593	28.45	0.055	584	28.41	0.058
Canberra Airport	590	36	0.120	581	36.08	0.116	535	35.4	0.149	581	36.11	0.104	595	36.83	0.079	586	36.96	0.073
Hume Dam	590	38.27	0.179	581	38.32	0.177	535	37.86	0.197	578	37.86	0.197	595	38.54	0.168	586	38.64	0.163
Lake Victoria	590	20.79	0.101	581	20.82	0.099	535	20.28	0.112	580	21.25	0.061	595	21.17	0.068	586	21.18	0.067
Laxton Met	590	17.69	0.093	581	17.66	0.095	535	17.21	0.141	572	17.41	0.121	595	17.86	0.075	586	17.83	0.078
Melbourne Airport	428	29.23	0.057	419	29.22	0.057	373	28.75	0.087	422	29.15	0.062	433	29.16	0.061	424	29.07	0.067
Mildura Airport	590	22.34	0.081	581	22.41	0.075	535	22.34	0.081	580	22.44	0.073	595	22.62	0.057	586	22.71	0.05
Murray Bridge	478	22.61	0.096	469	22.74	0.085	423	21.33	0.195	461	22.37	0.114	484	22.48	0.104	475	22.6	0.094
Sydney Obs Hill	590	89.77	0.070	581	89.19	0.081	535	90.49	0.055	593	91.48	0.034	595	90.73	0.049	586	90.21	0.06

temperature	Model 1			Model 2			Model 3			Model 4			Model 5			Model 6		
	DF	std	R^2_{adj}	DF	std	R^2_{adj}	DF	std	R^2_{adj}	DF	std	R^2_{adj}	DF	std	R^2_{adj}	DF	std	R^2_{adj}
Adelaide Airport	590	2.399	0.895	581	2.387	0.897	535	2.34	0.901	583	2.376	0.898	595	2.535	0.883	586	2.397	0.896
Broken Hill	588	3.084	0.643	579	3.094	0.640	533	2.82	0.703	584	3.761	0.469	593	3.095	0.64	584	3.103	0.638
Canberra Airport	590	2.215	0.913	581	2.178	0.915	535	2.14	0.918	589	2.19	0.925	595	2.274	0.908	586	2.225	0.912
Hume Dam	590	1.568	0.944	581	1.516	0.948	535	2.507	0.949	539	1.576	0.944	595	1.622	0.941	586	1.53	0.947
Lake Victoria	590	3.41	0.558	581	3.419	0.555	535	3.327	0.579	586	3.382	0.565	595	3.441	0.549	586	3.449	0.547
Laxton Met	590	1.434	0.937	581	1.385	0.941	535	1.405	0.94	595	1.444	0.936	595	1.478	0.933	586	1.415	0.939
Melbourne Airport	428	2.58	0.898	419	2.525	0.902	373	2.436	0.905	428	2.579	0.898	433	2.632	0.894	424	2.569	0.899
Mildura Airport	590	1.487	0.940	581	1.433	0.944	535	1.453	0.943	592	1.487	0.94	595	1.53	0.937	586	1.461	0.942
Murray Bridge	478	1.849	0.836	469	1.848	0.836	423	1.765	0.851	476	1.823	0.841	484	1.899	0.827	475	1.875	0.831
Sydney Obs Hill	590	2.931	0.720	581	2.875	0.731	535	2.867	0.732	588	2899	0.726	595	2.964	0.714	586	2.882	0.73

RM 3 has extended to RM include the main effects of CIs and their interaction effects. Evidence of improvement in the model 3 is, shown in Table 6.8. The influence of CIs and their interaction effects were varied at 5% level even 1% level. Therefore, the degrees of freedom are varied in RM 4, which leads to distance dependency of climatic influences on rainfall and temperature in the MDB areas and eastern Australia. No evidence of improvement by the use of this RM is shown in Table 6.8.

This study investigated multi indices influences on rainfall and temperature patterns in the MDB areas and eastern Australia. It is rational to reduce the multi dimension effects by using the factor score. The factor score is extracted by the PCA method, before RM data adequacy has been tested, and the multicollinearity and singularity problem removed. The extracted PCA factors shown in Table 6.7 were applied for the fitting RM 5 and 6. Fitted regression lines for rainfall and temperature series are given for all locations in Appendix 6.8 (a and b) and Appendix 6.9 (a and b) respectively. There is statistically significant evidence that the average rainfall and temperature patterns were an influence by the three extracted principal components. However, comparison with the RM 1 and 2, model 5 and 6 does not achieve significantly improvement.

Table 6.8 shows that for Model 1, for example at the Hum Dam, the estimated standard deviation of rainfall was 23.53 mm and the model fitted by 29.2%. The estimated standard deviation of temperature is 1.568^0C and model fitted by 94.4%., and all locations the models output are given in Table 6.8. For RM 2, as shown in Table 6.8, there is no improvement on model 1.

The outcomes of RM 5 by factor score are shown in Table 6.8 shows a very close to fit the variability of rainfall and temperature pattern compared with model 1, and also that model 4 is fits close to model 2 is shown in Table 6.8. Furthermore, understanding a particular climatic influence on rainfall and temperature patterns, the best influence of CIs on rainfall and temperature patterns will yield minimum AIC criteria, minimum standard deviation (std) and maximum adjusted R^2 in Table 6.9.

Table 6. 9: RM fitted by individual CI for rainfall and temperature.

Model7 for rainfall	Adelaide Airport		Broken hill		Canberra Airport		Hume dam		lake Victoria		Loxton		Melbourne Airport		Mildura Airport		Murray bridge		Sydney obs Hill	
	std	R^2_{adj}	std	R^2_{adj}	std	R^2_{adj}	std	R^2_{adj}	std	R^2_{adj}	std	R^2_{adj}	std	R^2_{adj}	std	R^2_{adj}	std	R^2_{adj}	std	R^2_{adj}
Nino1+2	23.990	0.264	29.220	0.004	37.52	0.044	39.680	0.117	21.520	0.038	18.190	0.041	29.580	0.034	22.910	0.033	22.69	0.039	91.51	0.033
Nino3	24.000	0.264	28.970	0.020	37.22	0.060	39.390	0.130	21.510	0.038	18.140	0.046	29.470	0.041	22.940	0.031	22.69	0.039	91.40	0.035
Nino4	23.990	0.264	28.590	0.046	37.17	0.062	39.390	0.130	21.420	0.046	18.070	0.053	29.370	0.048	23.190	0.010	22.67	0.091	91.30	0.037
Nino34	23.990	0.264	28.680	0.040	37.13	0.064	39.280	0.135	21.470	0.042	18.090	0.051	29.400	0.046	23.030	0.021	22.69	0.039	91.34	0.037
N-Atl	24.020	0.262	29.240	0.002	37.65	0.038	39.990	0.104	21.590	0.031	18.200	0.040	29.580	0.034	23.080	0.013	22.69	0.039	91.49	0.034
S-Atl	24.010	0.263	29.250	0.002	37.66	0.037	39.960	0.105	21.500	0.039	18.110	0.049	29.500	0.039	23.090	0.020	22.64	0.093	91.14	0.041
G. tropi	24.030	0.262	29.030	0.016	37.51	0.045	39.680	0.117	21.560	0.034	18.170	0.043	29.630	0.031	22.950	0.029	22.69	0.039	91.49	0.033
DMI	23.780	0.277	29.240	0.002	37.28	0.056	39.320	0.133	21.480	0.041	18.090	0.051	29.540	0.037	23.190	0.009	22.6	0.096	91.30	0.033
PDO	24.030	0.261	29.150	0.008	37.65	0.037	39.990	0.103	21.550	0.035	18.200	0.040	29.620	0.032	23.260	0.004	22.65	0.092	91.40	0.036
SOI	23.730	0.280	28.400	0.059	36.49	0.096	38.300	0.169	21.040	0.080	17.830	0.079	29.440	0.043	22.730	0.049	22.67	0.090	90.94	0.045
SAM	24.010	0.263	29.040	0.016	37.31	0.055	39.970	0.104	21.470	0.041	18.180	0.042	29.400	0.046	23.130	0.015	22.65	0.092	90.36	0.057
Model7 formula	Adelaide Airport		Broken hill		Canberra Airport		Hume dam		lake Victoria		Loxton		Melbourne Airport		Mildura Airport		Murray bridge		Sydney obs Hill	
	std	R^2_{adj}	std	R^2_{adj}	std	R^2_{adj}	std	R^2_{adj}	std	R^2_{adj}	std	R^2_{adj}	std	R^2_{adj}	std	R^2_{adj}	std	R^2_{adj}	std	R^2_{adj}
Nino1+2	2.581	0.879	4.809	0.131	2.315	0.904	1.629	0.940	3.430	0.552	1.484	0.933	2.634	0.893	1.531	0.937	1.893	0.828	91.510	0.033
Nino3	2.557	0.881	5.105	-0.002	2.288	0.907	1.643	0.939	3.427	0.553	1.491	0.932	2.627	0.894	1.541	0.936	1.891	0.829	91.400	0.035
Nino4	2.569	0.880	5.113	0.018	2.313	0.905	1.654	0.938	3.430	0.552	1.492	0.932	2.666	0.891	1.544	0.936	1.885	0.830	91.300	0.037
Nino34	2.560	0.881	5.106	0.020	2.296	0.906	1.651	0.938	3.427	0.553	1.492	0.932	2.647	0.892	1.544	0.936	1.888	0.829	91.340	0.037
N-Atl	2.531	0.884	4.894	0.100	2.347	0.902	1.645	0.939	3.425	0.554	1.487	0.932	2.670	0.891	1.540	0.936	1.883	0.830	91.490	0.034
S-Atl	2.550	0.882	4.884	0.104	2.349	0.902	1.655	0.938	3.429	0.552	1.492	0.932	2.685	0.889	1.544	0.936	1.885	0.830	91.140	0.041
G. tropi	2.473	0.889	5.137	0.006	2.317	0.904	1.654	0.938	3.430	0.552	1.486	0.932	2.663	0.891	1.543	0.936	1.867	0.833	91.490	0.033
DMI	2.538	0.883	5.160	0.000	2.319	0.904	1.627	0.940	3.430	0.552	1.473	0.934	2.648	0.892	1.527	0.937	1.887	0.829	91.500	0.033
PDO	2.581	0.879	5.141	0.007	2.352	0.901	1.655	0.938	3.422	0.554	1.492	0.932	2.680	0.890	1.544	0.936	1.888	0.829	91.400	0.036
SOI	2.578	0.879	5.166	-0.003	2.297	0.906	1.648	0.939	3.419	0.555	1.490	0.932	2.645	0.893	1.537	0.936	1.893	0.828	90.940	0.045
SAM	2.581	0.879	5.165	-0.002	2.310	0.905	1.654	0.938	3.425	0.554	1.483	0.933	2.663	0.891	1.537	0.936	1.893	0.828	90.360	0.057

This study suggested that the SOI is significantly the largest influence on rainfall and temperature patterns in the MDB and is well fitted $R^2_{\text{adjusted in}}$ by the model 7,

Furthermore, this study extended the RM 7 for consistent influence of SOI by adding PDO influence and their interaction effects on rainfall and temperature variability in the MDB areas. The coefficients of SOI, PDO and the fitted RM 8 and a statistical summary are shown in Table 6.10.

Table 6. 10: Regression coefficient of SOI, PDO and their interaction in a rainfall and temperature model 8.

Rainfall	Adelaide Airport	Broken Hill	Canberra Airport	Hume Dam	Lake Victoria	Loxton Met	Melbourne Airport	Mildura Airport	Murray Bridge	Sydney obs Hill
Intercept	38.54***	24.57***	52.79***	63.72***	22.17***	22.19***	46.81***	24.44***	29.19***	108.40***
Linear term	0.0028	0.0059	-0.0066	0.0028	-0.0060	0.0025	-0.0196	-0.0056	0.0018	-0.0082
Quadratic	-0.0001	1.3820	0.0000	-0.0001*	0.0000	0.0000	-0.0001	0.0000	0.0000	-0.0001
Cosine	-17.3600***	-2.6590	9.8160***	-11.460***	-0.9875	-2.3460	-4.929*	0.0667	-4.1720**	-2.0460
Sin	-10.8200***	-0.0001	-3.9950	-15.350***	-5.5850***	-5.3420***	4.6520*	-5.0710***	9.6060***	26.20***
SOI	0.4196***	0.7000***	0.9965	1.1570***	0.4977***	0.3994***	0.3294*	0.5331***	0.1717***	0.9624***
PDO	0.7955	-0.4764	1.7090	2.7170	-0.2075	0.6839	-0.3834	0.5898	1.6580	-1.8560
SOI*PDO	-0.1715*	-0.3091**	-0.2019	-0.0669	-0.2260**	-0.1433*	-0.0784	-0.2150**	-0.1573	-0.1748
SD	23.67	28.23	36.43	38.47	20.92	17.76	29.49	22.64	22.57	91.06
$R^2_{adjusted}$	0.286	0.0722	0.09912	0.1705	0.08994	0.08512	0.03976	0.0555	0.09862	0.04251
F value	35.22	10.1	10.51	18.77	9.542	9.042	3.62	8.11	8.705	4.837
Temperature	Adelaide Airport	Broken Hill	Canberra Airport	Hume Dam	Lake Victoria	Loxton Met	Melbourne Airport	Mildura Airport	Murray Bridge	Sydney obs Hill
Intercept	30.31***	24.04***	25.85***	21.17***	23.32***	23.38***	27.79***	23.59***	22.79***	29.19***
Linear term	0.0024***	0.0013	0.0023***	0.0018***	0.0011	0.0012**	0.0030**	0.0013***	0.0022***	0.0012
Quadratic	0.0000	0.0000	0.0000**	0.0000**	0.0000	0.0000*	0.0000	0.0000**	0.0000	0.0000
Cosine	5.3220***	4.9710***	8.9550***	7.5860***	4.5420***	6.7520***	-9.3080***	7.2190***	0.3583***	-6.1810***
Sine	8.2680***	-3.0230***	4.5560***	4.9960***	2.8480***	3.8680***	-5.4230***	4.1010***	-5.8190***	-2.1960***
SOI	-0.0160	-0.0330*	-0.0533***	-0.0178*	-0.0383**	-0.0117	-0.0430***	-0.0169**	-0.0043	-0.0262*
PDO	-0.0502	-0.2445	-0.0399	-0.0995	-0.3878	-0.0889	0.0267	-0.0727	-0.1734	0.1381
SOI*PDO	0.0087	0.0115	0.0131	-0.0023	-0.0072	0.0012	0.0027	0.0049	-0.0056	-0.0157
SD	2.579	3.096	2.298	1.649	3.406	1.49	2.651	1.537	1.893	2.967
$R^2_{adjusted}$	0.8793	0.6399	0.9058	0.9396	0.5585	0.932	0.8921	0.9361	0.8283	0.7135
F value	630.5	154.1	970.8	1322	110.4	1186	524.2	1267	476.6	216.2

6.4. Discussion and Conclusion

The variability of rainfall and temperature has been analyses in depth recognized in this study. It is important to take this into account when developing strategies on water resources management, because the hydrological baselines are uncertain due to climate change. The SST in the Pacific Ocean, Atlantic Ocean, and Indian Ocean and the SLP anomalies between Darwin, Australia and Tahiti were analyses.

This research provided evidence of seasonality. A deterministic trend and seasonal change in CIs series were highlighted by the various use RM. Strategies were superimposed to detect the trend of influence of CIs on the SST and SLP in the Pacific and Atlantic Ocean. It is concluded that evidence of an increasing trend of SST in the Atlantic Ocean over time. Moreover, these indices are not significant influential on Australian rainfall and temperature patterns. The analytical evidence has shown that Australian rainfall and temperature subject to SOI and PDO influences. The evidence was of an increasing trend in PDO influence from the mid 20^{th} century on the Australian subcontinent. This study concluded that the SOI had a significant influence and that its interaction with the PDO categorizes Australian rainfall patterns. It is further concluded that a reduction in future SOI influence could reduce Australia's future rainfall, and that the interaction between PDO and SOI is likely to be more pronounced during periods of negative PDO. However, it is recommended that the periods of negative PDO could reduce temperature influence, which might increase future rainfall in the MDB areas. It is also recommended to further study the effect of rainfall and temperature pattern in the MDB areas.

CHAPTER 7: EFFECT OF HYDROLOGICAL MODEL

7.1. Introduction

Evidence of global warming is becoming widely accepted, for example, IPCC (2007) and BOM (2008). However, evidence of change on a local scale can be more equivocal. Within Australia, the effect of changing climatic conditions in the MDB which covers 14% of the country's land area is of particular concern because the MDB produces one third of Australia's food supply and supports over a third of Australia's total gross value of agricultural production including export (Craik, and Cleaver, 2008). Over the last one hundred and twenty years, there have been three particularly notable droughts affecting the MDB: the Federation drought which began in the mid-1890s and reached its devastating climax in 1902; the World War II drought which started in 1937 and lasted until 1945; and the current drought which began in 2002 and is now in its seventh year.

Providing statistically significant evidence of climate change from time series data is not necessarily straightforward because non-stationarity can be present in a myriad of ways and is not restricted to approximately linear trends (Timbal and Jones, 2008). So, fitting RM with linear or more general polynomial, trends may not provide evidence of change in the rainfall and temperature time series when more general statistical tests may do so (Bates *et al*., 2008). For example, in Australia, the relatively low rainfall in the first half of the twentieth century mirrors decreases since 1990. It is plausible that there are a few abrupt changes in rainfall and temperature time series, perhaps influenced by changes in ocean currents, rather than some more systematic trend. One objective of this study is to suggest statistical analyses that are sensitive to small, but highly influential, climatic changes. The second, more specific objective is to investigate possible systematic changes in rainfall and temperature time series at six stations in the MDB and four capital cities near the eastern seaboard of Australia. Finally, in this study is to investigate the hydrological changes in the MDB rainfall and temperature series.

7.2. Study approach

This study analyses the time series of rainfall and temperature patterns in the MDB areas and the capital cities in eastern Australia. Initially, a sinusoidal model will apply for testing the amplitude of effects on rainfall and temperature time series in the MDB areas with four capital cities in eastern Australia. The second analysis presented in this chapter is based on RM for rainfall and temperature that allow for seasonal variations and underlying climate states, categorized in terms of the PDO and the Southern Oscillation Index (SOI) which are thought to affect weather patterns in eastern Australia.

The third analysis is based on the Holt-Winters seasonal forecasting method. This forecasting procedure is applied interactively and is well suited to identify any changes in seasonal patterns as well as any changes in the underlying level. The Holt-Winters method relies on exponential smoothing and in a forecasting context the most recent observation is typically given a weight of 0.2, making the procedure sensitive to rapid changes in the underlying conditions. However, in the context of climate change plots are more informative, from a retrospective point of view, if the smoothing is increased and the weight given to the most recent observation is reduced. The Holt-Winters method is less convenient for demonstrating statistically significant non-stationarity than is the regression based approach, but given evidence of non-stationarity it is ideal for tracking changes.

7.3. Results analysis

7.3.1. Trend detected using RM

7.3.1.1. Sinusoidal model study

Modelling the phases of sinusoidal period of a year is tricky because it involves a non-linear regression analysis. Polynomial regression provides a straightforward way to model simple forms of departure from the linearity. Fitting regression of rainfall or temperature on sine and cosine function of time with the period 1 year follows

$$y_i = \beta_0 + \beta_1 * \mathrm{Sin}(2\pi f t_i) + \beta_2 * \mathrm{Cos}(2\pi f t_i). + \varepsilon_i$$

here, y_i is defined as rainfall or temperature time series and $i = 1,2,3.....n$, and f=1/T, and T is the period (1 year) of fitted sinusoidal waves. The coefficients of $\beta_o, \beta_1,$ and β_3 are the unknown's to be determined. The estimated coefficients of RM with a sinusoidal period of a year in observed areas have been shown in Table 7.1.

Table 7. 1: Coefficient of regression for rainfall and temperature with and fitted RM by sinusoidal period a year in the MDB, and the eastern Australia.

	Coefficient	Model	Adelaide Airport	Broken hill	Canberra Airport	Hume dam	Lake Victoria	Loxton met	Melbourne Airport	Mildura Airport	Murray bridge	Sydney obs. hill
Mean	β_0	Rainfall	37.221	22.474	51.446	57.531	21.5825	22.7846	44.714	22.9794	30.15	100.038
		Temperature	30.181	23.947	26.055	21.556	23.560	23.648	28.092	24.011	22.678	29.354
Sine	β_1	Rainfall	-17.8927	-2.475	3.554	-14.595	-3.4596	4.1231	6.949	-2.5024	-9.651	-2.902
		Temperature	9.805	-5.584	8.410	8.908	6.469	-7.583	-0.057	8.231	4.391	6.658
Cosine	β_2	Rainfall	-10.0319	-2.684	8.991	9.165	3.068	-3.7099	-2.68	3.4901	-4.146	26.519
		Temperature	0.526	-1.670	5.534	-2.584	0.047	1.856	-10.754	-1.974	3.894	1.416

Station name	Degrees of freedom	Amplitude Effect*s		Residual std error		R^2		P-value		F-value	
		Rainfall	Temperature	Rainfall	Temperature	Rainfall	Temperature	Rainfall	Temperature	Rainfall	Temperature
Adelaide Airport	638	84.94	370.76	24.15	2.648	0.266	0.873	0.000	0.000	115.50	2199
Broken hill	601	12.50	187.34	29.21	3.111	0.008	0.638	0.095	0.000	2.36	528.7
Canberra Airport	830	24.81	417.87	38.97	2.409	0.030	0.898	0.000	0.000	12.83	3635
Hume dam	1287	43.52	510.01	39.6	1.818	0.087	0.929	0.000	0.000	61.09	8391
Lake Victoria	1022	21.24	228.09	21.77	2.836	0.022	0.723	0.000	0.000	11.56	1332
Loxton met	1179	28.60	508.61	19.39	1.535	0.039	0.928	0.000	0.000	24.18	7644
Melbourne Airport	454	25.16	394.08	29.6	2.729	0.031	0.887	0.001	0.000	7.22	1778
Mildura Airport	1287	19.13	493.34	22.44	1.716	0.018	0.924	0.000	0.000	11.81	7849
Murray bridge	491	46.42	307.77	22.63	1.907	0.098	0.827	0.000	0.000	26.55	1169
Sydney obs. hill	1300	29.73	223.75	89.72	3.042	0.042	0.715	0.000	0.000	28.78	1632

Table 7.1 have shown the amplitude effect of sine waves on rainfall and temperature pattern varies at the different locations. The amplitude effect (sine wave) has a higher effect on temperature variability than rainfall variability. There is evidence of decreasing seasonal effects on rainfall and temperature over the MDB areas and the eastern seaboard of Australia. The study suggests that the average climate pattern over the MDB areas and its strong spatial and temporal variations of rainfall and temperature are caused by the influence of various synoptics that affect the MDB areas during different seasons and by the topography of the MDB areas.

7.3.1.2. RM linear and Quadratic term

Having allowed for seasonal effects, a linear, quadratic or polynomial term may be applied in the fitted RM, in order to detect a trend in rainfall and temperature time series in the MDB areas and the eastern Australia. However, a linear term in the mean adjusted and polynomial term is highly correlated $(r = 0.9165)$. That the estimated uncertainties of rainfall and temperature are significantly different from zero for the fitted model, including linear and quadratic terms is shown in Table 7.2. This has been indicated that rainfall would be fluctuating positively or negatively. Table 7.2, the fitted R^2 for rainfall range is (from 0.0002 to 0.0163), for temperature range is (from 0.0009 to 0.0057) shows that extrapolating the trend provides the implausible scenario for future the rainfall patterns and contemporary temperature as the number is very small, and it gives a weak prediction the MDB areas and eastern Australia.

Table 7. 2: Fitted linear and quadratic model in MDB areas and eastern Australia

	Coefficient	Model	Adelaide Airport	Broken hill	Canberra Airport	Hume dam	Lake Victoria	Loxton met	Melbourne Airport	Mildura Airport	Murray bridge	Sydney obs.hill
Mean	β_0	Rainfall	38.350	25.080	54.480	59.310	23.460	21.760	45.670	23.640	38.430	103.700
		Temperature	30.290	23.990	25.720	21.060	23.380	23.470	28.030	23.610	22.760	29.400
linear	β_1	Rainfall	-0.005	0.002	-0.006	0.005	0.000	-0.001	-0.028	0.000	0.002	0.010
		Temperature	0.0030	0.0012	0.0017	-0.0004	0.0001	-0.0002	0.0038	-0.0007	0.0023	0.0006
Quadratic	β_2	Rainfall	-0.00003	-0.00009	-0.00005	-0.00001	-0.00002	0.00001	-0.00006	0.00000	-0.00001	-0.000025
		Temperature	-0.000003	-0.000002	0.000005	0.000004	0.000002	0.000002	0.000002	0.000003	-0.000005	0.000000

Station name	Degree of freedom	Residual std error		R^2_{adj}		P-value		F-value	
		Rainfall	Temperature	Rainfall	Temperature	Rainfall	Temperature	Rainfall	Temperature
Adelaide Airport	638	28.15	7.42	0.0024	0.0057	0.4713	0.1599	0.7532	1.8380
Broken hill	601	29.22	5.163	0.0065	0.0018	0.1397	0.5784	1.9750	0.5479
Canberra Airport	830	39.44	7.51	0.0061	0.0042	0.0775	0.1742	2.5650	1.7510
Hume dam	1287	41.37	6.796	0.0032	0.0050	0.1283	0.0400	2.0570	3.2280
Lake Victoria	1022	21.95	5.384	0.0059	0.0010	0.0475	0.6145	3.0570	0.4871
Loxton met	1179	19.75	5.734	0.0028	0.0009	0.1959	0.5768	1.6320	0.5506
Melbourne Airport	454	29.82	8.095	0.0163	0.0038	0.0241	0.4171	3.7570	0.8762
Mildura Airport	1287	22.64	6.217	0.0007	0.0053	0.6244	0.0333	0.4712	3.4100
Murray bridge	491	23.82	4.565	0.0002	0.0056	0.9410	0.2519	0.0609	1.3830
Sydney obs hill	1300	91.56	5.695	0.0028	0.0016	0.1570	0.3645	1.8540	1.0100

In practice, there is evidence of significant amplitude effects on rainfall and contemporary temperature. However, the uncertainties associated with estimating the rainfall are much higher than for temperature over the MDB areas, as shown in the Table 7.2. The rainfall and temperature behaviour using a GLS approach under an auto regressive process (AR [1]) model is shown in Appendix 7.1. In the case of temperature, there is significant evidence of increasing trend in five out of ten weather stations, leading to a spatial variability of temperature pattern over the MDB areas and eastern seaboard Australia.

7.3.2. Alternative Approach: Detected trend

7.3.2.1. Exponential smoothing

The time series $\{x_t\}$ and t = 1 , 2……n., for example, rainfall and temperature series, has a history up to time n. This study aim to predict some sequential future $\{x_{t+k}\}$based on historical rainfall and temperature series. We presume that there are no systematic trends or seasonal effects in the process or that these have been identified and removed. It has also been established the equation (10.1) that the mean process can be changed from one step to the next step. However, the climatic variability, particularly for rainfall pattern and contemporary temperature were implausible to predict for long term climatic behavior in the MDB and eastern Australia. For example, the Hume Dam in the MDB areas rainfall and temperature pattern have been checked for any marked systematic trend or seasonal effects as highlighted in Figure 7.1. Furthermore, we have no information about like the direction of these changes.

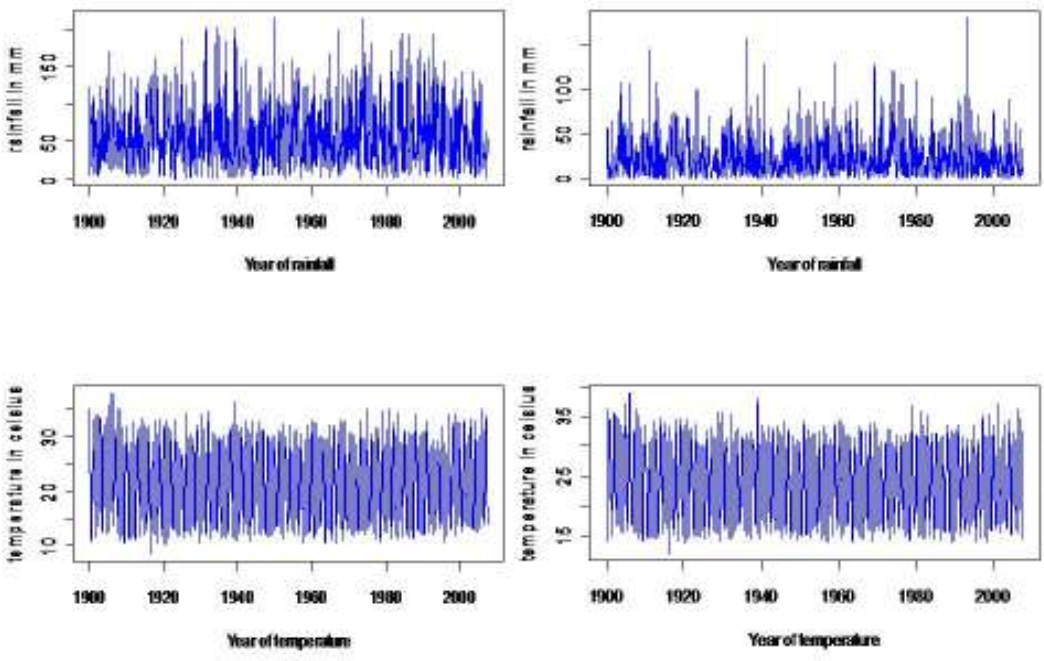

Figure 7. 1: Monthly rainfall (upper row) and temperature (bottom row) pattern observed at Hum Dam (left side) and Mildura airport (right side) stations in the MDB areas.

It is plausible to detect the systematic trends or seasonal effects using an exponential smoothing equation (43) for rainfall and temperature time series. Exponential smoothing is a special case of the Holt-Winters Algorithm (Cowpertwait and Metcalf, 2009). Implement in R routine, using the Holt-Winters function, estimated the smoothing parameter α and also estimate to specify the value for $\alpha = 0.2$.

Table 7. 3: Fitted EWMA model by Holt-Winters function.

Locations	Holt winter exponential smoothing without trend and seasonal component						Choice smooth paparamet, alpha=0.2			
	Smooth parameter (α) (Column 1)		Coefficient of EWMA (a_t) (Column 2)		Sum of Square Error (Column 3)		Coefficient of EWMA (a_t) (Column 4)		Sum of Square Error (Column 5)	
	Rainfall	Temperature	Rainfall	Temperature	Rainfall	Temperature	Rainfall	Temperature	Rainfall	Temperature
Adelaide Airport	0.417223	0.9999339	32.28479	20.50026	543920	15505.59	28.367	23.11226	545663	62444.5
Broken Hill	0.048091	0.9999339	21.76108	12.90054	515981	6058.78	29.247	23.88111	525583	16894
Canberra Airport	0.056913	0.9999339	40.25379	16.50003	1338755	17811.5	36.1747	23.81387	1385124	48945.3
Hume Dam	0.000054	0.9999339	57.96863	13.69034	2209773	19929.08	35.7888	23.11226	2281297	62444.5
Lake Victoria	0.004173	0.9999339	20.68834	14.70046	497025	11317.89	18.528	24.19634	534899	31275.5
Laxton Met	0.023676	0.9999339	22.91031	14.80044	470171	13865.01	22.8	24.02078	495459	40824.8
Melbourne Airport	0.054868	0.9999339	34.1489	17.30006	424941	12467.6	30.3093	25.87661	442846	31411.15
Mildura Airport	0.001146	0.9999339	22.69736	14.15045	2209773	17453.96	16.6407	24.01879	701418	52271.2
Murray Bridge	0.001442	0.9999339	29.42712	15.50038	279618	4040.823	29.3993	23.84451	303191	10700.2
Sydney Obs. Hill	0.016585	0.9218128	96.37292	40.39768	11072733	28879.89	103.936	32.13466	1.2E+07	44654.2

In the Table 7.3, the values of smoothing parameter (α) are given in column 1 for rainfall and temperature patterns in six MDB areas and four capital cities in eastern Australia. The minimum sum of squares one step ahead predictive errors (SS1PE) of rainfall and temperature respectively are shown in column 3. The sum of square in column 3 may be compared with those obtained from specifying the smooth parameter $\alpha = 0.2$ in column 5, for example, for the Hume Dam. The estimated value of the mean rainfall per month and contemporary temperature at the end of 2007 is 35.788 and 23.11 in column 4 and SS1PE was slightly increased in contemporary

rainfall pattern and highly increased in temperatures pattern were highlighted in Table 7.3. Therefore, the optimum value for α is a particularly important criterion on SS1PE and need to remove any choice value. Moreover, the optimum estimate can be close to 0 if the time series is a long one over a stable period and its makes the EWMA unresponsive to any future change in the mean level. For example Figure 7.2 below observations at the Hume Dam and Mildura Airport stations are presented and details for other weather stations are given in Appendix 7.2. With values of smoothing parameter close to 0, highly smoothed estimates for the mean level of rainfall are obtained as shown in column 1 of Table 7.3 contemporary the values of the smoothing parameter are close to 1, leading to EWMA are temperature time series pattern.

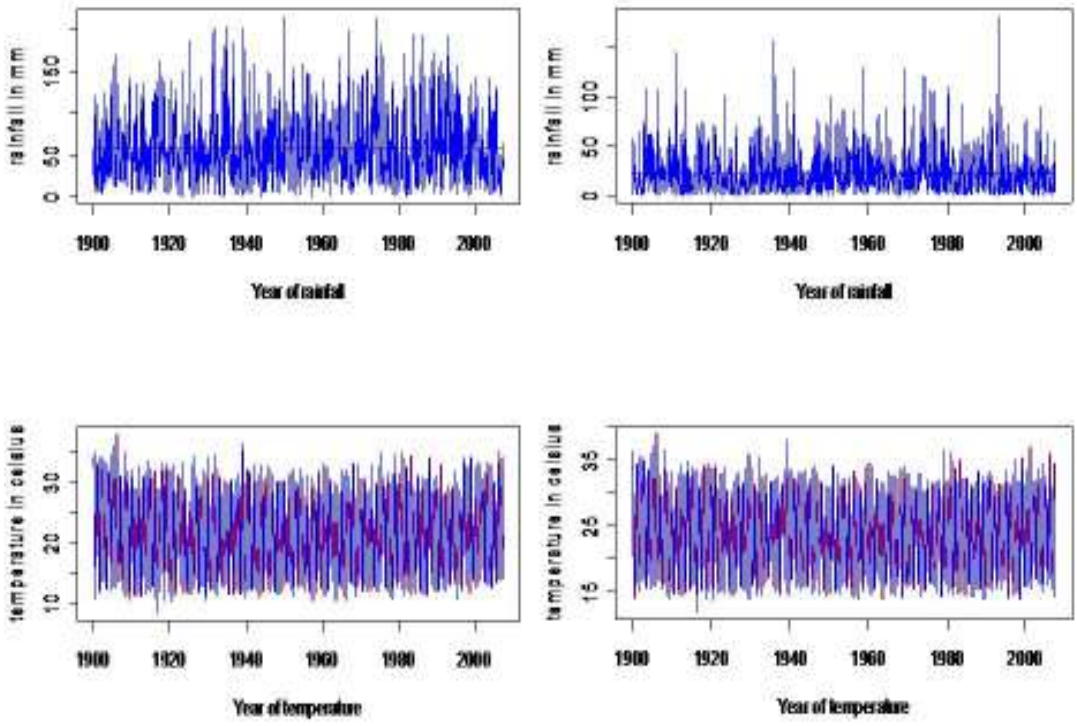

Figure 7. 2: Holt-Winters exponential smoothing without trend and without seasonal component in Hume Dam (left side) and Mildura Airport (right side) : rainfall series (upper row) and temperature series (bottom row) .

7.3.2.2. Holt-Winters method

The Holt-Winter (Holt, 1957 and Winter, 1960) method provides an alternative approach to that described in chapter 2, section 4.3.3. The Holt-Winter model assumes an underlying level with the addition of a possible trend and seasonal effects. Its versatility is that the level, trend and seasonal effects are allowed to change over time. Thus it is a non-stationary model, and is useful for tracking changes in the underlying parameters of a time series. The level, trend and seasonal effects are updated as data become available using exponential smoothing.

The updating equations for a series x_t with period p are:

$$a_t = \alpha * (x_t - s_{t-p}) + (1-\alpha) * (a_{t-1} + b_{t-1}) \quad 0<\alpha<1$$

$$b_t = \beta * (a_t - a_{t-1}) + (1-\beta) * b_{t-1} \quad 0<\beta<1$$

$$s_t = \gamma (x_t - a_t) + (1-\gamma) * s_{t-p} \quad 0<\gamma<1$$

where a_t, b_t and s_t are the estimated level, trend and seasonal effect at time t, and α, β and γ are smoothing parameters. The first of these three equations updates the estimate of the level. It is a weighted average of the seasonally adjusted latest observations (x_t-s_{t-p}) and the sum of the estimates of the level and trend one time step ago (a_{t-1}+b_{t-1}). The weights are α, the smoothing parameter and 1- α. A smaller α corresponds to increased smoothing. The second of the three equations above updates the estimate of trend b_t. It takes a weighted average of the latest estimate of trend, difference in levels are one time step forwarded (a_t-a_{t-1}), and the estimate of trend one time step back b_{t-1}. The last of the three equations updates the estimate of the seasonal effect. It is a weighted average of the latest estimate of the seasonal effect. This is the difference between the observation and the estimated level (x_t-a_t), and the last estimate of the seasonal effect which was made at time t-p. In forecasting applications, the smoothing parameters can be optimised by minimising the sum of

squared one step ahead predictions. For the purpose of tracking the underlying level, trend and seasonal effects, a choice of 0.04 and 0.05 for α, β and γ is made for rainfall and temperature series respectively which gives enhanced smoothing as shown in Table 7.4,

Table 7. 4: Optimised smoothing parameter using the Holt Winter algorithm, based on SS1PE.

i. Rainfall Model	α	β	γ	a	b	S	SSE
1	0.2	0.2	0.2	39.512	2.91246	–	2672671
2	0.1	0.1	0.1	28.682	-1.281	–	2388544
3	0.01	0.01	0.01	47.3711	-0.0693	–	2840846
4	0.02	0.02	0.02	42.3628	-0.191		2383134
5	0.03	0.03	0.03	40.7473	-0.2098	–	2288852
6	**0.04**	**0.04**	**0.04**	**41.9316**	**-0.2878**	–	**2264396**
7	0.05	0.05	0.05	40.703	-0.4262	–	2267449
ii. Temperature Model	**α**	**β**	**γ**	**a**	**b**	**S**	**SSE**
1	0.2	0.2	0.2	24.1138	-0.0249		4292.12
2	0.1	0.1	0.1	24.1046	0.0896	–	3868.92
3	0.01	0.01	0.01	23.2325	0.0066	–	12723.8
4	0.02	0.02	0.02	23.3533	0.0155	–	5585.36
5	0.03	0.03	0.03	23.5219	0.01795	–	4477.211
6	0.04	0.04	0.04	23.3001	0.0238	–	4086.07
7	**0.05**	**0.05**	**0.05**	**23.3788**	**0.0352**	–	**3919.95**

The optimum values for the smoothing parameters, based on SS1PE for both rainfall and temperature series are marked bold in Table 7.4. It follows that the mean level and seasonal variation adapt swiftly, whereas the trend is slow. The average value of the trend over the entire period is -0.2878 for rainfall and 0.0352 for temperature over Hume Dam reservoir. The estimated values of level both in terms of rainfall and temperature are 41.9316 and 23.3788 respectively. Finally, for comparison the mean square one – step a head prediction error equals 41.89685 for rainfall and 1.743193

for temperature, and the standard deviation (s) of the original series 41.40059 for rainfall and 6.80811 for temperature, which is no substantially larger than S . So, there is no reason to suspect occasional shifts in the mean. However, it can be seen in Figure 7.3 (a and b) that the estimated level has been decreasing for the rainfall pattern and increasing for the contemporary temperature pattern over the last 10 year.

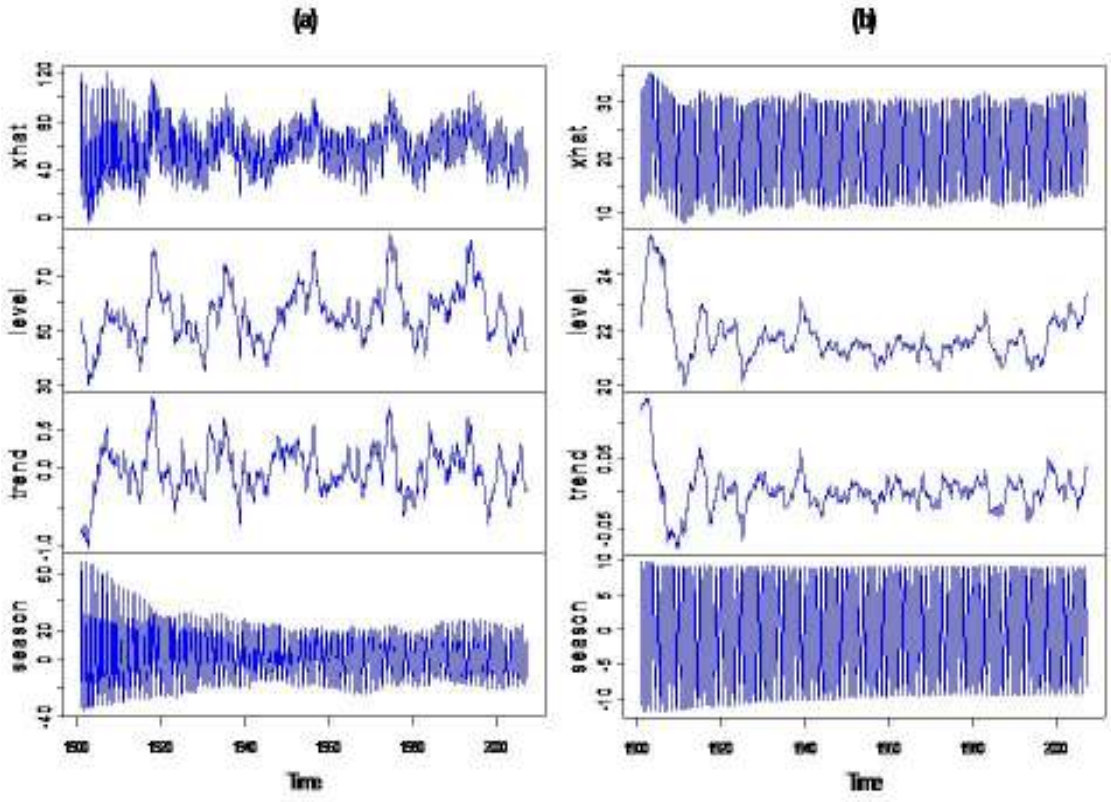

Figure 7. 3: Holt-Winters exponential smoothing with a) trend (β= 0.04) and a seasonal component (γ = 0.04) for rainfall and b) trend (β= 0.05) and a seasonal component (γ = 0.05) for temperature at Hume dam in the MDB.

The algorithm was applied to the time series, after adjusting for PDO, SOI and their interaction by subtracting the regression estimates of these effects. The tracking plots take some time to settle down in Figure 7.3. However, for rainfall it can be seen that the estimated level has been decreasing over the last 10 years, and the estimated trend is becoming more negative. The opposite effects can be seen for temperature. The average value of the trend over the entire period is -0.02398 mm per month for rainfall and 0.00293°C per month for temperature, respectively.

7.3.3. Correlation and RM

7.3.3.1. Correlation pattern climatic indicator and seasonality

The strengthening and the weakening of correlations provide an evaluation of the relationship between rainfall and temperature from season to season. There is significant evidence of negative correlation between temperature and rainfall pattern at the Hume dam and across the other MDB areas. This study suggests that the probability of temperature decreasing would be increasing the future rainfall pattern at the Hume dam and over MDB areas. Moreover, temperature allows for seasonal variation and association with low rainfall. The association with the PDO and the SOI was investigated. There was evidence that rainfall is reduced during periods of negative SOI, and the interaction between PDO and SOI makes this effect more pronounced during periods of negative PDO as shown in Table 7.5.

Table 7. 5: Association between the climatic indicator and seasonality

Pearson Correlation	Rain	Temp	PDO	SOI	Jan	Feb	Mar	Apr	May	June	July	Aug	Sep	Oct	Nov	Dec	PDO*SOI
rain	1.000																
Temp	-0.357***	1.000															
PDO	-0.038*	-0.016	1.000														
SOI	0.235***	-0.009	-0.301***	1.000													
Jan	-0.100***	0.410***	-0.012	0.011	1.000												
Feb	-0.130***	0.396***	-0.005	0.009	-0.091**	1.000											
Mar	-0.086***	0.239***	0.013	0.010	-0.091**	-0.091***	1.000										
Apr	-0.062**	0.001	0.051*	-0.019	-0.091**	-0.091***	-0.091***	1.000									
May	0.022	-0.219**	0.064*	-0.023	-0.091***	-0.091***	-0.091***	-0.091***	1.000								
June	0.108***	-0.380***	0.042	0.003	-0.091**	-0.091***	-0.091***	-0.091***	-0.091***	1.000							
July	0.140***	-0.419**	0.028	0.009	-0.091**	-0.091***	-0.091***	-0.091***	-0.091***	-0.091***	1.000						
Aug	0.124***	-0.325***	-0.029	-0.013	-0.091***	-0.091***	-0.091***	-0.091***	-0.091***	-0.091***	-0.090***	1.000					
Sep	0.040	-0.102***	-0.054*	-0.004	-0.091***	-0.091***	-0.091***	-0.091***	-0.091***	-0.091***	-0.090***	-0.09***	1.000				
Oct	0.080***	-0.014	-0.044	-0.016	-0.091***	-0.091***	-0.091***	-0.091***	-0.091***	-0.091***	-0.090***	-0.09***	-0.09***	1.000			
Nov	-0.061**	0.132**	-0.045	0.003	-0.091***	-0.091***	-0.091***	-0.091***	-0.091***	-0.091***	-0.090***	-0.09***	-0.09***	-0.09***	1.000		
Dec	-0.066**	0.319**	-0.005	0.031	-0.091***	-0.091***	-0.091***	-0.091***	-0.091***	-0.091***	-0.090***	-0.09***	-0.09***	-0.090***	-0.09***	1.000	
PDO*SOI	-0.026	0.010	-0.065*	0.114*	0.042	-0.055**	-0.010	-0.022	0.031	0.007	0.001	-0.045	0.011	-0.011	0.033	0.014	1.000

*coefficients are statistically significant at the 5% level
**coefficients are statistically significant at the 1% level
***coefficients are statistically significant at the 0.1% level

In Table 7.5 have been shown the rainfall and temperature pattern, which are categorized by the PDO and SOI and their interaction effects, and also by seasonal indicators from January to December over the MDB areas, and those for all other weather stations are given in Appendix 7.3.

7.3.3.2. Fitting RMs with climatic and seasonal indicators

The first stage is to fit regressions of rainfall and temperature on PDO, SOI and their interaction (PDOxSOI), together with additive monthly seasonal effects. The RS from the regressions are then considered in detail, in particular, for evidence against a hypothesis that they are from a stationary random process. The model has the form:

$$Y_t = \beta_0 + \beta_1 \times \text{PDO}_t + \beta_2 \times \text{SOI}_t + \beta_3 \times \text{PDO}_t \times \text{SOI}_t + \beta_4 \times \text{Jan}..... + \beta_{14} \times \text{Nov} + \varepsilon_t$$

where t is time in months, Y_t is monthly rainfall, or monthly average maximum temperature, the indicator variables:

$$\text{Jan}=\begin{cases}1 & \text{if January}\\ 0 & \text{Otherwise}\end{cases} \quad \text{Feb}=\begin{cases}1 & \text{if February}\\ 0 & \text{otherwise}\end{cases} \quad ....\text{Nov}=\begin{cases}1 & \text{if November}\\ 0 & \text{otherwise}\end{cases}$$

allow additive seasonal effects. With this choice of parameterization, the coefficients β_4 to β_{14} represent seasonal effects relative to the month of December. Therefore β_0 represent the intercept for December. Lastly, ε_t is a time series of variables with mean = 0 that are referred to as errors. The mathematical form of the model does not restrict rainfall to be positive, but in this application there were only a few months with zero rain recorded. For example, Hume Dam had 9 dry months out of the 1290 months rainfall record and the fitted values are all positive. The device of using the logarithm of the rainfall as the response in the regression resulted in a slightly poorer fit and in this study choice was made not to follow this approach. The estimated regression coefficients for all 10 stations, and the two dependent variables (rainfall and temperature), are presented in Appendix 7.4 (a and b). In most cases, the coefficients of PDO, SOI, and their interaction $(\text{PDO} \times \text{SOI})$, are statistically significantly different from 0 at the 5% level (e.g. Verzani, 2005) when the regression

is fitted by generalised least squares assuming appropriate AR(p) models for the errors.

Table 7. 6: Fit of RMs for rainfall and temperature for 10 stations

Station name	Record length (months)	Rainfall model				Temperature model			
		Estimated standard dev. error	R^2_{adj}	P-value	F test	Estimated standard dev. error	R^2_{adj}	P-value	F test
Adelaide Airport	641	23.58	0.298	< 2.2e-16	20.39	2.487	0.888	< 2.2e-16	363.3
Broken Hill	604	28.17	0.074	1.255e-07	4.451	3.102	0.638	< 2.2e-16	77.03
Hume Dam	1290	38.24	0.147	< 2.2e-16	16.83	1.726	0.936	< 2.2e-16	1342
Lake Victoria	1024	21.23	0.068	2.420e-12	6.352	2.806	0.728	< 2.2e-16	196.8
Loxton Met	1183	18.85	0.090	< 2.2e-16	9.39	1.446	0.936	< 2.2e-16	1243
Mildura Airport	1290	21.89	0.064	7.177e-15	7.322	1.63	0.932	< 2.2e-16	1253
Murray Bridge	494	22.58	0.097	2.485e-08	4.812	1.876	0.831	< 2.2e-16	174.7
Canberra Airport	833	37.83	0.084	2.157e-12	6.428	2.279	0.908	< 2.2e-16	588.1
Melbourne Airport	457	29.46	0.036	0.007272	2.198	2.631	0.894	< 2.2e-16	276.6
Sydney Obs. Hill	1303	89.18	0.053	5.712e-12	6.15	2.907	0.740	< 2.2e-16	265

In Table 7.6 gives the record length, estimated standard deviation of the errors, and adjusted R^2 values, $R^2_{adjusted} = 1 - (\sum_{t=1}^{n} r_t^2 /(n-15)) /(\sum_{t=1}^{n} y_t - \overline{y})^2 /(n-1))$, where the residual (r_t) is the difference between the observations (y_t) and the expected values calculated from the fitted RM, $(\hat{y}_t)$. Thus the RSs are estimates of the errors, and are treated as a realisation of the error time series. For the temperature model, the high $R^2_{adjusted}$ are mainly attributable to seasonal variation. About half the coefficients of the climatic indicators are statistically significantly different from 0 at the 5% level, as shown in Appendix 7.4 (a, and b). For the rainfall model, $R^2_{adjusted}$ are lower because rainfall at these stations was markedly less seasonal than temperature. However all the coefficients of SOI, and the interaction coefficients for 6 out of 10 stations, are statistically significantly different from 0 at the 5% level, as shown in Appendix 7.4(a and b). There is a negative correlation between the RSs from the rainfall and temperature model (e.g. Hume Dam, r = -0.36), which is explained by the rain-bearing atmospheric conditions being colder.

A realisation of significant effects on rainfall and temperature patterns is shown in Appendix 7.5 (a and b). This study realised using GLS with auto regressive process of the first order, and provides significant evidence of rainfall variation from 1.91 mm to 8.61 mm and contemporary temperature variations from 0.14 ^{0}C to 0.44 ^{0}C at the 5% level. The variation of rainfall pattern is significantly influenced by the variation of SOI (from 0.05 mm to 0.25 mm) and the variation of interaction between SOI and PDO (from 0.05 mm to 0.22 mm) at the 5% level in the MDB areas and eastern Australia. However, the variations of temperature have also been significantly influenced by SOI variations and seasonality effect at the 5 % level as shown in Appendix 7.6 (a and b)

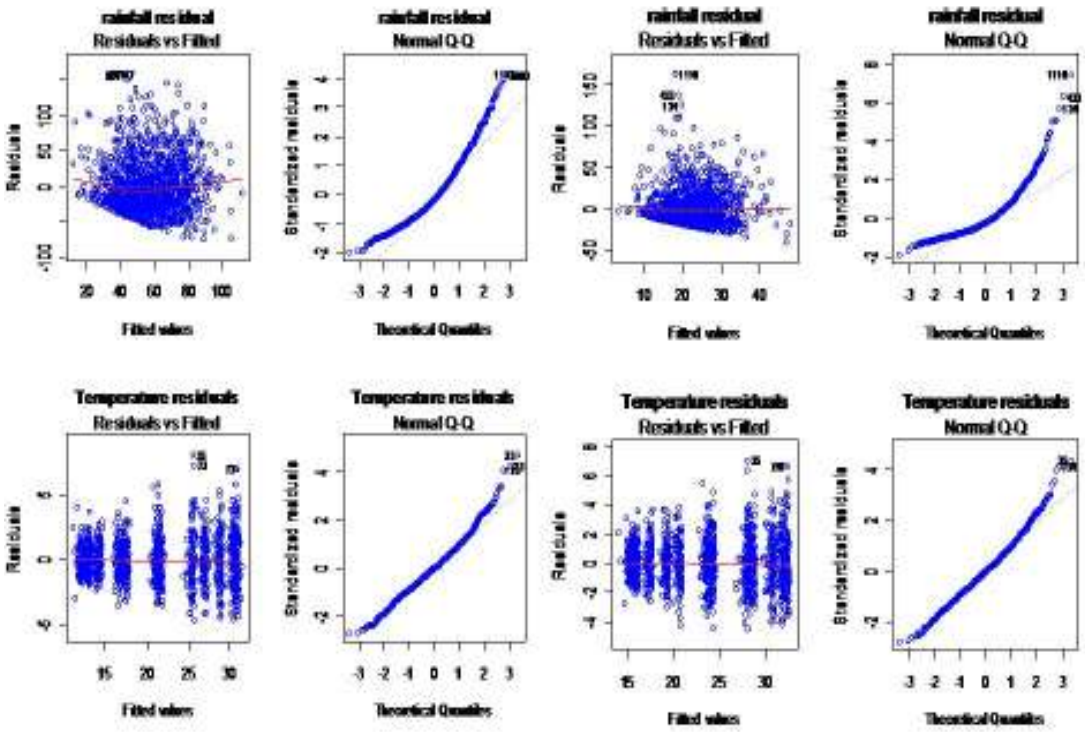

Figure 7. 4: **Rainfall RS versus fitted values (upper left); normal q-q plot of rainfall RS (upper right); temperature RS versus fitted value (lower left); normal q-q plot of temperature RS (lower right) for the Hume Dam station**

Having allowed for climatic indicators and seasonal variations, analysed the RS were analysis. The RS, for example, the Hume Dam and Mildura Airport data are now randomly considered in more detail. The plots of rainfall and temperature RS against fitted values shown in Figure 7.4 (upper and lower row first and third snapshot), and

details for all other weather stations as given in Appendix 7.7, suggests that the variability may increase slightly as the fitted value increases (e.g. Cook and Weisberg, 1982) . A plot of ordered RS against the expected order statistics from a normal distribution is shown in Figure 7.4 (upper and lower row second and fourth snapshot), and the clear departure from linearity indicates that the RS have a positively skewed distribution. This feature can also be seen clearly in the histogram of Figure 7.5 and Detail for other weather stations is given in Appendix 7.8.

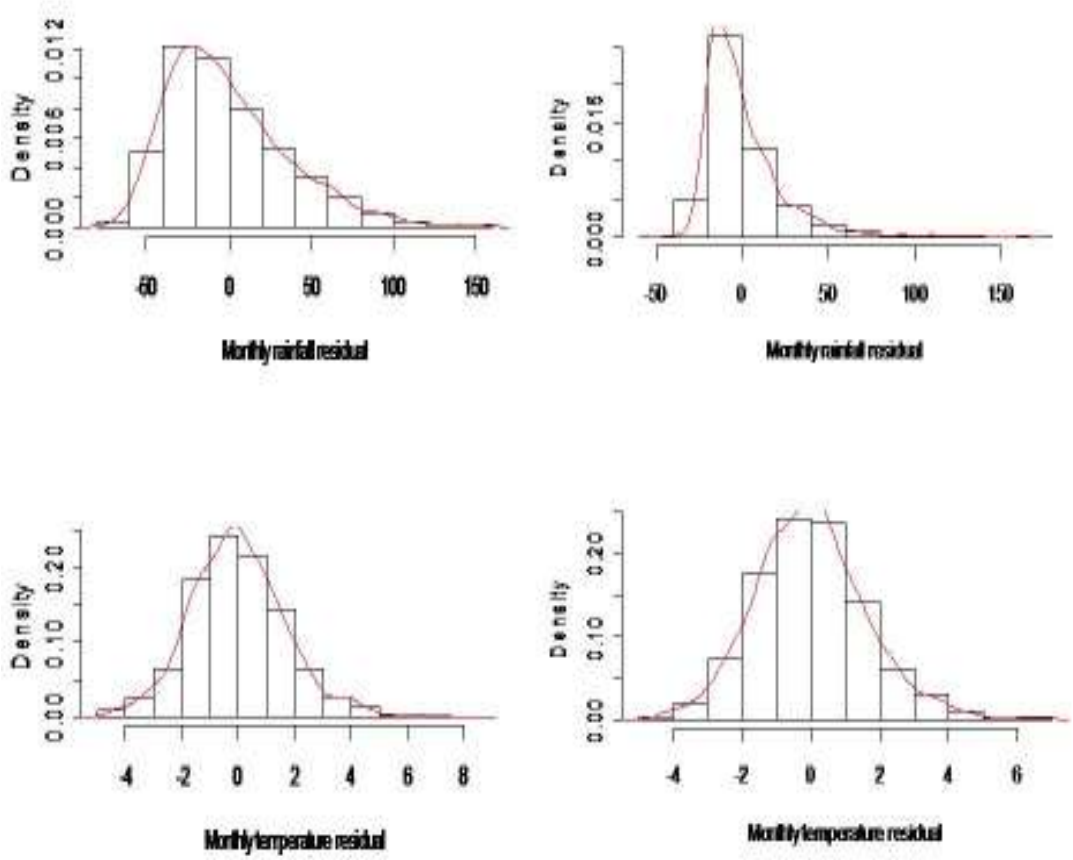

Figure 7. 5: Histograms of RS rainfall (upper row) and temperature 8bottom row) for the Hume Dam (left side) and Mildura (right side) station

This skewness is a consequence of rainfall being a non-negative variable with occasional extreme values. In contrast, the temperature RSs show a more marked heteroskedasticity, with the variability increasing with fitted value, but are reasonably well modelled as a normal distribution.

7.4. Discussion and conclusions

The initial regression analysis of rainfall, and temperature could only be performed with some transform of rainfall or temperature as the response, such as a fractional power or logarithm. The power could be chosen so that the RS have a distribution that is close to normal. However, the transform had the little effect on the correlation structure of the RS and did not affect the evidence of shifts in the process mean. The dynamics of ocean currents are highly non-linear and sudden changes have been observed over the past century. It might be argued that as this is a likely explanation of sudden shifts in the mean of the rainfall and temperature time series. It is, however, inappropriate to include known indicators of currents, in particular, SOI, in the initial regression analysis. Conversely, if PDO and SOI are omitted from the initial regression the evidence of non-stationarity remains, as can be seen from the Holt Winter analysis.

The regression based analysis provided evidence of shifts in the underlying mean rainfall and temperature over the past hundred years, after allowing for seasonal variation and the established effects of PDO and SOI. The Holt-Winters analysis provided qualitatively similar results without making allowance for PDO and SOI. However, the uncertainty associated with estimating the sensitivity of rainfall in the MDB areas and eastern Australia. By the realization of significant evidence of rainfall and temperature patterns, this study concluded that there was a trend of increasing temperature patterns in the MDB areas. This effect may be made more pronounce in the future, and would tend to lower rainfall in the MDB. This is what might be expected given the strong endorsement of global warming by IPCC. For three stations, there is evidence of a quadratic trend in temperature, which corresponds to the beginning and end of the 20^{th} century records being warmer. It has been suggested by Stevenson screens that some Australian weather stations at the beginning of the 20^{th} century may not have been up to modern standards, and that this may account for some of the high readings at the beginning of that century. It is therefore, further recommended to project the temperature to aid in understanding the variability of rainfall patters in the MDB.

To facilitate the WRMS for policy makers, this study realized the significantly effect on rainfall and temperature over the MDB areas and eastern Australia. Furthermore, it is concluded that the influence of the SOI and the PDO if serially correlated up to two years, would lead to changing rainfall patterns over this time. This is an influence well understood by TAR by IPCC and by the Australian BOM (IPCC, 2001 and BoM, 2008). It is recommended that modelling rainfall and temperature patterns would provide a better understanding of future water availability in the MDB areas.

The evidence of increasing or decreasing trends in rainfall and temperature suggested that there is distance dependency, which is categorized by ENSO and other hydrological parameters. To facilitate WRMS, however, more research is required on how rainfall and temperature patterns change the mean step and evidence of persistency. Furthermore, it is recommended to continue to seek evidence of change in rainfall and temperature patterns in the MDB areas.

.

CHAPTER 8: PERSISTENCY OF HYDROLOGICAL MODEL

.

8.1. Introduction

In the previous chapter, the evidence of rainfall and temperature pattern have been shown as non-stationarity because seasonal effect or trends. Moreover, variability of rainfall and temperature series may have demonstrated that the serially correlated, which usually results in periods of volatility. One idea is to modelling series of this nature is to use an AR model for the variance i.e. called auto regressive conditional heteroskedasticity (ARCH) model for the variance. Some of the CIs exhibits marked correlations at high lags and idea referred to as a long-memory process. Long memory process is a feature of many geophysical time series. Hurst (1951) demonstrated that this affected the optimal design capacity of a dam. Mudelsee (2007) shows that long memory result of a hydrological response that can be leads to prolong the drought, or extreme event of flood.

The aim of this chapter will design the climatic variability based on location in MDB areas. Distance dependence correlation model with periodic function will be applying for assessing the strength of rainfall and temperature pattern in the MDB areas, allowing CIs. One the particular objective of this study is to investigate the temporal properties of deseasonalized rainfall and temperature pattern, which plays a key role of the water resources across the MDB area and eastern Australia. Further more study will highlight the mathematical persistent of rainfall and temperature pattern and their step change across the MDB areas and eastern Australia.

8.2. Study approach

Chapter 5 discussed various RMs for rainfall and temperature that allow for seasonal variations and underlying climate states, categorized in terms of the PDO and the Southern Oscillation Index (SOI) which are thought to have significant effect on weather patterns in eastern Australia. The RSs from these regressions represent stochastic components which give random variation about the fitted values. The RSs are investigated in some detail, with the aim of detecting any shifts in the underlying mean or standard deviation of this random variation. The marginal distribution of the

RS and the possibility that the standard deviation depends on the magnitude of predicted values was also discussed. In the present chapter, the time series structure of the RS is investigated, in particular: the autocorrelations; possible bursts of high variability, and evidence for mathematical persistence. In chapter 8 the spatial correlation is modeled. Then, cumulative sum (CUSUM) plots are used to identify potential changes in the underlying mean. In such plots step changes in the mean of a process are indicated by a linear trend in the CUSUM. In contrast to a step change, a linear trend in the process mean would show up as a quadratic trend in the CUSUM. Even if the process mean is constant, there will be apparent trends in a CUSUM and there is a standard test, the V-mask or its algebraic equivalent, which identifies statistically significant trends in the CUSUM. However, the V-mask test is sensitive to an assumption that random variation is independent, an assumption that is not appropriate for the RS. Instead, a Monte-Carlo procedure is used to test the significance of apparent trends in the CUSUM plots.

8.3. Results analysis

Deseasonalized rainfall and temperature series are considered in detail with particular emphasis on evidence of non-stationarity.

8.3.1. Spatial correlation model

8.3.1.1. Distance between the weather stations.

For the spatial correlation model, six weather stations in the MDB areas and one in each four capital cities were considered. Their locations are identified by a red mark o the map shown as Figure 8.1.

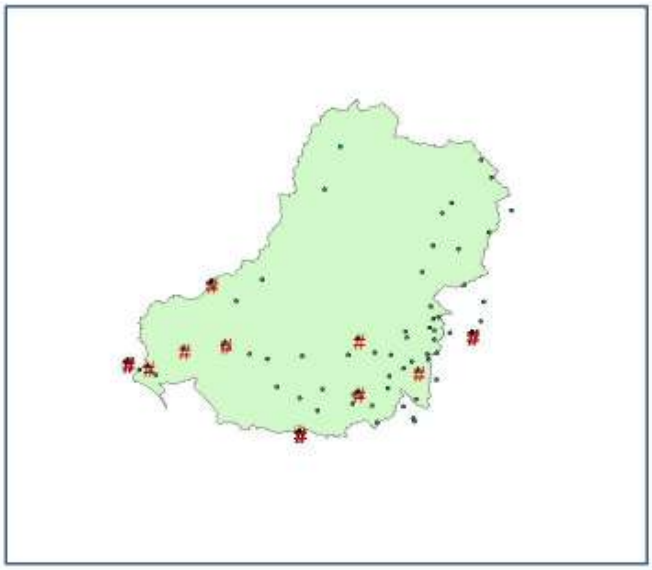

Figure 8. 1: Location of weather stations marked by red star.

The distance between weather stations was calculated based on latitude (north-south) and longitude (east – west) using web link calculator, shown in Table 8.1 and also distance from North –South (latitude) and East-West (longitude) were calculated and placed in Appendix 8.1.

Table 8. 1: Distance (km) calculated by latitude and longitude for six stations in the MDB and four state capital cities in Australia

	Adelaide Airport	Broken Hill	Canberra Airport	Hume Dam	Lake Victoria	Loxton Met	Melbourne Airport	Mildura Airport	Murray Bridge	Sydney observatory Hill
Adelaide Airport	0	463.8	1188	954.8	322.1	234.6	763.8	404.7	84.43	1416
Broken Hill		0	934.1	767.7	227.9	290.2	732.6	258.4	425.1	1102
Canberra Airport			0	257.2	892.8	964.2	552.7	799.3	1105	274.9
Hume Dam				0	680.1	741.3	300.5	586.9	870.8	527.2
Lake Victoria					0	90.2	565.2	93.85	253.7	1105
Loxton Met						0	593.6	170.6	163.6	1185
Melbourne Airport							0	488	681	825.8
Mildura Airport								0	329.5	1015
Murray Bridge									0	1336
Sydney Observatory Hill										0

8.3.1.2. The correlation of RS

The RS of rainfall and temperature were measured for the above mentioned locations on the map Figure 8.1. The number of pairs of stations is 45 the number of choices of 2 stations from 10 (i.e. ${}^{10}C_2$). Deriving the spatial correlation coefficient provides evidence of strength of association between locations. There is a very weak correlation of rainfall and temperature pattern between the stations. It is statistically significant but some correlations are negative in the temperature series in Appendix 8.2 (i) and 8.2 (ii), and plots of the sample correlation against distance are given in Figure 8.2.

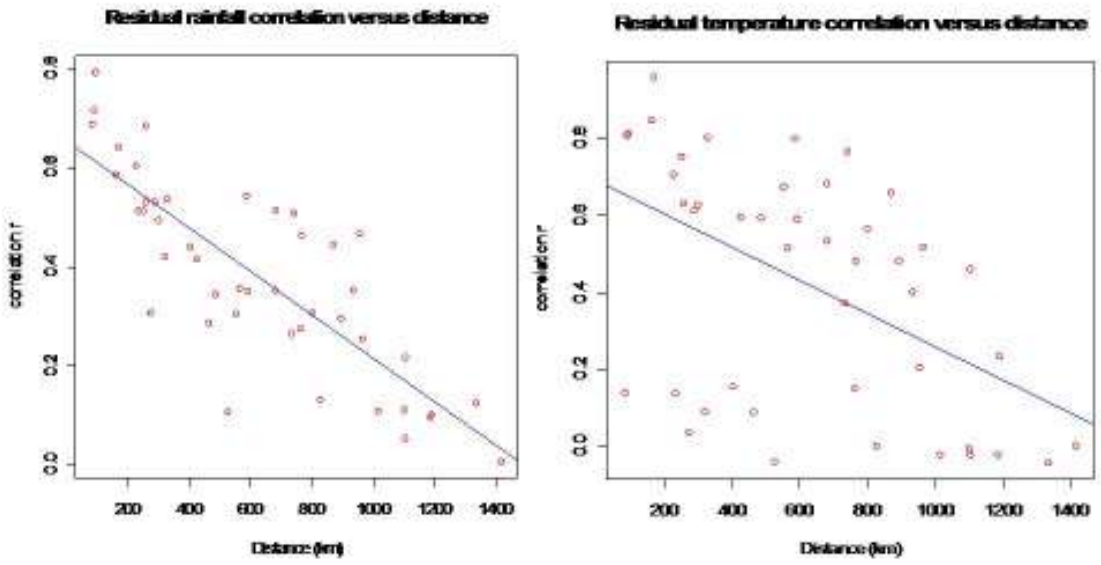

Figure 8. 2: RS rainfall correlation (left) and RS temperature correlation (right) versus distance

Figure 8.2, shows a clear distance dependence of the coefficients. The graphical representations in Figure 8.2 highlight this. They both have negative slope, i.e. the correlations of rainfall and temperature pattern between stations increase as distance between the locations is decreased.

8.3.1.3. Correlation model

The RS at different stations are correlated when they are, or are nearly, synchronous. The spatial correlation model for rainfall or temperature is:

$$\rho_{ij} = e^{-kd_{ij}}$$

Where d_{ij} is defined as the distance between stations i and j. The model is fitted to the 45 (distance correlation) pairs by fitting a regression of the logarithm of the sample correlation, or log (0.001) if the sample correlation is negative, against distance, without an intercept. The spatial correlation model for rainfall and temperature presented in Table 8.2, shows a best-fit linear regression line with 85% and 56% effect of distance on rainfall and temperature series respectively in model 1. In addition, model 1, the estimate of noise standard deviation is substantially small and estimated coefficient of distance effect is statistically significant. .

Table 8. 2: The spatial correlation model designed; i. coefficient distance for rainfall and temperature series in model 1, ii) coefficient of north-south and east-west distance for rainfall and temperature series in model 2.

Model 1.	Co-efficient	Std. error	t value	P-value	R^2	Adjusted R^2
Distance for rain	-0.0018798	0.0001143	-16.36	<2e-16	0.8589	0.8557
Distance for temp	-0.0031175	0.0004058	-7.683	1.16E-9	0.5729	0.5632
Model 2.	**Co-efficient**	**Std. error**	**t value**	**P-value**	**R^2**	**Adjusted R^2**
NS Dist for rain	-0.0007561	0.0004600	-1.644	0.108	0.8523	0.8454
EW Dist for rain	-0.0017999	0.0001586	-11.352	0.000015		
NS Dist for temp	0.0003945	0.0015745	0.251	0.803	0.5843	0.565
EW Dist for temp	-0.00341134	0.0005427	-6.286	1.40e-07		

In model 1, the stations are close enough for spatial correlations to be substantial, and a model of exponential decay of correlation with distance provides a good fit, and could be used to define a Variogram. A model 2 was also fitted treating the north-south and east-west distances as separate predictor variables, but there was no evidence to suggest that this model provided a better fit. In practical terms the spatial correlation between stations noise standard error in rainfall and temperature model like 80km appears to negligible

8.3.2. Temporal properties of RSs

8.3.2.1. Autocorrelation

The RSs shows in term of both short term and long term correlations which case a fractional autoregressive integrating moving average model (FARIMA [p, d, q]). However, the hydrological model is reasonably well by AR processes of order 1 (AR [1] processes). The purpose of a correlogram is to determine whether there is autocorrelation in the series. In this, correlations that decay very slowly to zero suggest that separated observations are related and long memory or long range dependence is present. Bern (1994) provides mathematical evidence of persistence in the correlogram of time series. Persistence causes the correlogram to decay hyperbolically with r(k) approximating $k^{-\alpha}$ as the lag increases. The autocorrelation lag at 0 is included by default; this always takes the values 1, since it represents the correlation between the data and themselves. In this study particularly interests are the autocorrelations at another lags these are shown in Table 8.3.

Table 8.3 shows that the autocorrelations continue to decrease as the lag become larger. Contemporary variation is increased indicating that there is no linear association among the observations separated by lags larger than 3. The correlogram plots for rainfall and temperature RSs in Hume Dam are shown in Figure 8.3 and others correlograms of RSs are shown in Appendix 8.3. In particular, for Hume Dam station, the rainfall RS typically have significant serial correlation at lag 1, at least. The temperature RSs have higher serial correlations up to lags of about two years, as shown in Figure 8.3

Table 8. 3: Lag 1 to 3 serial correlations from rainfall and temperature RSs for all 10 stations

Station name	Record length (months)	Rainfall residuals			Temperature residuals		
		Lag 1	Lag 2	Lag 3	Lag 1	Lag 2	Lag 3
Adelaide Airport	641	0.104	0.075	-0.006	0.138	0.111	0.078
Broken Hill	604	0.105	0.095	0.116	0.068	0.093	0.008
Hume Dam	1290	0.159	0.098	0.057	0.385	0.270	0.179
Lake Victoria	1024	0.077	0.014	0.003	0.199	0.122	0.108
Loxton Met Station	1183	0.066	0.027	0.022	0.201	0.165	0.134
Mildura Airport	1290	0.092	0.049	0.026	0.298	0.236	0.179
Murray Bridge	494	0.103	0.015	-0.045	0.508	0.296	0.077
Canberra Airport	833	0.073	-0.010	0.013	0.267	0.207	0.130
Melbourne Airport	457	0.068	0.031	0.038	0.385	0.270	0.179
Sydney Observatory Hill	1303	0.018	0.008	0.022	0.077	0.115	0.032

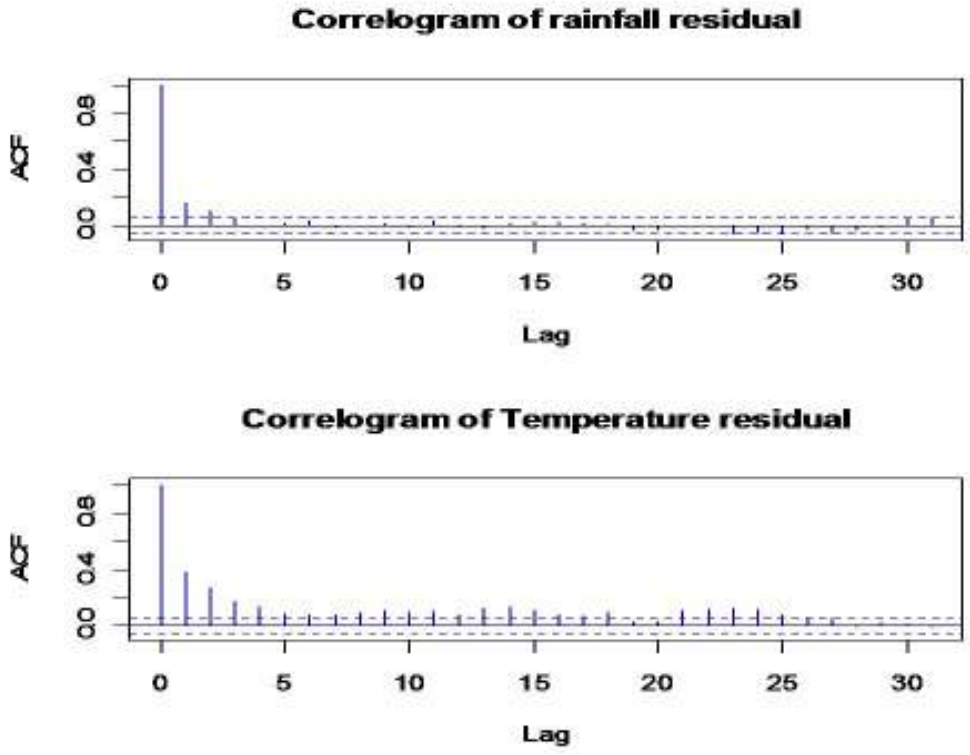

Figure 8. 3: Correlogram of rainfall (upper) and temperature (lower) RS for the Hume Dam station.

Figure 8.3 shows the correlogram, for the Hume Dam RS, detail are shown in Appendix 8.3. Autocorrelations outside the dashed lines on the correlogram are statistically significantly different from 0 at the 5% level.

8.3.2.2. GARCH model

Non-stationarity in the variance of the time series is known as volatility, and it can be approximated using GARCH models. A test for non-stationarity in the variance of a stationary time series involves first fitting a suitable ARMA (p, q)) model and then calculating the correlogram of the squared RSs from that ARMA model. If the squared RS have significant autocorrelation, bursts of increased variability are indicated. To investigate volatility, the correlogram of the squared RS are shown in Figure 8.4 for Hume Dam. Details are shown in Appendix 8.4.

For the Hume Dam rainfall RSs, there is a suggestion of volatility because of the significant autocorrelations of the squared RSs after fitting an AR (2) model to the regression RSs. However, the volatility appears slight in practical terms. For the Hume Dam temperature RSs, there is a seasonal pattern to the autocorrelations of the squared RSs after fitting an AR (24) model to the regression RSs. This suggests some seasonal variability in the standard deviation, which corresponds to the already noted tendency for the standard deviation to increase with the mean value.

Moreover, the correlogram of rainfall RSs shows no obvious patterns or significant values in Appendix 8.4, but the correlogram of temperature RS appear to be more practical term at the Loxton Met stations in the MDB. Hence satisfactory performance of the GRACH model fit has been demonstrated.

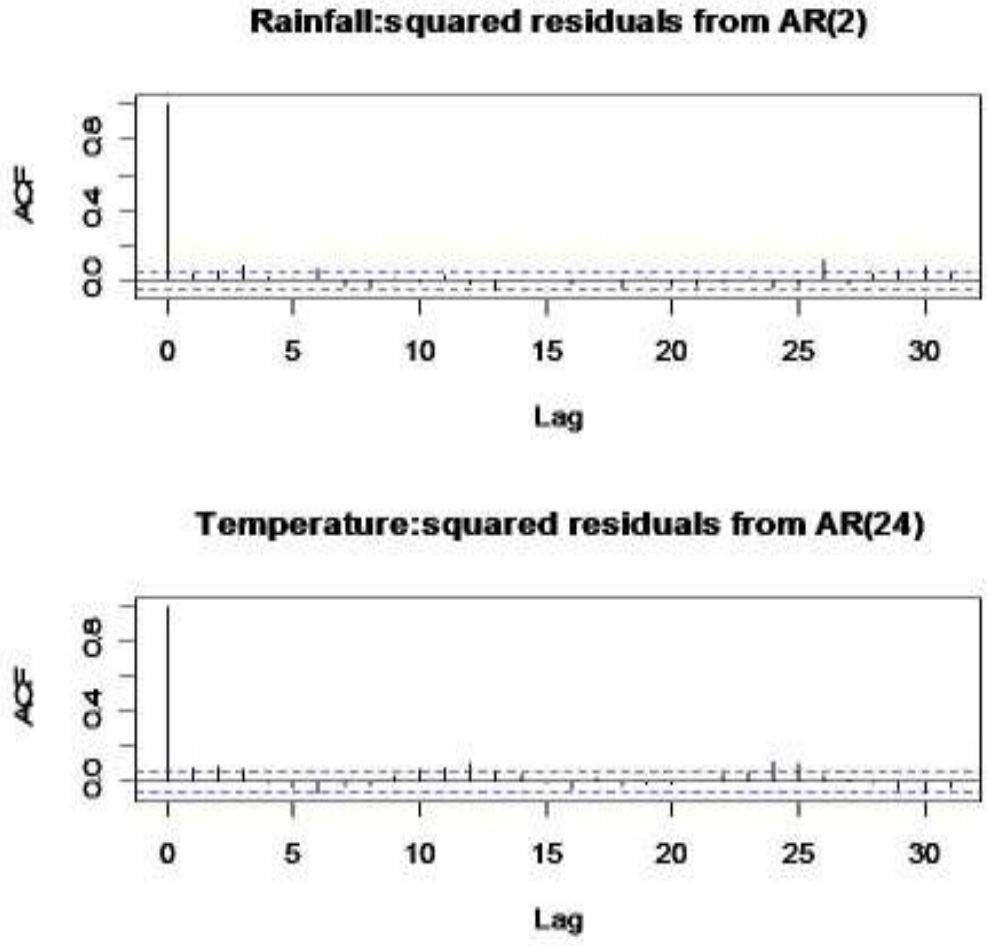

Figure 8. 4: Correlogram of GRACH model squared rainfall (upper) and temperature (lower) RSs for the AR models for Hume Dam

8.3.3. Hurst Phenomena

The mathematical definition of Hurst phenomenon (H>0.5) section 4.4.7, corresponds to long range dependence and H equals 0.5 if correlations decay exponentially. However, in realisations of time series, which are necessarily finite, sample estimates of H are biased above 0.5. A time series should have an estimated trend removed before calculation of H in order to distinguish long-term memory from any trend. One method of estimating H for a time series $\{\varepsilon_t\}$ is to regress the logarithm of the rescaled adjusted range R_m, calculated from a subseries of length m (where m is less

than or equal to the length n of the whole series) against the logarithm of m. Calculated values of the rescaled adjusted range are shown in Table 8.4.

Table 8. 4: The Hurst coefficient for rainfall and temperature for all 10 stations

Station Name	length	Estimated Hurst coefficient		AR process		Realisation of P-values	
		Rainfall	Temperature	Rainfall	Temperature	Rainfall	Temperature
Adelaide Airport	641	0.4751901	0.570015	2	2	0.10	0.16
Broken Hill	604	0.6233186	0.579108	3	2	0.07	0.15
Canberra Airport	833	0.5021439	0.626324	1	2	0.32	0.07
Hume Dam	1290	0.5532967	0.750545	2	5	0.17	0.01
Lake Victoria	1025	0.547199	0.562474	1	3	0.15	0.21
Loxton met	1182	0.5798934	0.5360469	1	5	0.09	0.02
Melbourne Airport	457	0.5671415	0.599891	1	3	0.17	0.3
Mildura Airport	1290	0.5093299	0.742117	2	5	0.49	0.03
Murray bridge	494	0.4201007	0.608266	1	3	0.15	0.04
Sydney Observatory Hill	1303	0.5719091	0.547859	5	6	0.11	0.22

The regression estimates of the Hurst coefficient for rainfall and temperature are shown in column 3 of Table 8.4. The estimated Hurst coefficient H is less than 0.5 for rainfall patterns at Adelaide Airport and Murray Bridge and the temperature pattern at the Loxton Met. These evidence of independent random variation and it is not required to realised the long rang dependency by the AR process. The realisations of the estimated H coefficient by different order (order chosen by the GRACH model) are shown in column 5 in Table 8.4. Sequentially, significant evidence is H calculated from realisations of the AR process with parameters estimated by fitting to the RS. For example the rescaled adjusted ranges for the Hume Dam station monthly rainfall and temperature RSs were calculated at block sizes from 2 up to the record length of 1284 months, as shown in Figure 8.4. The regression estimate of the Hurst coefficient for rainfall is 0.553, and this is not significantly greater than values of H calculated from realisations of an AR(2) process with parameters estimated by fitting to the RS (17% of realisations from Monte-Carlo simulation had Hurst coefficients greater than 0.553). The regression estimate of the Hurst coefficient for temperature is 0.751, and

this is significantly greater than values of H calculated from realisations of an AR (5) process with parameters estimated by fitting to the RS (P ≈ 0.01 by Monte-Carlo simulation) as shown in Table 8.4. Therefore there is no evidence of long memory in the rainfall but there is some evidence of long memory in temperature patterns in MDB areas.

The rescaled adjusted range plots ln (R_m) versus ln (m) for the Hume Dam station monthly rainfall and temperature RSs were calculated at block sizes from 2 up to the record length of 107 years as shown in Figure 8.5. Similar rescaled adjusted range plots are given in Appendix 8.5.

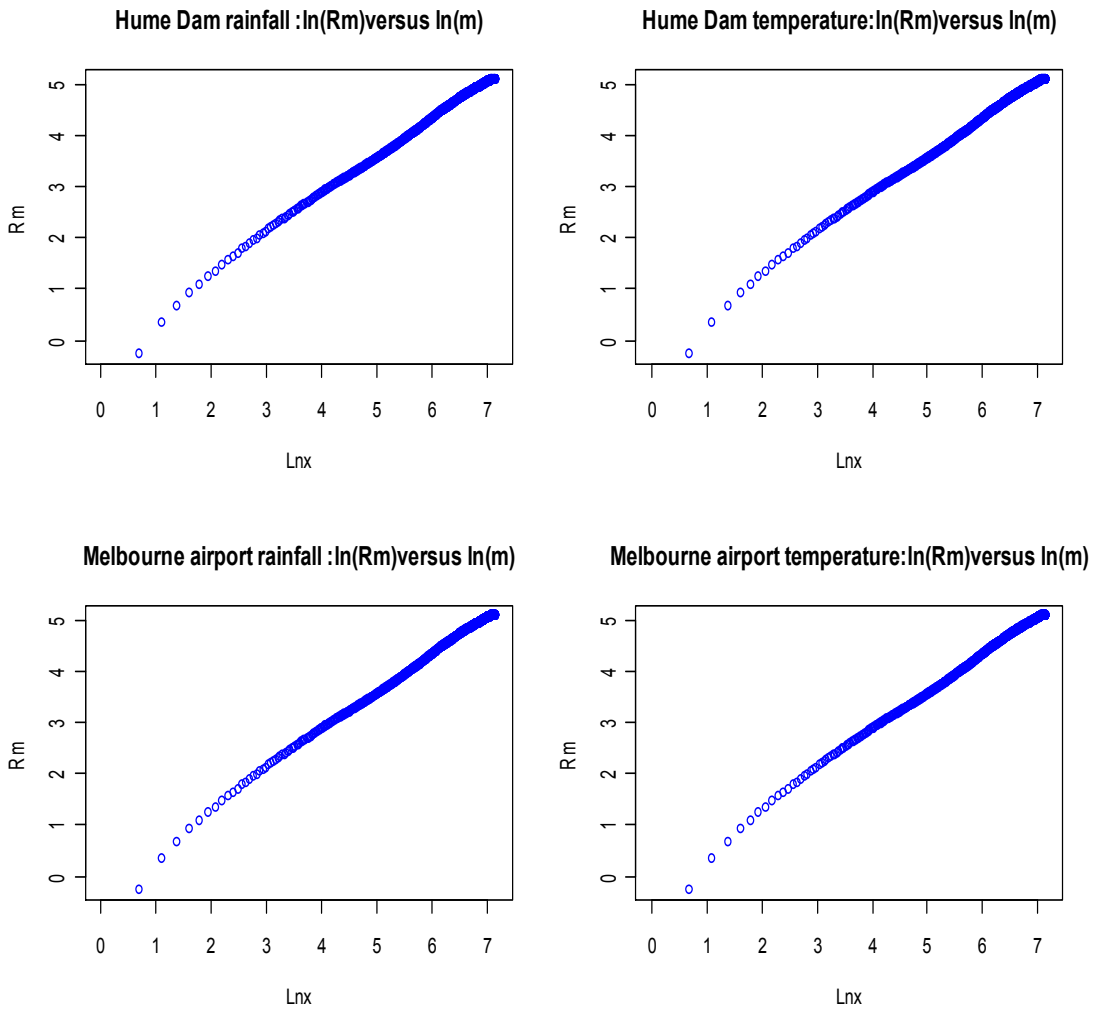

Figure 8. 5: Rescaled adjusted range for monthly rainfall (left) and temperature RS (right) for the Hume Dam station and Melbourne airport.

8.3.4. CUMSUM method

In the cumulative sum (CUSUM) method, the RSs are analysed in more detail for indications of a step change in the average rainfall and temperature patterns in the MDB areas in eastern Australia. CUSUM statistics for the assessment of the rainfall and temperature patterns are shown in Table 8.5.

Table 8. 5: CUSUM method test statistics with fitted ARMA process

		Cumulative sum of residual with fitted AR process						Simulation process run 1000 noise series with length residual series, realisation at lag 10 independent random variation				
	Length (Column 1)	Rainfall (Column 2)			Temperature (Column 3)			Gumbel distribution factor (Column 4)	Rainfall (Column 5)		Temperature (Column 6)	
		Standard deviation (a)	Estimated standard deviation (b)	Q statistic (c)	Standard deviation (a)	Estimated standard deviation (b)	Q statistic (c)		Q statistics (a)	P-values (b)	Q statistics (a)	P-values (b)
Adelaide Airport	641	23.322	20.101	34.286	2.460	2.261	61.662	1.164	27.084	0.20	51.128	0.02
Broken Hill	604	27.836	17.752	72.055	1.242	0.613	68.360	1.162	63.608	0.00	47.787	0.10
Canberra Airport	833	37.506	29.207	53.656	2.260	2.023	86.670	1.167	43.916	0.03	73.412	0.01
Hume Dam	1290	38.035	32.294	81.008	1.717	1.520	178.620	1.166	67.426	0.03	157.733	0.00
Lake Victoria	1025	21.083	14.457	66.922	1.262	0.874	80.154	1.165	52.432	0.22	67.001	0.04
Loxton met	1182	13.991	12.936	61.537	12.547	2.804	206.171	1.166	213.349	0.00	113.789	0.00
Melbourne Airport	457	29.006	21.828	48.817	2.590	2.518	47.386	1.168	40.177	0.00	40.667	0.02
Mildura Airport	1290	21.768	15.192	72.605	1.621	1.491	174.069	1.166	65.382	0.05	162.760	0.00
Murray Bridge	494	22.258	17.430	25.058	1.263	1.142	54.286	1.165	18.144	0.03	52.307	0.01
Sydney Obs. Hill	1303	88.701	69.692	72.797	2.891	2.854	71.936	1.168	69.532	0.01	67.016	0.05

Column 2b and 3b of Table 8.5 show that the median range of estimated standard deviation ($\tilde{\sigma}$) is substantially smaller the standard deviation of RSs of the rainfall and temperature series shown in Columns 2a and 3a respectively. There is no reason to

suspect that both rainfall and temperature series exhibit occasional large shifts under the mean process.

In the simulation process, to calculate $\tilde{\sigma}$, the moving ranges of the RS at some chosen lag are calculated and the median of this range is multiplied by factors from the Gumbel distribution. In the case of independent random variations, a lag of 1 suffices and is used. However, in this study the RSs are not considered independent and a lag of 10 is chosen so that the ranges can reasonably be assumed to be the absolute values of differences of independent variables. The marginal distribution of the RSs is well modelled by Gumbel distribution. The factor 1.16 is found by simulation from a Gumbel distribution as shown in Column 4 in Table 8.5. However, this factor is irrelevant for calculating the statistical significance as a Monte-Carlo procedure is used to test the null hypothesis of a constant underlying population mean. Fitting a suitable ARMA (p, q) model with random variation from a Gumbel distribution to the RS, running 1000 simulations of the same length as the RS and calculating yields the Q statistic shown at Columns 5a and 6a for each rainfall and temperature series respectively. The statistical significance of calculated values of Q (in Columns 2c and 3c of Table 8.5) is the proportion of simulated Q values (in Column 5a and 6a) that exceed Q.

CUSUM plots for the rainfall and temperature RSs from the Hume Dam and Mildura Airport stations are shown in Figure 8.6. Detailed CUSUM plots are shown in Appendix 8.6. Similar details for the other sites are also provided in Appendix 8.6.

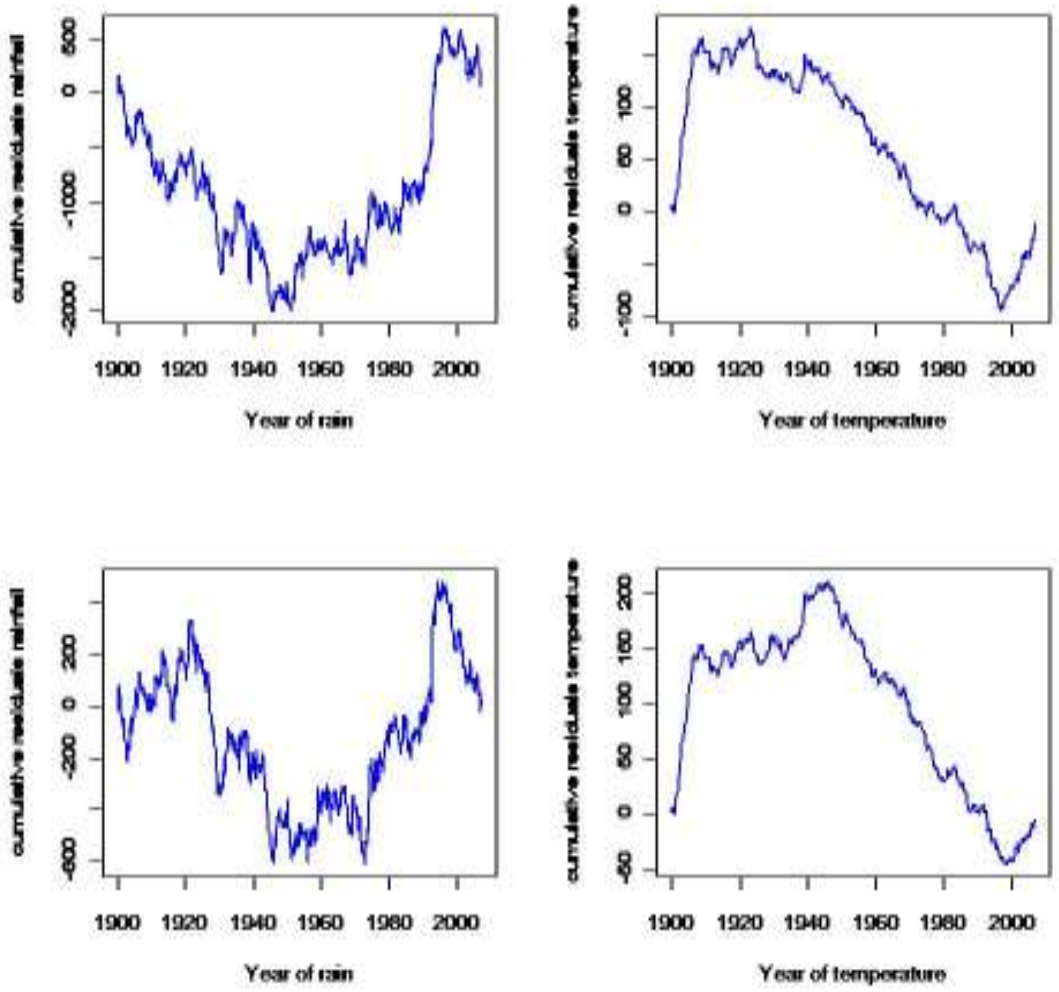

Figure 8. 6: Cumulative sum plots for Hume Dam and Mildura Airport rainfall (left) and temperature (right) RSs

In both cases Q is statistically significant (at the 5% and 10% level respectively) and there is evidence of non-stationarity in the mean. For example for Hume Dam, the rainfall CUSUM indicates a period of below average rainfall (1900-1949) followed by a period of above average rainfall (1950-2000), and a recent period of below average rainfall (2001-2007). Similarly for the Mildura Airport station, the rainfall CUSUM indicates a period of below average rainfall (1925-1958) followed by a period of above average rainfall (1969-1999) and a recent period of below average rainfall (2000-2007). This is shown in Table 8.6 and similar CUSUM indicating average rainfall and temperature per month are given in Appendix 8.6

Statistics for these periods are given on the left side of Table 8.6. The temperature CUSUM suggests broadly similar periods, which may be due to the negative correlation between rainfall and temperature, and the associated statistics for these periods are given in the right side of Table 8.6

Table 8. 6: Average rainfall and temperature by period determined by CUSUM of rainfall RSs

		Period determined by CUSUM of rainfall residuals	
Area	Periods	Mean rainfall / month(mm)	Mean Temperature / month (mm)
Hume Dam	1990-1949	54.91	21.73
	1950-2000	61.38	21.25
	2001-2007	47.07	22.67
Mildura Airport	1925-1958	22.15	23.95
	1969-1999	24.73	23.64
	2000-2007	19.07	24.62

Steep slopes in CUSUM plots typically correspond to periods of below average or above average values rather than trends. These would correspond to quadratically increasing or decreasing slope respectively. Moving average plots are a useful means for distinguishing more clearly shifts in level from trends. Five year (60 point) moving averages of the rainfall and temperature RSs, the regression having removed the effects of the seasonality and climatic indicators, for the Hume Dam and Mildura

Air port station are shown in Figure 8.7. The current relatively warm and dry climate is apparent, but not extraordinary relative to the 107 year period.

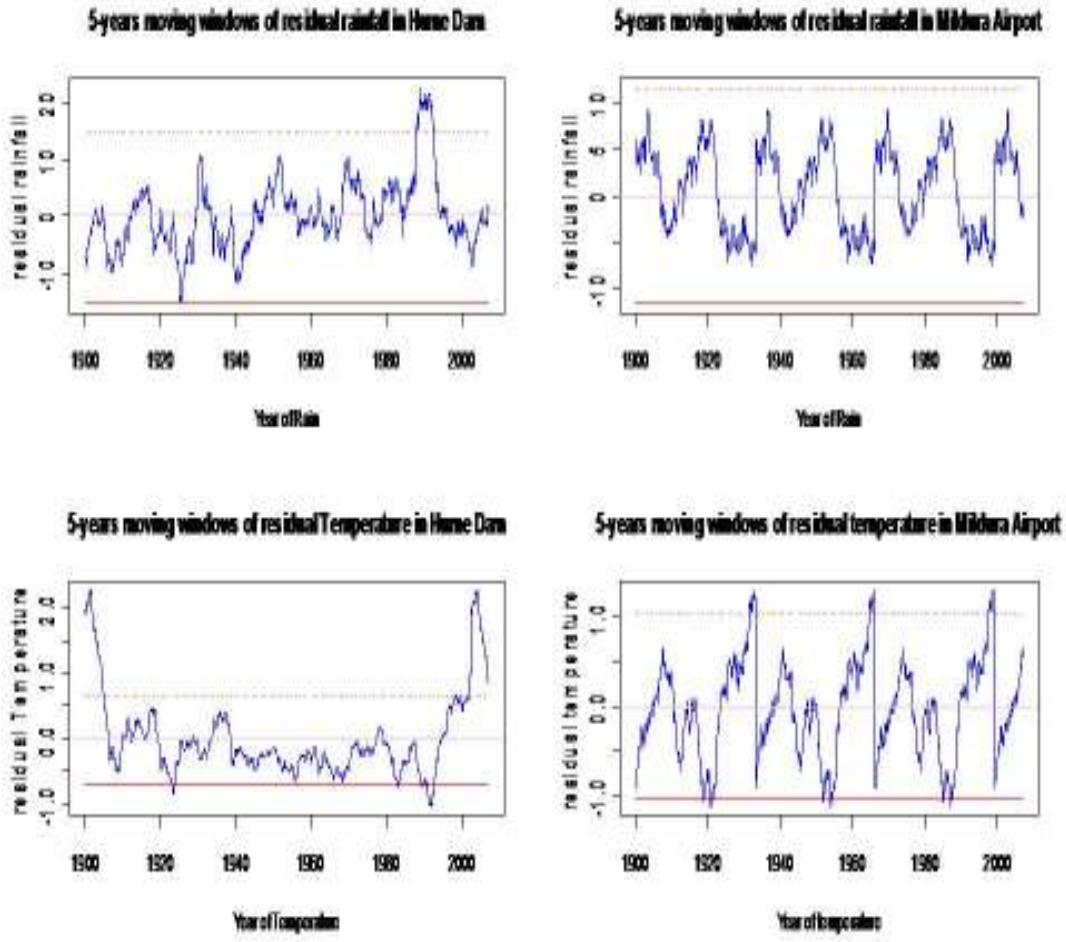

Figure 8. 7: Five-years Moving averages of for rainfall and temperature RSs for Hume Dam (left side) and Mildura Airport (right side).

8.3.5. Robust regression technique

The strategy is to fit known effects, including seasonal and climatic indicators Therefore, it reinforces the local weighted smoothing curves of the original time series with a parameter of 0.2, corresponding to local weighted robust regression over 20% of the length of the time series, which is small enough to show low frequency changes in the underlying level of the time series, could compared with the RM with

climatic indicators of SOI, PDO and their interaction effects, as shown in Appendix 8.9 (a and b)

Following up robust RM, the strategy is to fit with removed lowess trend and re-assess the significance of the climatic indicators in the Hume dam patterns, Figure 8.8 show the estimated effects of climatic indicators superimposed on the lowess trend

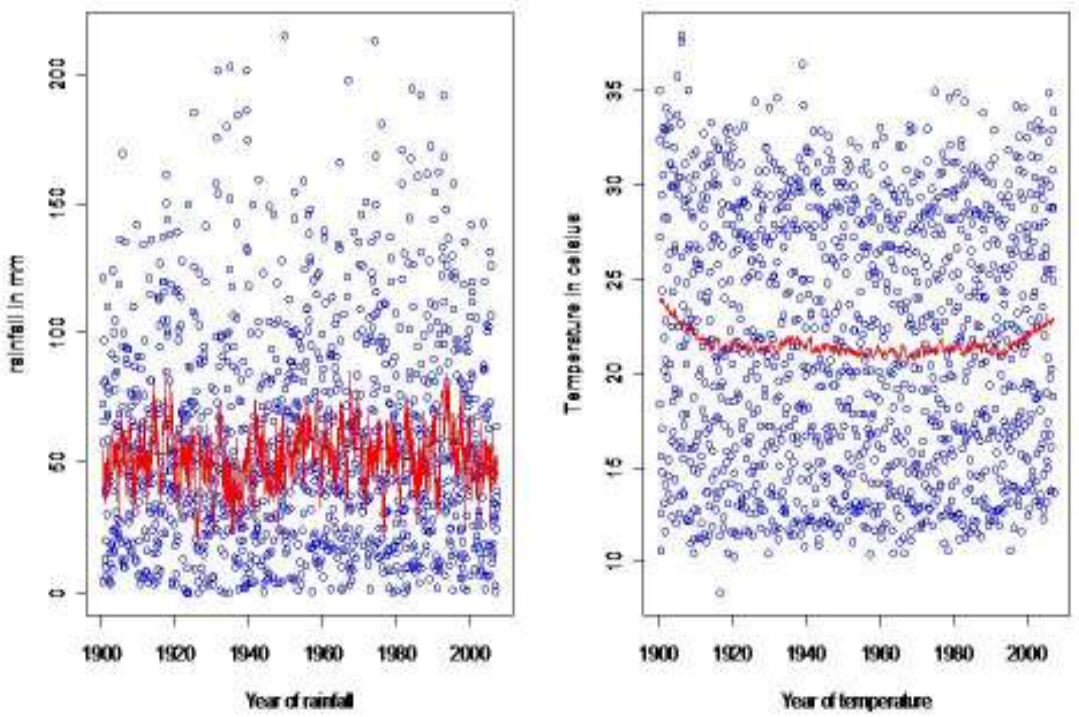

Figure 8. 8: Local weighted robust regression a) smooth parameter 0.2 (black line), b) removed lowess trend (red line) in rainfall (left side) and temperature (right side) at Hume dam in the MDB area.

8.3.6. Rainfall and Temperature projection

The recommended strategies were based on a Monte Carlo simulation process using a Gumbel distribution. The simulation process revealed evidence of step change in rainfall and temperature as shown in Table 8.5. Furthermore, it was recommended that long range persistency in temperature patterns in the MDB areas as shown in Table 8.4, would lead to reduce rainfall. This study re-analyzed the climatic indicators

and removed any trend in the rainfall and temperature series, and superimposed to project the next 100 years at the Hume dam in the MDB areas, as shown in Figure 8.9.

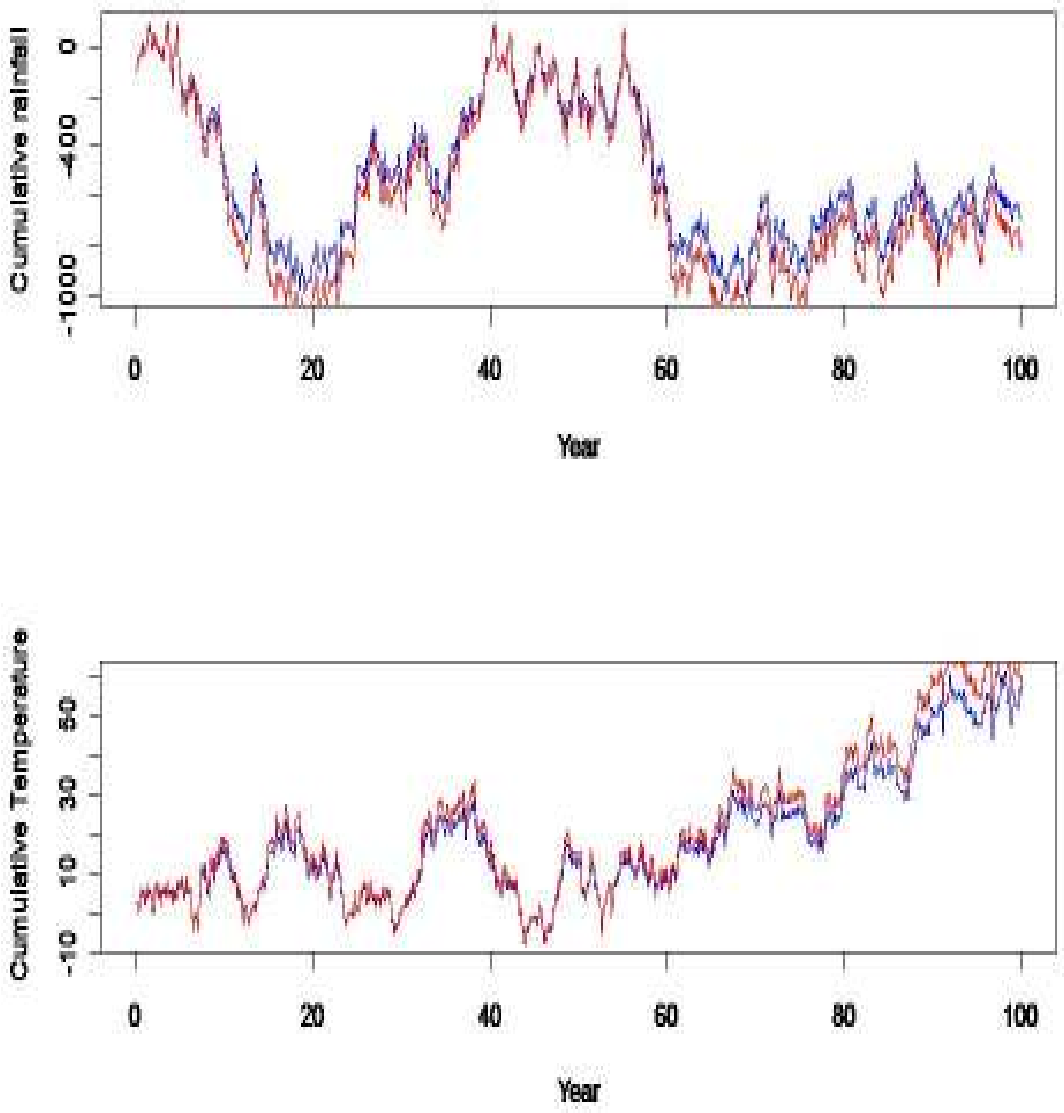

Figure 8. 9: Projected rainfall and temperature a) blue line white noise series b) red line white noise series multiple by Gumbel factor.

8.4. Discussion and conclusions

There are many ways in which non-stationarity in rainfall and temperature time series could be investigated. The strategy of identifying seasonal variation and the effect of global climatic indicators, and removing these features before attempting to discern evidence of trends or step changes in climatic time series provides a powerful test of supposed stationarity. This study concluded that there was evidence of non stationarity in rainfall and temperature patterns in the MDB areas. This study found that post 2000 period, was characterized by above average temperature and below average rainfall, as shown in Table 8.4 and Appendix 8.7. It also recognized evidence of step change in rainfall and temperature in both the long and the short term. It was recommended a 5-year moving average to smooth and show the trend but that is a relatively short period. The last 10 years rainfall was significantly reduced due to increasing temperature as shown in Figure 7.3. Evidence was also found of long range memory in the temperature patterns as shown in Table 8.4. Development of the robust RM for better understanding rainfall and temperature pattern in the MDB areas was achieved. This evidence may be superimposed to plot the temperature and rainfall patterns in the MDB areas expectations of the next 100 year.

This chapter concludes the research with recommendations regarding the development of WRMS in the GRB and the MDB. Moreover, a holistic approach is proposed to resolve conflicts over water resources management in developed and developing countries. A valuable lesson in IWRM strategy can be learned from the holistic approach adapted in the MRB. This is discussed and a possible strategy adapted for the GRB. A statistical downscaling technique has been applied to assess the relevant climatic drivers and a hydrological model then developed for implementation in water resources management in the MDB.

Water conflict involves the question of "equity". A vague and relative term in any event. Criteria for equity are particularly difficult to determine in water conflicts, where international water law is ambiguous and often contradictory. Also no mechanism exists to enforce principles which are agreed-upon. In addition, the term “equitable” can not always be focused. When implementing the water resources development projects, ignoring this fact may initiate the social conflict. For example in case of the Farraka Barrage the conflict between Bangladesh and India, arises due to unequitable distribution of the water during the monsoon season and the post monsoon period. The conflict is further worsened on the Indian part by not regulating the water flow in the monsoon season which ultimately increases flooding in Bangladesh and also by not releasing a proper quantity of water during the dry season. The latter makes it necessary for Bangladeshi farmers to irrigate during the dry season. This study recommends resolution of these issues of water sharing by proper negotiation and cooperation between the two countries and also by adaptation of UN principles of transboundary water resources management.

Equitable sharing of water resources is clearly the best solution for mitigating the conflict related to the water sharing between transboundary countries. When establishing the equitable principles, it is necessary to consider both the types of river basins and the populations depending on them and also the past history of water use in those river basins. This study recommends also that the conditions of the aquifers

involved, both confined and unconfined, need to be considered as part of the resolution. This would complete the minimisation of social conflict and the analysis of the dependency factors on the water resources. Some of the recommendations given below may be helpful in mitigating social conflict especially in developing countries;

1. The Institutional framework should focus on in depth studies of the socio-economic conditions and also pre EIA and post EIA reports, and other monitoring and evaluation reports of any relevant water resources management programs or projects.

2. UN principles should be adapted to compensate for the impact on peoples in the community, providing alternatives livelihoods activities where necessary.

3. An international framework of cooperation should be established incorporating the above mentioned UN principles on transboundary water management especially with regard to mitigating social conflicts over shared water resources between the two or more than two countries involved

4. An international reference committee should also be established. This should take an active part in the resolution of social conflicts from an international standpoint.

A case study has been presented of the Ganges River Basin, and in particular, the transboundary water sharing issues between Bangladesh and India. The vital issues of why water sharing treaties are violated and why India currently rejects the proposal to augment the flow at the Farakka Barrage in the GRB are confronted. This study drew attention to the agreement on water sharing of Ganges of 1996 (valid until 2026). Steps are needed to ensure the availability of water for sharing. A Stackelberg leader-follower model is proposed to develop win-win strategies for mitigation of transboundary water sharing issue between Bangladesh and India. The recommendations of this study can be implemented in any river basin, particularly ones involving upstream – downstream co riparian states.

The model developed highlighted how augmenting flow at Farakka could resolve the water sharing conflicts between Bangladesh and India. Implementation of a long-term solution based upon the Stackelberg model would achieve the optimal water sharing arrangement. Optimization of the flow augmentation in the Ganges River during the dry season is recommended instead of political bickering about the Farakka issue. A strategy involving water transfer from a third party (Nepal) is involved.

To develop WRMS in the MDB, a scenario based upon relevant climatic drivers was generated by a statistical downscaling technique. A large number of statistical methods applied for analysing hydrological series were examined. Rainfall and temperature patterns were analysed to assess future water availability. Also, parametric and a non-parametric statistical tools were superimposed to characterise the respective patterns.

The variability of rainfall and temperature patterns was characterized by statistical tools. Rainfall followed a decreasing pattern whereas temperature followed an increasing pattern, in both the long term and the short term. Non parametric statistical tests showed that there was no evidence of trend between the rainfall and temperature patterns in the MDB areas. The relationship between rainfall and temperature was negative. The increasing trend of temperature could further reduce rainfall in the MDB areas. Moreover, this study provided evidence of the temporal and spatial variation of rainfall and temperature patterns. Projecting rainfall and temperature patterns for future water availability in the MDB areas, this study provided recommendation for minimizing temporal and spatial variability.

i. **Minimize spatial variation**: The height values from 0 to 2.587 represent the spatial variation. Considering height value 2.587 would be convenient way to minimize the spatial variation and furthermore develop strategies for future water availability in the MDB areas.

ii. **Minimize temporal variation**: the height values from 0 to 1.18 represent temporal variation. Considering the height value 1.18 could minimize the temporal variation in rainfall and temperature pattern in the MDB areas.

It is recommended to further assess rainfall and temperature patterns and further examine how rainfall and temperature pattern are influenced by relevant CIs across the MDB areas.

The variability of rainfall and temperature has been analysed recognized and in depth in this study. It is important to take this into account when developing strategies on water resources management, because the hydrological baselines are uncertain due to climate change. The SST in the Pacific Ocean, Atlantic Ocean, and Indian Ocean and the SLP anomalies between Darwin, Australia and Tahiti were analysed. This study provided evidence of an increasing trend of SST in the Atlantic Ocean over time. The evidence was of an increasing trend in PDO influence from the mid 20th century on the Australian subcontinent. This study concluded that the SOI had a significant influence and that its interaction with the PDO categorizes Australian rainfall patterns. It is further concluded that a reduction in future SOI influence could reduce Australia's rainfall, and that the interaction between PDO and SOI is likely to be more pronounced during periods of negative PDO. However, periods of negative PDO could reduce temperature influence, which might increase future rainfall in the MDB areas. It is recommended to further study the effects of rainfall and temperature patterns in the MDB areas.

Allowing for seasonality, rainfall and temperature have been modelled with a focus on the effects on future water availability in the MDB areas. By the realization of significant evidence of rainfall and temperature patterns, this study concluded that there was a trend of increasing temperature patterns in the MDB areas. This effect may be more pronounced in future, and would tend to lower rainfall in the MDB. It is therefore further recommended to project the temperature effects to aid in understanding the variability of rainfall patterns in the MDB. Furthermore, the influence of the SOI and the PDO if serially correlated up to 2 years, would lead to changing rainfall patterns over this time. It is recommended that modelling rainfall and temperature patterns be used to provide a better understanding of future water availability in the MDB areas. Furthermore it is recommended to continue to seek evidence of change in rainfall and temperature patterns in the MDB areas.

Removing seasonality and any trend effects, this study concluded that there was evidence of non stationarity in rainfall and temperature patterns in the MDB areas. This study found that the post 2000 period was characterized by above average temperature and below average rainfall. It also recognized evidence of step change in rainfall and temperature in both the long and the short term. A 5-year moving average was recommended to smooth and show the trend but that is a relatively short period. The last 10 years rainfall was significantly reduced due to increasing temperature. Evidence was also found of long range memory in the temperature patterns. Development of a robust RM for better understanding rainfall and temperature patterns in the MDB areas was achieved.

The strategy is to fit known effects, seasonal and climatic indicators. Therefore, it is reinforce the local weighted smoothing curves of the original time series with a parameter of 0.2, corresponding to local weighted robust regression over 20% of the length of the time series. This is small enough to show low frequency changes in the underlying level of the time series, could compared with the RM with climatic indicators of SOI, PDO and their interaction effects. Following up robust RM, the strategy is to fit with removed lowess trend and re-assess the significance of the climatic indicators, then to show the estimated effects of climatic indicators superimposed on the lowess trend.

The recommended strategies were based on a Monte Carlo simulation process using a Gumbel distribution. The simulation process revealed evidence of step change in rainfall and temperature. Furthermore, it was recommended that long range persistency in temperature patterns in the MDB areas, would lead to reduced rainfall. This study re-analyzed the climatic indicators and removed any trend in the rainfall and temperature series, and superimposed to project the next 100 years in the MDB areas.

Further it is required to check the conditional consistent evidence of change in climatic drivers corresponding with local rainfall and temperature.

10. REFERENCES

Abbas, B. M., 1992. Development of Water Resources in the Ganges and Brahmaputra River Basins; In the Ganges Brahmaputra Basin, edited by D. J. Eaton. Austin, Texas: The University of Texas at Austin

Adel, MM 2001, 'Effect on water resources from upstream water diversion in the Ganges Basin', Journal of Environmental Quality, vol. **30**, no. 2, pp. 356-368

Adel, MM 2002, 'Man-made climatic changes in the Ganges Basin', *International Journal of Climatology,* vol. **22**, no. 8, pp. 993-1016

Alam, U.Z. 2002: Questioning the water wars rationale: A case study of the Indus Waters Treaty. *The Geographical Journal*, **168(4)**, pp 341-353.

Alcamo, J., DoK ll, P., Kaspar, F., Siebert, S., 1997: Global Change and Global Scenarios of Water Use and Availability: An Application of Water GAP 1.0. University of Kassel, Germany. 47pp

Arabi, M., R.S. Govindaraju, and M.M. Hantush., 2007: A Probabilistic Approach for Analysis of Uncertainty in the Evaluation of Watershed Management Practices. *Journal of Hydrology,* Vol **333**, Issue 2-4, 459-471.

Arnell, N.W. and E.K. Delaney, 2006: Adapting to climate change: public water supply in England and Wales, *Climatic Change*, **78**, 227-255.

Arnell**,** N.W., 1996: *Global Warming, River Flows and Water Resources*. John Wiley and Sons, Chichester, United Kingdom, 226 pp

Barnston A. G., and R. E. Livezey, 1987: Classification, seasonality and persistence of low-frequency atmospheric circulation patterns. *Monitoring Weather Review* Vol. **115**, 1083-1126.

Barsugli, J., Anderson, C., Smith, J.B., and Vogel, J.M. 2009 : "Options for Improving Climate Modeling to Assist Water Utility Planning for Climate Change. [Online].Available:http://www.wucaonline.org/assets/pdf/actionswhitepaper 120909.pdf. [Access June 9, 2010]

Bates, B.C., Z.W. Kundzewicz, S. Wu, and J.P. Palutikof, Eds., 2008: Climate Change and Water. Technical Paper of the Intergovernmental Panel on Climate Change, IPCC Secretariat, Geneva, 210 pp

Beecham, S. and Chowdhury, R., 2009: Temporal Characteristics and Variability of Point Rainfall: A Statistical and Wavelet Analysis, International Journal of Climatology, Royal Meteorological Society, **30**(3), pp458-473.

Beuhler, M., 2003: Potential impacts of global warming on water resources in southern California. *Water Sci. Technol.*, **47**(7–8), 165–168.

Biswas, AK, Seetharam, K.E., 2007: 'Achieving water security for Asia', *Water Resources Development*, vol. **24**, No. 1, pp. 145-176

Bras, RL 1990, *Hydrology: an introduction to hydrological science*, Addison-Wesley, Reading MA, 643 p.

Burns, JF 2008, Sharing Ganges Waters, India and Bangladesh Test the Depth of Cooperation, New York Times, 27th August 2008.

BWDB (Bangladesh Water Development Board), 2008, *Guideline and manual for Bank protection works*, Bangladesh Water Development Board, Dhaka.

Chiew, F.H.S. and McMahon, T.A., 2003: El Niño-Southern Oscillation and Australian Rainfall and Stream Flow. *Australian Journal of Water Resource,* **6**, 115–129.

Chiew, F.H.S., T.C. Piechota, J.A. Dracup, and T.A. McMahon, 1998: El Niño Southern Oscillation and Australian rainfall, river flow and drought— links and potential for forecasting. *Journal of Hydrology*, **204,** 138–149.

Chowdhury, R. and Beecham, S., 2010: Australian Rainfall Trends and their Relation to the Southern Oscillation Index, Journal of Hydrological Processes, Wiley, **24**, pp504-514.

Chowdhury, R.K. and Rahman, R., 2008. Multi criteria Decision Analysis in Water Resources Management: the *Malnichara* Channel Improvement. *International Journal Environmental Science Technology,* Spring, e(2), 195-204.

Collins, M., and The CMIP Modelling Groups, 2005: El Niño or La Niña like climate change? *Climatic Dynamic*, **24**, 89-104.19.

Compagnucci, R.H. and W.M. Vargas, 1998: Inter annual variability of the Cuyo River's river flow in the Argentinian Andean Mountains and ENSO events. *International Journal of Climatology*, **18,** 1593–1609.

Conca, K. 2006: "The new face of water conflict". Woodrow Wilson International Centre for Scholars. Website: http://www.wilsoncenter.org/topics/pubs/NavigatingPeaceIssue3.pdf, [Dated 6th Oct, 2009]

Cook, R.D., and Weisberg, S., 1982: Residuals and Influence in Regressions London, UK: Chapman and Hall/CRC cited in A Handbook of Statistical Analyses Using R pp84-85.

Cosgrove, WJ, 2003, *Water Scarcity and Peace: A Synthesis of case studies prepared under the PCCP-Water for Peace Process,* PPCP Publications

Cowpertwait, P.S.P and Metcalf, A.V. 2009: Introductory time series with R. Springer

Crow, B. & Singh, N 2000, 'Impediments and innovation in international rivers: the waters of South Asia', *World Development,* vol. **28,** pp. 1907–1925.

De Kort, I.A.T., and M.J. Booij. 2007: Decision Making under Uncertainty in a Decision Support System for the Red River. *Environmental Modeling & Software,* **22**, 128-13

De Villiers, M. 2001, Water: the fate of our most precious resource, Houghton Mifflin, Boston, 368 pp.

Dessai, S., X. Lu and J.S. Risbey, 2005: On the role of climate scenarios for adaptation planning. *Global Environment Chang*, **15**, 87–97.

Drosdowsky, W., 1993: An analysis of Australian seasonal rainfall anomalies: 1950–1987:"Temporal variability and teleconnection patterns". *International Journal Climatol*, **13**, 111–149.

Easter, K.W., 2000: Asia's Irrigation Management in Transition: A Paradigm Shift Faces High Transaction Costs. *Review of Agricultural Economics*, 22(2), 370-388.

Faruqui, N.I.,A.K. Biswas andM.J. Bino, Eds., 2001: *Water Management in Islam*. United Nations University Press, Tokyo, 149 pp

Feldman, DL 2007: 'Water Policy for Sustainable Development', Johns Hopkins University Press, Baltimore, 371 p.

Field,A.P 2005: Discovering Statistics Using SPSS (2nd edition), London, chapter 11, and 15

Franks, S.W., 2002. Assessing hydrological change: deterministic general circulation models or spurious solar correlation? *Hydrological Process,* **16**, 559–564.

Galaz, V., 2005: Social-ecological resilience and social conflict: Institutions and strategic adaptation in Swedish water management. *Ambio*, **34**, 567-572.

Gleick, P, Water Conflict Chronology, web site: http://worldwater.org/ conflictchronology.pdf . [Access 26th august 2008]

Gleick, P. 2008: *Water Conflict Chronology*. *Global Policy Forum*. 1- 46 pp.

Gleick, P.H., (1993): Water and Conflict- Fresh water resources and International security, *International Security*, **18(1)**, 79-112

Gleick, PH 1998, 'Water in crisis paths to sustainable water use', *Ecological Applications*, vol. **8**, pp. 571-579:

Gutowski, W.J., Jr., Wilby, R.L., Hay, L.E., Anderson, C.J., Arritt, R.W., Clark, M.P., Leavesley, G.H.,Pan, Z., Da Silva, R., and Takle, E.S. 2000: Statistical and Dynamical Downscaling of Global Model Output for US National Assessment Hydrological Analyses. 11th Symposium on Global Change Studies, Long Beach, CA, January 9-14, 2000.

Haddadin, MJ & Shamir U, 2003: *Jordan Case Study,* PCCP Publications.

Haftendorn, H 2000, 'Water and international conflict', *Third World Quarterly,* vol. **21**, no. 1, pp. 51 – 68

Hooper, B. 2006: Integrated water resources management: governance, best practice, and research challenges. *Journal of Contemporary Water Research & Education*, Issue **135**, 1-7.

Hossain, I 1998, 'Bangladesh-India Relations: The Ganges Water-Sharing Treaty and Beyond.', *Asian Affairs: An American Review,* vol.**13***,* 1-13

Hughes, J.P. and Guttorp, P. 1994: A class of stochastic models for relating synoptic atmospheric patterns to regional hydrologic phenomena. *Water Resources Research,* **30**: 1535-1546.

ICWE, 1992: “International Conference on Water and Environment”; The Dublin Statement on Water and Sustainable Development, website http://www.unesco.org/science/waterday2000/dublin.htm. [Access October 5, 2007]

IPCC, 2001: “Climate Change 2000”. The Science of Climate Change, Summary for Policy makers and Technical Summary of Working Group,. Cambridge University Press, page 98.

Islam, MR, Begum, SF, Yamaguchi, Y, Ogawa, K 1999: ‘The Ganges and Brahmaputra rivers in Bangladesh: Basin denudation and sedimentation’, *Hydrological Processes*, vol. **13**, pp. 2907-2923.

Iyer, RR 2003: ‘Water – Perspectives, Issues, Concerns’, *Sage Publications*, New Delhi, 369 pp.

JRC, 1997: Bangladesh Nepal task force on flood control, Report on flood mitigation measures and multi-purpose use of water resources, Joint Rivers Commission Bangladesh

Kaplan, A., Cane, M. A., Kushnir, Y., Clement, A. C., Blumenthal, M. B., and Rajagopalan, B., 1998: “Analysis of Global Sea Surface Temperature 1856-1991”. *Journal of Geophysical Research Oceans,* **103 (C9),** 18567-18589.

Karl, T.R. and R.W. Knight, 1998: Secular trends of rainfall amount, frequency and intensity in the United States. *Bulletin of the American Meteorological Society*, **79,** 231–241.

Keremane, GB, McKay, J 2006, ‘Self-created rules and conflict management processes: the case of water user’s associations on Waghad canal in Maharasshtra, India’, *Water Resources Development*, vol. **22**, No.4, 543-559 pp.

Khan, TA 1996, 'Management and sharing of the ganges', *Natural Resources Journal,* vol. **36**, no. 3, pp. 455-479

Klijn, F., J. Dijkman and W. Silva, 2001: *Room for the Rhine in the Netherlands. Summary of Research Results*. RIZA Report 2001.033, Rijkswaterstaat, Utrecht. Cited in, Bates, B.C., Z.W. Kundzewicz, S. Wu, and J.P. Palutikof, Eds., 2008: Climate Change and Water. Technical Paper of the Intergovernmental Panel on Climate Change, IPCC Secretariat, Geneva, 210 pp

Kodikara, P.N. 2008. : Multi-Objective Optimal Operation of Urban Water Supply Systems. PhD thesis, *Victoria University, Australia,* pp.1-290

Krol, M.S., Fuhr, D., Do¨ring, A., 2005. Semi-arid northeast Brazil: integrated modelling of regional development and global change impacts. In: Unruh, J., Krol, M.S., Kliot, N. (Eds.), Environmental Change and its Implications for Population Migrations, Advances in Global Change Research, vol. 20. Kluwer Academic Publishers, Dordrecht, pp. 119–144.

Lankford, B.A., Merrey, D.J., Cour, J. and Hepworth, N. 2007: From Integrated to Expedient: An Adaptive Framework for River Basin Management in Developing Countries. Research Report 110: International Water Management Institute, Colombo, Sri Lanka, 39pp.

Lankford. B.B., van koppen, T. Franks, ands H. Mahoo (2004): Entrenched views or insufficient science?: contested causes and solutions of water allocations; insights from the great Rusha River basin, Tanzania, Agricultural Water Management **69(2)**, 135-153.

Latif, M., Kleeman, R. and Eckert, C., 1997: Greenhouse Warming, Decadal Variability, or El Nino? An Attempt to Understand the Anomalous 1990s, *J. Climate,* **10**, 2221–2239.

Madulu, N.F. 2003: Linking poverty levels to water resource use and conflicts in rural Tanzania. *Physics and Chemistry of the Earth (B),* **28**, pp 911-917

Malkina-Pykh, IG 2003, *Sustainable water resources management*, WIT Press, Southampton.

Mantua, N., Hare, S.R., Zhang, Y., Wallace, J.M. and Francis, R.C., 1997. A Pacific inter-decadal climate oscillation with impacts on salmon production. *Bull. Amer. Meteorol. Soc.,* **78**, 1069–1079.

Marengo, J.A., 1995: Variations and change in South American river flow. *Climatic Change*, **31,** 99–117.

Marshall, G. J., 2003: Trends in the Southern Annular Mode from observations and reanalyses. *Journal of Climate,* **16,** 4134-4143.

Maxwell, J.W. and Reuveny, R. 2000: "Resource scarcity and conflict in developing countries". *Journal of Peace Research,* **37(3)**, 301-322

McBride JL, Nicholls N. 1983. Seasonal relationships between Australian rainfall and the Southern Oscillation. *Monthly WeatherReview* **111**: 1998–2004.

McCabe, G.J., 1996: Effects of winter atmospheric circulation on temporal and spatial variability in annual river flow in the western United States. *Hydrological Sciences Journal*, **41,** 873–888.

McCarthy, J.J., Canziani, O.F., Leary, N.A., Dokken, D.J., White, K.S. (Eds.), 2001. Climate Change 2001: Impacts, Adaptation and Vulnerability. Cambridge University Press, Cambridge.

McInnes, K.L., K.J.E. Walsh, G. D. Hubbert and T. Beer, 2003: Impact of Sea-level Rise and Storm Surges on a Coastal Community. Natural Hazards, (in press)

Mearns LO, Bogárdi I, Matyasovszky I, Palecki M. 1999: Comparison of climate change scenarios generated from regional climate model experiments and statistical downscaling. *Journal of Geophysical Research* **104**: 6603-6621.

Mehta, L. (2007): Whose scarcity? Whose property? The case of water in western India. Land Use Policy. **24**, Page 654-663.

Mekong River Commission, 2001: Procedures for Data and Information Exchange and Sharing, Website: http://www.mrcmekong.org/download/programmes/wup Procedures.pdf. [Dated 12th August 2008]

Mirza, MMQ 1997, 'Hydrological changes in the Ganges system in Bangladesh in the post-Farakka period', Hydrological Sciences, vol. **42**, no. 5, pp. 613-631

Mirza, MMQ, 1998: Diversion of the Ganges water at Farakka and its effects on salinity in Bangladesh', *Environmental Management,* vol. **22**, no. 5, pp. 711-722.

Mirza, MMQ, Warrick, RA, Ericksen, NJ 2003, 'The implications of climate change on floods of the Ganges, Brahmaputra and Meghan rivers in Bangladesh', *Climatic Change,* vol. **57**, pp. 287–318

Morgan, M.G. and Henrion, M. 1990: Uncertainty: A Guide to Dealing with Uncertainty in Quantitative Risk and Policy Analysis. Cambridge University Press, Cambridge, 332 pp.

Moss, R.H. and Schneider, S.H. 2000: Towards Consistent Assessment and Reporting of Uncertainties cited in the IPCC TAR (2001): Initial Recommendations for Discussion by Authors. New Delhi: TERI,

Mostert, E, 2003, Conflict and Cooperation in the management of International Freshwater Resources: A Global Review, PCCP Publications.

Muckelston, KW, 2003: "International Management in the Columbia River System". UNESCO, IHP, WWAP, "Technical *documents in hydrology". PC –CP series number* **12***,* 1-66 pp.

Mudelsee, M. 2007: long memory of river from spatial aggregation. Water resources research, 43 (W01202)

Murphy J. 1999: An evaluation of statistical and dynamical techniques for downscaling local climate. *Journal of Climate* **12**: 2256-2284.

Nicholls, N., Kariko, A., 1993: East Australia rainfall events: inter annual variations, trends, and relationships with the southern oscillation. *Journal Climate* **6**, 1141–1152.

Nilsson, C., C. A. Reidy., M. Dynesius., & C. Revenga. 2005: *Fragmentation and flow regulation of the world's large river systems*. Science **308**:405-408.

Nishat, A. & Faisal, IM 2000 :'An assessment of the institutional mechanisms forwater negotiations in theGanges–Brahmaputra–Meghna System', *International Negotiation,* vol. **5**, pp. 289–310

OECD 2005, Water and violent conflict, Preventing Conflict and Building Peace, Issues Brief 2005, web site: www.oecd.org, [Dated 27th Sept 2009]

Ohlsson, L., 2000: Water conflicts and social resource scarcity. *Physics and Chemistry of the Earth* (B). **25(3)**, 213-220.

Olsen, J.R., J.R. Stedinger, N.C. Matalas, and E.Z. Stakhiv, 1999: Climate variability and flood frequency estimation for the Upper Mississippi and Lower Missouri Rivers. *Journal of the American Water Resources Association*, **35,** 1509–1523.

Onn, L P, 2003: The Water Issue between Singapore and Malaysia: No solution in sight? Institute of Southeast Asian Studies, web site: http://www.iseas.edu.sg/pub .html. [Access August 27 2008],

Opoku-Ankomah, Y., Cordery, I., 1993: Temporal variation of relations between New South Wales rainfall and the southern oscillation. *International Journal of Climatology*. **13**, 51–64.

Osborn, T.J., M. Hulme, P.D. Jones, and T.A. Basnet, 2000: Observed trends in the daily intensity of United Kingdom rainfall. *International Journal of Climatology*, **20,** 347–364.

Pahl-Wostl, C., 2002: Agent based simulation in integrated assessment and resources management. In: Rizzoli, A., Jakeman, T. (Eds.), "Integrated Assessment and

Decision Support". Proceedings of the First Biennial Meeting of the International Environmental Modelling and Software Society, vol. **2**, pp 239–250.

Pearce, F., (2006): Uganda pulls plug on Lake Victoria, New Scientist **2538**, 12.

Piechota, T.C., J.A. Dracup, and R.G. Fovell, 1997: Western U.S. river flow and atmospheric circulation patterns during El Niño-Southern Oscillation. *Journal of Hydrology*, **201,** 249–271.

Piechota, T.C., J.A. Dracup, F.H.S. Chiew, and T.A. McMahon, 1998: Seasonal river flow forecasting in eastern Australia and the El Niño- Southern Oscillation. *Water Resources Research*, **34,** 3035–3044.

PMSEIC. 2007. Climate Change in Australia, Regional Impacts and adaptation/ Managing the Risk for Australia. *PMSEIC, Independent Working Group.* Report Prepared for the Prime Minister's Science, Engineering and Innovation Council, Canberra, June, 1-63.

Popplestone G, 2008: "Arguing over the World's Water Resources", website: http: //www.nowpublic.com/environment/arguing-over-worlds-water-resources.[Dated 4th August 2008]

Priscoli, JD, 2003: *Participation, Consensus Building and Conflict Management Training Course (Tools for achieving PCCP)*, PCCP Publications.

Prudhomme C, Reynard N, Crooks S. 2002. Downscaling of global climate models for flood frequency analysis: where are we now? *Hydrological Processes* **16**: 1137-1150

Pun, S.B. (2004) Overview: Conflicts over the Ganges?, In: Subba, B. & Pradhan, K. (eds.) Disputes over the Ganga, pp.3-20, Panos Institute South Asia, Nepal.

Rahman, MM 2006, 'The Ganges Water Conflict: A Comparative Analysis of 1977 Agreement and 1996 Treaty', *Asteriskos - Journal of International & Peace Studies,* vol. **1/2**, pp. 195-208

Raisanen, J., and T. N. Palmer, 2001: A Probability and Decision-Model Analysis of a Multi model Ensemble of Climate Change Simulations. *Journal of Climate,* Vol, **14**, 3212-3226.

Richardson, C. W. 1981: Stochastic Simulation of Daily Precipitation, Temperature, and Solar Radiation. *Water Resources Research*, **17(1)** 182-190

Romilly, P. 2005: Time series modelling of global mean temperature for managerial decision making. *Journal of Environmental management,* **76,** pp 61-60,

Ropelewski, C.F., and Halperts, M. S., 1996: "Quantifying Southern Oscillation-Precipitation Relationships". *Journal of Climate*, 9(5), 1043-1059.

Rudra, K 2000, 'Living On the Edge: The Experience along The Bank of the Ganga in Malda District, West Bengal', *Indian Journal of Geography & Environment*, vol. **5**, pp. 57-67

Rummel, R.J, 1979: "*War, Power, and Peace,* Vol.4, Sage Publications, Sage, California.

Saji, N.H, Goswami, P.N, Vinayachandran and Yamagata, T., 199: "A dipole mode in the tropical Indian Ocean", *Nature*, 401, 360-363

Salidjanova N, 2007: "Chinese Damming of Mekong and Negative Repercussions for Tonle Sap, ICE Case Studies". Website: http://www.american.edu/ted/ice/mekong-china.htm. [Access 11th August, 2008].

Salman, SMA & Uprety, K 1999, 'Hydro-politics in South Asia: A comparative analysis of the Mahakali and the Ganges treaties', *Natural Resources Journal,* vol. **39**, no. 2, pp. 295-343

Savenije, H.H.G. and Van der Zaag, P. 2008: Integrated water resources management: Concepts and issues. *Physics and Chemistry of the Earth (B)*, **33**, pp 290-297.

Schulze, R.E., 1997: Impacts of global climate change in a hydrological vulnerable region: challenges to South African hydrologists. *Progress in Physical Geography*, **21,** 113–136.

Semenov, M.A., Brooks, R.J., Barrow, E.M., and Richardson, C.W. 1998: Comparison of the WGEN and LARS-WG stochastic weather generators in diverse climates. *Climate Research,* **10**: 95-107.

Semenov, Mikhail A., and Barrow, E.M. 1997: Use of Stochastic Weather Generator in the Development of Climate Change Scenarios**,** *Climatic Change*, **35**: 397-414

Shorthouse, C. and N.W. Arnell, 1997: Spatial and temporal variability in European river flows and the North Atlantic Oscillation. *FRIEND'97: International Association of Hydrological Science Publications*, **246,** 77–85.

Simmonds I, Hope P. 1997: Persistence characteristics of Australian rainfall anomalies. *International Journal of Climatology* **17**: 597–613.

Simonovic, S.P. and L.H. Li, 2003: Methodology for assessment of climate change impacts on large-scale flood protection system. *Journal of Water Research, Pl.-ASCE*, **129**(5), 361–371.

Singh, KP, Mohan, D, Sinha, S, Dalwani, R 2004: 'Impact assessment of treated/untreated wastewater toxicants discharged by sewage treatment plants on health, agricultural, and environmental quality in the wastewater disposal area', *Chemosphere*, vol. 55, pp. 227–255.

Smith, N., 1995: Recent hydrological changes in the Avoca River catchment, Victoria. Australian Geographical Studies **33 (1),** 6–18.

Stainforth, D. A., T. E. Downing, R. Washington, A. Lopez, and M. New. 2007b: Issues in the Interpretation of Climate Model Ensembles to Inform Decisions. *Philosophical Transactions of the Royal Society.* Volume **365**, 2163-2177

Stone, R., Auliciems, A., 1992: SOI phase relationships with rainfall in eastern Australia. *International Journal Climatology* **12**, 625–636.

Suppiah, R., Hennessy, K.J., 1996: Trends in the intensity and frequency of heavy rainfall in tropical Australia and links with the southern oscillation. Australian Meteorological Magazine **45**, 1–17.

Thebaud, B. and Batterbury, S. 2001: Sahel pastoralists: opportunism, struggle, conflict and negotiation - A case study from eastern Niger. *Global Environmental Change,* **11**, 69-78.

Tkatch, R. J., and S. P. Simonovic, 2006: A New Approach to Multi-Criteria Decision Making in Water Resources. *Journal of Geographic Information & Decision Analysis.* Volume **1**, No. 1, 25-43.

Troup, A.J. 1965: "The Southern Oscillation", *Quarterly Journal of the Royal Meteorological Society*, **91,** 490-506.

Tsering T, 2008: Mekong: Managing a Transboundary River,
Website: http://www. tibetjustice.org/reports/mekong.pdf. [Dated: 10 August 2008]

UN (United Nations). 2004: *World population to 2300*. Website: http://www.un. Org / esa/Population/publications/longrange2/WorldPop2300final.pdf, [Access: 20th Oct 2009]

UNDP (United Nations Development Programme), 2009: Millennium Development Goals, website: http://www.undp.org/mdg/basics.shtml. [Dated 2nd Oct 2009]

UNESCO (United Nations Educational, Scientific and Cultural Organization) 2009: *Water in a changing world: the United Nations World Water Development Report 3*, Earthscan, London

UNESCO, 2008, "*The Danube River Basin", W*ebsite: http://www.unesco.org/water/wwap/wwdr/wwdr2/case_studies/pdf/danube.pdf [Access: August 29, 2008]

UNESCO, 2008: *From Potential Conflict to Co-operation Potential (PCCP),* website: http:// www.unesco.org/water/pccp.html. [Dated 30th August, 2008]

Verzani, J. 2005: "Using R for introductory statistics". Chapman & Hall/CRC: page 414.

Visbeck, M. Hall A. 2004: Comments on "Synchronous variability in the Southern Hemisphere atmosphere, sea ice, and ocean resulting from the annular mode" – Reply. *Journal of Climate* **17**: 2255–2258.

Vo, PL 2007, 'Urbanization and water management in Ho Chi Minh City, Vietnam, issues, challenges and perspectives', *Geo Journal,* vol. **70**, pp. 75- 89

Vogel, R.M., C.J. Bell, and N.M. Fennessey, 1997: Climate, riverflow and water supply in the northeastern United States. *Journal of Hydrology*, **198,** 42–68.

Waage, M. 2009: Developing New Methods for Incorporating Climatic Uncertainties into Water Planning. "EPA Sustainable Water Infrastructure and Climate Change Workshop, Washington, DC. January 6. cited in Edward, M. Maryline, L. Jennifer, D., Laurna, K., and Marc, W., 2010: Decision Support Planning Methods: Incorporating Climate Change Uncertainties into Water Planning. Report prepared for Water Utility Climate Alliance white paper, San Francesco, January 2010.

Water Aid, 2003:" Social conflict and water: lessons from north-east Tanzania". Discussion Paper, website, http://www.wca-infonet.org/cds_static/en/social_conflict water_lessons_from_north_en_30137_102479.html, [dated 11 August 2008].

Wilby R.L., Conway, D., Jones, P.D. 2002b: Prospects for downscaling seasonal precipitation variability using conditioned weather generator parameters. *Hydrological Processes* **16**: 1215-1234.

Wilby, R.L., 2006: When and where might climate change be detectable in UK river flows? *Geophysical Research Letter.*, **33**(19), L19407, doi: 10.1029/2006GL027552.

Wilby, R.L., Dawson, C.W., and Barrow, E.M. 2002a: SDSM – a decision support tool for the assessment of regional climate change impacts. *Environmental Modelling & Software,* **17**: 147-159.

Wilhite, D.A., 2000: Drought*:* A Global Assessment. Rout ledge, London: Vol 1, 396 pp; Vol **2**, 304 pp.

Wilks, D.S. 1998: Multisite Generalization of a Daily Stochastic Precipitation Generation Model**,** *Journal of Hydrology,* **210**: 178-191.

Wilks, D.S., and Wilby, R.L. 1999: The Weather Generation Game: A Review of Stochastic Weather Models, *Progress in Physical Geography,* **23(3):** 329-357.

Wolf, A, Stahl, K, Macomber, M 1999, *Water, conflict, and cooperation*, International Centre of Excellent in Water Resource Management,

Wolf, A. T. 1999. *Criteria for equitable allocations: The heart of international water conflict*. Natural Resources Forum **23(1),** pp3-30.

Wolf, A.T. and Newton J.T. 2008: Managing and Transforming Water Conflicts". *International Hydrology Series,* Cambridge University Press, website: http:// www.transboundarywaters.orst.edu/research/case_studies. [Access 17th Aug 2008].

Wolf, AT 2007, 'Share waters: conflict and cooperation', *Annual Review of Environment and Resources*, vol. **32**, pp. 241-269

Wolf, AT, Stahl, K & Macomber, MF 2003, 'Conflict and cooperation within international river basins: The importance of institutional capacity', *Water Resources Update,* vol. **125**

Wolter, K. and Timlin, M.S. 1998: "Measuring the strength of ENSO-how does rank 1997/1998 rank?" Weather, **53**, 315-324.

World Bank, 2005: "*Water Crisis"* World Water Council. Website http://www.world watercouncil.org/index.php?id=25 , [Access 10th Oct 2009]

WSJ. 2008. *China Evacuates Last Town Near Three Gorges Dam*. Website: http:// chi nese.wsj.com/gb/20080724/bch094619.asp. [Dated 15th Oct, 2009]

Xu C-Y. 1999: From GCMs to river flow: a review of downscaling methods and hydrologic modeling approaches. *Progress in Physical Geography* **23(2),** 229-249.

Yarnal, B., Comrie, A.C., Frakes, B., and Brown, D.P. 2001: Developments and Prospects in Synoptic Climatology, I*nternational Journal of Climatology,* **21**, 1923-1950.

Yoff, S., A.T. Wolf and M. Giordano (2003): Conflict and cooperation over the International fresh water Resources, Indicators of basin at risk. Journal of American Water Resources Associations **39(5)**, 1109-1126.

Yohe, G. and Tol, R.S.J. 2002 Indicators for social and economic coping capacity - moving toward a working definition of adaptive capacity, Global Environmental Change, **12**, 25–40

Zhang, X.-G., Casey, T.M., 1992: Long-term variations in the southern oscillation and relationships with Australian rainfall. Aust. *Meteorology Magazine*. **40 (4)***,* 211–225.

Zhang, Y., Wallace, J.M. and Battisti, D.S., 1997. ENSO-like Inter-decadal Variability: 1900-93. *Journal Climate,* **10**, 1004–1020.

Website address:

Australian Bureau of Meteorology (BoM), available at:
http://www.bom.gov.au/climate/data/index.shtml

Climate Prediction Centre (CPC) of the National weather service, at available
http://www.cpc.noaa.gov/data/indices/

Japan Agency for Marin Earth Science and Technology (JAMSTEC), at available:
http://www.jamstec.go.jp/frsgc/research/d1/iod/

Natural Environment research Council based in the British Antarctic Survey, at available, http://www.nerc-bas.ac.uk/icd/gjma/sam.html, and http://www.Antarctica.ac.uk. [

Probe International 30.06.2006. The Hydrolancang cascade, website available, http://www.probeinternational.org/catalog/contentfullstory.php. [Dated on 25th Nov 2010].

11. APPENDIX

Appendix 4 1: Ratio of water sharing at the Farakka Barrage on GRB between Bangladesh and India

Period		Agreement 1977	MOU ' 82	MOU ' 85	Treaty ' 96
	1949-1973	1978-82	1983-84	1986-88	1997-07
Month	Average BD	BD:IND	BD:IND	BD:IND	BD:IND
January I	109830	62:38	62:38	66:34	65:35
January II	101285	60:40	60:40	61:39	61:39
January III	94092	59:41	58:42	58:42	59:41
February I	90618	61:39	58:42	58:42	57:43
February II	87407	61:39	58:42	58:42	55:45
February III	83025	60:40	56:46	57:43	53:47
March I	78414	61:39	59:41	59:41	52:48
March II	73706	61:39	60:40	60:40	53:47
March III	69256	61:39	59:41	59:41	45:55
April I	66276	61:39	60:40	59:41	54:46
April II	63191	63:37	63:37	63:37	47:53
April III	61611	63:37	63:37	63:37	54:46
M ay I	63730	62:38	62:38	62:38:	52:48
May II	69475	61:39	59:41	59:41	54:46
May III	77372	64:36	61:39	60:40	61:39

Note that I= 1-10days, II= 11-20 days, III=21-30days

Appendix 4. 2: Flow available at Farakka 1997 – 2007 on the GRB

	m³/s											Average
Month	1997	1998	1999	2000	2001	2002	2003	2004	2005	2006	2007	1997-2007
Jan I	102180	204814	135181	131608	104511	108722	85844	118194	96582	95840	77966	114677
II	89635	175566	120633	110876	91952	92854	85968	113867	85112	80471	73141	101825
III	88672	145866	118742	97686	89740	93951	83409	107844	84257	70562	70037	95524
Feb I	85604	128186	102433	92253	82454	93470	83099	111099	84455	64118	67454	90420
II	81015	101841	99878	87517	73971	87921	86566	102534	86341	58701	69072	85032
III	77399	94738	89343	84905	65703	89561	87672	84392	76854	53566	93280	81583
Mar I	66170	85323	78920	82439	64517	84251	89132	67625	66715	52340	86441	74898
II	56769	75967	72413	72966	61085	71160	76328	65626	62459	53040	78063	67807
III	48487	71570	69108	69849	54898	68694	70486	63344	60309	50727	77321	64072
April I	50481	78588	65244	71449	59123	69960	76474	64784	64120	50674	82445	66667
II	54526	90955	63826	70570	55813	74856	72992	65416	60037	50118	85068	67652
III	63933	87901	65910	85124	62078	82152	76789	71754	58371	54889	82496	71945
May I	66728	102203	73928	88719	62039	80155	92199	72746	67015	56534	75862	76193
II	66055	122062	85128	90767	84218	86215	91018	67490	74175	67490	87100	83793
III	63309	121210	100644	138675	99808	124218	90601	101060	65902	73926	94937	97663
Average flow	70731	112453	89422	91694	74127	87209	83238	85185	72847	62200	80046	82650
Flow variation	-14	36	8	11	-10	6	1	3	-12	-25	-3	

Appendix 4 3: Seasonal variation (%) flow available at Farraka on the GRB from 1997 – 2007

	1997	1998	1999	2000	2001	2002	2003	2004	2005	2006	2007
Jan I	44	82	51	44	41	25	3	39	33	54	-3
II	27	56	35	21	24	6	3	34	17	29	-9
III	25	30	33	7	21	8	0	27	16	13	-13
Feb I	21	14	15	1	11	7	0	30	16	3	-16
II	15	-9	12	-5	0	1	4	20	19	-6	-14
III	9	-16	0	-7	-11	3	5	-1	6	-14	17
Mar I	-6	-24	-12	-10	-13	-3	7	-21	-8	-16	8
II	-20	-32	-19	-20	-18	-18	-8	-23	-14	-15	-2
III	-31	-36	-23	-24	-26	-21	-15	-26	-17	-18	-3
Apr I	-29	-30	-27	-22	-20	-20	-8	-24	-12	-19	3
II	-23	-19	-29	-23	-25	-14	-12	-23	-18	-19	6
III	-10	-22	-26	-7	-16	-6	-8	-16	-20	-12	3
May I	-6	-9	-17	-3	-16	-8	11	-15	-8	-9	-5
II	-7	9	-5	-1	14	-1	9	-21	2	9	9
III	-10	8	13	51	35	42	9	19	-10	19	19

Note that I= 1-10days, II= 11-20 days, III=21-30days

Appendix 4 4: comparative static

$$\frac{\partial \alpha^*}{\partial \beta} = \frac{\partial \alpha^*}{\partial Y}.\frac{\partial Y}{\partial X} + \frac{\partial \alpha^*}{\partial Y}.\frac{\partial Y}{\partial X}.\frac{\partial Y}{\partial \beta} \quad \text{..... (A1)}$$

$$\frac{\partial \alpha^*}{\partial Y} = \frac{1}{\theta} Y^{\frac{1}{\theta}-1} > 0, \text{ as } \theta > 0 \text{ and } Y = \left[\frac{(p-c)Av_1 X^b (a-\delta(b))}{-\delta(\gamma+1)k\beta(X^{\gamma+1})}\right] > 0 \text{ .....(A2)}$$

Y can be expressed as $Y = Z_1 \beta^{-1}$, where $Z_1 = \left[\frac{(p-c)Av_1 X^b (\alpha-\delta(b))}{-\delta(\gamma+1)k(X^{\gamma+1})}\right] > 0$

$$\frac{\partial Y}{\partial \beta} = -Z_1 \beta^{-2} < 0 \text{ ..... (A3)}$$

Y can expressed as $Y = Z_2 X^{b-\gamma-1} > 0$ where $Z_2 = \left[\frac{(p-c)Av_1(\alpha-\delta(b))}{-\delta(\gamma+1)k}\right] > 0$

$\frac{\partial Y}{\partial X} = (b-\gamma-1)Z_2 X^{b-\gamma-2} > 0$, as $\frac{\partial \ln((NTB)_1}{\partial \ln S} > \frac{\partial \ln(TC)_1}{\partial \ln S}$. where $(NTB)_1$ is the net total benefit of India and $(TC)_1$ is the total cost of India for buying water from Nepal.

X can be written from (10) as $X = Z_3(1-\beta)^{-\frac{\delta}{c}}$ where $Z_3 = \left[\frac{(p-c)Bv_2 d}{k(\gamma+1)}\right]^{\frac{\delta}{c}} > 0$

$$\frac{\partial X}{\partial \beta} = \frac{\delta}{c}(1-\beta)^{-\frac{\delta}{c}-1} Z_3 < 0, \qquad \delta < 0, c > 0 \text{ ..... (A4)}$$

Taking into account of the signs of the derivations in (2), (3) and (4) and substituting in (A1),

We get, $\frac{\partial \alpha^*}{\partial \beta} = -\frac{1}{\theta} Y^{\frac{1}{\theta}-1}.Z_1 \beta^{-2} + \frac{1}{\theta} Y^{\frac{1}{\theta}-1}.Z_2 X^{b-\gamma-1}.\frac{\delta}{c}(1-\beta)^{-\frac{\delta}{c}} Z_3 < 0$ ..... (A5)

Appendix 5 1: Seasonal variability in the MDB areas and the eastern of Australia using box plots.

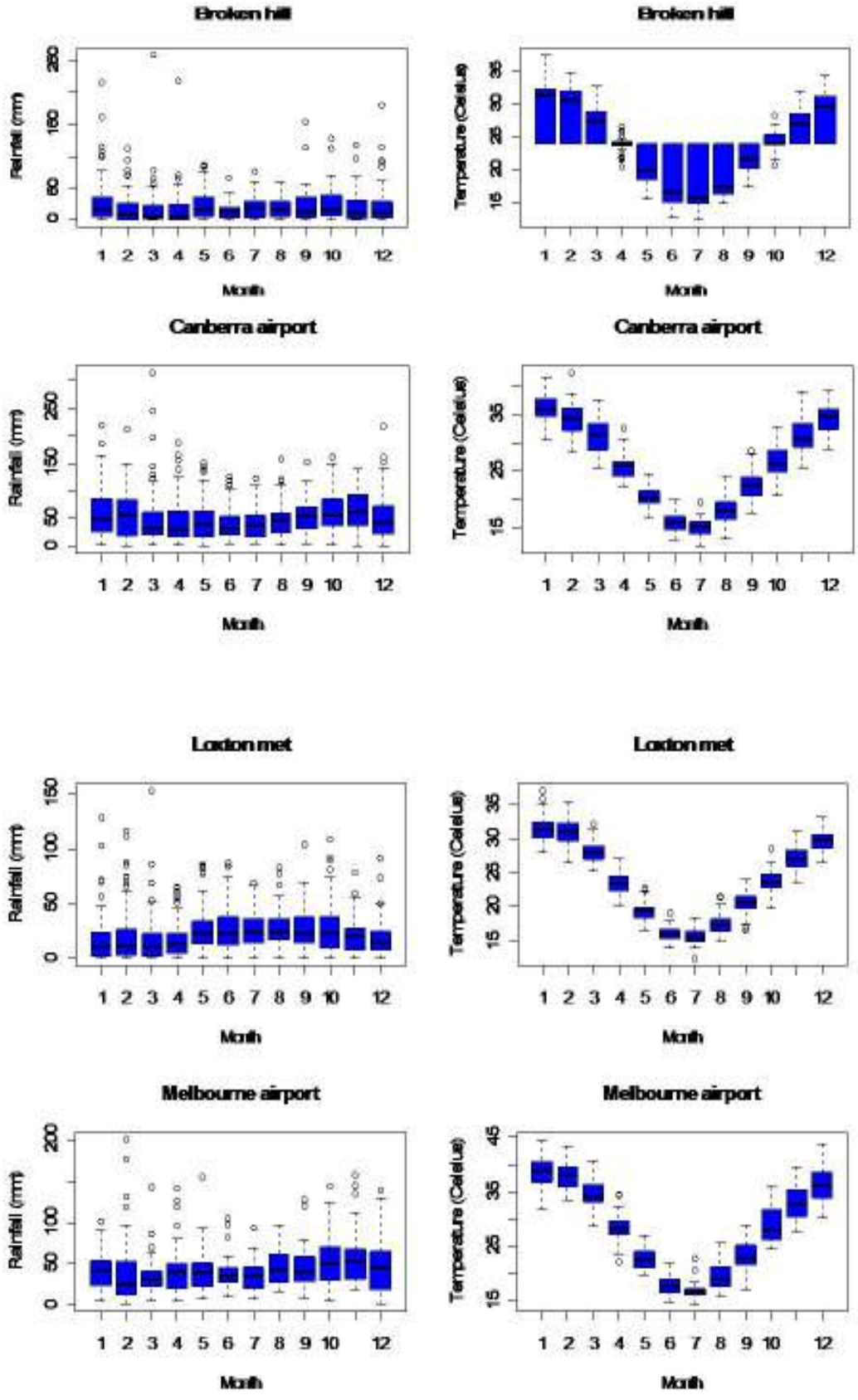

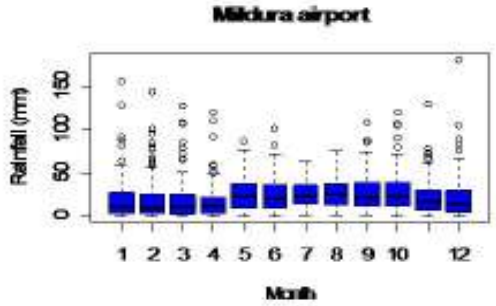
Mildura airport
Rainfall (mm)
0
50
100
150
1 2 3 4 5 6 7 8 9 10 12
Month

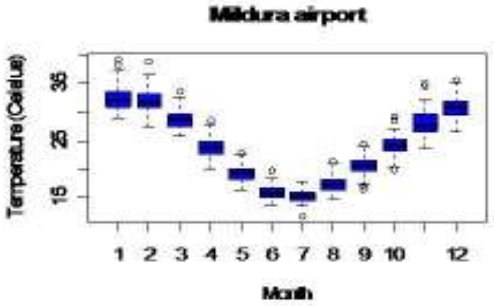
Mildura airport
Temperature (Celsius)
15
25
35
1 2 3 4 5 6 7 8 9 10 12
Month

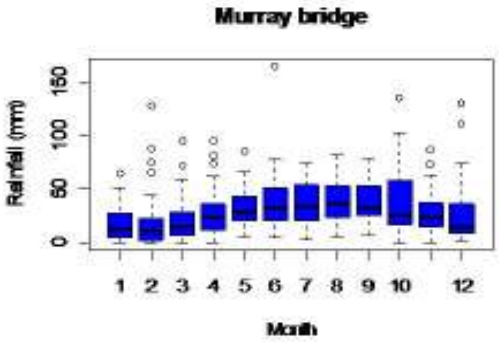
Murray bridge
Rainfall (mm)
0
50
100
150
1 2 3 4 5 6 7 8 9 10 12
Month

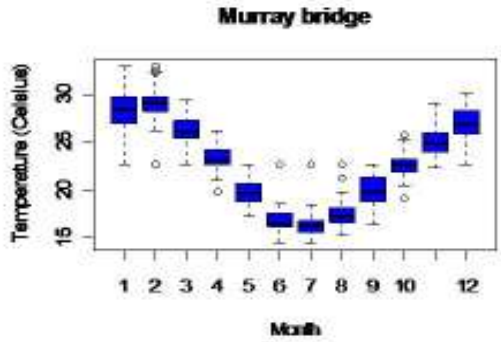
Murray bridge
Temperature (Celsius)
15
20
25
30
1 2 3 4 5 6 7 8 9 10 12
Month

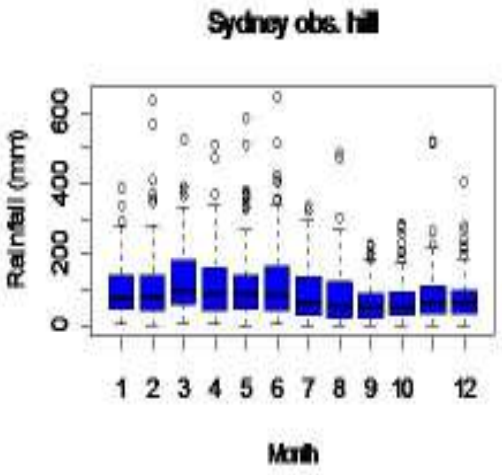
Sydney obs. hill
Rainfall (mm)
0
200
400
600
1 2 3 4 5 6 7 8 9 10 12
Month

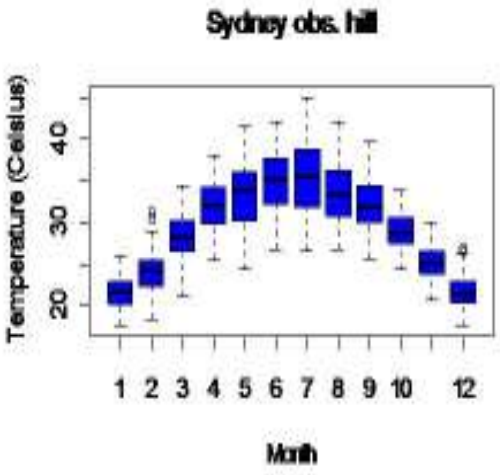
Sydney obs. hill
Temperature (Celsius)
20
30
40
1 2 3 4 5 6 7 8 9 10 12
Month

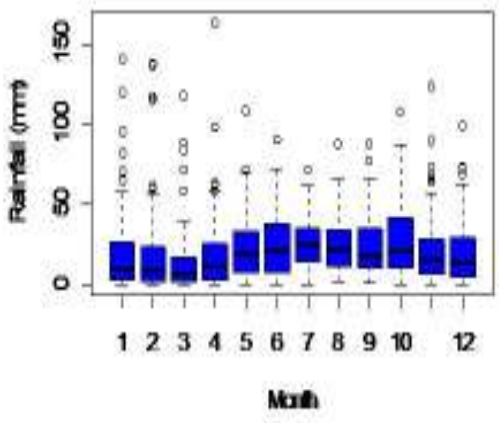
Lake Victoria
Rainfall (mm)
0
50
100
150
1 2 3 4 5 6 7 8 9 10 12
Month

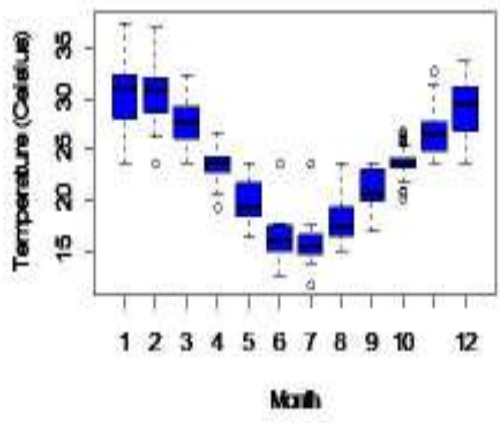
Lake Victoria
Temperature (Celsius)
15
20
25
30
35
1 2 3 4 5 6 7 8 9 10 12
Month

Appendix 5. 2: Monthly mean step change for rainfall (left side) and temperature (right side) pattern change in both short term and long term in the MDB areas and the eastern of Australia .

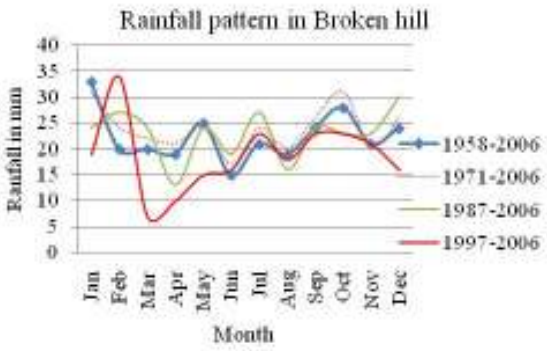

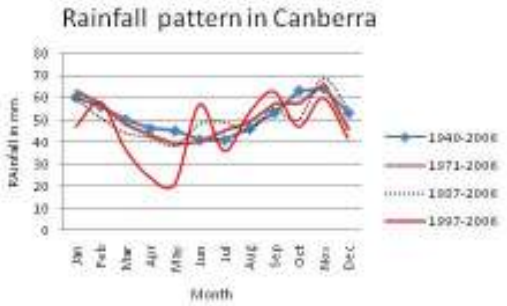

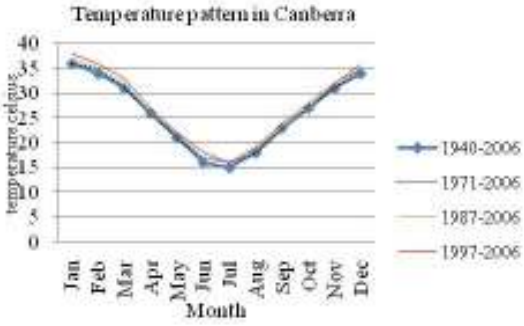

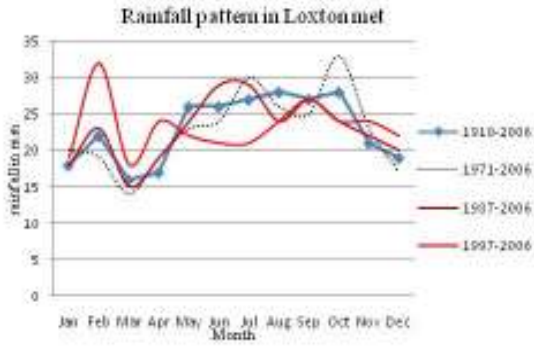

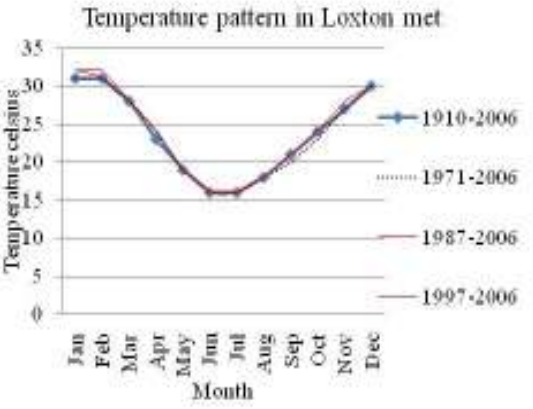

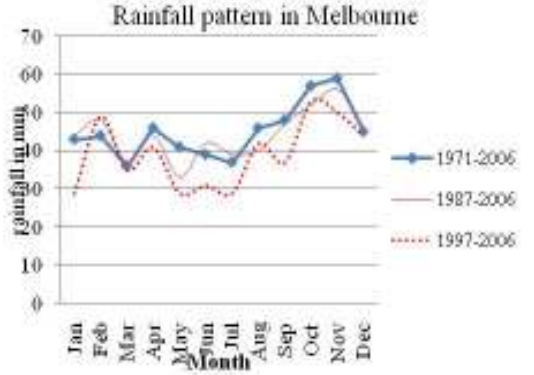

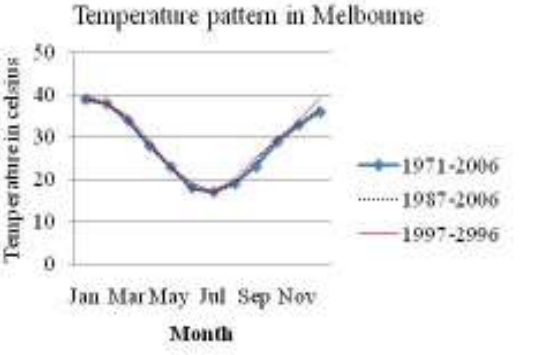

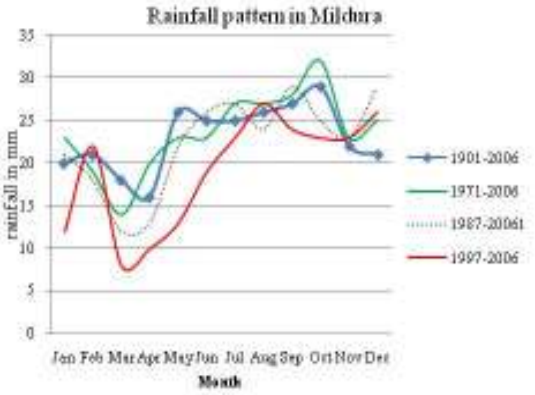
Rainfall pattern in Mildura
rainfall in mm
Jan Feb Mar Apr May Jun Jul Aug Sep Oct Nov Dec
Month
1901-2006
1971-2006
1987-20061
1997-2006

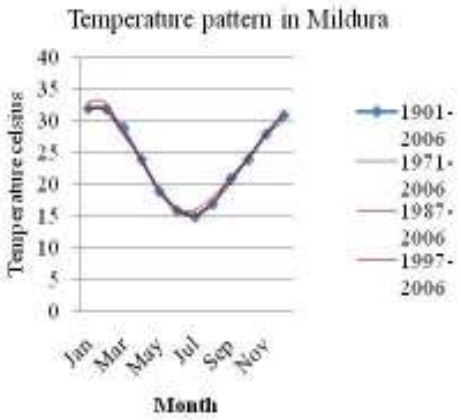
Temperature pattern in Mildura
Temperature celsius
Jan Mar May Jul Sep Nov
Month
1901-2006
1971-2006
1987-2006
1997-2006

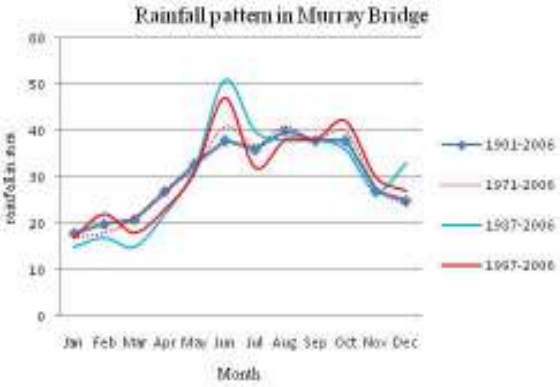
Rainfall pattern in Murray Bridge
rainfall in mm
Jan Feb Mar Apr May Jun Jul Aug Sep Oct Nov Dec
Month
1901-2006
1971-2006
1987-2006
1997-2006


Temperature pattern in Murray Bridge
Temperature in celsius
Jan Feb Mar Apr May Jun Jul Aug Sep Oct Nov Dec
Month
1967-2006
1971-2006
1987-2006
1997-2006

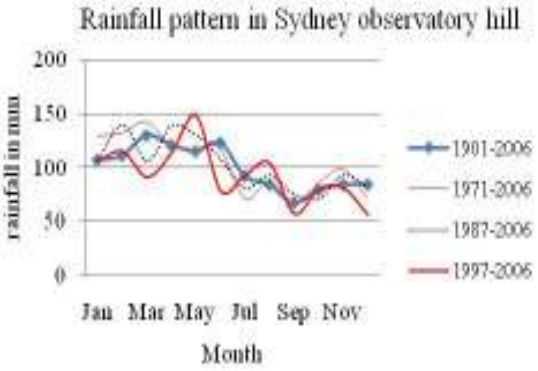
Rainfall pattern in Sydney observatory hill
rainfall in mm
Jan Mar May Jul Sep Nov
Month
1901-2006
1971-2006
1987-2006
1997-2006

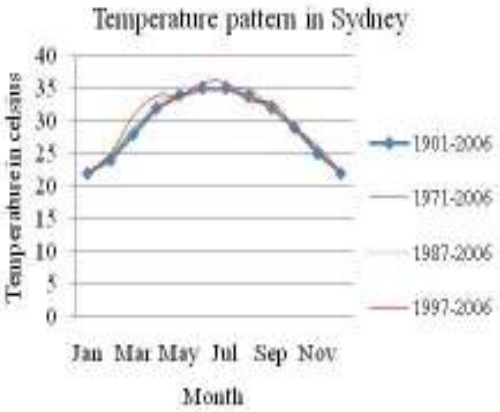
Temperature pattern in Sydney
Temperature in celsius
Jan Mar May Jul Sep Nov
Month
1901-2006
1971-2006
1987-2006
1997-2006


Rainfall pattern in Lake victoria
rainfall in mm
Jan Feb Mar Apr May Jun Jul Aug Sep Oct Nov Dec
Month
1923-2006
1971-2006
1987-2006
1997-2006


Temperature pattern in Lake Victoria
Temperature celsius
Jan Feb Mar Apr May Jun Jul Aug Sep Oct Nov Dec
Month
1923-2006
1971-2006
1987-2006
1991-2006

Appendix 5. 3: Spatial characteristics of rainfall and temperature in the MDB areas and eastern Australia categorized using clustering form

Method: Single Linkage clustering method

Stage 1: we merge the Broken hill and Mildura airport as a cluster C1 height=0.040774

	Hume dam	Adelaide airport	C1	Canberra airport	Loxtonn et	Melbourne airport	Murray bridge	Sydney obs hill	Lake victoria
Hume dam	0								
Adelaide airport	3.075634	0							
C1	1.657979	2.185881	0						
Canberra airport	1.538793	1.559734	1.361636	0					
Loxtonn et	1.601061	2.30015	0.118162	1.42393	0				
Melbourne airport	2.283803	0.801939	1.64376	0.75801	1.743969	0			
Murray bridge	1.217158	2.548072	0.509461	1.41722	0.416873	1.900532	0		
Sydney obs hill	3.14967	2.587441	3.618675	2.25704	3.678361	2.281905	3.616759	0	
Lake victoria	1.627171	2.333404	0.141794	1.47096	***0.047127***	1.783354	0.43002	3.725976	0

Stage 2: we merge Loxton met and lake Victoria as a cluster C2 height 0.047127

Stage 2	Hume dam	Adelaide airport	C1	Canberra airport	C2	Melbourne airport	Murray bridge	Sydney obs hill
Hume dam	0							
Adelaide airport	3.075634	0						
C1	1.657979	2.185881	0					
Canberra airport	1.538793	1.559734	1.361636	0				
C2	1.601061	2.30015	***0.118162***	1.423933	0			
Melbourne airport	2.283803	0.801939	1.64376	0.758005	1.74397	0		
Murray bridge	1.217158	2.548072	0.509461	1.417224	0.41687	1.900532	0	
Sydney obs hill	3.14967	2.587441	3.618675	2.257041	3.67836	2.281905	3.616759	0

Stage 3: we merge C1 and C2 as a cluster C3 height= 0.118162

Stage 3	Hume dam	Adelaide airport	C3	Canberra airport	Melbourne airport	Murray bridge	Sydney obs hill
Hume dam	0						
Adelaide airport	3.075634	0					
C3	1.601061	2.185881	0				
Canberra airport	1.538793	1.559734	1.361636	0			
Melbourne airport	2.283803	0.801939	1.64376	0.758005	0		
Murray bridge	1.217158	2.548072	***0.416873***	1.417224	1.900532	0	
Sydney obs hill	3.14967	2.587441	3.618675	2.257041	2.281905	3.616759	0

Stage 4: we merge Murray bridge and C3 as a cluster C4 height =0.416873

Stage 4	Hume dam	Adelaide airport	C4	Canberra airport	Melbourne airport	Sydney obs hill
Hume dam	0					
Adelaide airport	3.075634	0				
C4	1.217158	2.185881	0			
Canberra airport	1.538793	1.559734	1.361636	0		
Melbourne airport	2.283803	0.801939	1.64376	***0.758005***	0	
Sydney obs hill	3.14967	2.587441	3.616759	2.257041	2.281905	0

Stage 5: we merge Canberra airport and Melbourne as a cluster C5 height =0.758005

Stage 5	Hume dam	Adelaide airport	C4	C5	Sydney obs hill
Hume dam	0				
Adelaide airport	3.075634	0			
C4	1.217158	2.185881	0		
C5	1.538793	***0.801939***	1.361636	0	
Sydney obs hill	3.14967	2.587441	3.616759	2.281905	0

Stage 6: we merge Adelaide airport and C5 as a cluster C6 height =0.801939

Stage 6	Hume dam	C6	C4	Sydney obs hill
Hume dam	0			
C6	1.538793	0		
C4	***1.217158***	2.185881	0	
Sydney obs hill	2.281905	2.587441	3.616739	0

Stage 7: we merge Hume dam and C4 as a cluster C7 height = 1.217157864

Stage 7	C7	C6	Sydney obs hill
C7	0		
C6	***1.538793***	0	
Sydney obs hill	2.281905	2.587441	0

Stage 8: we merge C6 and C7 as a cluster C8 height = 1.538793443

Stage 8	C8	Sydney obs hill
C8	0	
Sydney obs hill	***2.587441***	0

Stage 9, we merge the Sydney observatory hill and C8 as a cluster C9 height = 2.587441

Appendix 5. 4: Temporal characteristics of rainfall and temperature in the MDB areas and eastern of Australia categorized using clustering form

Stage 1: We can merged Jun with August as a cluster C1, height = 0.18357

	Jan	Feb	Mar	Apr	May	C1	Jul	Sep	Oct	Nov	Dec
Jan	**0**										
Feb	0.26066	**0**									
Mar	0.57554	0.67706	**0**								
Apr	1.4142	1.48734	0.83866	**0**							
May	2.41169	2.52474	1.85142	1.0657	**0**						
C1	3.35332	3.51207	2.83910	2.14783	1.18000	0					
Jul	3.69094	3.84311	3.16781	2.44941	1.40438	***0.22719***	0				
Sep	2.44867	2.58721	1.91029	1.19133	0.28268	0.95651	1.26484	0			
Oct	2.33878	2.53244	1.89279	1.42301	0.94749	1.28905	1.48087	0.63866	0		
Nov	0.87725	1.00744	0.33332	0.58178	1.53444	2.50609	2.83577	1.58081	1.56972	0	
Dec	0.4838	0.69865	0.3327	1.05615	1.97655	2.87772	3.21849	1.98947	1.85304	0.47525	0

Stage 2: We can merged July with C1 as a cluster C2, height = 0.22719

	Jan	Feb	Mar	Apr	May	C2	Sep	Oct	Nov	Dec
Jan	**0**									
Feb	***0.26066***	0								
Mar	0.57554	0.67706	0							
Apr	1.4142	1.48734	0.83866	0						
May	2.41169	2.52474	1.85142	1.0657	0					
C2	3.35332	3.51207	2.83910	2.14783	1.18000	0				
Sep	2.44867	2.58721	1.91029	1.19133	0.28268	0.95651	0			
Oct	2.33878	2.53244	1.89279	1.42301	0.94749	1.28905	0.63866	0		
Nov	0.87725	1.00744	0.33332	0.58178	1.53444	2.50609	1.58081	1.56972	0	
Dec	0.4838	0.69865	0.3327	1.05615	1.97655	2.87772	1.98947	1.85304	0.47525	0

Stage 3: We can merged January with February as a cluster C3, height = 0.26066

	C3	Mar	Apr	May	C2	Sep	Oct	Nov	Dec
C3	0								
Mar	0.57554	0							
Apr	1.4142	0.83866	0						
May	2.41169	1.85142	1.0657	0					
C2	3.35332	2.83910	2.14783	1.18000	0				
Sep	2.44867	1.91029	1.19133	***0.28268***	0.95651	0			
Oct	2.33878	1.89279	1.42301	0.94749	1.28905	0.68866	0		
Nov	0.87725	0.33332	0.58178	1.53444	2.50609	1.50081	1.56972	0	
Dec	0.4858	0.3327	1.05615	1.97655	2.87772	1.98947	1.85304	0.47525	0

Stage 4: We can merged May with September as a cluster C4, height = 0.28268

	C3	Mar	Apr	C4	C2	Oct	Nov	Dec
C3	0							
Mar	0.57554	0						
Apr	1.4142	0.83866	0					
C4	2.41169	1.85142	1.0657	0				
C2	3.35332	2.83910	2.14783	1.18000	0			
Oct	2.33878	1.89279	1.42301	0.94749	1.28905	0		
Nov	0.87725	0.33332	0.58178	1.53444	2.50609	1.56972	0	
Dec	0.4858	***0.3327***	1.05615	1.97655	2.87772	1.85304	0.47525	0

Stage 5: We can merged March with December as a cluster C5, height = 0.3327

	C3	C5	Apr	C4	C2	Oct	Nov
C3	0						
C5	0.4858	0					
Apr	1.4142	0.83866	0				
C4	2.41169	1.85142	1.0657	0			
C2	3.35332	2.83910	2.14783	1.18000	0		
Oct	2.33878	1.89279	1.42301	0.94749	1.28905	0	
Nov	0.87725	***0.33332***	0.58178	1.53444	2.50609	1.56972	0

Stage 6: We can merged C5 with November as a cluster C6, height = 0.3332

	C3	C6	Apr	C4	C2	Oct
C3	0					
C6	***0.4858***	0				
Apr	1.4142	0.83866	0			
C4	2.41169	1.85142	1.0657	0		
C2	3.35332	2.83910	2.14783	1.18000	0	
Oct	2.33878	1.89279	1.42301	0.94749	1.28905	0

Stage 7: We can merged C3 with C6 as a cluster C7, height = 0.4858

	C7	Apr	C4	C2	Oct
C7	0				
Apr	***0.83866***	0			
C4	1.85142	1.0657	0		
C2	2.83910	2.14783	1.18000	0	
Oct	1.89279	1.42301	0.94749	1.28905	0

Stage 8: We can merged C7 with April as a cluster C8, height = 0.83866

	C8	C4	C2	Oct
C8	0			
C4	1.0657	0		
C2	2.14783	1.18000	0	
Oct	1.42301	***0.94749***	1.28905	0

Stage 9: We can merged C4 with October as a cluster C9, height = 0.94749

	C8	C9	C2
C8	0		
C9	1.0657	0	
C2	2.14783	1.18000	0

Stage 10: We can merged C8 with C9 as a cluster C10, height = 1.0657

	C10	C2
C10	0	
C2	1.18000	0

Stage 11: We can merged C10 with C2 as a cluster C11, height = 1.1800

Appendix 6. 1: Correlation plots between the CIs.

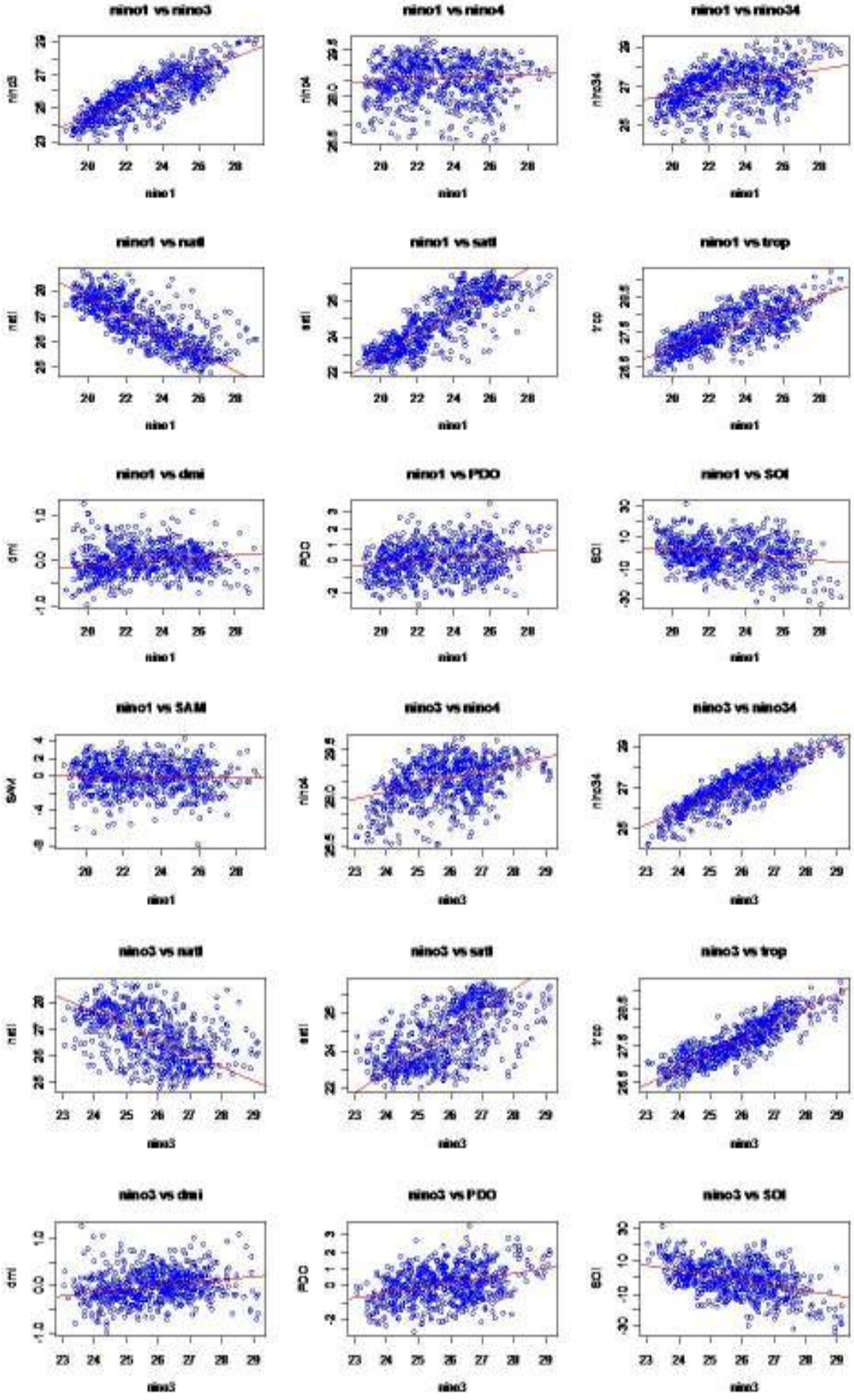

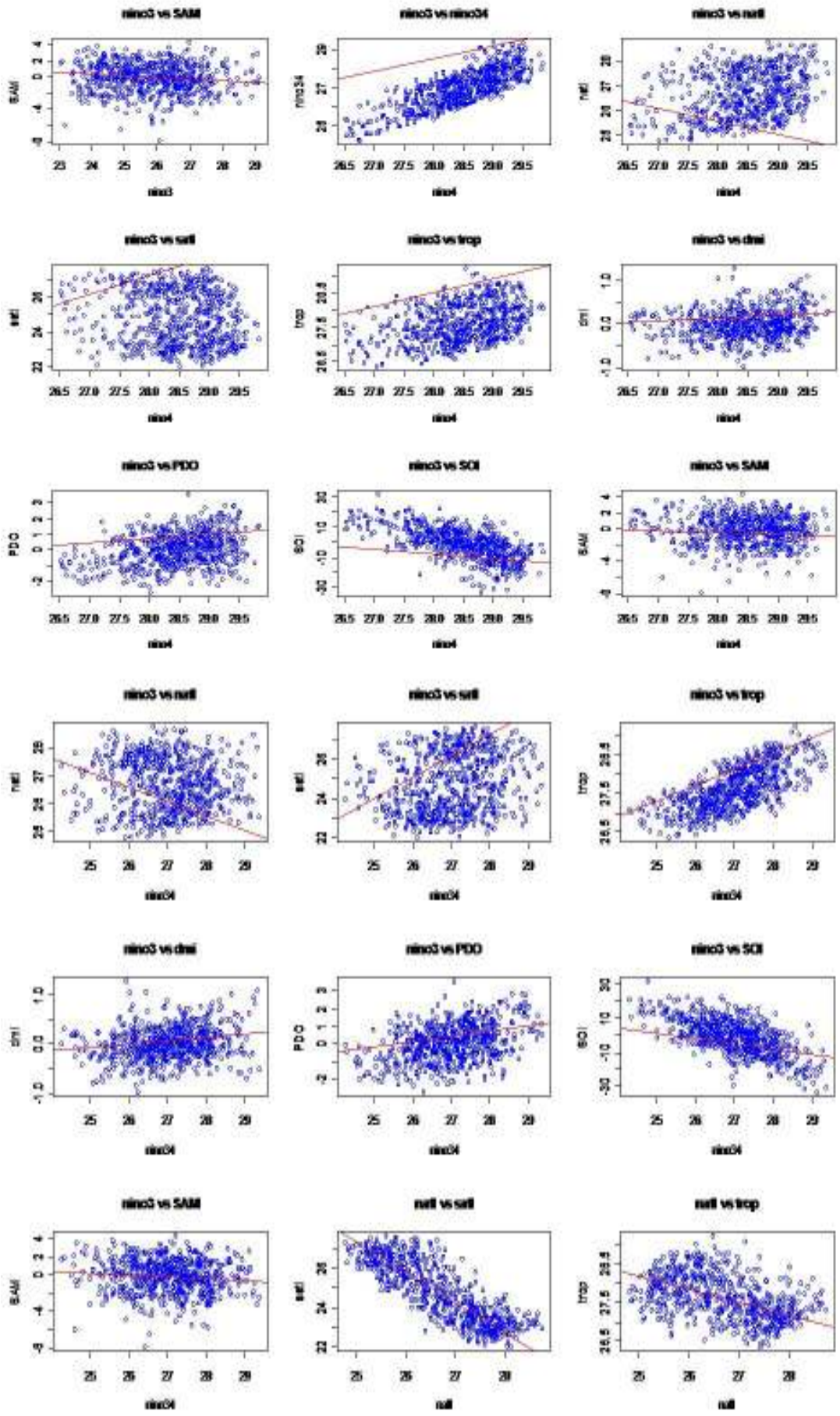
nino3 vs SAM
nino3 vs nino34
nino3 vs nao
nino3 vs sati
nino3 vs trop
nino3 vs dmi
nino3 vs PDO
nino3 vs SOI
nino3 vs SAM
nino3 vs nao
nino3 vs sati
nino3 vs trop
nino3 vs dmi
nino3 vs PDO
nino3 vs SOI
nino3 vs SAM
nao vs sati
nao vs trop
nino3
nino34
nao
sati
trop
dmi
PDO
SOI
SAM

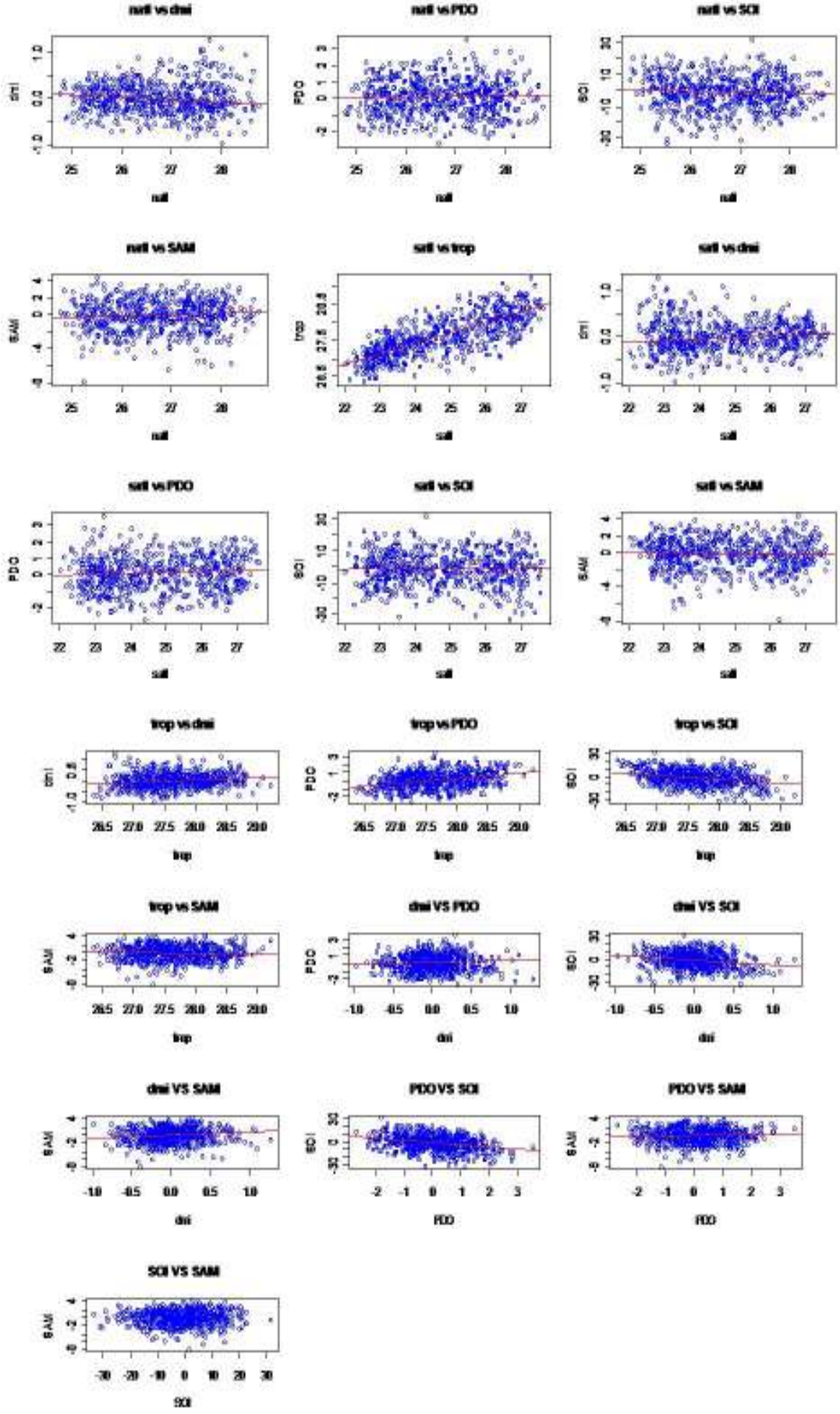
natl vs dmi
natl vs PDO
natl vs SOI
natl vs SAM
satl vs trop
satl vs dmi
satl vs PDO
satl vs SOI
satl vs SAM
trop vs dmi
trop vs PDO
trop vs SOI
trop vs SAM
dmi VS PDO
dmi VS SOI
dmi VS SAM
PDO VS SOI
PDO VS SAM
SOI VS SAM

Appendix 6. 2: Coefficients of RM for CIs by linear, quadratic and sinusoidal function.

Reg. Model	Coefs.	Nino1+2	Nino3	Nino4	Nino3.4	N. Atl	S. Atl	G. Tropic	DMI	PDO	SOI	SAM
Intercept	β_0	23.120	25.800	28.370	26.940	26.560	24.800	27.580	-0.003	0.218	-1.357	-0.122
(t-304.5)	β_1	0.00021660	0.00041070	0.00070090	0.00024820	0.00057820	0.00086830	0.00091290	0.00003143	0.00157100	-0.00724100	0.00175600
$(t-304.5)^2$	β_2	-0.00000183	0.00000042	0.00000360	0.00000228	0.00000502	-0.00000066	0.00000162	0.00000016	-0.00000469	0.00000638	0.00000006
Cosine	β_3	1.96200000	1.18900000	0.00195100	0.54690000	-0.85870000	1.50700000	0.50950000	-0.00624600	0.21560000	-0.71320000	-0.05808000
Sine	β_4	-2.09400000	-0.37800000	0.23570000	0.15920000	0.82530000	-1.36900000	-0.25480000	-0.02172000	0.06847000	-0.28960000	0.07350000
	R^2	0.767700	0.482900	0.116300	0.180500	0.847100	0.932100	0.620200	0.002728	0.110200	0.018560	0.030390
	Ad. R^2	0.766200	0.479400	0.110500	0.175100	0.846100	0.931700	0.617700	-0.003888	0.104300	0.012050	0.023960

Appendix 6. 3: Fitted ARMA model with (1,0,1) process for climatic indicators

Model	Order (p,d,q)	AR(1)	MA(1)	Intercept	AIC	Estimated sigma^2	Log-likelihood
Nino1+2	(1,0,0)	0.8695	0	23.0357	1899.26	1.315	-946.63
	(0,0,1)	0	0.8777	23.0749	2099.73	1.828	-1046.87
	(1,0,1)	0.8136	0.6409	23.038	1555.24	0.743	-773.62
Nino3	(1,0,0)	0.886	0	25.79	1094.43	0.3499	-544.22
	(0,0,1)	0	0.8421	25.8199	1404.43	0.5828	-699.21
	(1,0,1)	0.8276	0.5404	25.7905	856.88	0.2357	-424.44
Nino4	(1,0,0)	0.924	0	28.4791	72.61	0.06512	-33.3
	(0,0,1)	0	0.778	28.4795	688.57	0.1796	-341.28
	(1,0,1)	0.8977	0.1966	28.4767	49	0.06243	-20.5
Nino3.4	(1,0,0)	0.9116	0	26.9906	603.02	0.1571	-301.01
	(0,0,1)	0	0.8087	27.0156	1095.79	0.3509	-544.89
	(1,0,1)	0.8634	0.3927	26.9949	494.39	0.1298	-243.2
North Atlantic	(1,0,0)	0.8623	0	26.7065	822.42	0.2237	-408.21
	(0,0,1)	0	0.8632	26.7093	1010.9	0.305	-502.45
	(1,0,1)	0.8051	0.6141	26.7134	493.01	0.1295	-242.5
South Atlantic	(1,0,0)	0.8604	0	24.7667	1402.39	0.5308	-698.19
	(0,0,1)		0.9125	24.7812	1534.13	0.7208	-764.06
	(1,0,1)	0.8198	0.726	24.764	941.15	0.2704	-466.58
Global Tropic	(1,0,0)	0.8424	0	27.6263	260.9	0.08886	-127.45
	(0,0,1)	0	0.8991	27.6349	346.77	0.1023	-170.38
	(1,0,1)	0.7792	0.7185	27.6284	-139.9	0.04571	73.95
DMI	(1,0,0)	0.7859	0	0.0015	-186.83	0.04257	96.41
	(0,0,1)	0	0.9843	0.0018	-318.04	0.03417	162.02
	(1,0,1)	0.6706	0.9712	0.0021	-675.62	0.01888	341.81
SAM	(1,0,0)	0.2313	0	-0.1213	2419.9	5.105	-1206.95
	(0,0,1)	0	0.2357	-0.1208	2419.94	5.103	-1206.97
	(1,0,1)	0.1143	0.1222	-0.1209	2421.83	5.102	-1206.91
PDO	(1,0,0)	0.8257	0	0.0635	1080.06	0.3419	-537.03
	(0,0,1)	0	0.6838	0.0734	1360.13	0.5424	-677.06
	(1,0,1)	0.8129	0.0404	0.0646	1081.5	0.3416	-536.75
SOI	(1,0,0)	0.6414	0	-1.1165	4236.38	61.5	-2115.19
	(0,0,1)	0	0.4607	-1.1308	4368.8	76.51	-2181.4
	(1,0,1)	0.8726	-0.424	-1.0965	4186.56	56.46	-2089.28

Appendix 6. 4: The correlograms of the series RS for the ARMA (3, 0, 3) model fitted to CIs from 1957 to 2007

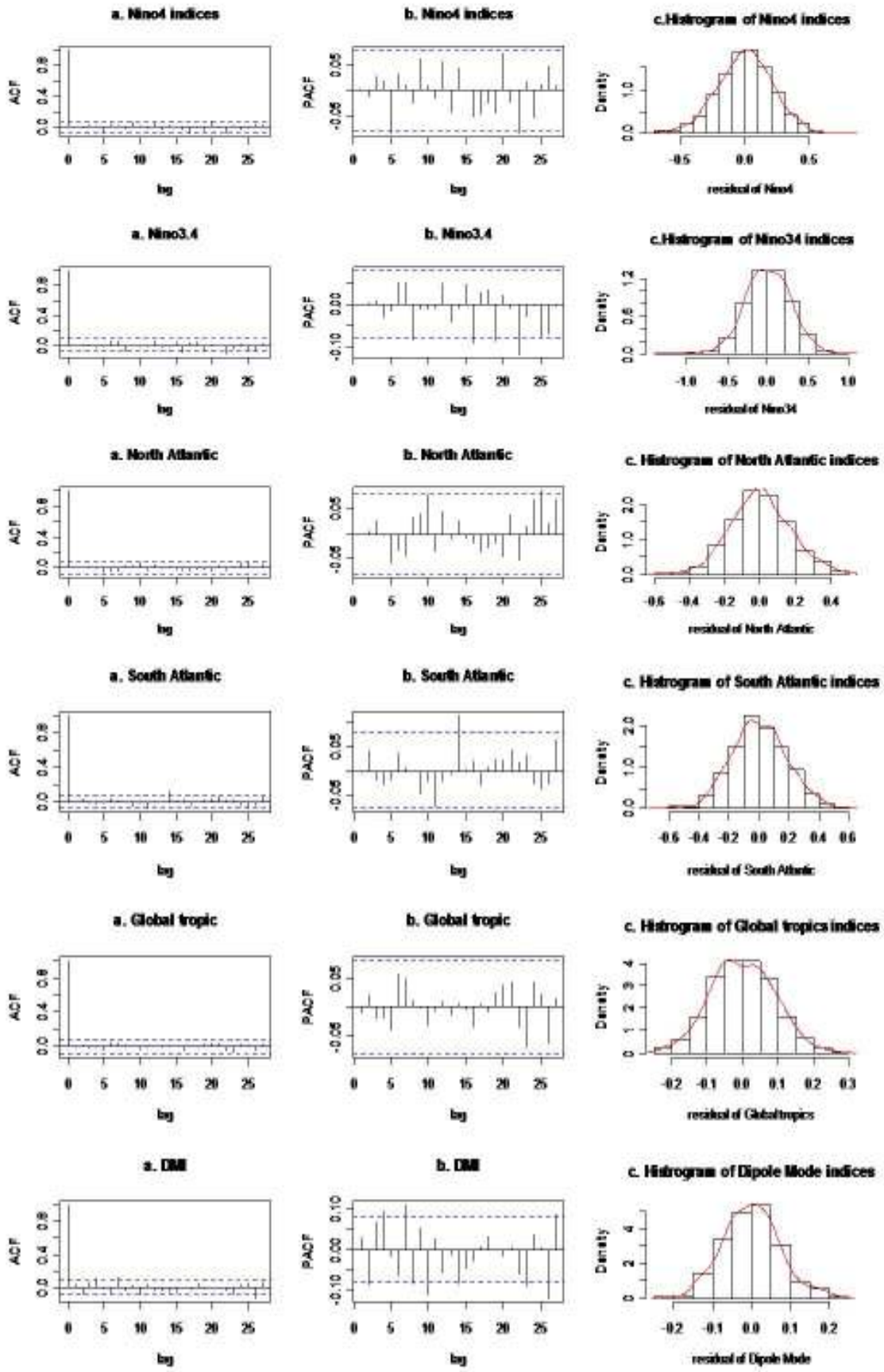

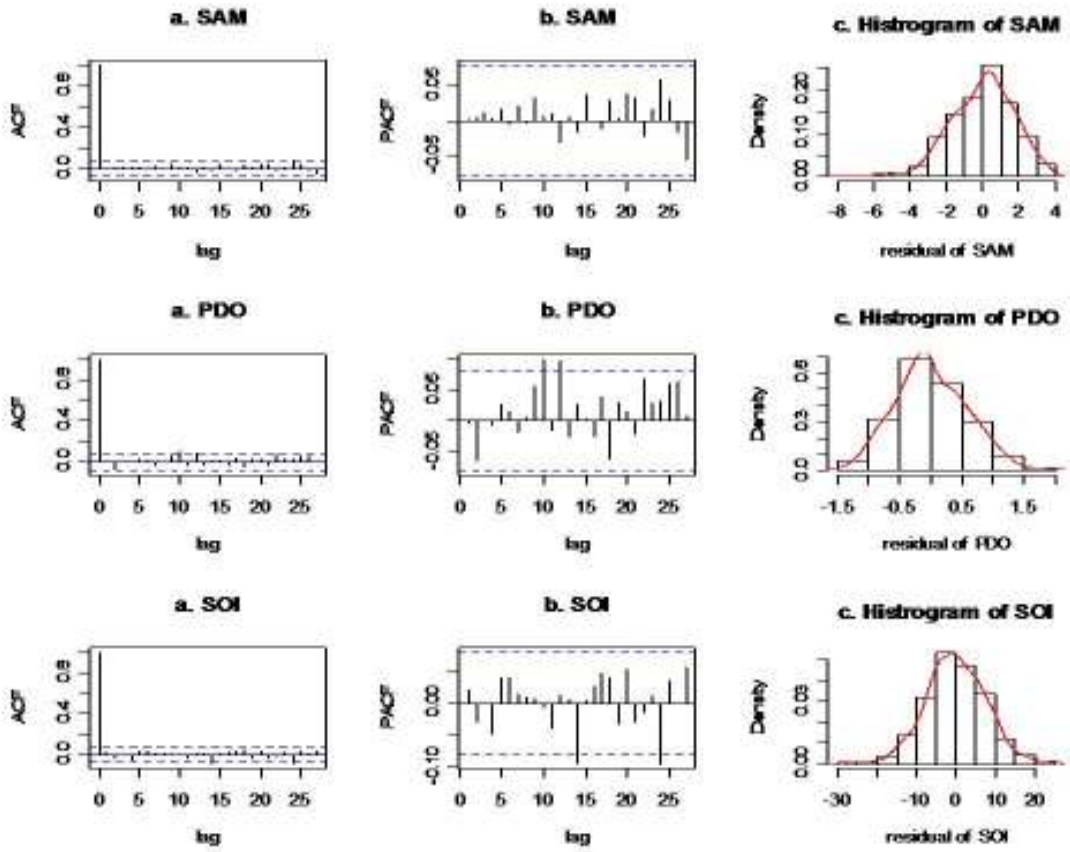

Appendix 6. 5: Cr-C of climatic indicators of white noise with (3, 0, 3)

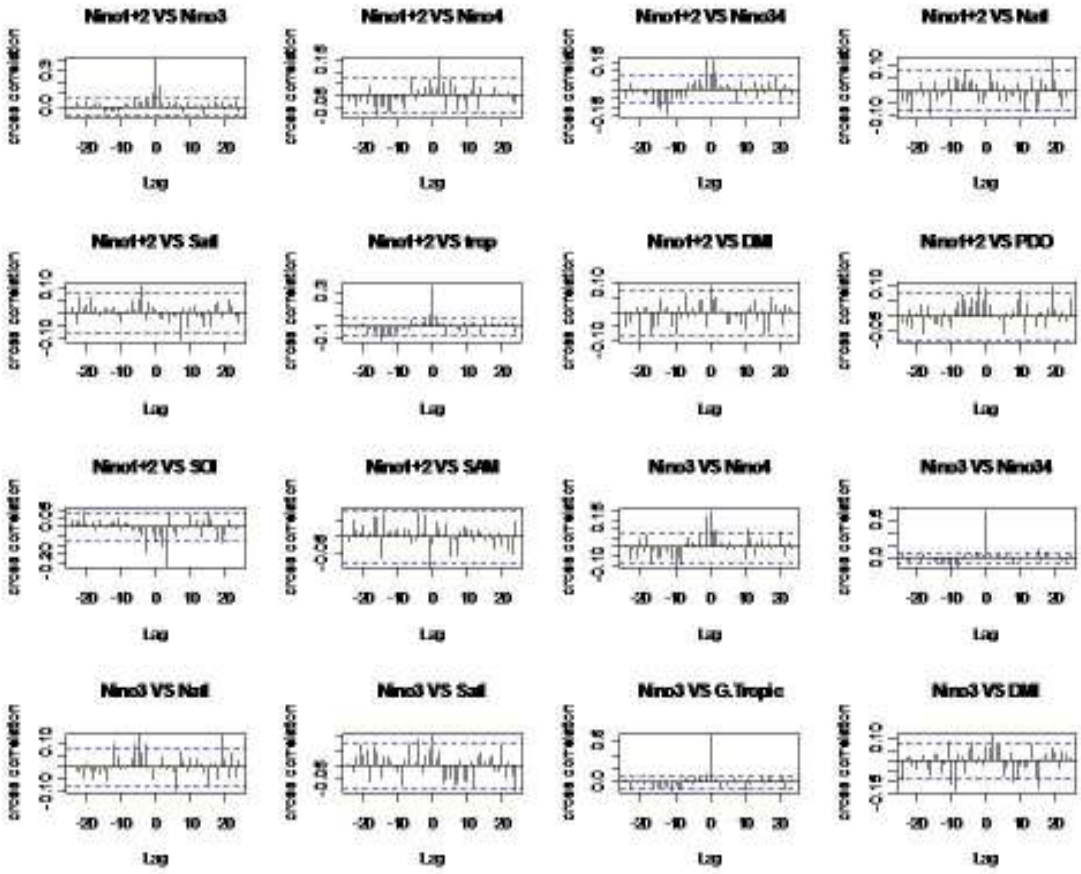

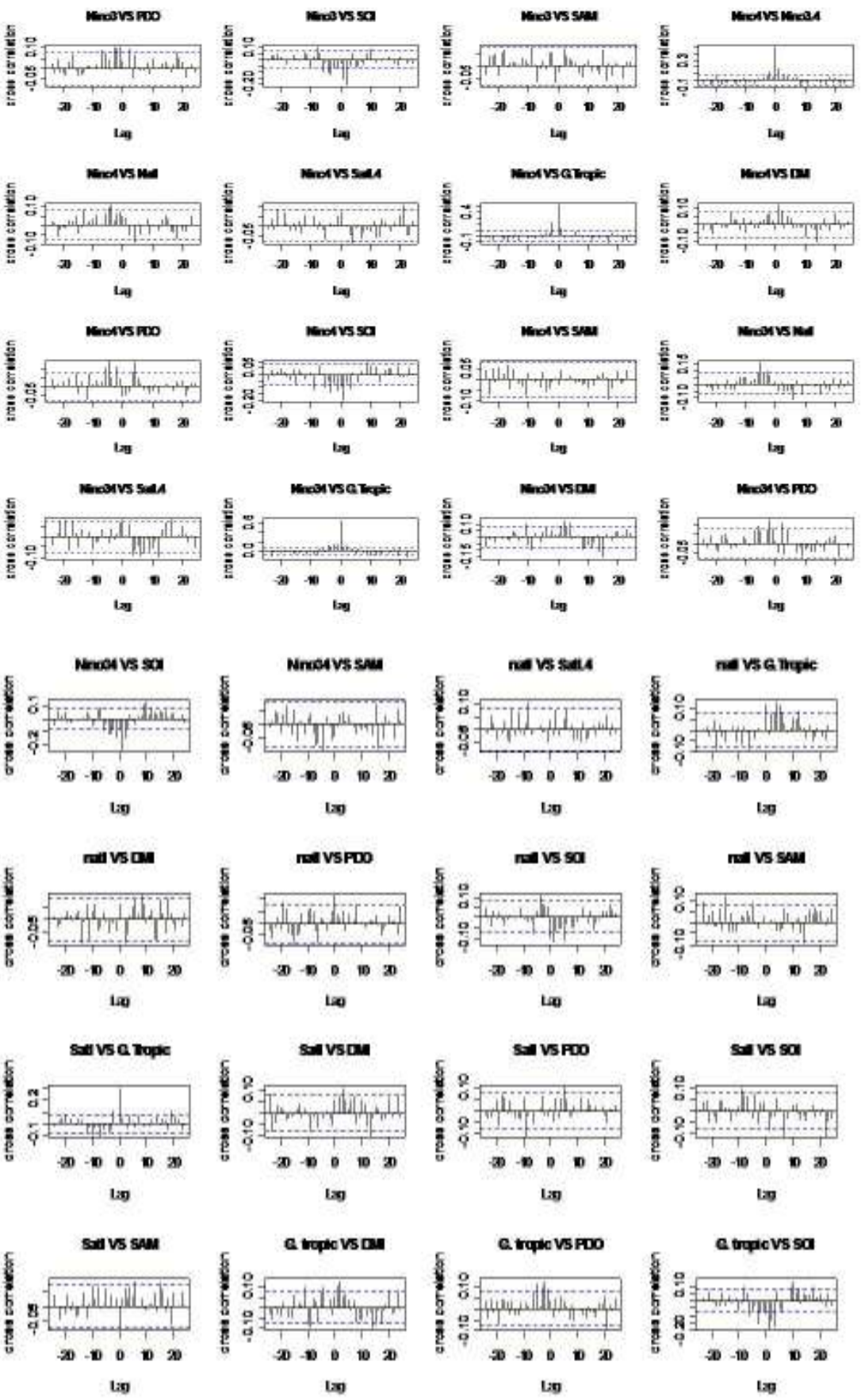
Nino3 VS PDO
Nino3 VS SOI
Nino3 VS SAM
Nino4 VS Nino3.4
Nino4 VS Nat
Nino4 VS Sat.4
Nino4 VS G.Tropic
Nino4 VS DMI
Nino4 VS PDO
Nino4 VS SOI
Nino4 VS SAM
Nino34 VS Nat
Nino34 VS Sat.4
Nino34 VS G.Tropic
Nino34 VS DMI
Nino34 VS PDO
Nino34 VS SOI
Nino34 VS SAM
nat VS Sat.4
nat VS G.Tropic
nat VS DMI
nat VS PDO
nat VS SOI
nat VS SAM
Sat VS G.Tropic
Sat VS DMI
Sat VS PDO
Sat VS SOI
Sat VS SAM
G.tropic VS DMI
G.tropic VS PDO
G.tropic VS SOI
cross correlation
Lag

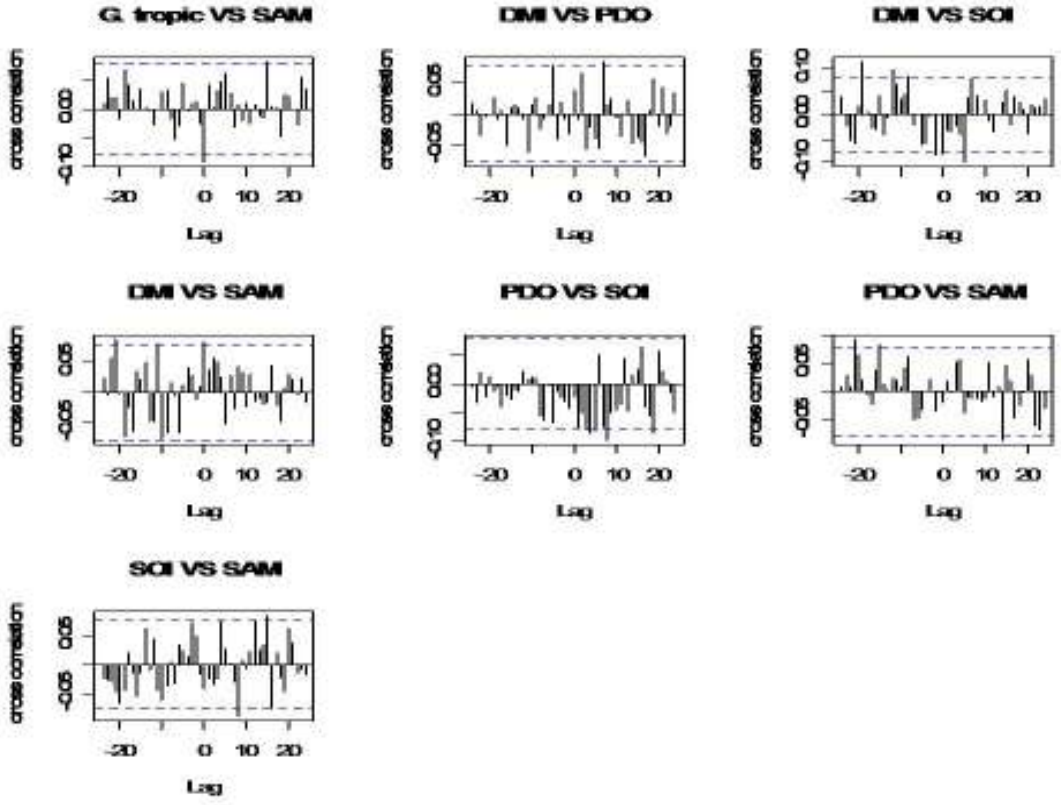
G. tropic VS SAM
DMI VS PDO
DMI VS SOI
DMI VS SAM
PDO VS SOI
PDO VS SAM
SOI VS SAM
cross correlation
Lag

Appendix 6. 6: Regression coefficients of rainfall series by CIs for 6 stations in the MDB and 4 stations in eastern Australia

a) RM with linear, quadratic and climatic indicators with one year periodic function

	Coefficient	Adelaide Airport	Broken hill	Canberra Airport	Hume Dam	Lake Victoria	Location met	Melbourne Airport	Mildura Airport	Murray Bridge	Sydney obs Hill
Intercept	β_0	-165.900	179.400	-241.400	-93.880	-137.700	-122.00	-218.500	-22.430	-32.960	-703.600
linear	β_1	-0.001	0.007	-0.013	0.0003	-0.011	0.000	-0.039**	-0.009	-0.001	-0.022
quadratic	β_2	0.000	0.000	0.000	0.00012*	0.000	0.000	0.000	0.000	0.000	0.000
Cosine	β_3	-15.53***	-5.459	6.858*	-12.18***	1.072	-2.09**	-3.804	1.860	-12.960	-9.110
Sine	β_4	-14.220	-7.370	-7.121	-15.56	-14.33*	-15.650	15.760	-8.811	8.631***	-25.200
Niño1+2	β_5	-0.961	-0.437	6.902*	0.964	-0.707	0.961	2.624	-1.646	0.402	20.46*
Niño3	β_6	1.763	1.253	-22.790*	-0.939	1.972	0.969	-9.725	4.585	-2.585	-55.51*
Niño4	β_7	4.292	-1.038	-7.298	3.846	2.560	3.487	-8.113	5.263	-3.086	-17.190
Niño3.4	β_8	-1.240	1.551	20.670	1.182	0.942	-0.342	5.662	-2.506	4.891	59.310
N-Atlantic	β_9	-0.882	-3.141	4.159	6.706	-0.525	1.375	2.616	-1.530	-0.554	11.910
S-Atlantic	β_{10}	1.317	3.857	1.346	6.611	4.890	6.154**	3.664	3.078	4.167	28.33*
Global tropics	β_{11}	3.032	-7.303	8.329	-11.720	-2.885	-6.584	13.450	-5.462	-0.484	-12.860
DMI	β_{12}	-8.793**	1.581	-11.030	-15.810**	-5.443	-4.77*	-4.651	-4.139	-5.657	-2.007
PDO	β_{13}	0.083***	0.226***	0.888	2.199	-0.525*	0.320	0.077	0.567	1.717	-3.114
SOI	β_{14}	0.549	0.663*	1.029***	1.078***	0.615***	0.462***	0.049	0.632***	0.135	1.339*
SAM	β_{15}	-0.534*	1.616*	2.841***	0.915	1.202*	0.519	1.971*	1.323*	0.887	8.306**
PDO*SOI	β_{16}	-0.225	-0.273	-0.130	-0.044	-0.234**	-0.141*	0.033	-0.237**	-0.118	0.036

b) RM with linear, quadratic and climatic indicators with seasonal indicator

	Coefficient	Adelaide Airport	Broken hill	Canberra Airport	Hume Dam	Lake Victoria	Location met	Melbourne Airport	Mildura Airport	Murray Bridge	Sydney obs Hill
Intercept	β_0	-195.200	485.700	-376.900	-221.900	-81.710	-68.550	248.800	87.760	60.050	-944.700
linear	β_1	-0.002	0.019	-0.017	-0.005	-0.009	0.002	-0.010	-0.005	0.004	-0.034
Quadratic	β_2	0.000	0.000	0.000	0.000*	0.000	0.000	0.000	0.000	0.000	0.000
Niño1+2	β_3	-2.097	0.492	6.810	-0.310	-0.744	0.770	5.961	-1.509	1.121	19.130
Niño3	β_4	9.665	9.101	-31.98**	5.176	5.346	4.205	-9.517	9.197	-3.323	-57.400
Niño4	β_5	6.808	5.680	-13.790	5.424	4.310	4.767	-2.488	8.415	-2.573	-17.980
Niño3.4	β_6	-8.626	-4.061	29.23*	-5.594	-1.776	-2.625	7.832	-6.243	6.322	57.580
N-Atlantic	β_7	1.186	0.389	1.181	7.693	0.770	2.773	4.466	0.181	-0.375	8.491
S-Atlantic	β_8	4.044	9.293*	-4.026	7.686	6.603*	7.773**	8.288	5.707	4.507	25.540
Global tropics	β_9	-2.505	-36.08*	27.790	-8.903	-9.899	-13.340	-20.250	-17.340	-6.549	6.177
DMI	β_{10}	-9.299**	0.190	-10.420	-16.48**	-5.958*	-5.015*	-6.393	-4.765	-6.247	0.170
PDO	β_{11}	-0.055	0.349	0.754	1.857	-0.559	0.325	0.487	0.601	1.763	-2.627
SOI	β_{12}	0.498***	0.625***	1.067***	1.052***	0.595***	0.439***	0.062	0.611***	0.132	1.368*
SAM	β_{13}	-0.584	1.551*	2.885***	0.769	1.188	0.544	1.953	1.309*	0.909	8.479***
PDO*SOI	β_{14}	-0.243**	-0.275*	-0.123	-0.061	-0.236	-0.142	0.073*	-0.239**	-0.111	0.015
Jan	β_{15}	-8.550	-2.694*	10.990	-4.348	-6.707	-7.212	-14.130	-6.886	-3.626	5.684
Feb	β_{16}	-13.420	-22.790	12.720	-17.440	-15.350	-11.740	-18.200	-15.400	-7.085	3.726
Mar	β_{17}	-14.650	-18.920	4.066	-16.920	-22.86*	-19.44*	-20.41	-18.290	-0.561	6.247
Apr	β_{18}	-2.329	-9.362	-3.164	-4.504	-14.33	-10.910	0.413	-12.230	6.807	-9.763
May	β_{19}	19.74*	3.202	-10.570	9.641**	-6.044	0.163	2.065	-4.316	17.01*	-1.214
Jun	β_{20}	24.41***	-7.244	-7.013	13.37*	-3.851	3.530	1.215	-5.818	17.24**	62.86**
Jul	β_{21}	35.39***	-4.593	0.257	31.630	5.776	13.78**	-2.991	-1.232	22.75**	26.120
Aug	β_{22}	27.7**	-6.196	5.111	32.140	8.085	13.520*	8.142	0.967	23.81*	65.9*
Sep	β_{23}	24.53**	1.072	11.200	21.750	10.880	14.790*	11.640	2.743	25.48*	37.960
Oct	β_{24}	16.910*	10.430	12.420	18.740	14.230*	17.050**	20.210	7.383	15.130	47.300
Nov	β_{25}	1.124	3.374	10.790	-0.980	4.847	8.368	19.820	1.601*	11.550	40.950

*coefficients are statistically significant at the 5% level
**coefficients are statistically significant at the 1% level
***coefficients are statistically significant at the 0.1% level

Appendix 6. 7: Regression coefficients of temperature series by CIs for 6 stations in the MDB and 4 stations in eastern Australia

a) **RM with linear, quadratic and climatic indicators with one year periodic function**

	Coefficient	Adelaide Airport	Broken hill	Canberra Airport	Hume Dam	Lake Victoria	Loxton met	Melbourne Airport	Mildura Airport	Murray Bridge	Sydney obs Hill
Intercept	β_0	-37.05**	16.480	13.590	44.70***	54.05***	41.98***	26.640	39.140***	64.34***	9.218
linear	β_1	0.000	0.002	0.003***	0.003***	0.002*	0.002***	0.004**	0.002***	0.004***	0.000
quadratic	β_2	0.000*	0.000	0.000*	0.000***	0.000	0.000**	0.000	0.000***	0.000	0.000
Cosine	β_3	5.794***	5.813***	9.107***	7.575***	4.815***	6.641***	-9.372***	7.107***	1.344	-5.794***
Sine	β_4	8.276***	-2.29***	4.173***	4.237***	3.170**	3.507***	-6.436***	3.516	-5.761***	-3.512***
Niño1+2	β_5	-0.416	0.102	-0.159	-0.011	-0.365	-0.021	-0.157	0.002**	-0.196	-0.564*
Niño3	β_6	0.315	0.920	1.474*	1.521**	1.136	1.153**	1.831*	1.206*	1.211	3.041***
Niño4	β_7	-0.776	1.327*	0.474	0.802*	-0.167	0.583	0.283	0.720**	0.207	1.081
Niño3.4	β_8	-0.491	-1.047	-1.079	-1.241*	-0.339	-1.242*	-1.217	-1.349	-0.802	-3.121**
N-Atlantic	β_9	0.244	1.034*	0.642*	0.046	-0.131	0.121	1.262**	0.097	0.362	0.251
S-Atlantic	β_{10}	-0.507	0.276	0.506	0.430*	0.024	0.240	0.208	0.313	0.071	0.567
Global tropics	β_{11}	3.995***	-2.257*	-1.308	-2.310***	-1.264	-1.453***	-2.035*	-1.492**	-2.312***	-0.463
DMI	β_{12}	1.219***	-0.020	0.898**	0.738***	-0.100	0.690***	0.935*	0.598**	0.544*	0.143
PDO	β_{13}	-0.113	-0.335*	-0.114	-0.102	-0.361*	-0.067	-0.137	-0.059	-0.124	0.118
SOI	β_{14}	-0.008	-0.018	-0.038**	-0.008	-0.041*	-0.016	-0.033	-0.020*	-0.019	-0.035*
SAM	β_{15}	-0.030	-0.014	-0.249***	-0.043	-0.101	-0.109**	-0.200	-0.092**	-0.019	0.011
PDO*SOI	β_{16}	0.004	0.010	0.011	0.001	-0.005	0.003	0.006**	0.006	0.000	-0.013

b) RM with linear, quadratic and climatic indicators with seasonal indicator

	Coefficient	Adelaide Airport	Broken hill	Canberra Airport	Hume Dam	Lake Victoria	Loxton met	Melbourne Airport	Mildura Airport	Murray Bridge	Sydney obs Hill
Intercept	β_0	-5.773	40.960	7.721	17.590	41.920	20.76*	-2.505	12.610	45.01**	54.200
linear	β_1	0.001	0.003	0.002**	0.001*	0.002	0.001	0.001	0.000	0.003**	0.002
Quadratic	β_2	0.000	0.000	0.000	0.000**	0.000	0.000*	0.000	0.000*	0.000	0.000
Niño1+2	β_3	-0.225	0.286	-0.172	-0.140	-0.452	-0.099	-0.324	-0.114	-0.342	-0.089
Niño3	β_4	-0.258	0.317*	0.554	0.487	0.536	0.102	0.361	0.128	1.129	1.658
Niño4	β_5	-0.813	1.282	-0.158	-0.113	-0.696	-0.272	-0.875	-0.209	-0.101	1.098
Niño3.4	β_6	0.285	-0.329	-0.263	-0.431	0.190	-0.361	-0.031	-0.482	-0.878	-1.451
N-Atlantic	β_7	0.257*	0.96*	0.232	-0.471*	-0.396	-0.336	0.616*	-0.409*	0.217	0.176
S-Atlantic	β_8	-0.518***	0.179	-0.140	-0.416	-0.461	-0.525*	-1.003	-0.527**	-0.171*	0.484
Global tropics	β_9	2.711	-3.073*	0.907	1.405	0.687	1.723*	2.567**	2.158***	-0.461	-2.954
DMI	β_{10}	1.233	-0.057	0.858**	0.787***	-0.028	0.732***	1.176	0.655	0.593	0.109
PDO	β_{11}	-0.080	-0.315	-0.144	-0.143*	-0.376*	-0.101	-0.145	-0.098	-0.159	0.176
SOI	β_{12}	-0.006	-0.015	-0.033*	-0.003	-0.038	-0.011	-0.027*	-0.014	-0.018	-0.026
SAM	β_{13}	-0.011***	-0.004	-0.252***	-0.042	-0.090	-0.107**	-0.178	-0.090**	-0.026	0.031
PDO*SOI	β_{14}	0.007***	0.012	0.012	0.000	-0.005	0.003	0.006***	0.006	-0.003	-0.008
Jan	β_{15}	2.907***	1.394	2.419***	2.548	1.426	2.195***	4.090***	2.189***	0.864	-0.809
Feb	β_{16}	5.223	1.633	0.548	2.084***	2.104	1.910***	4.319	1.817**	-1.554	1.100
Mar	β_{17}	3.599***	0.208***	-3.052**	-1.675***	-0.505	-1.56**	0.253***	-1.957**	-4.351***	5.361***
Apr	β_{18}	-0.091***	-2.321***	-9.04***	-7.301*	-4.164***	-6.187***	-7.354***	-7.10***	-8.024***	9.721***
May	β_{19}	-5.458***	-6.013***	-14.22***	-12.270***	-7.408***	-10.68***	-13.64***	-11.75***	-10.790***	11.660***
Jun	β_{20}	-11.15***	-9.419***	-18.27***	-15.250***	-9.715***	-13.34***	-19.05***	-14.28***	-11.77***	12.68***
Jul	β_{21}	-14.91***	-11.23***	-18.93***	-15.77***	-10.15***	-13.56***	-19.92***	-14.45***	-10.94***	12.55***
Aug	β_{22}	-16.78***	-10.71***	-16.07***	-13.57***	-9.227***	-11.8***	-18.0***	-12.34***	-9.227***	11.44***
Sep	β_{23}	-13.95***	-8.399***	-11.87***	-10.630***	-7.937***	-8.99***	-14.58***	-9.464***	-6.694***	10.03***
Oct	β_{24}	-9.515***	-5.240***	-7.71***	-7.042***	-4.652***	-5.874***	-9.453***	-6.131***	-3.987***	7.261***
Nov	β_{25}	-4.594***	-2.215**	-3.18***	-3.164***	-2.131*	-2.587***	-4.52***	-2.714***	-1.776***	3.812***

*coefficients are statistically significant at the 5% level
**coefficients are statistically significant at the 1% level
***coefficients are statistically significant at the 0.1% level

Appendix 6. 8: Regression coefficient of rainfall series by factor score for 6 stations in the MDB and 4 stations in eastern Australia

a) RM with linear, quadratic and climatic indicators with one year periodic function

	Co efficient	Adelaide Airport	Broken hill	Canberra Airport	Hume Dam	Lake Victoria	Lexton met	Melbourne Airport	Mildura Airport	Murray Bridge	Sydney obs. Hill
Intercept	β_0	38.770***	24.63***	52.31***	62.55***	22.09***	22.09***	46.01***	24.74***	30.06***	106.4***
linear	β_1	0.004	0.005	-0.003	0.009	-0.006	0.003	-0.020	-0.005	0.002	-0.014
quadratic	β_2	-0.00006	-0.00007	-0.00003	-0.00012*	-0.00001*	0.00002	-0.00006	-0.00004	0.00001	-0.00009
Cosine	β_3	-16.97***	0.764	8.386***	-13.010	-0.843***	-2.119	-4.797	-0.202	-14.16*	-2.580
Sine	β_4	-19.32**	-15.17*	-11.900	-23.180	-17.750*	-15.720***	13.70***	-12.48*	9.053***	-10.510
Factor 1	β_5	5.387	7.860	4.682	4.038	8.250	7.162*	5.187*	4.680	6.584	25.140
Factor 2	β_6	-1.452	-5.23***	-7.111***	-7.672	-3.404***	-2.403***	-3.326**	-3.132**	0.005	-9.313**
Factor 3	β_7	-3.292**	1.108	-0.481	-4.304	-0.136**	-0.849	1.864	0.058	-0.661	7.404
Factor 1x2	β_8	0.481	0.731	1.738	2.226	1.056	1.074	2.451	0.174	0.629	-1.349
Factor 1x3	β_9	1.154	2.384*	1.985	2.565	1.162	1.540	1.953*	1.721	0.888	-1.530
Factor 2x3	β_{10}	-3.520***	-3.142*	-3.888*	-5.946	-2.432***	-1.777**	-3.812*	-2.969**	-3.585***	-5.009

b) Regression model with linear, quadratic and climatic indicators with seasonal indicators

	Co efficient	Adelaide Airport	Broken hill	Canberra Airport	Hume Dam	Lake Victoria	Lexton met	Melbourne Airport	Mildura Airport	Murray Bridge	Sydney obs. Hill
Intercept	β_0	26.05***	35.99***	51.71***	50.76***	20.970***	17.900***	45.64***	25.550***	18.38***	88.36***
linear	β_1	0.005	0.005	-0.003	0.009	-0.006	0.003	-0.020	-0.005	0.002	-0.015
quadratic	β_2	0.000	0.000	0.000	0.000	0.000***	0.000	0.000	0.000	0.000	0.000
Factor 1	β_3	7.123	6.365	2.005	5.138	8.528*	7.358*	1.863*	5.323	5.566	24.180
Factor 2	β_4	-1.765	-5.305***	-7.093***	-7.76***	-3.58***	-2.391**	-3.586*	-3.279**	0.001	-9.252**
Factor 3	β_5	-3.592***	1.301	-0.436	-4.614	-0.362	-0.789	1.475	-0.149	-0.753	8.301***
Factor 1x2	β_6	0.087	0.784	1.844	1.974	0.811	1.213	1.924	-0.061	0.495	-0.179
Factor 1x3	β_7	0.925	2.396*	2.128	2.337	1.013	1.613*	1.698	1.589	0.907	-1.058
Factor 2x3	β_8	-3.721***	-3.104*	-4.189**	-6.07***	-2.664**	-2.004**	-4.30**	-3.104**	-3.682***	-4.980
Jan	β_9	-11.330*	4.702	3.562	-6.798	-7.167	-5.072	-5.878	-5.968	-2.484	12.680
Feb	β_{10}	-15.390*	-14.880	-0.207	-18.250	-14.74*	-6.688	-4.619*	-13.260	-4.760	12.890
Mar	β_{11}	-15.970	-20.330	-7.459	-17.250	-22.40**	-15.81*	-12.530**	-17.93*	-0.139	17.570
Apr	β_{12}	0.745	-23.310	-8.797	-1.585	-12.430	-9.708	-2.227	-12.110	5.899	-0.783
May	β_{13}	24.19***	-19.680	-9.629	15.300	-3.260	0.810	-3.631	-3.246	16.29*	-4.517
Jun	β_{14}	29.18***	-26.310	-8.579	18.97*	0.750	4.837*	-4.321	-1.637	17.44***	51.95**
Jul	β_{15}	40.47***	-15.860	-3.266	38.11***	11.47*	16.200***	-5.915	6.000	24.90***	3.869
Aug	β_{16}	33.93***	-13.020	0.632	39.82***	14.47*	16.840***	5.599	9.352	26.74***	37.760
Sep	β_{17}	33.7***	-5.242	10.480	34.54**	18.510**	19.320**	7.923	11.750	28.02***	12.480
Oct	β_{18}	25.34***	1.659	16.520	31.00**	20.11***	20.060**	17.050	12.9*	17.30*	30.940
Nov	β_{19}	6.648	-3.294	15.930	6.933	8.085	9.560	16.08*	3.949	11.96*	34.230

*coefficients are statistically significant at the 5% level
**coefficients are statistically significant at the 1% level
***coefficients are statistically significant at the 0.1% level

Appendix 6. 9: Regression coefficient of temperature series by factor score for 6 stations in the MDB and 4 stations in eastern Australia

a) Regression model with linear, quadratic and climatic indicators with one year periodic function

	Coefficient	Adelaide Airport	Broken hill	Canberra Airport	Hume Dam	Lake Victoria	Lorton met	Melbourne Airport	Mildura Airport	Murray Bridge	Sydney obs Hill
Intercept	β_0	30.26***	24.04***	25.83***	21.14***	23.32***	23.36***	27.84***	23.56***	22.76***	29.30***
linear	β_1	0.002**	0.001	0.002***	0.002***	0.001	0.001**	0.003**	0.001**	0.002	0.001
quadratic	β_2	-0.000001	-0.000003	0.00001**	0.00001***	0.000005	0.00001**	0.000012	0.00001**	-0.00004	0.000006
Cosine	β_3	5.457***	-4.871***	9.146***	7.650***	-4.641***	6.770***	-9.433***	7.250***	0.514***	-6.019***
Sine	β_4	7.228***	-1.091	3.770***	3.934***	2.616**	3.354***	-4.624***	3.586***	-5.751***	-3.68***
Factor 1	β_5	0.784	-1.376*	0.653	0.796**	0.156	0.374	0.679	0.382	-0.132	1.15*
Factor 2	β_6	0.234*	0.143	0.481***	0.029	0.111	-0.011	0.382**	0.042	-0.140	0.297*
Factor 3	β_7	0.326**	0.246	-0.030	0.116	-0.057	0.007	-0.025	0.017	0.090	0.099
Factor 1x2	β_8	0.169	0.107	-0.016	-0.122	-0.103	-0.20**	-0.141	-0.186**	-0.157	-0.021
Factor 1x3	β_9	-0.179	-0.047	-0.177	-0.197**	-0.016	-0.103	-0.218	-0.107	-0.048	-0.047
Factor 2x3	β_{10}	0.002	0.186	0.254**	0.110	0.022	0.067	0.226	0.080	0.007	0.104

b) RM with linear, quadratic and climatic indicators with seasonal indicators

	Coefficient	Adelaide Airport	Broken hill	Canberra Airport	Hume Dam	Lake Victoria	Lorton met	Melbourne Airport	Mildura Airport	Murray Bridge	Sydney obs Hill
Intercept	β_0	35.68***	27.26***	34.12***	28.00***	27.58***	29.37***	36.10***	30.04***	28.25***	22.07***
linear	β_1	0.002***	0.001	0.002***	0.002***	0.001	0.001**	0.003**	0.001**	0.002***	0.001
quadratic	β_2	-0.000003	-0.000003	0.00001**	0.00001***	0.000005	0.00001**	0.000012	0.00001**	-0.000003	0.000005
Factor 1	β_3	0.079	-1.052	0.329	0.702*	0.024	0.190	0.185	0.203	0.019	0.207
Factor 2	β_4	0.138	-0.158	0.532***	0.117	-0.151	0.054	0.45**	0.114	-0.093	0.311
Factor 3	β_5	0.256*	0.27*	-0.030	0.175*	-0.005	0.045	0.040	0.064	0.119	0.096
Factor 1x2	β_6	0.024	0.145	0.005	-0.014	-0.032	-0.128*	-0.065	-0.102	-0.097	-0.039
Factor 1x3	β_7	-0.215*	-0.049*	-0.129	-0.124	0.025	-0.045	-0.157	-0.042	-0.019	-0.007
Factor 2x3	β_8	-0.066	0.214*	0.246*	0.116	-0.016	0.060	0.191	0.075	0.029	0.064
Jan	β_9	1.891***	1.625	1.974***	2.107***	0.848	1.754***	2.404***	1.807***	0.429	-0.165
Feb	β_{10}	3.748***	2.031	-0.011	1.380**	1.253	1.247***	1.666	1.297**	-2.219***	2.066*
Mar	β_{11}	2.613**	0.534	-3.405***	-2.232***	-1.166	-2.054***	-2.007	-2.201***	-4.968***	5.887***
Apr	β_{12}	0.073	-1.938	-9.021***	-7.398***	-4.264***	-6.199***	-8.339***	-6.814***	-8.337***	9.408***
May	β_{13}	-4.91***	-4.838**	-14.100***	-12.15***	-7.299***	-10.52***	-13.91***	-11.36***	-10.970***	11.01***
Jun	β_{14}	-10.80***	-7.438***	-18.17***	-15.04***	-9.135***	-13.36***	-18.82***	-14.25***	-11.380***	12.56***
Jul	β_{15}	-14.860***	-8.573***	-18.94***	-15.56***	-9.548***	-13.74***	-19.43***	-14.76***	-10.37***	13.05***
Aug	β_{16}	-16.590***	-7.927***	-15.91***	-13.34***	-8.499***	-11.96***	-16.81***	-12.77***	-8.261***	12.18***
Sep	β_{17}	-13.380***	-6.204***	-11.56***	-10.35***	-7.275***	-9.02***	-12.83***	-9.746***	-5.613***	10.55***
Oct	β_{18}	-8.568***	-4.146***	-7.311***	-6.714***	-4.05***	-5.73***	-7.608***	-6.156***	-3.106***	7.259***
Nov	β_{19}	-3.802	-1.968**	-2.864***	-2.88***	-1.804*	-2.379***	-3.28***	-2.558***	-1.332***	3.537***

*coefficients are statistically significant at the 5% level
**coefficients are statistically significant at the 1% level
*** coefficients are statistically significant at the 0.1% level

Appendix 7. 1: Realization of linear, quadratic and sinusoidal of one year period with AR (1) process model

Locations	Coefficient	Rainfall				Temperature			
		Value	Std.Error	t-value	p-value	Value	Std.Error	t-value	p-value
Adelaide Airport	Intercept	38.457670	1.657185	23.206633	0.000000	30.284896	0.181074	167.251260	0.000000
	tSin	-17.892400	1.523315	-11.745696	0.000000	9.799139	0.165848	59.085040	0.000000
	tCos	-10.062800	1.521968	-6.611705	0.000000	0.522922	0.165711	3.155630	0.001700
	time	-0.004960	0.005967	-0.831187	0.406200	0.002868	0.000652	4.398940	0.000000
	time2	-0.000040	0.000036	-1.010458	0.312700	-0.000003	0.000004	-0.792420	0.428400
Broken Hill	Intercept	25.058752	2.102504	11.918526	0.000000	24.005572	0.481803	49.824470	0.000000
	tSin	-2.473537	1.925272	-1.284773	0.199400	-5.610438	0.240722	-23.306750	0.000000
	tCos	-2.625284	1.920818	-1.366753	0.172200	-1.657060	0.241156	-6.871310	0.000000
	time	0.001461	0.008034	0.181832	0.855800	0.000752	0.001826	0.411590	0.680800
	time2	-0.000085	0.000052	-1.650604	0.099300	-0.000003	0.000012	-0.227770	0.819900
Canberra Airport	Intercept	54.402420	2.285593	23.802323	0.000000	25.688548	0.166608	154.185870	0.000000
	tSin	3.572370	2.111757	1.691659	0.091100	8.405467	0.145868	57.623810	0.000000
	tCos	8.939470	2.110099	4.236515	0.000000	5.539470	0.145841	37.982880	0.000000
	time	-0.006010	0.006334	-0.948923	0.342900	0.001609	0.000461	3.486550	0.000500
	time2	-0.000050	0.000029	-1.730945	0.083800	0.000006	0.000002	2.939880	0.003400
Hume Dam	Intercept	59.270820	1.996223	29.691488	0.000000	21.066854	0.108179	194.740920	0.000000
	tSin	-14.576200	1.814612	-8.032680	0.000000	8.908788	0.091347	97.527080	0.000000
	tCos	9.142220	1.815325	5.036137	0.000000	-2.578214	0.091422	-28.201140	0.000000
	time	0.004490	0.003572	1.255494	0.209500	-0.000418	0.000193	-2.162030	0.030800
	time2	-0.000010	0.000011	-1.171461	0.241600	0.000004	0.000001	6.076450	0.000000
Lake Victoria	Intercept	23.447757	1.117780	20.977076	0.000000	23.376875	0.298639	78.278000	0.000000
	tSin	-3.455149	1.038663	-3.326535	0.000900	6.483546	0.174441	37.167520	0.000000
	tCos	3.040783	1.037915	2.929702	0.003500	0.050756	0.174699	0.290530	0.771500
	time	-0.000268	0.002518	-0.106482	0.915200	-0.000005	0.000670	-0.007880	0.993700
	time2	-0.000021	0.000010	-2.239828	0.025300	0.000002	0.000003	0.832250	0.405500

Locations	Co efficient	Rainfall				Temperature			
		Value	Std.Error	t-value	p-value	Value	Std.Error	t-value	p-value
Laxton Met station	Intercept	21.741483	0.923517	23.542059	0.000000	23.481932	0.085022	276.186910	0.000000
	tSin	4.123949	0.858566	4.803299	0.000000	-7.583594	0.076079	-99.680480	0.000000
	tCos	-3.722891	0.858759	-4.335201	0.000000	1.854930	0.076121	24.368040	0.000000
	time	-0.001477	0.001804	-0.818746	0.413100	-0.000183	0.000166	-1.103980	0.269800
	time2	0.000009	0.000006	1.514315	0.130200	0.000001	0.000001	2.616430	0.009000
Melbourne Airport	Intercept	45.668600	2.251632	20.282441	0.000000	27.987057	0.227250	123.155340	0.000000
	tSin	6.853890	2.097407	3.267795	0.001200	-0.043338	0.207157	-0.209200	0.834400
	tCos	-2.678430	2.091798	-1.280443	0.201000	-10.756897	0.206522	-52.086080	0.000000
	time	-0.027420	0.011376	-2.410161	0.016300	0.003783	0.001147	3.296920	0.001100
	time2	-0.000060	0.000096	-0.572045	0.567600	0.000006	0.000010	0.613880	0.539600
Mildura Airport	Intercept	23.624569	1.056615	22.358723	0.000000	23.615200	0.093215	253.341020	0.000000
	tSin	-2.497672	0.976319	-2.558252	0.010600	8.232563	0.081885	100.537600	0.000000
	tCos	3.481164	0.976571	3.564681	0.000400	-1.969894	0.081936	-24.041750	0.000000
	time	0.000335	0.001891	0.176976	0.859600	-0.000708	0.000167	-4.245560	0.000000
	time2	-0.000005	0.000006	-0.821868	0.411300	0.000003	0.000001	5.692090	0.000000
Murray Bridge	Intercept	30.455835	1.739458	17.508811	0.000000	22.747294	0.223137	101.943030	0.000000
	tSine	-9.659281	1.607955	-6.007182	0.000000	4.387076	0.169743	25.845470	0.000000
	tCos	-4.148769	1.601922	-2.589870	0.009900	3.897651	0.169123	23.046320	0.000000
	time	0.002831	0.008128	0.348272	0.727800	0.001935	0.001039	1.862420	0.063100
	time2	-0.000015	0.000064	-0.237506	0.812400	-0.000004	0.000008	-0.471160	0.637700
Sydney Observatory Hill	Intercept	103.819940	3.849772	26.967819	0.000000	29.404899	0.142935	205.722800	0.000000
	tSin	-2.910290	3.611251	-0.805894	0.420500	6.658334	0.131885	50.485990	0.000000
	tCos	26.564000	3.614352	7.349588	0.000000	1.416722	0.132015	10.731520	0.000000
	time	0.009800	0.006823	1.436463	0.151100	0.000568	0.000253	2.243360	0.025000
	time2	-0.000030	0.000020	-1.318689	0.187500	0.000000	0.000001	-0.479150	0.631900

Appendix 7. 2: Exponential smoothing of rainfall series (upper row) and temperature series (bottom row) without trend and without seasonal component series observed over MDB areas and eastern Australia using the Holt-Winters approach.

i. Adelaide Airport and Broken Hill rainfall and temperature series

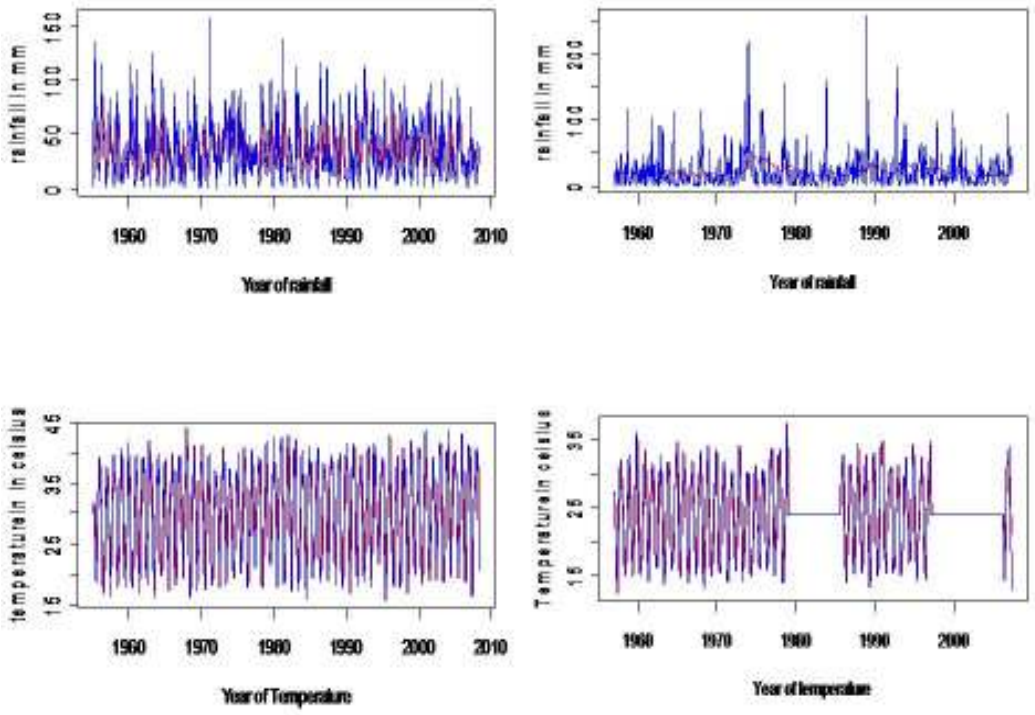

ii. Canberra Airport and Lake Victoria rainfall and temperature series

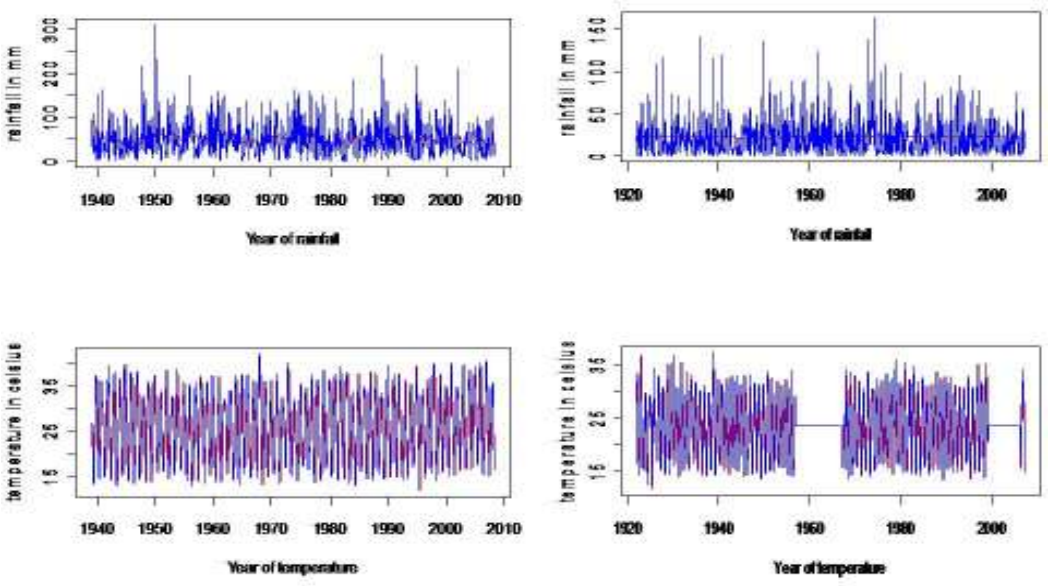

iii. Loxton met and Melbourne Airport rainfall and temperature series

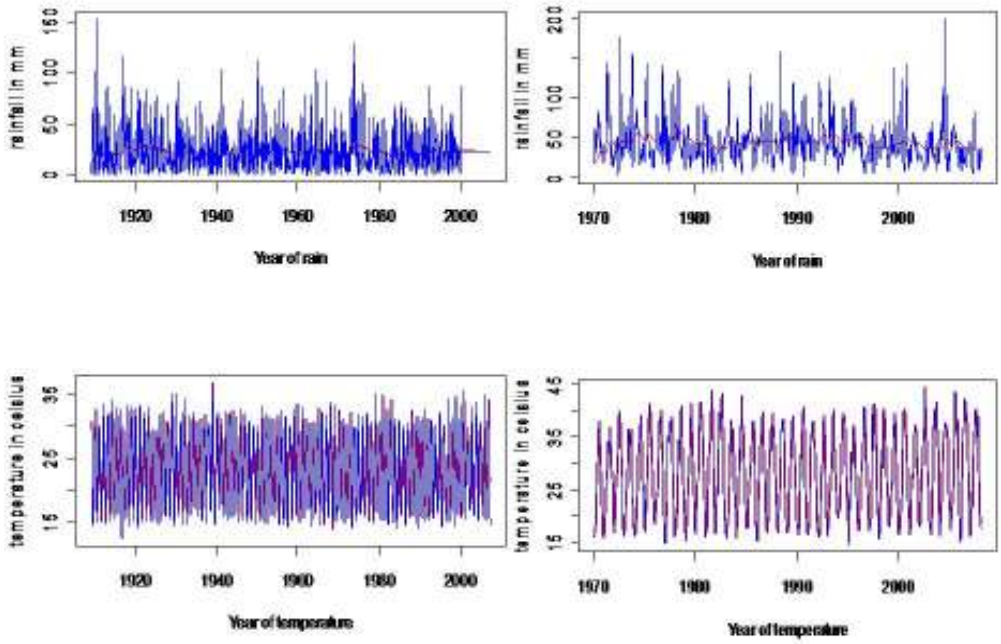

iv. Murray Bridge and Sydney Observatory Hill rainfall and temperature series

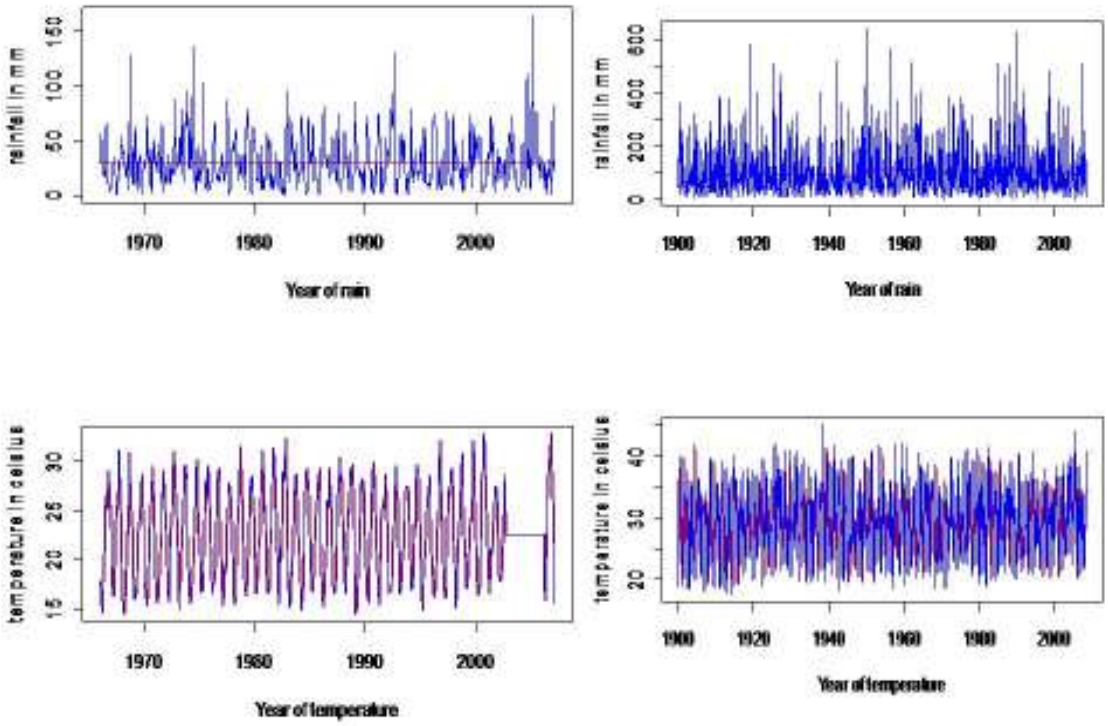

Appendix 7. 3: correlation between the rainfall and temperature pattern with seasonal indicators over the MDB areas and the eastern seaboard in Australia

i. Correlation pattern for Adelaide Airport

	Rainfall	Temp	PDO	SOI	Int	Jan	Feb	Mar	Apr	May	June	July	Aug	Sep	Oct	Nov	Dec
Rainfall	1																
Temp	-.420***	1															
PDO	.015	.007	1														
SOI	.127**	-.018	-.393***	1													
Int	-.075	-.022	-.052	.013	1												
Jan	-.205***	.299***	-.020	.017	.024	1											
Feb	-.201***	.371***	.004	.010	-.047	-.090*	1										
Mar	-.177***	.325***	.034	-.012	-.048	-.091*	-.091*	1									
Apr	-.026	.228***	.044	-.039	-.048	-.091*	-.091*	-.092*	1								
May	.132**	.026	.063	-.006	.046	-.091*	-.091*	-.092*	-.092*	1							
June	.201***	-.222***	.022	-.019	.027	-.091*	-.091*	-.092*	-.092*	-.092*	1						
July	.240***	-.396***	.041	-.009	.031	-.091*	-.091*	-.092*	-.092*	-.092*	-.092*	1					
Aug	.130***	-.456***	.019	-.012	-.015	-.090*	-.090*	-.091*	-.091*	-.091*	-.091*	-.091*	1				
Sep	.099*	-.322***	-.015	.016	.002	-.090*	-.090*	-.091*	-.091*	-.091*	-.091*	-.091*	-.090*	1			
Oct	.020	-.129***	-.051	.005	-.020	-.090*	-.090*	-.091*	-.091*	-.091*	-.091*	-.091*	-.090*	-.090*	1		
Nov	-.124***	.061	-.035*	.033	.018	-.090*	-.090*	-.091*	-.091*	-.091*	-.091*	-.091*	-.090*	-.090*	-.090*	1	
Dec	-.141***	.216***	-.059	.016	.031	-.090*	-.090*	-.091*	-.091*	-.091*	-.091*	-.091*	-.090*	-.090*	-.090*	-.090*	1

*coefficients are statistically significant at the 5% level
**coefficients are statistically significant at the 1% level
*** coefficients are statistically significant at the 0.1% level

ii. Correlation pattern for Broken hill

	Rainfall	temp	PDO	SOI	Int	Jan	Feb	Mar	Apr	May	June	July	Aug	Sep	Oct	Nov	Dec
Rainfall	1																
temp	-.009	1															
PDO	-.067	-.103*	1														
SOI	.235**	-.031	-.341**	1													
Int	-.096*	-.001	-.210**	.121**	1												
Jan	.119**	.397**	-.019	.016	.028	1											
Feb	-.025	.379**	.002	.008	-.055	-.090*	1										
Mar	-.024	.222**	.036	-.011	-.061	-.091*	-.091*	1									
Apr	-.035	-.008	.055	-.033	-.067	-.091*	-.091*	-.092*	1								
May	.024	-.242**	.066	-.005	.043	-.091*	-.091*	-.092*	-.092*	1							
June	-.071	-.394**	.029	-.023	.039	-.091*	-.091*	-.092*	-.092*	-.092*	1						
July	-.018	-.424**	.044	-.011	.040	-.090*	-.090*	-.091*	-.091*	-.091*	-.091*	1					
Aug	-.035	-.332**	.011	-.013	-.020	-.090*	-.090*	-.091*	-.091*	-.091*	-.091*	-.090*	1				
Sep	.008	-.163**	-.027	.024	-.009	-.090*	-.090*	-.091*	-.091*	-.091*	-.091*	-.090*	-.090*	1			
Oct	.051	.025	-.047	-.001	.000	-.090*	-.090*	-.091*	-.091*	-.091*	-.091*	-.090*	-.090*	-.090*	1		
Nov	-.017	.193**	-.086*	.036	.026	-.090*	-.090*	-.091*	-.091*	-.091*	-.091*	-.090*	-.090*	-.090*	-.090*	1	
Dec	.023	.319**	-.066	.014	.033	-.090*	-.090*	-.091*	-.091*	-.091*	-.091*	-.090*	-.090*	-.090*	-.090*	-.090*	1

*coefficients are statistically significant at the 5% level
**coefficients are statistically significant at the 1% level
*** coefficients are statistically significant at the 0.1% level

iii. Correlation pattern for Canberra Airport

	Rainfall	Temp	PDO	SOI	Int	Jan	Feb	Mar	Apr	May	June	July	Aug	Sep	Oct	Nov	Dec
Rainfall	1																
Temp	.044	1															
PDO	-.103***	-.056	1														
SOI	.247***	-.035	-.399***	1													
Int	-.060	.020	-.107***	.026	1												
Jan	.060	.403***	-.034	.012	.027	1											
Feb	.036	.329***	-.016	.024	-.050	-.090***	1										
Mar	-.005	.212***	.028	.009	-.030	-.091***	-.091***	1									
Apr	-.041	-.004	.046	-.030	-.027	-.091***	-.091***	-.092***	1								
May	-.052	-.219***	.068	-.025	.031	-.091***	-.091***	-.092***	-.092***	1							
June	-.081*	-.398***	.044	-.016	.002	-.091***	-.091***	-.092***	-.092***	-.092***	1						
July	-.077*	-.434***	.041	-.006	.001	-.091***	-.091***	-.092***	-.092***	-.092***	-.092***	1					
Aug	-.037	-.317***	.014	-.010	-.014	-.090***	-.090***	-.091***	-.091***	-.091***	-.091***	-.091***	1				
Sep	.007	-.141***	-.025	.005	.023	-.090***	-.090***	-.091***	-.091***	-.091***	-.091***	-.091***	-.090***	1			
Oct	.086*	.035	-.044	-.003	-.007	-.090***	-.090***	-.091***	-.091***	-.091***	-.091***	-.091***	-.090***	-.090***	1		
Nov	.098***	.208***	-.085*	.025	.033	-.090***	-.090***	-.091***	-.091***	-.091***	-.091***	-.091***	-.090***	-.090***	-.090***	1	
Dec	.008	.333***	-.040	.014	.013	-.090***	-.090***	-.091***	-.091***	-.091***	-.091***	-.091***	-.090***	-.090***	-.090***	-.090***	1

*coefficients are statistically significant at the 5% level
**coefficients are statistically significant at the 1% level
*** coefficients are statistically significant at the 0.1% level

iv. Correlation pattern for Lake Victoria

	rainfall	temp	PDO	SOI	Int	Jan	Feb	Mar	Apr	May	June	July	Aug	Sep	Oct	Nov	Dec
rainfall	1																
temp	-.174***	1															
PDO	-.066*	-.047	1														
SOI	.194***	.013	-.332***	1													
Int	-.081***	.023	-.065*	.102***	1												
Jan	-.034	.395***	-.013	.020	.039	1											
Feb	-.040	.400***	-.014	.018	-.049	-.091***	1										
Mar	-.112***	.242***	.025	.021	-.015	-.091***	-.092***	1									
Apr	-.045	-.010	.057	-.014	-.003	-.091***	-.092***	-.092***	1								
May	.029	-.231***	.071*	-.020	.021	-.091***	-.092***	-.092***	-.092***	1							
June	.020	-.396***	.045	-.011	.002	-.091***	-.092***	-.092***	-.092***	-.092***	1						
July	.051	-.419***	.024	-.008	-.002	-.090***	-.091***	-.091***	-.091***	-.091***	-.091***	1					
Aug	.033	-.321***	-.018	-.034	-.039	-.090***	-.091***	-.091***	-.091***	-.091***	-.091***	-.090***	1				
Sep	.042	-.165***	-.048	-.004	.011	-.090***	-.091***	-.091***	-.091***	-.091***	-.091***	-.090***	-.090***	1			
Oct	.085***	.005	-.045	-.005	-.009	-.090***	-.091***	-.091***	-.091***	-.091***	-.091***	-.090***	-.090***	-.090***	1		
Nov	.007	.185***	-.068*	.012	.026	-.090***	-.091***	-.091***	-.091***	-.091***	-.091***	-.090***	-.090***	-.090***	-.090***	1	
Dec	-.036	.321***	-.019	.024	.018	-.090***	-.091***	-.091***	-.091***	-.091***	-.091***	-.090***	-.090***	-.090***	-.090***	-.090***	1

*coefficients are statistically significant at the 5% level
**coefficients are statistically significant at the 1% level
*** coefficients are statistically significant at the 0.1% level

v. Correlation pattern for Loxton met

	Rainfall	Temp	PDO	SOI	Int	Jan	Feb	Mar	Apr	May	June	July	Aug	Sep	Oct	Nov	Dec
Rainfall	1																
Temp	-.248**	1															
PDO	-.038	-.031	1														
SOI	.190**	.013	-.312**														
Int	-.107**	.027	-.057*	.068*	1												
Jan	-.079**	.409**	-.029	.012	.044	1											
Feb	-.018	.388**	-.010	.013	-.052	-.091**	1										
Mar	-.115**	.227**	.013	.014	-.001	-.091**	-.091**	1									
Apr	-.089**	-.013	.050	-.027	-.008	-.091**	-.091**	-.091**	1								
May	.056	-.231**	.069*	-.024	.026	-.091**	-.091**	-.091**	-.091**	1							
June	.056	-.398**	.045	.004	.000	-.091**	-.091**	-.091**	-.091**	-.091**	1						
July	.062*	-.418**	.030	.006	-.004	-.091**	-.091**	-.091**	-.091**	-.091**	-.091**	1					
Aug	.079**	-.321**	-.022	-.027	-.041	-.091**	-.091**	-.091**	-.091**	-.091**	-.091**	-.090**	1				
Sep	.072*	-.156**	-.047	-.002	.009	-.091**	-.091**	-.091**	-.091**	-.091**	-.091**	-.090**	-.090**	1			
Oct	.077*	.006	-.045	-.011	-.014	-.091**	-.091**	-.091**	-.091**	-.091**	-.091**	-.090**	-.090**	-.090**	1		
Nov	-.031	.186**	-.054	.010	.031	-.091**	-.091**	-.091**	-.091**	-.091**	-.091**	-.090**	-.090**	-.090**	-.090**	1	
Dec	-.068*	.321**	.000	.032	.010	-.091**	-.091**	-.091**	-.091**	-.091**	-.091**	-.090**	-.090**	-.090**	-.090**	-.090**	1

*coefficients are statistically significant at the 5% level
**coefficients are statistically significant at the 1% level
*** coefficients are statistically significant at the 0.1% level

vi. Correlation pattern for Melbourne Airport

	Rainfall	temp	PDO	SOI	Int	Jan	Feb	Mar	Apr	May	June	July	Aug	Sep	Oct	Nov	Dec
Rainfall	1																
temp	-.028	1															
PDO	-.061	-.063	1														
SOI	.128**	.004	-.385**	1													
Int	-.006	-.056	-.203**	.179**	1												
Jan	-.021	.391**	-.033	.040	.035	1											
Feb	-.014	.365**	-.007	.021	-.073	-.091	1										
Mar	-.088	.242**	.059	-.016	-.080	-.091	-.091	1									
Apr	.001	.006	.055	-.051	-.083	-.091	-.091	-.091	1								
May	-.038	-.200**	.085	-.023	.072	-.091	-.091	-.091	-.091	1							
June	-.067	-.386**	.007	-.039	.044	-.091	-.091	-.091	-.091	-.091	1						
July	-.086	-.425**	.052	-.015	.037	-.092*	-.092*	-.092*	-.092*	-.092*	-.092*	1					
Aug	.014	-.321**	.032	-.031	-.014	-.091	-.091	-.091	-.091	-.091	-.091	-.092*	1				
Sep	.021	-.178**	-.025	.033	.018	-.091	-.091	-.091	-.091	-.091	-.091	-.092*	-.091	1			
Oct	.104*	.025	-.065	.010	-.003	-.091	-.091	-.091	-.091	-.091	-.091	-.092*	-.091	-.091	1		
Nov	.147**	.182**	-.092	.055	.003	-.091	-.091	-.091	-.091	-.091	-.091	-.092*	-.091	-.091	-.091	1	
Dec	.028	.303**	-.066	.017	.043	-.091	-.091	-.091	-.091	-.091	-.091	-.092*	-.091	-.091	-.091	-.091	1

*coefficients are statistically significant at the 5% level
**coefficients are statistically significant at the 1% level
*** coefficients are statistically significant at the 0.1% level

vii. Correlation pattern for Mildura Airport

	Rainfall	temp	PDO	SOI	Int	Jan	Feb	Mar	Apr	May	June	July	Aug	Sep	Oct	Nov	Dec
Rainfall	1																
temp	-.176**	1															
PDO	-.076**	-.009	1														
SOI	.193**	-.006	-.301**	1													
Int	-.079**	.020	-.065*	.114**	1												
Jan	-.036	.404**	-.018	.011	.042	1											
Feb	-.035	.384**	-.005	.009	-.053	-.091**	1										
Mar	-.068*	.224**	.013	.010	-.010	-.091**	-.091**	1									
Apr	-.080**	-.017	.051	-.019	-.022	-.091**	-.091**	-.091**	1								
May	.039	-.231**	.064*	-.023	.031	-.091**	-.091**	-.091**	-.091**	1							
June	.031	-.393**	.042	.008	.007	-.091**	-.091**	-.091**	-.091**	-.091**	1						
July	.024	-.419**	.028	.009	.001	-.091**	-.091**	-.091**	-.091**	-.091**	-.091**	1					
Aug	.047	-.319**	-.029	-.018	-.043	-.091**	-.091**	-.091**	-.091**	-.091**	-.091**	-.090**	1				
Sep	.047	-.163**	-.054	-.004	.011	-.091**	-.091**	-.091**	-.091**	-.091**	-.091**	-.090**	-.090**	1			
Oct	.073**	.009	-.044	-.016	-.011	-.091**	-.091**	-.091**	-.091**	-.091**	-.091**	-.090**	-.090**	-.090**	1		
Nov	-.015	.193**	-.045	.003	.033	-.091**	-.091**	-.091**	-.091**	-.091**	-.091**	-.090**	-.090**	-.090**	-.090**	1	
Dec	-.026	.325**	-.005	.031	.014	-.091**	-.091**	-.091**	-.091**	-.091**	-.091**	-.090**	-.090**	-.090**	-.090**	-.090**	1

*coefficients are statistically significant at the 5% level
**coefficients are statistically significant at the 1% level
*** coefficients are statistically significant at the 0.1% level

viii. Correlation pattern for Murray Bridge

	rainfall	temp	PDO	SOI	Int	Jan	Feb	Mar	Apr	May	June	July	Aug	Sep	Oct	Nov	Dec
rainfall	1																
temp	-.370**	1															
PDO	.021	-.080	1														
SOI	.104*	.013	-.363**	1													
Int	-.026	-.058	-.228**	.179**	1												
Jan	-.153**	.385**	-.034	.031	.041	1											
Feb	-.133**	.419**	-.006	.015	-.065	-.091*	1										
Mar	-.121**	.237**	.059	-.012	-.079	-.091*	-.091*	1									
Apr	-.027	.043	.052	-.060	-.074	-.091*	-.091*	-.091*	1								
May	.027	-.198**	.070	-.014	.064	-.092*	-.092*	-.092*	-.092*	1							
June	.110*	-.385**	.015	-.014	.037	-.092*	-.092*	-.092*	-.092*	-.093*	1						
July	.061	-.413**	.061	-.007	.034	-.091*	-.091*	-.091*	-.091*	-.092*	-.092*	1					
Aug	.121**	-.335**	.014	-.022	-.021	-.091*	-.091*	-.091*	-.091*	-.092*	-.092*	-.091*	1				
Sep	.099*	-.188**	-.030	.029	.016	-.091*	-.091*	-.091*	-.091*	-.092*	-.092*	-.091*	-.091*	1			
Oct	.092*	-.006	-.055	.000	-.007	-.091*	-.091*	-.091*	-.091*	-.092*	-.092*	-.091*	-.091*	-.091*	1		
Nov	-.039	.166**	-.087	.046	.007	-.091*	-.091*	-.091*	-.091*	-.092*	-.092*	-.091*	-.091*	-.091*	-.091*	1	
Dec	-.058	.291**	-.060	.009	.046	-.091*	-.091*	-.091*	-.091*	-.092*	-.092*	-.091*	-.091*	-.091*	-.091*	-.091*	1

*coefficients are statistically significant at the 5% level
**coefficients are statistically significant at the 1% level
*** coefficients are statistically significant at the 0.1% level

ix. Correlation pattern for Sydney Observatory hill

	Rainfall	temp	PDO	SOI	Int	Jan	Feb	Mar	Apr	May	June	July	Aug	Sep	Oct	Nov	Dec
Rainfall	1																
temp	.008	1															
PDO	-.060*	.087**	1														
SOI	.085**	-.087**	-.304**	1													
Int	-.059*	-.016	-.061*	.108**	1												
Jan	.020	-.413**	-.018	.013	.040	1											
Feb	.039	-.276**	-.004	.013	-.055*	-.091**	1										
Mar	.097**	-.059*	.014	.011	-.011	-.091**	-.091**	1									
Apr	.070*	.142**	.048	-.020	-.022	-.091**	-.091**	-.091**	1								
May	.054	.224**	.062*	-.025	.034	-.091**	-.091**	-.091**	-.091**	1							
June	.080**	.306**	.041	.007	.006	-.091**	-.091**	-.091**	-.091**	-.091**	1						
July	-.020	.315**	.028	.006	.002	-.091**	-.091**	-.091**	-.091**	-.091**	-.091**	1					
Aug	-.056*	.237**	-.025	-.019	-.041	-.091**	-.091**	-.091**	-.091**	-.091**	-.091**	-.091**	1				
Sep	-.110**	.157**	-.052	-.005	.012	-.091**	-.091**	-.091**	-.091**	-.091**	-.091**	-.091**	-.090**	1			
Oct	-.071*	-.014	-.045	-.017	-.012	-.091**	-.091**	-.091**	-.091**	-.091**	-.091**	-.091**	-.090**	-.090**	1		
Nov	-.048	-.217**	-.045	.003	.032	-.091**	-.091**	-.091**	-.091**	-.091**	-.091**	-.091**	-.090**	-.090**	-.090**	1	
Dec	-.055*	-.405**	-.004	.032	.014	-.091**	-.091**	-.091**	-.091**	-.091**	-.091**	-.091**	-.090**	-.090**	-.090**	-.090**	1

*coefficients are statistically significant at the 5% level
**coefficients are statistically significant at the 1% level
***coefficients are statistically significant at the 0.1% level

Appendix 7. 4: RM Coefficients for a) rainfall series, b) temperature Series in the MDB areas and four eastern Australian capital cities

Rainfall Model	Co-efficient	Broken Hill	Hum Dume	Lake Victoria	Leeton Met	Mildura Airport	Murray Bridge	Adelaide Airport	Canberra Airport	Melbourne Airport	Sydney Obs. hill
Constant	β_0	24.27***	46.92***	18.15***	16.96***	20.05***	25.67***	23.49***	51.92***	47.48***	81.19***
PDO	β_1	-0.13	1.43	0.06	0.37	-0.35	1.24	0.86	0.46	0.33	-5.8*
SOI	β_2	70***	1.03***	47***	42***	45***	32**	42***	97***	34*	640*
Jan	β_4	9.28	-3.74	0.35	-0.03	-0.26	-7.88	-6.17**	6.96*	-5.15	23.5
Feb	β_5	-5.6	-9.21	-0.7	3.31	-0.88	-6.66	-6.45	2.66	-4.63	27.64*
Mar	β_6	-5.11	-2.27	-5.71	-2.85	-2.95	-5.81	-3.85	-2.06	-11.53	46.67***
April	β_7	-5.73	1.81	-0.25	-0.7	-3.49	2.21	10.52*	-5.59	-2.34	39.45**
May	β_8	0.73	13.69**	5.42	9.24**	5.90*	6.47**	30.17***	-6.63	-6.1	36.25**
June	β_9	-8.1	24.37***	4.48	8.67**	4.66	13.07*	32.06***	-11	-8.84	42.29***
July	β_{10}	-3.18	28.84***	6.68*	9.05**	4.03	10.57**	35.48***	-10.77	-10.95	11.79
Aug	β_{11}	-5.63	27.54***	5.51	10.36***	5.79	13.87*	25.13***	-5.52	-1.02	-0.6
Sept	β_{12}	-2.19	15.98**	6.08	10.22***	5.90	11.93*	22.07***	0.16	-1	-16.87
Oct	β_{13}	2.7	21.68***	9.12**	10.56***	7.91**	11.66	14.76**	10.61	7.51	-4.93
Nov	β_{14}	-4.439	1.953	3.37	3.36	1.38	1.04	1.38	11.62	11.36	2.45
PDO*SOI	β_3	-.348***	-0.188*	-.19***	-.21***	-.21***	-0.11	-.24**	-0.22	-0.07	-.57*

Temperature Model	Co-efficient	Broken Hill	Hum Dume	Lake Victoria	Leeton Met	Mildura Airport	Murray Bridge	Adelaide Airport	Canberra Airport	Melbourne Airport	Sydney Obs. Hill
Constant	β_0	30.48***	28.81***	30.24***	29.79***	30.77***	27.30***	35.57***	34.41***	36.20***	21.72***
PDO	β_1	-0.07	0.06	0.01	0.09*	0.15**	-0.07	0.12	0.05	-0.02	0.16
SOI	β_2	-.03**	-.02***	-.01*	-0.01*	-0.02**	-0.01	-0.01	-.05***	-.04***	-.03**
Jan	β_4	1.60*	2.01***	1.49**	1.63***	1.58***	1.50**	2.05*	1.76***	2.41***	-.12
Feb	β_5	1.28*	1.69***	1.35**	1.26***	1.2***	2.06***	3.83*	-.02	1.73**	2.45***
Mar	β_6	-1.95*	-1.85***	-1.78**	-1.81***	-2.11***	-.85	2.59*	-3.05***	-1.62**	6.54***
April	β_7	-6.68***	-7.24***	-6.88***	-6.39***	-7.16***	-3.97***	0.19	-8.47***	-8.02***	10.26***
May	β_8	-11.62***	-12.19***	-11.29***	-10.54***	-11.55***	-7.76***	-4.76*	-13.85***	-13.56***	11.80***
June	β_9	-14.73***	-15.81***	-14.69***	-13.68***	-14.85***	-10.70	-10.82*	-18.24***	-18.59***	13.39***
July	β_{10}	-15.37***	-16.72***	-15.09***	-14.08***	-15.41***	-11.14	-15.08*	-19.12***	-19.43***	13.57***
Aug	β_{11}	-13.45***	-14.58***	-13.19***	-12.23***	-13.32***	-9.91	-16.65*	-16.26***	-16.81***	12.12***
Sept	β_{12}	-9.89***	-11.34***	-10.04***	-9.08***	-10.09***	-7.60	-13.31*	-11.86***	-12.88***	10.64***
Oct	β_{13}	-6.02***	-7.55***	-6.56***	-5.98***	-6.53***	-4.75	-8.52*	-7.51***	-7.45***	7.38***
Nov	β_{14}	-2.53**	-3.34***	-2.95***	-2.56***	-2.72	-2.02***	-3.81*	-3.11***	-3.17***	3.56***
PDO*SOI	β_3	.011*	0.005	.01*	0.01	0.01*	.00*	0.01	.02**	0.01	0.002

*coefficients are statistically significant at the 5% level
**coefficients are statistically significant at the 1% level
***coefficients are statistically significant at the 0.1% level

Appendix 7. 5: Realisation of rainfall RM with GLS of AR [1] process

i. Rainfall variation over the 10 weather stations

Rainfall Model Std	Co-efficient	Broken Hill	Hum Dame	Lake Victoria	Loxton Met	Mildura Airport	Murray Bridge	Adelaide Airport	Canberra Airport	Melbourne Airport	Sydney Obs. Hill
Constant	β_0	4.00317	3.71074	2.309714	1.911382	2.123237	3.537889	3.260624	4.536821	4.796994	8.610301
PDO	β_1	1.310468	1.214872	0.693964	0.58478	0.670387	1.161646	1.012508	1.373115	1.512024	2.592118
SOI	β_2	0.12595	0.117144	0.074813	0.059477	0.065265	0.109175	0.103091	0.145755	0.142998	0.255101
PDO*SOI	β_3	0.110611	0.102269	0.059296	0.050439	0.057089	0.094133	0.083482	0.111654	0.12193	0.223848
Jan	β_4	5.320495	4.781824	3.125101	2.595773	2.843361	4.715865	4.330822	6.194226	6.512749	11.99355
Feb	β_5	5.617237	5.155965	3.240712	2.683094	2.976192	4.980203	4.567934	6.430364	6.771927	12.12038
Mar	β_6	5.629189	5.208175	3.249051	2.686279	2.985431	5.02085	4.576102	6.427622	6.806715	12.11166
April	β_7	5.638969	5.223401	3.252553	2.689566	2.989744	5.018986	4.581415	6.432425	6.806439	12.12302
May	β_8	5.638225	5.227048	3.254439	2.690811	2.990945	4.986855	4.581555	6.439211	6.809807	12.12778
June	β_9	5.62319	5.221002	3.251115	2.687916	2.987675	4.967734	4.569762	6.430067	6.77358	12.11477
July	β_{10}	5.656074	5.23116	3.258793	2.694038	2.993789	5.010751	4.574396	6.429385	6.74417	12.11262
Aug	β_{11}	5.646797	5.237539	3.261988	2.69826	2.997934	5.000453	4.591854	6.446612	6.780945	12.15585
Sept	β_{12}	5.637258	5.225904	3.258044	2.69604	2.995452	4.990156	4.583453	6.440366	6.766224	12.15184
Oct	β_{13}	5.60336	5.169109	3.24888	2.691118	2.983849	4.964374	4.559252	6.424164	6.747036	12.15233
Nov	β_{14}	5.317498	4.794314	3.127474	2.60339	2.851072	4.719112	4.329707	6.197717	6.515397	12.02771

ii. Statistical evidence of rainfall impact

Rainfall Model P-values	Co-efficient	Broken Hill	Hum Dame	Lake Victoria	Loxton Met	Mildura Airport	Murray Bridge	Adelaide Airport	Canberra Airport	Melbourne Airport	Sydney Obs. Hill
Constant	β_0	0.000	0.000	0.000	0.000	0.000	0.000	0.000	0.000	0.000	0.000
PDO	β_1	0.329	0.289	0.922	0.435	0.583	0.320	0.480	0.778	0.898	0.029
SOI	β_2	0.000	0.000	0.000	0.000	0.000	0.005	0.000	0.000	0.029	0.011
PDO*SOI	β_3	0.004	0.144	0.002	0.000	0.001	0.267	0.006	0.067	0.621	0.013
Jan	β_4	0.081	0.425	0.912	0.972	0.924	0.096	0.156	0.262	0.484	0.050
Feb	β_5	0.331	0.079	0.835	0.280	0.776	0.185	0.159	0.670	0.500	0.023
Mar	β_6	0.378	0.065	0.030	0.308	0.325	0.253	0.406	0.753	0.092	0.000
April	β_7	0.321	0.722	0.945	0.805	0.247	0.653	0.022	0.388	0.733	0.001
May	β_8	0.491	0.009	0.095	0.001	0.049	0.193	0.000	0.304	0.373	0.003
June	β_9	0.151	0.000	0.167	0.003	0.119	0.009	0.000	0.038	0.190	0.001
July	β_{10}	0.576	0.000	0.041	0.002	0.180	0.035	0.000	0.095	0.106	0.330
Aug	β_{11}	0.326	0.000	0.090	0.000	0.052	0.006	0.000	0.394	0.882	0.965
Sept	β_{12}	0.708	0.002	0.002	0.001	0.049	0.017	0.000	0.981	0.888	0.167
Oct	β_{13}	0.026	0.000	0.005	0.000	0.008	0.019	0.001	0.099	0.296	0.689
Nov	β_{14}	0.406	0.695	0.280	0.259	0.631	0.823	0.750	0.062	0.081	0.837

Appendix 7. 6: Realisation of temperature RM with GLS of AR [1] process

i. Temperature variations over the 10 weather stations

Temperature Model std	Co-effiment	Broken Hill	Hum Dame	Lake Victoria	Loxton Met	Mildura Airport	Murray Bridge	Adelaide Airport	Canberra Airport	Melbourne Airport	Sydney Obs Hill
Constant	β_0	0.449488	0.167536	0.307474	0.146092	0.158308	0.294686	0.344045	0.277041	0.428767	0.280723
PDO	β_1	0.152715	0.0589	0.097666	0.048349	0.054795	0.115657	0.109311	0.092242	0.144006	0.087726
SOI	β_2	0.011444	0.005434	0.008603	0.004804	0.00515	0.009336	0.011024	0.009264	0.013347	0.008574
PDO*SOI	β_3	0.010043	0.004695	0.007058	0.004079	0.00447	0.00809	0.008954	0.007203	0.011389	0.007513
Jan	β_4	0.330647	0.184489	0.247544	0.184089	0.185981	0.239771	0.447562	0.330712	0.552005	0.379007
Feb	β_5	0.431781	0.217417	0.318827	0.202004	0.212399	0.358214	0.479693	0.374	0.598601	0.393961
Mar	β_6	0.448792	0.228633	0.356938	0.205246	0.219518	0.389563	0.482405	0.383988	0.60749	0.394715
April	β_7	0.522428	0.233236	0.379162	0.20621	0.221993	0.402593	0.483323	0.387236	0.608495	0.395204
May	β_8	0.539817	0.234994	0.39071	0.206469	0.222752	0.407155	0.483405	0.38854	0.609092	0.395384
June	β_9	0.543216	0.23498	0.393527	0.206226	0.222583	0.406547	0.482108	0.387993	0.605318	0.394923
July	β_{10}	0.539649	0.234965	0.390291	0.206642	0.222838	0.408207	0.482613	0.387767	0.602964	0.394846
Aug	β_{11}	0.52106	0.233792	0.379443	0.206365	0.222559	0.400946	0.484345	0.387797	0.605837	0.395267
Sept	β_{12}	0.486998	0.229412	0.357456	0.206015	0.220273	0.38808	0.483104	0.384539	0.603386	0.394048
Oct	β_{13}	0.430128	0.217929	0.319035	0.202603	0.212917	0.356469	0.478754	0.373614	0.596105	0.395001
Nov	β_{14}	0.330091	0.184905	0.248122	0.184588	0.180425	0.29031	0.447439	0.331026	0.552296	0.380059

ii. Statistical evidence of temperature impact

Temperature model P-values	Co-effiment	Broken Hill	Hum Dame	Lake Victoria	Loxton Met	Mildura Airport	Murray Bridge	Adelaide Airport	Canberra Airport	Melbourne Airport	Sydney Obs Hill
Constant	β_0	0.000	0.000	0.000	0.000	0.000	0.000	0.000	0.000	0.000	0.000
PDO	β_1	0.874	0.211	0.635	0.149	0.033	0.909	0.369	0.512	0.899	0.091
SOI	β_2	0.218	0.011	0.026	0.050	0.008	0.236	0.203	0.000	0.004	0.003
PDO*SOI	β_3	0.349	0.720	0.909	0.218	0.404	0.855	0.480	0.016	0.333	0.857
Jan	β_4	0.001	0.000	0.000	0.000	0.000	0.000	0.000	0.000	0.000	0.755
Feb	β_5	0.038	0.000	0.000	0.000	0.000	0.000	0.000	0.920	0.004	0.000
Mar	β_6	0.004	0.000	0.001	0.000	0.000	0.045	0.000	0.000	0.008	0.000
April	β_7	0.000	0.000	0.000	0.000	0.000	0.000	0.695	0.000	0.000	0.000
May	β_8	0.000	0.000	0.000	0.000	0.000	0.000	0.000	0.000	0.000	0.000
June	β_9	0.000	0.000	0.000	0.000	0.000	0.000	0.000	0.000	0.000	0.000
July	β_{10}	0.000	0.000	0.000	0.000	0.000	0.000	0.000	0.000	0.000	0.000
Aug	β_{11}	0.000	0.000	0.000	0.000	0.000	0.000	0.000	0.000	0.000	0.000
Sept	β_{12}	0.000	0.000	0.000	0.000	0.000	0.000	0.000	0.000	0.000	0.000
Oct	β_{13}	0.000	0.000	0.000	0.000	0.000	0.000	0.000	0.000	0.000	0.000
Nov	β_{14}	0.000	0.000	0.000	0.000	0.000	0.000	0.000	0.000	0.000	0.000

Appendix 7. 7: Rainfall and temperature RSs versus fitted value and q-q plot of rainfall and temperature RSs over MDB areas and the eastern seaboard of Australia.

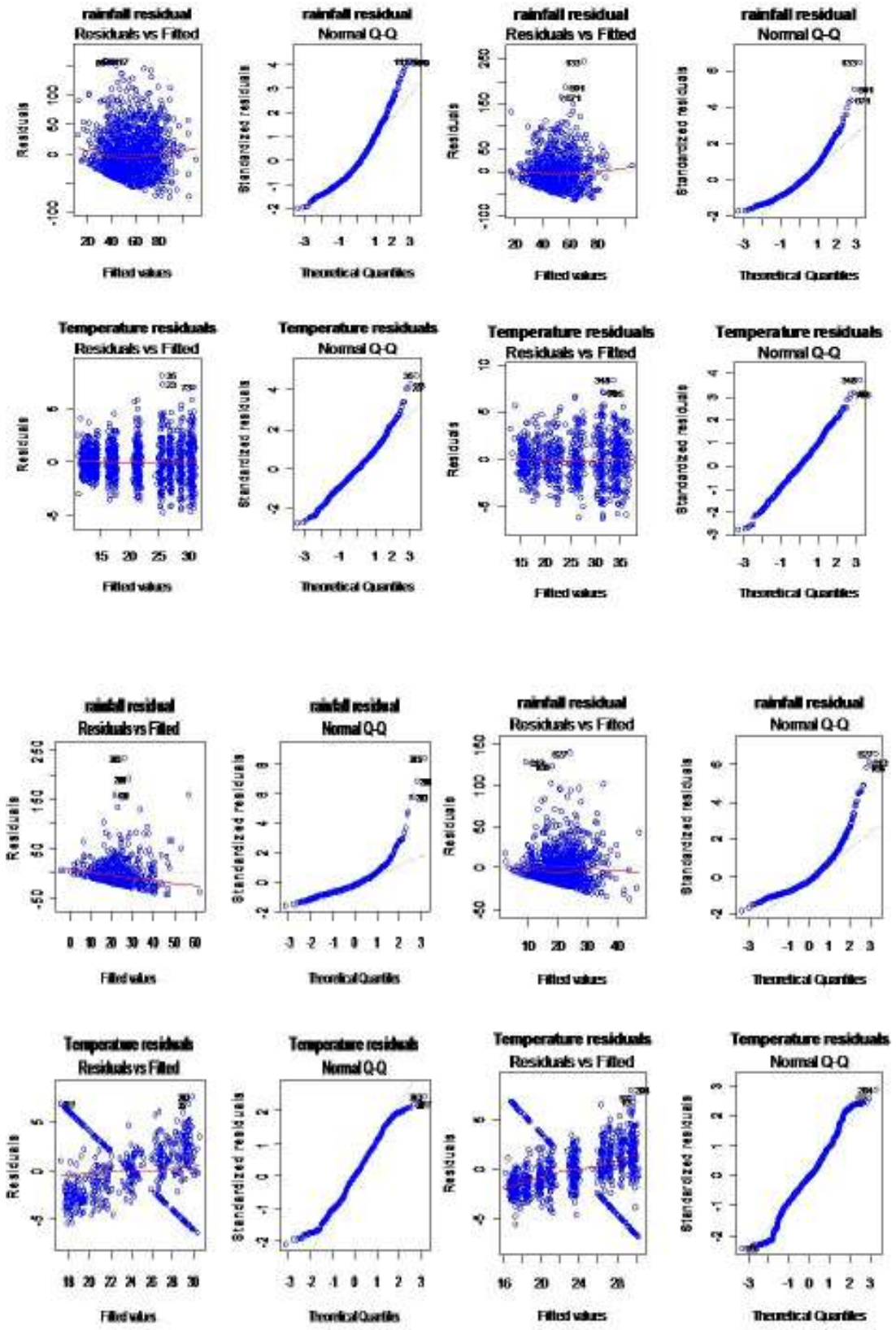

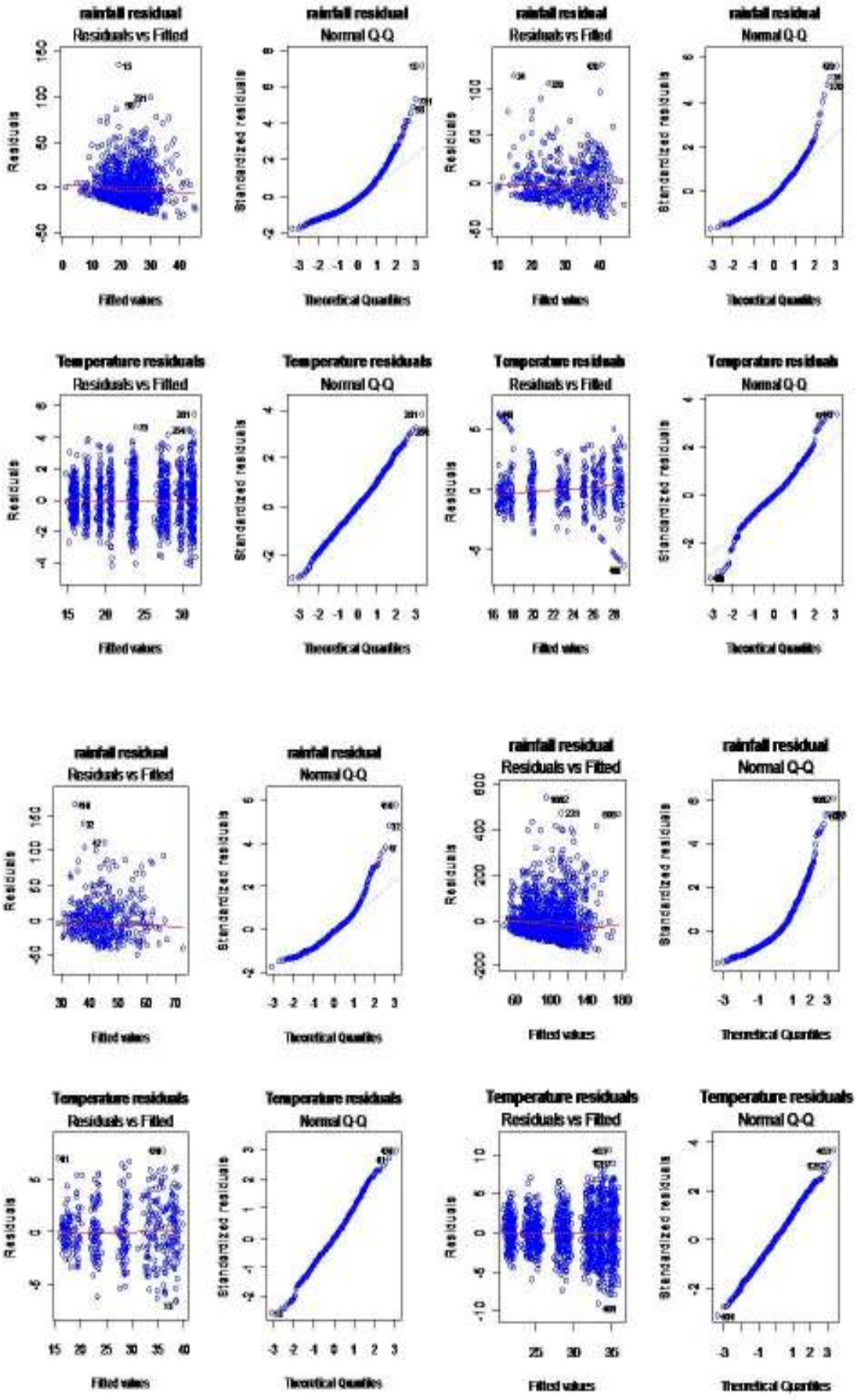
rainfall residual
Residuals vs Fitted
Residuals
Fitted values
rainfall residual
Normal Q-Q
Standardized residuals
Theoretical Quantiles
rainfall residual
Residuals vs Fitted
Residuals
Fitted values
rainfall residual
Normal Q-Q
Standardized residuals
Theoretical Quantiles
Temperature residuals
Residuals vs Fitted
Residuals
Fitted values
Temperature residuals
Normal Q-Q
Standardized residuals
Theoretical Quantiles
Temperature residuals
Residuals vs Fitted
Residuals
Fitted values
Temperature residuals
Normal Q-Q
Standardized residuals
Theoretical Quantiles
rainfall residual
Residuals vs Fitted
Residuals
Fitted values
rainfall residual
Normal Q-Q
Standardized residuals
Theoretical Quantiles
rainfall residual
Residuals vs Fitted
Residuals
Fitted values
rainfall residual
Normal Q-Q
Standardized residuals
Theoretical Quantiles
Temperature residuals
Residuals vs Fitted
Residuals
Fitted values
Temperature residuals
Normal Q-Q
Standardized residuals
Theoretical Quantiles
Temperature residuals
Residuals vs Fitted
Residuals
Fitted values
Temperature residuals
Normal Q-Q
Standardized residuals
Theoretical Quantiles

Appendix 7. 8: Distribution of rainfall and temperature over the MDB areas and eastern Australia

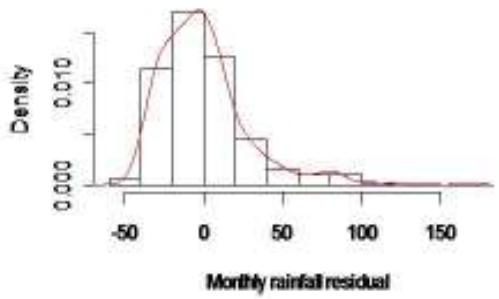

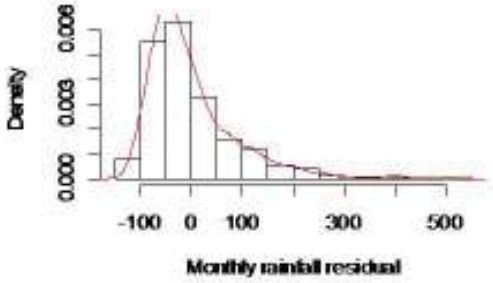

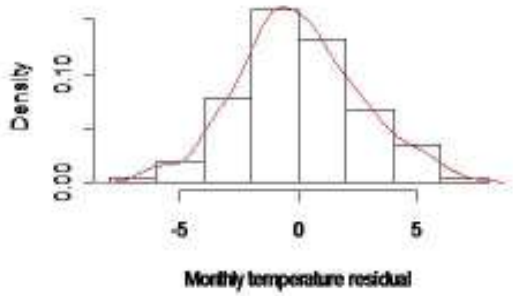

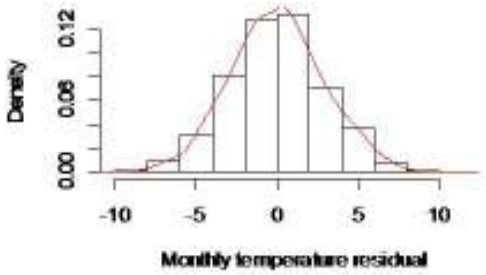

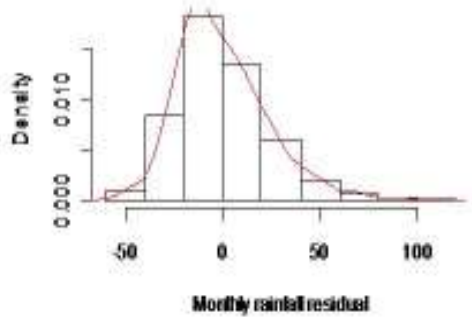

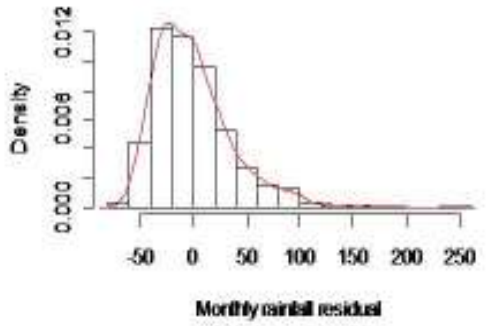

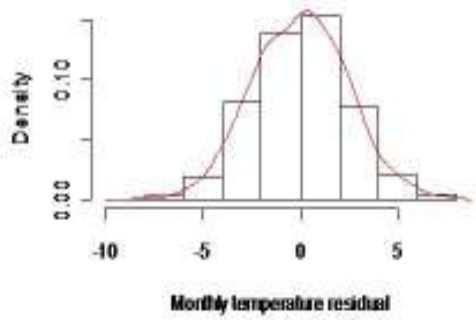

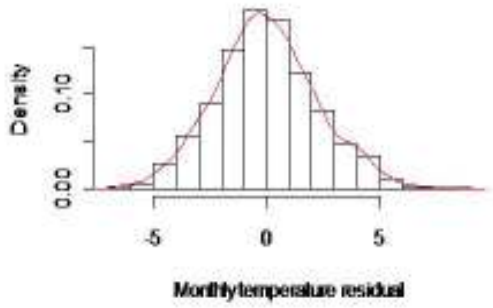

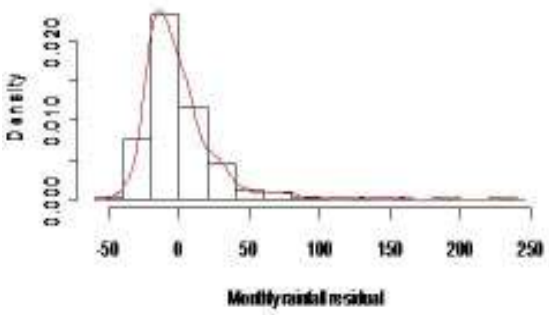
Density
0.000
0.010
0.020
-50
0
50
100
150
200
250
Monthly rainfall residual

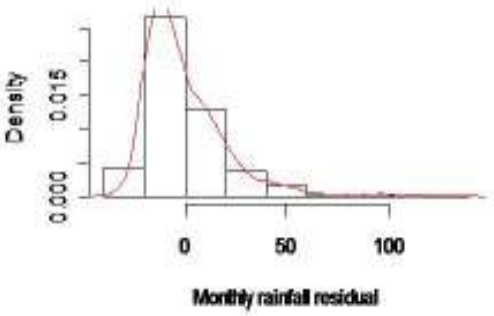
Density
0.000
0.015
0
50
100
Monthly rainfall residual

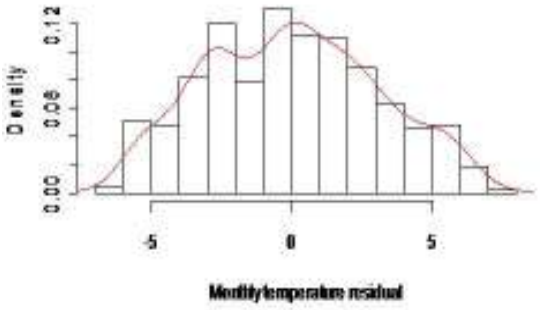
Density
0.00
0.08
0.12
-5
0
5
Monthly temperature residual

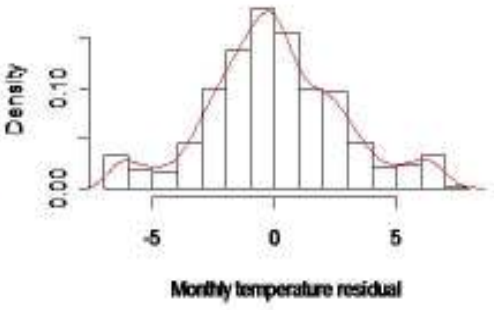
Density
0.00
0.10
-5
0
5
Monthly temperature residual

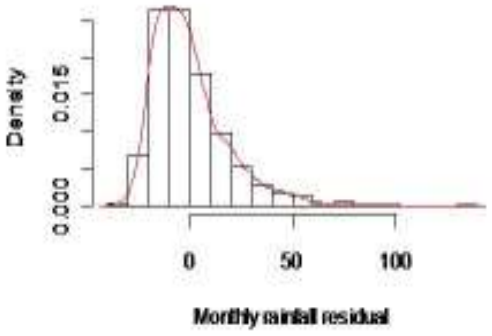
Density
0.000
0.015
0
50
100
Monthly rainfall residual

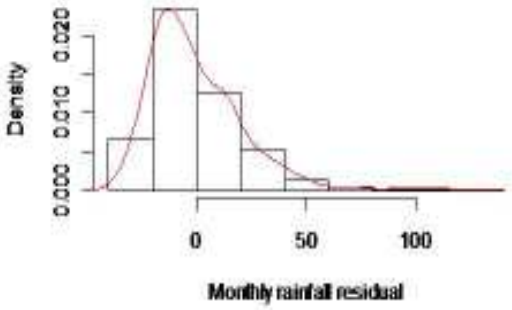
Density
0.000
0.010
0.020
0
50
100
Monthly rainfall residual

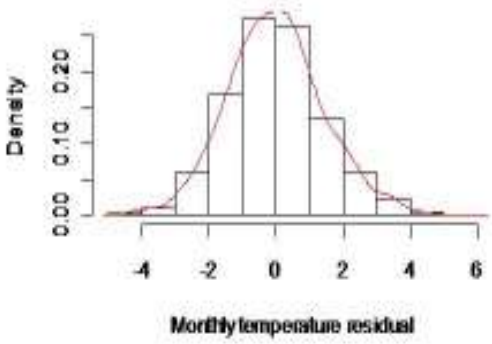
Density
0.00
0.10
0.20
-4
-2
0
2
4
6
Monthly temperature residual

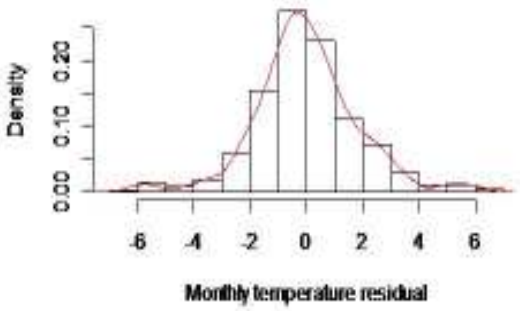
Density
0.00
0.10
0.20
-6
-4
-2
0
2
4
6
Monthly temperature residual

Appendix 8. 1: The distances calculate between stations i.) north-south (latitude) direction ii.) east- west (longitude) direction

N-S direction	Adelaide Airport	Broken Hill	Canberra Airport	Hume Dam	Lake Victoria	Loxton Met	Melbourne Airport	Mildura Airport	Murray Bridge	Sydney observatory Hill
Adelaide Airport	0	328.00	38.92	127.90	101.20	55.60	302.50	78.95	18.90	121.20
Broken Hill		0	366.90	455.90	226.80	272.40	630.50	249.10	346.90	206.80
Canberra Airport			0	88.96	140.10	94.52	263.50	117.90	20.02	160.10
Hume Dam				0	229.10	183.50	174.60	206.80	109.00	249.10
Lake Victoria					0	45.59	403.60	22.24	120.10	20.02
Loxton Met						0	358.00	23.35	74.50	65.61
Melbourne Airport							0	381.40	283.50	423.70
Mildura Airport								0	97.85	42.25
Murray Bridge									0	140.10
Sydney Observatory Hill										0

E-W direction	Adelaide Airport	Broken Hill	Canberra Airport	Hume Dam	Lake Victoria	Loxton Met	Melbourne Airport	Mildura Airport	Murray Bridge	Sydney observatory Hill
Adelaide Airport	0	328	1188	946.3	305.8	227.9	701.6	397	82.28	1411
Broken Hill		0	859.5	618.2	22.24	100	373.6	68.94	245.7	1083
Canberra Airport			0	241.3	881.8	959.6	485.9	790.6	1105	223.5
Hume Dam				0	640.5	718.3	244.6	549.3	864	464.8
Lake Victoria					0	77.4	395.9	91.18	223.5	1105
Loxton Met						0	473.7	169	145.7	1183
Melbourne Airport							0	304.7	619.4	709.4
Mildura Airport								0	314.7	1014
Murray Bridge									0	1329
Sydney Observatory Hill										0

Appendix 8. 2: The strength of spatial correlation of i) RS rainfall pattern and ii) temperature pattern in the MDB and four capital cities in Australia

i. rainfall pattern	Adelaide Airport	Broken Hill	Canberra Airport	Hume Dam	Lake Victoria	Loxton Met	Melbourne Airport	Mildura Airport	Murray Bridge	Sydney observatory Hill
Adelaide Airport	1.000									
Broken Hill	0.287	1.000								
Canberra Airport	0.102	0.352	1.000							
Hume Dam	0.466	0.462	0.530	1.000						
Lake Victoria	0.421	0.605	0.296	0.515	1.000					
Loxton Met	0.513	0.531	0.255	0.508	0.716	1.000				
Melbourne Airport	0.275	0.265	0.305	0.494	0.356	0.350	1.000			
Mildura Airport	0.441	0.684	0.307	0.543	0.793	0.640	0.344	1.000		
Murray Bridge	0.688	0.416	0.219	0.445	0.512	0.585	0.353	0.537	1.000	
Sydney Observatory Hill	0.007	0.111	0.309	0.108	0.054	0.098	0.132	0.110	0.125	1.000

ii Temperature pattern	Adelaide Airport	Broken Hill	Canberra Airport	Hume Dam	Lake Victoria	Loxton Met	Melbourne Airport	Mildura Airport	Murray Bridge	Sydney observatory Hill
Adelaide Airport	1.000									
Broken Hill	0.090	1.000								
Canberra Airport	0.234	0.400	1.000							
Hume Dam	0.206	0.481	0.631	1.000						
Lake Victoria	0.090	0.706	0.482	0.682	1.000					
Loxton Met	0.138	0.611	0.519	0.765	0.808	1.000				
Melbourne Airport	0.151	0.372	0.674	0.627	0.515	0.592	1.000			
Mildura Airport	0.156	0.631	0.565	0.799	0.811	0.959	0.593	1.000		
Murray Bridge	0.142	0.595	0.461	0.660	0.753	0.848	0.533	0.802	1.000	
Sydney Observatory Hill	0.003	-0.005	0.037	-0.039	-0.021	-0.019	0.003	-0.021	-0.041	1.000

Appendix 8. 3: Correlogram of rainfall (upper) and temperature (lower) RSs for all 10 stations.

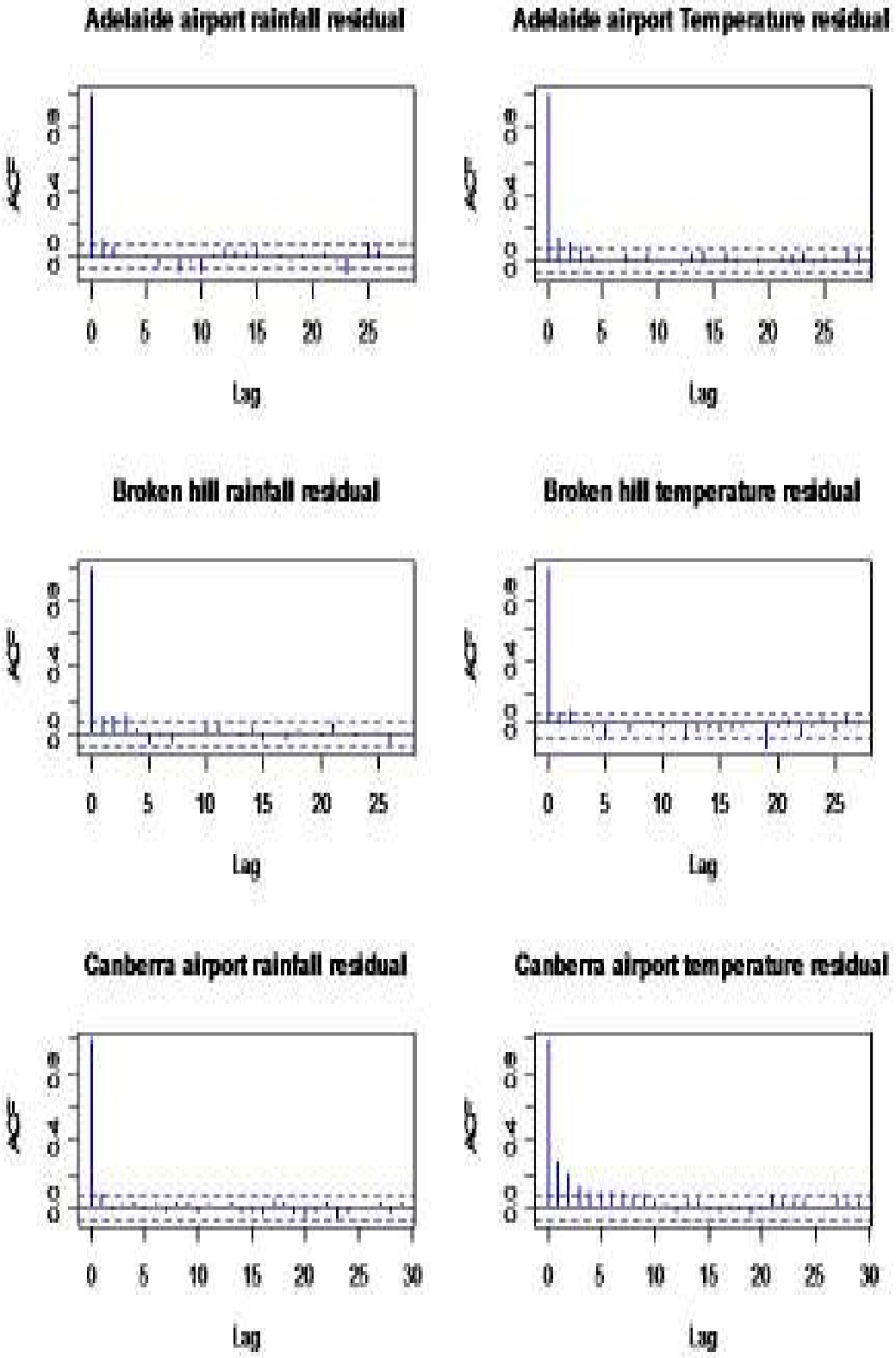

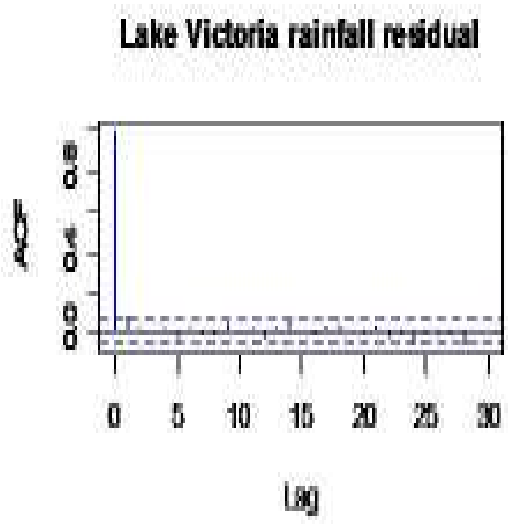
Lake Victoria rainfall residual
ACF
0.0
0.4
0.8
0
5
10
15
20
25
30
Lag

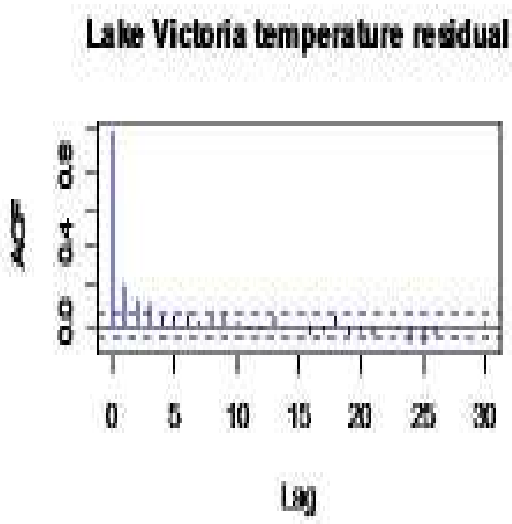
Lake Victoria temperature residual
ACF
0.0
0.4
0.8
0
5
10
15
20
25
30
Lag

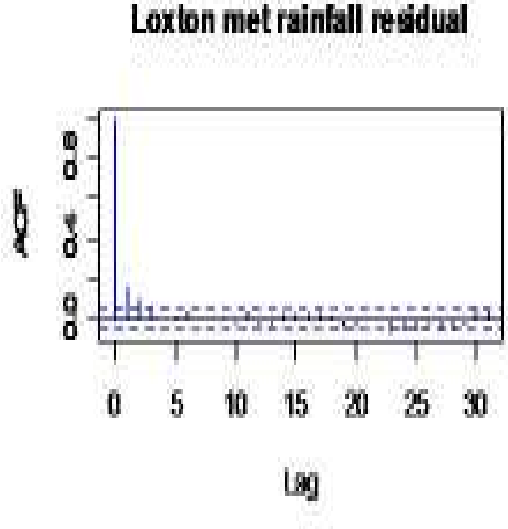
Loxton met rainfall residual
ACF
0.0
0.4
0.8
0
5
10
15
20
25
30
Lag

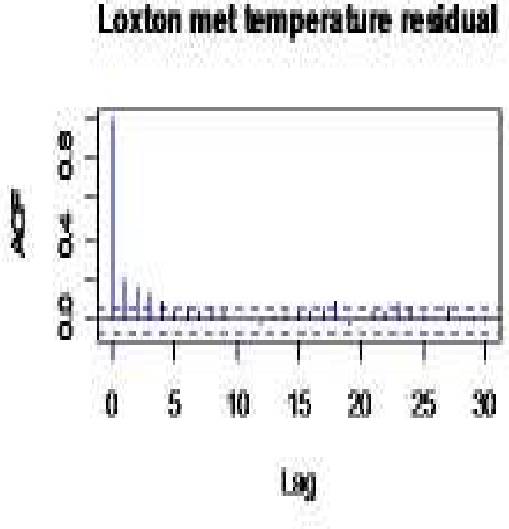
Loxton met temperature residual
ACF
0.0
0.4
0.8
0
5
10
15
20
25
30
Lag

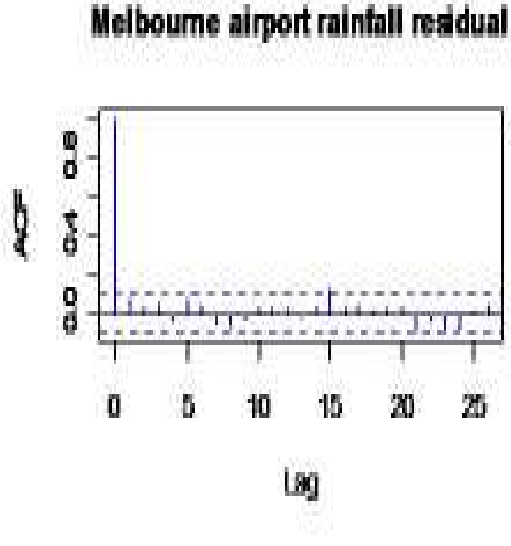
Melbourne airport rainfall residual
ACF
0.0
0.4
0.8
0
5
10
15
20
25
Lag

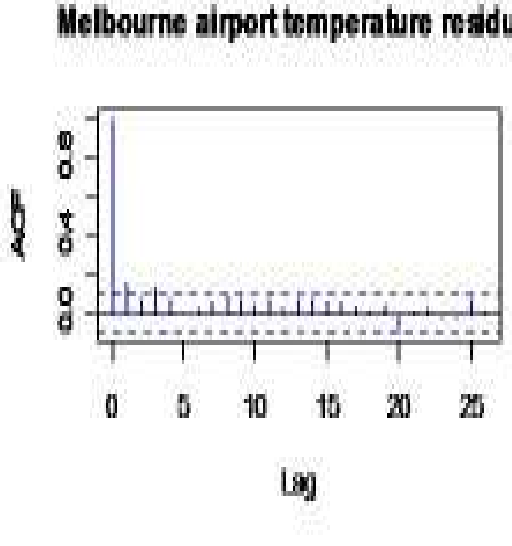
Melbourne airport temperature residual
ACF
0.0
0.4
0.8
0
5
10
15
20
25
Lag

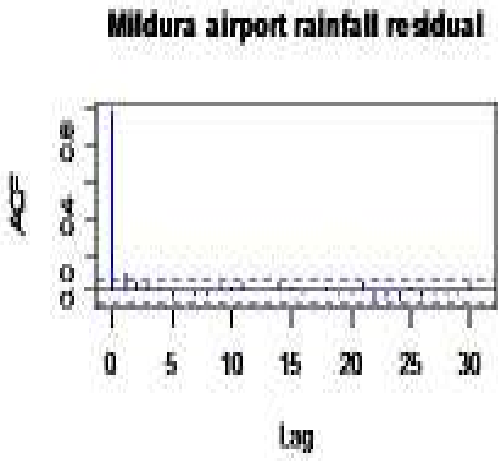
Mildura airport rainfall residual
ACF
0.0
0.4
0.8
0
5
10
15
20
25
30
Lag

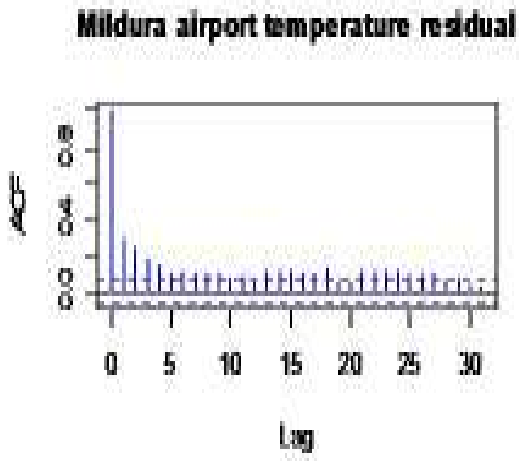
Mildura airport temperature residual
ACF
0.0
0.4
0.8
0
5
10
15
20
25
30
Lag

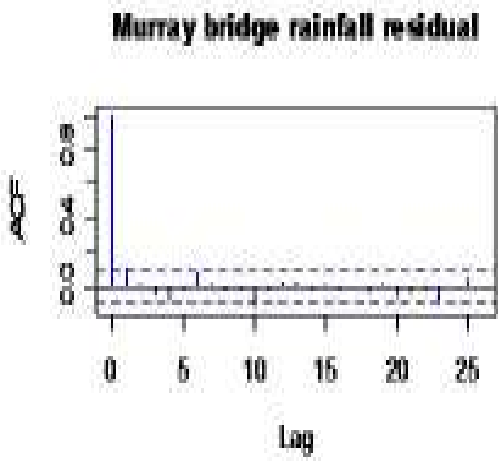
Murray bridge rainfall residual
ACF
0.0
0.4
0.8
0
5
10
15
20
25
Lag

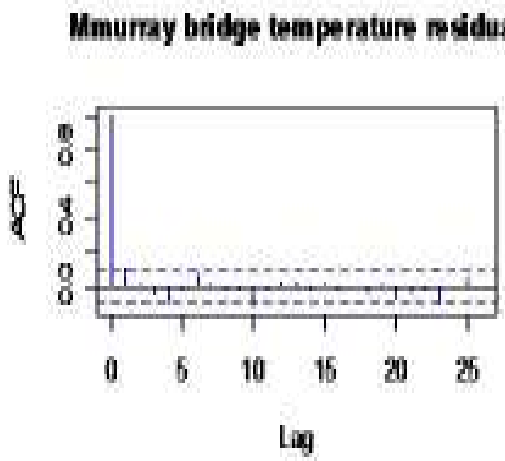
Mmurray bridge temperature residual
ACF
0.0
0.4
0.8
0
5
10
15
20
25
Lag

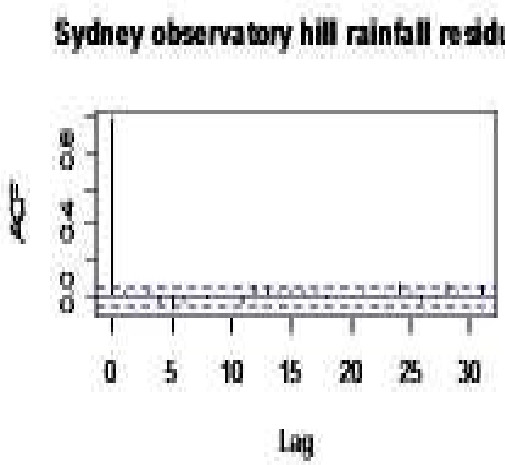
Sydney observatory hill rainfall residual
ACF
0.0
0.4
0.8
0
5
10
15
20
25
30
Lag

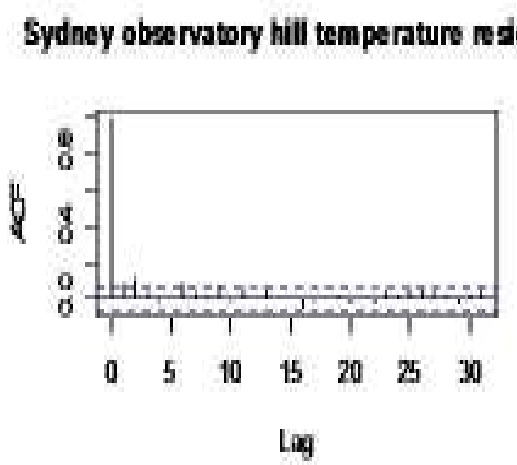
Sydney observatory hill temperature residu
ACF
0.0
0.4
0.8
0
5
10
15
20
25
30
Lag

Appendix 8. 4: Correlogram for GRACH model squared rainfall and temperature RSs for AR model.

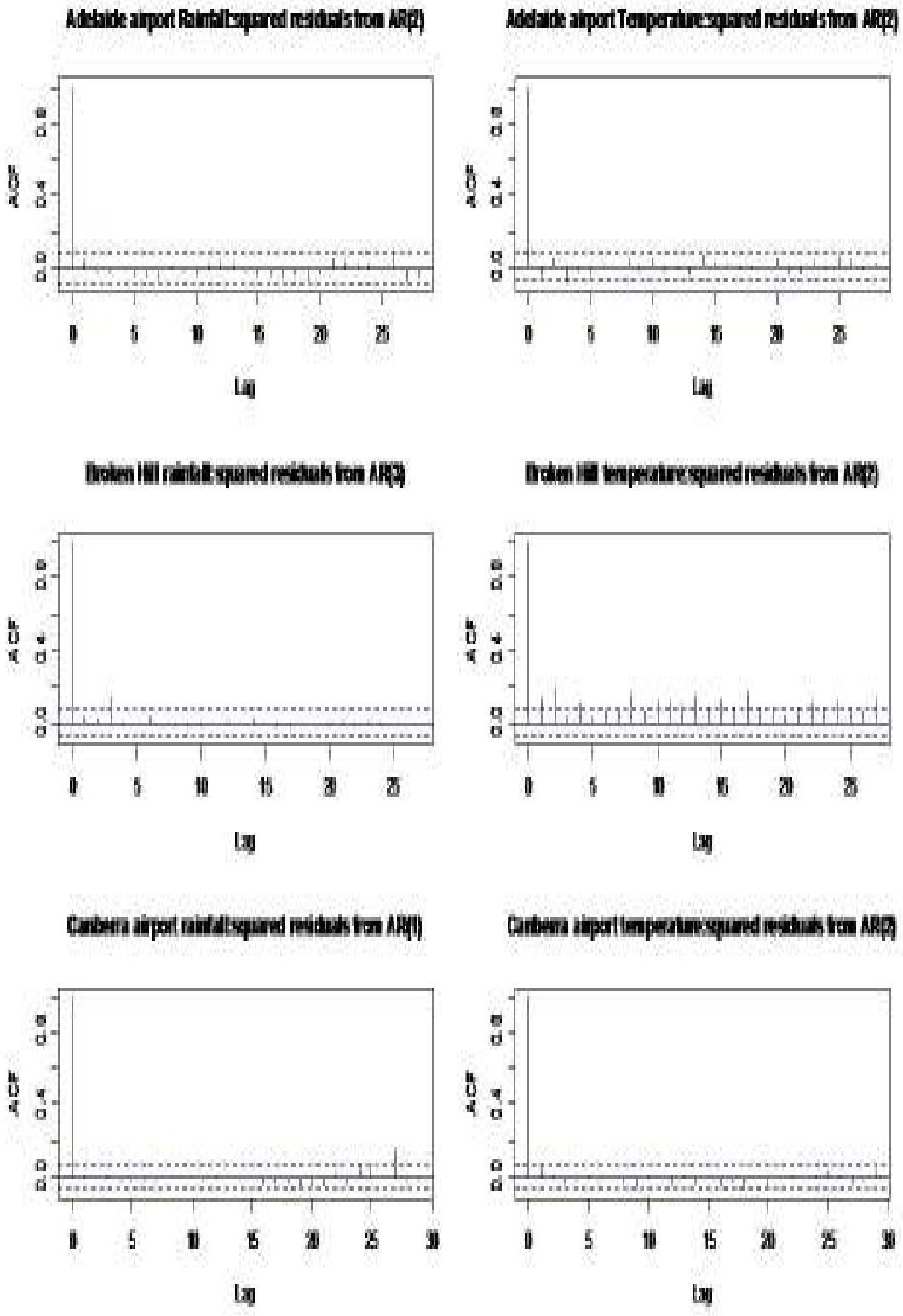

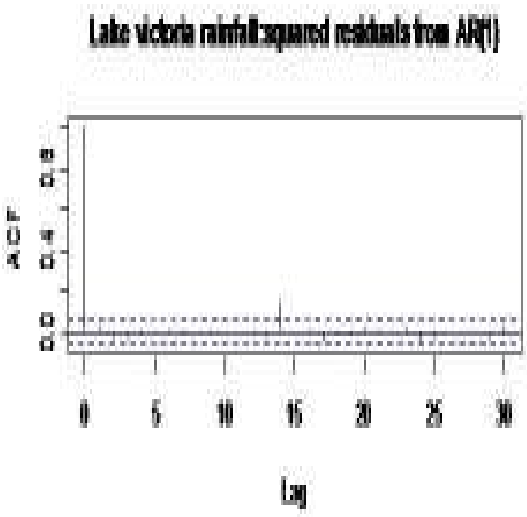
Lake victoria rainfall:squared residuals from AR(1)
ACF
0.0
0.4
0.8
0
5
10
15
20
25
30
Lag

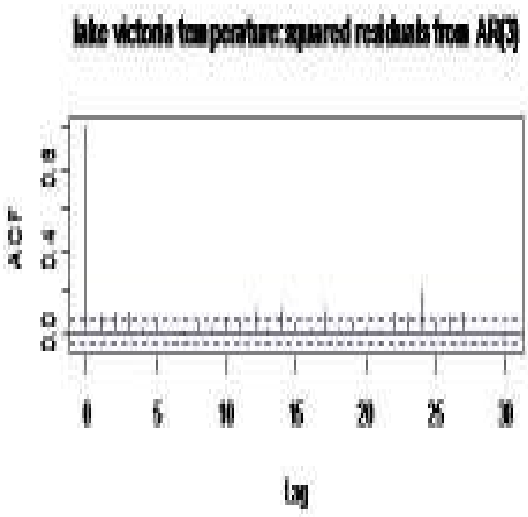
lake victoria temperature:squared residuals from AR(3)
ACF
0.0
0.4
0.8
0
5
10
15
20
25
30
Lag

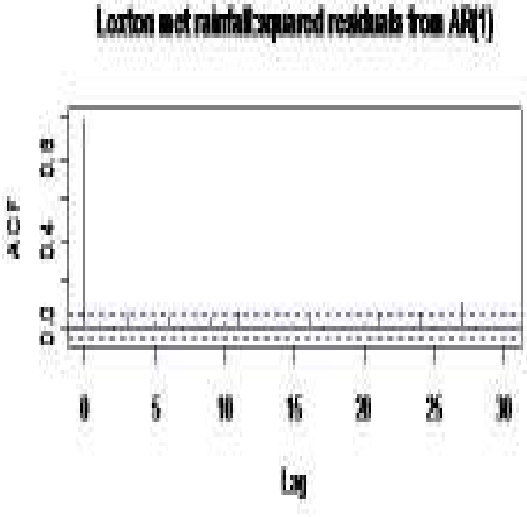
Lorton met rainfall:squared residuals from AR(1)
ACF
0.0
0.4
0.8
0
5
10
15
20
25
30
Lag

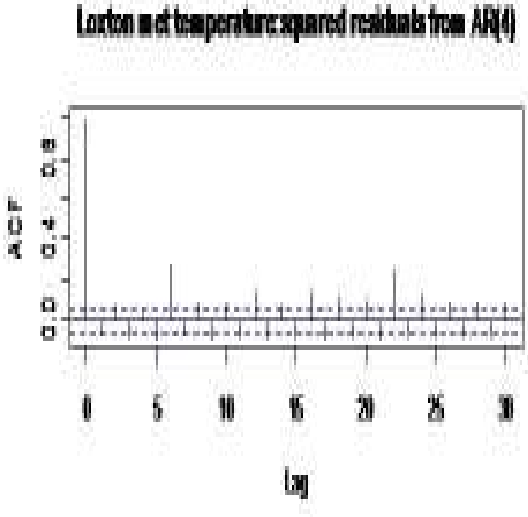
Lorton met temperature:squared residuals from AR(4)
ACF
0.0
0.4
0.8
0
5
10
15
20
25
30
Lag

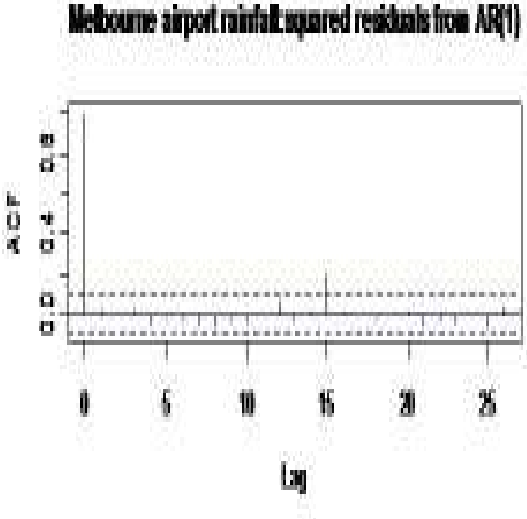
Melbourne airport rainfall:squared residuals from AR(1)
ACF
0.0
0.4
0.8
0
5
10
15
20
25
Lag

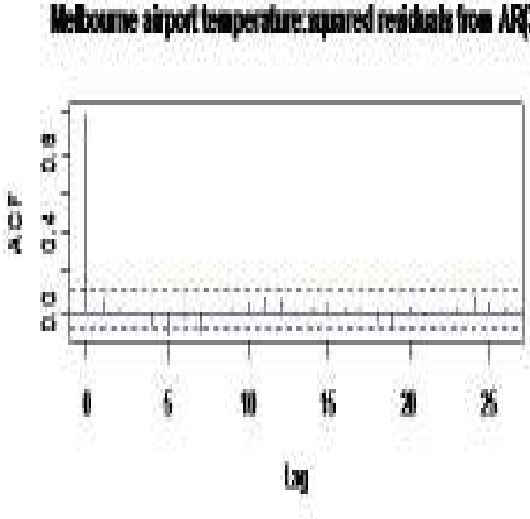
Melbourne airport temperature:squared residuals from AR(3)
ACF
0.0
0.4
0.8
0
5
10
15
20
25
Lag

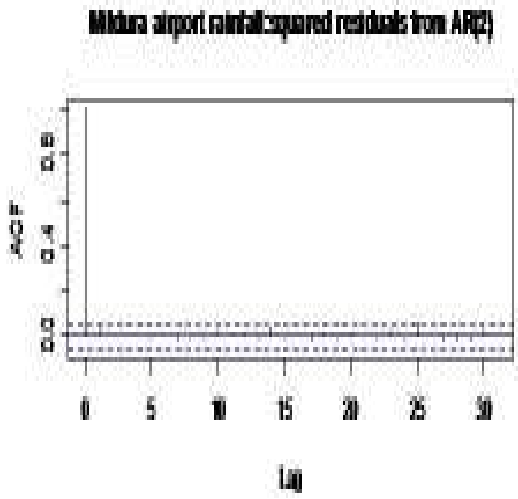
Mildura airport rainfall squared residuals from AR(2)
ACF
0.0
0.4
0.8
0
5
10
15
20
25
30
Lag

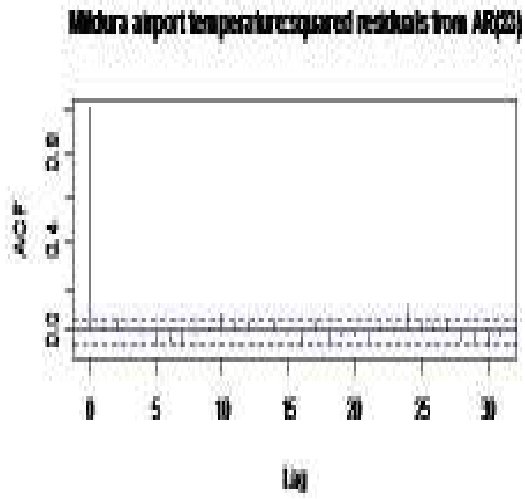
Mildura airport temperature squared residuals from AR(22)
ACF
0.0
0.4
0.8
0
5
10
15
20
25
30
Lag

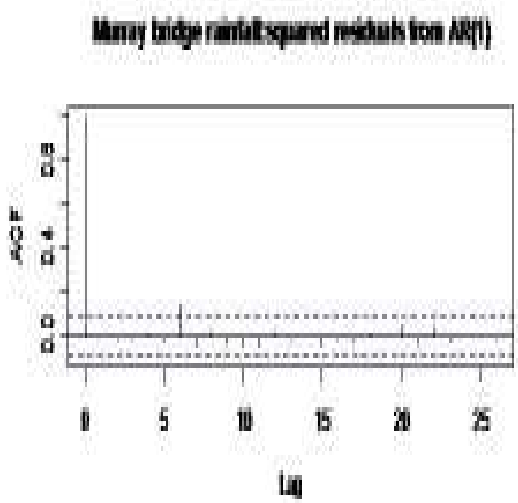
Murray bridge rainfall squared residuals from AR(1)
ACF
0.0
0.4
0.8
0
5
10
15
20
25
Lag

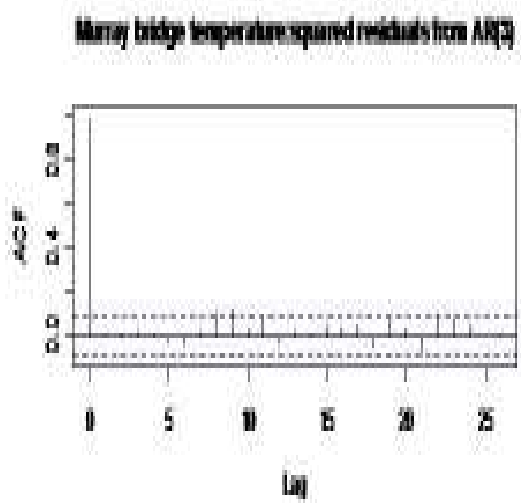
Murray bridge temperature squared residuals from AR(3)
ACF
0.0
0.4
0.8
0
5
10
15
20
25
Lag

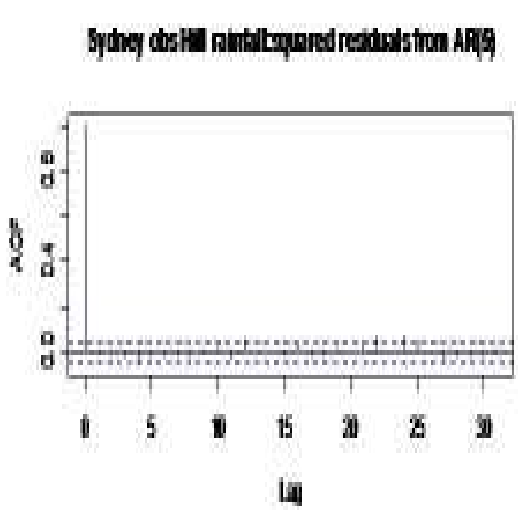
Sydney obs Hill rainfall squared residuals from AR(9)
ACF
0.0
0.4
0.8
0
5
10
15
20
25
30
Lag

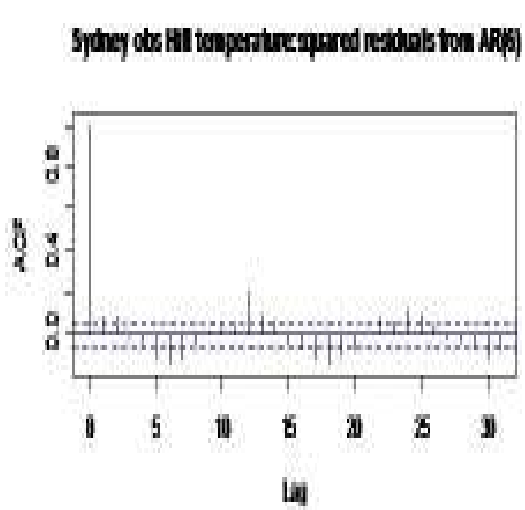
Sydney obs Hill temperature squared residuals from AR(6)
ACF
0.0
0.4
0.8
0
5
10
15
20
25
30
Lag

Appendix 8. 5: Rescaled adjusted ranges for monthly rainfall (left) and temperature RS (right).

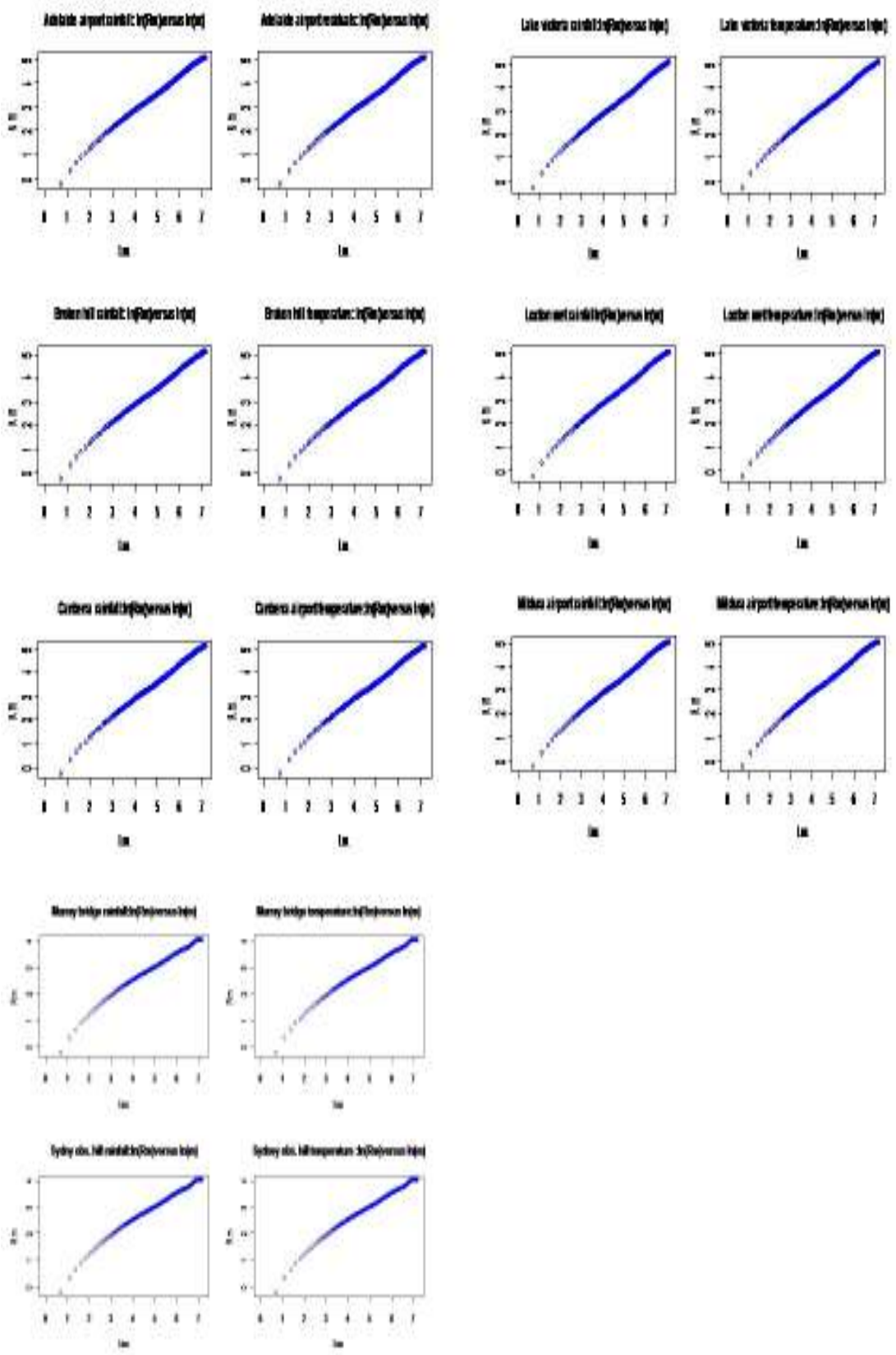

Appendix 8. 6: Cumulative sum plots rainfall and temperature RSs for 6 (six) stations in MDB areas and one of each four s capital city in Australia.

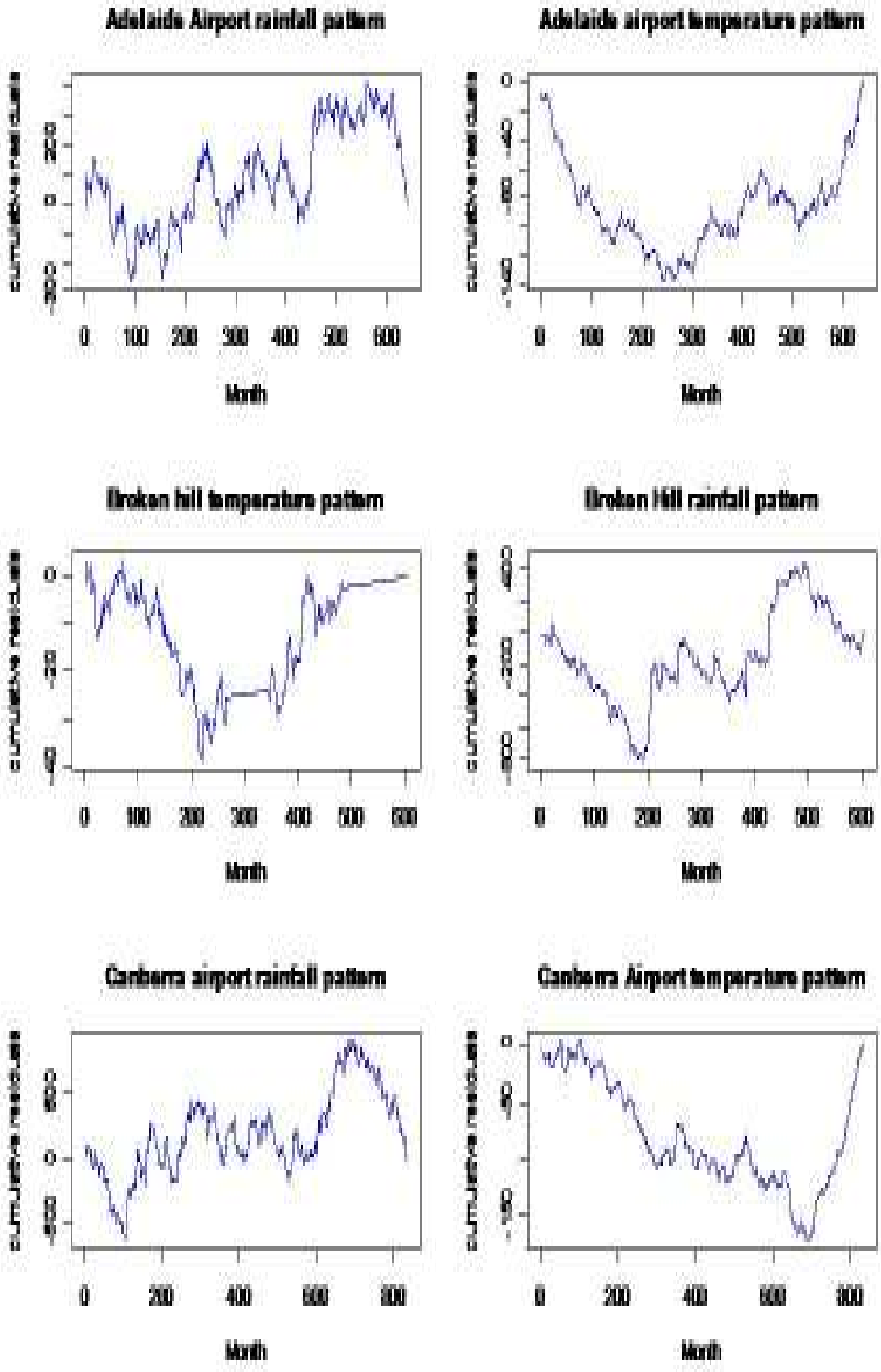

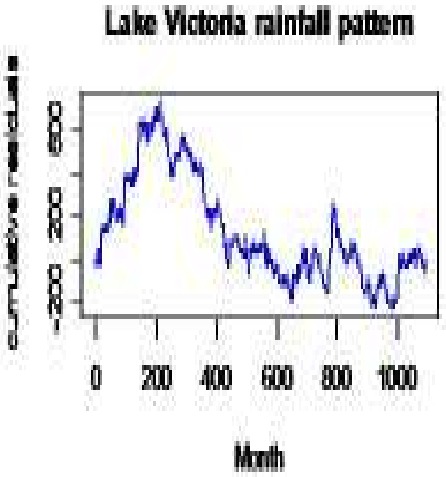
Lake Victoria rainfall pattern
cumulative residuals
-200
200
600
0
200
400
600
800
1000
Month

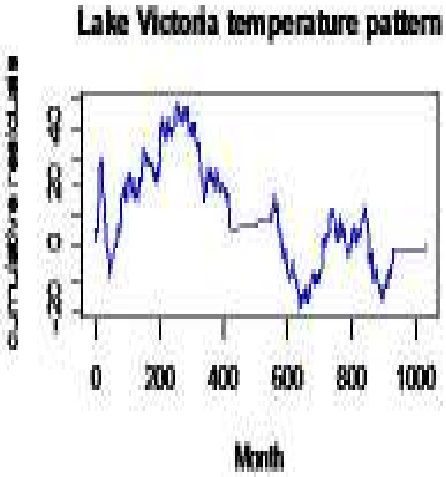
Lake Victoria temperature pattern
cumulative residuals
-20
0
20
40
0
200
400
600
800
1000
Month

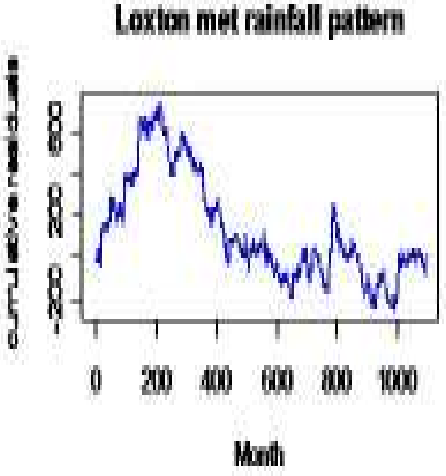
Loxton met rainfall pattern
cumulative residuals
-200
200
600
0
200
400
600
800
1000
Month

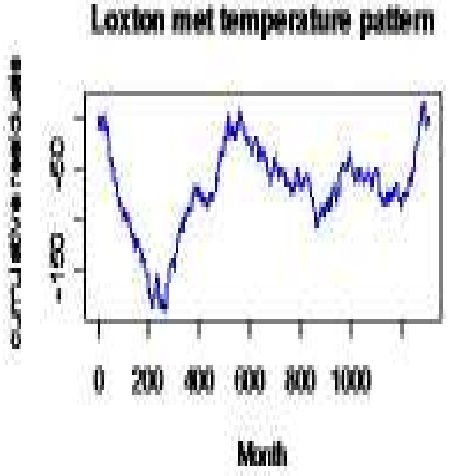
Loxton met temperature pattern
cumulative residuals
-150
-50
0
200
400
600
800
1000
Month

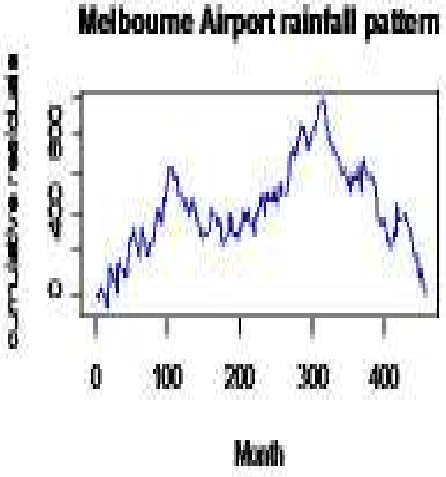
Melbourne Airport rainfall pattern
cumulative residuals
0
400
800
0
100
200
300
400
Month

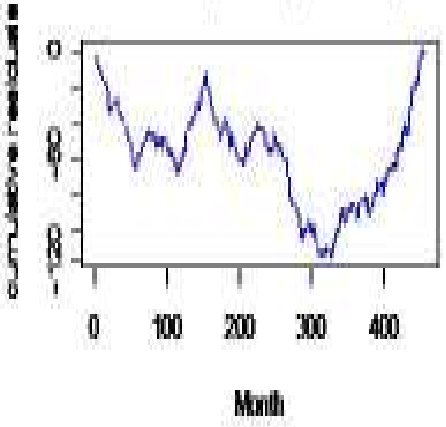
Melbourne airport temperature pattern
cumulative residuals
-120
-60
0
0
100
200
300
400
Month

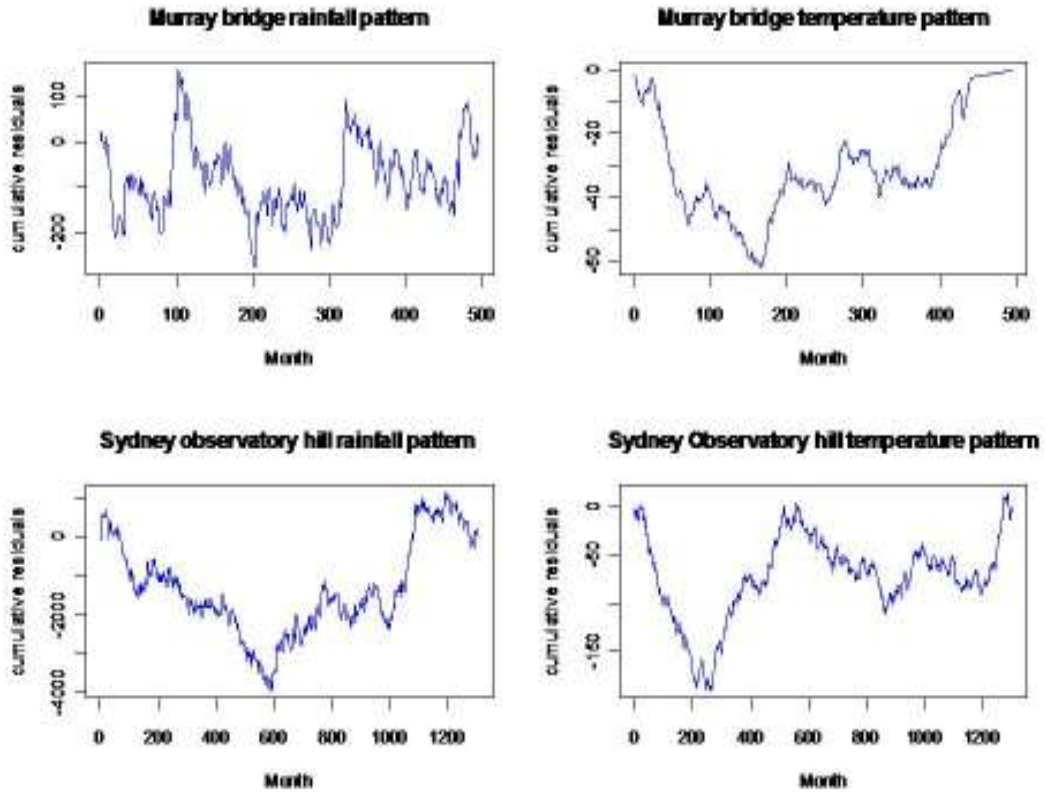

Appendix 8. 7: Average rainfall and temperature per month (in mm) by period determined by CUSUM of rainfall RSs

		Period determined by CUSUM of rainfall residuals	
Area	Period	Mean rainfall/ month(mm)	Mean Temp/ month(mm)
Hume Dam	1890-1949	54.91	21.73
	1950-2000	61.38	21.25
	2001-2007	47.07	22.67
Broken Hill	1958-1972	18.73	23.71
	1973-1996	26.26	24.02
	2000-2007	19.38	24.56
Loxton Met Station	1909-1925	26.18	23.67
	1926-1960	21.23	23.73
	1974-1998	21.29	23.54
Lake Victoria	1922-1944	19.86	23.69
	1945-1999	22.77	23.45
	2000-2007	18.89	26.04
Melbourne Airport	1970-1999	46.5	27.82
	2000-2007	38.12	29.26

		Period determined by CUSUM of rainfall residuals	
Area	Period	Mean rainfall/ month(mm)	Mean Temp/ month(mm)
Canberra Airport	1949-1980	54.48	25.69
	1983-1999	54.41	25.97
	2000-2008	43.97	27.33
Sydney Observatory Hill	1900-1948	91.67	29.33
	1949-1997	109.07	29.23
	2000-2008	89.76	30.36
Adelaide Airport	1956-1962	31.98	29.58
	1962-1974	39.93	29.75
	1977-1989	36.94	30.65
	1995-1999	38.06	29.97
	1999-2009	32.98	31.33
Murray Bridge	1976-1990	28.81	22.74
	1993-1999	27.76	22.85
	2001-2007	29.91	23.72
Mildura	1925-1958	22.15	23.95
Airport	1969-1999	24.73	23.64
	2000-2007	19.07	24.62

Appendix 8. 8: Five-years Moving averages of for rainfall and temperature RSs for six station in the MDB areas and one of each four capital city station in Australia

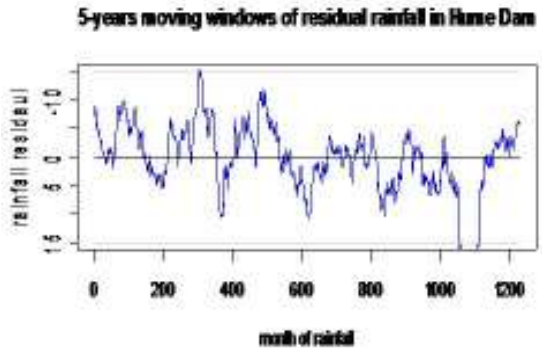

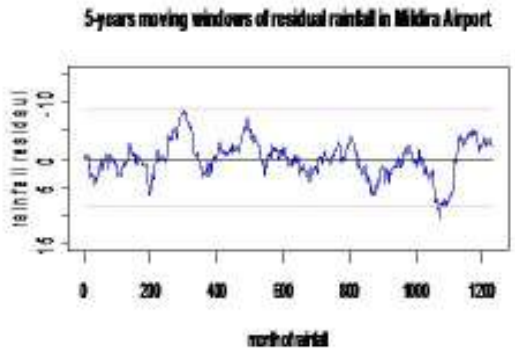

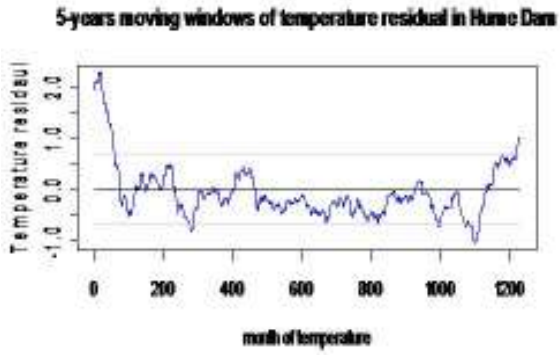

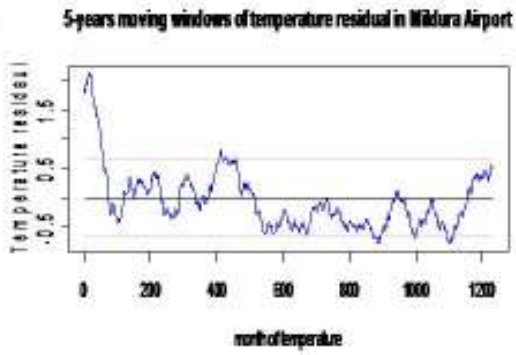

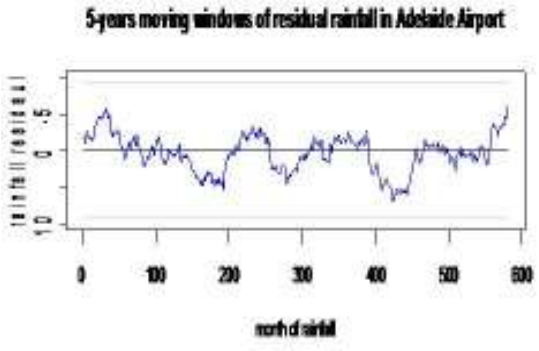

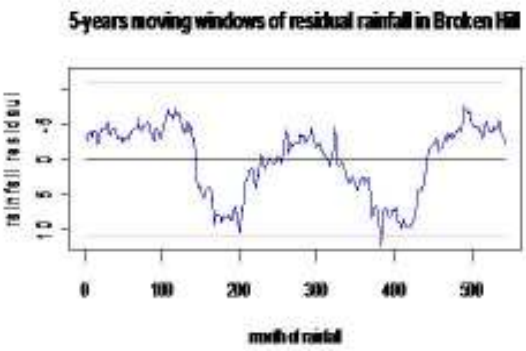

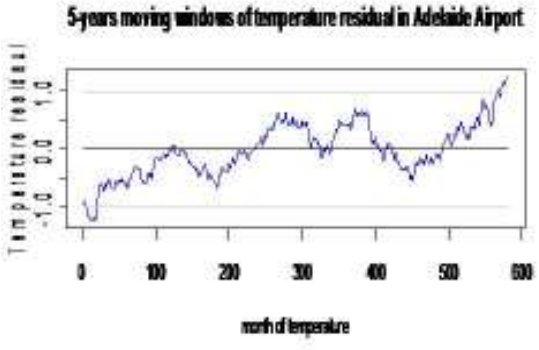

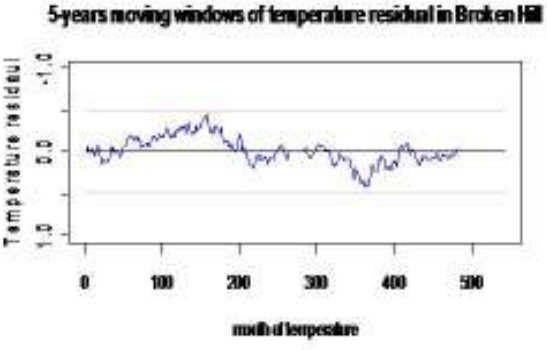

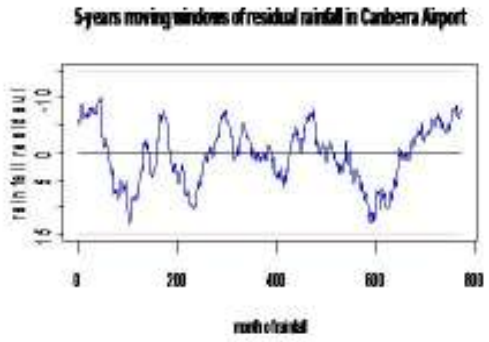
5-years moving windows of residual rainfall in Canberra Airport
rainfall residual
month of rainfall

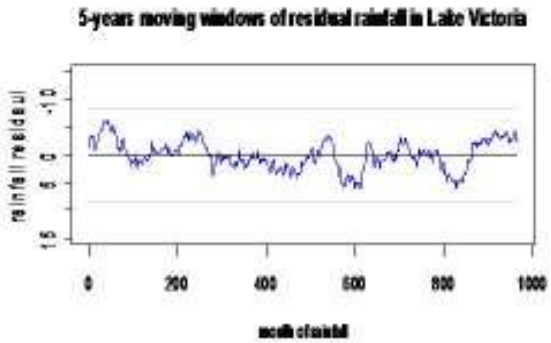
5-years moving windows of residual rainfall in Lake Victoria
rainfall residual
month of rainfall

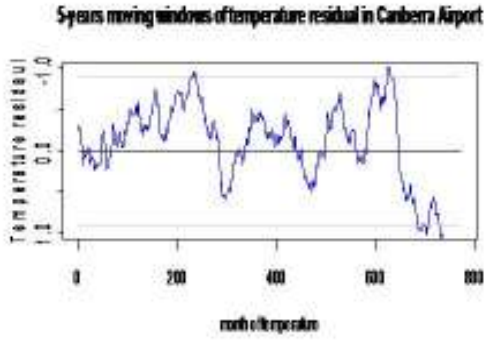
5-years moving windows of temperature residual in Canberra Airport
Temperature residual
month of temperature

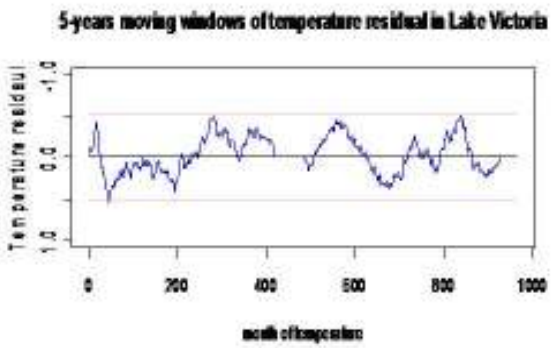
5-years moving windows of temperature residual in Lake Victoria
Temperature residual
month of temperature

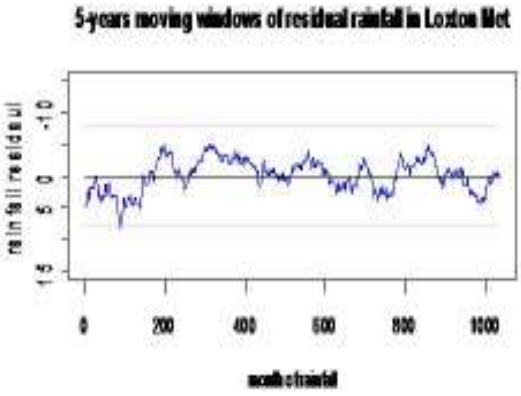
5-years moving windows of residual rainfall in Loxton Met
rainfall residual
month of rainfall


5-years moving windows of residual rainfall in Melbourne Airport
rainfall residual
month of rainfall

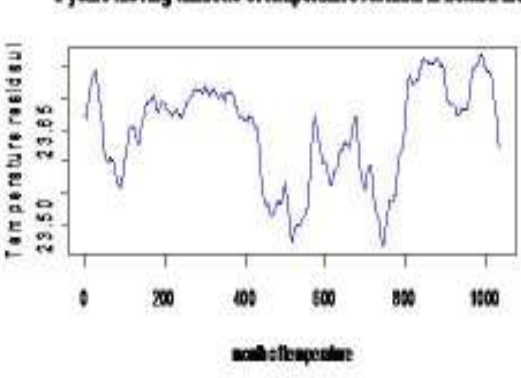
5-years moving windows of temperature residual in Loxton Met
Temperature residual
month of temperature

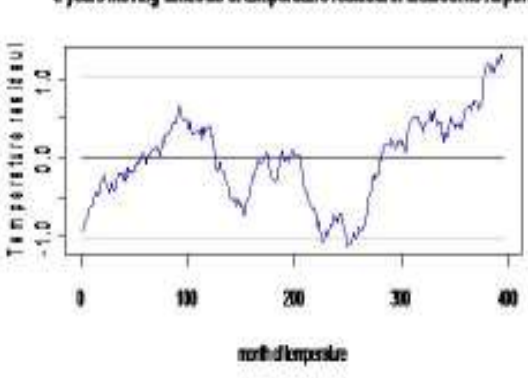
5-years moving windows of temperature residual in Melbourne Airport
Temperature residual
month of temperature

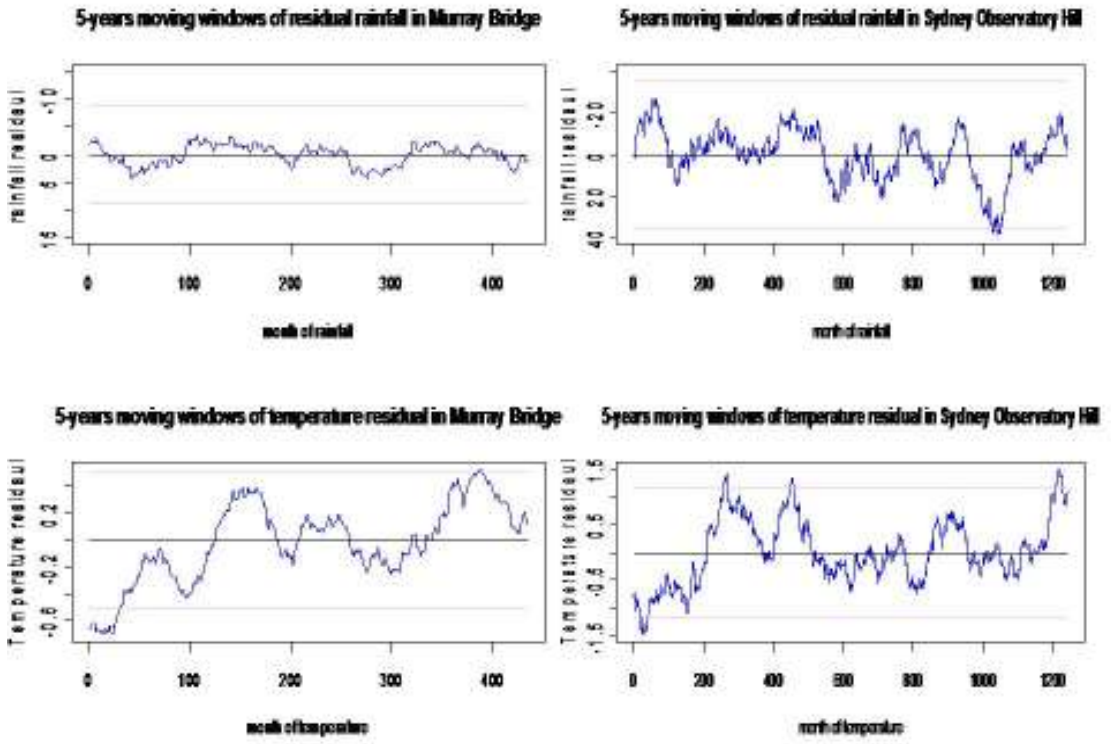

Appendix 8. 9: coefficient of robust RM and original series of regression

a. Rainfall series

Temp Model		Constant	PDO	SOI	PDO*SOI	Jan	Feb	Mar	April	May	June	July	Aug	Sept	Oct	Nov
Co-efficient		β_0	β_1	β_2	β_3	β_4	β_5	β_6	β_7	β_8	β_9	β_{10}	β_{11}	β_{12}	β_{13}	β_{14}
Broken Hill	1	30.48***	-0.07	-.03**	0.11*	1.60*	1.28*	-1.95*	-6.68***	-11.62***	-14.73***	-15.37***	-13.43***	-9.89***	-6.02***	-2.53**
	2	4.516***	-0.269*	-0.031*	0.0123	1.1620	0.9503	-1.34*	-4.574***	-7.785***	-10.001***	-10.491***	-9.305***	-6.806***	-4.193***	-1.774**
Hume Dam	1	28.31***	0.06	-.02***	0.005	2.01***	1.69***	-1.85***	-7.24***	-12.19***	-15.81***	-16.72***	-14.58***	-11.34***	-7.55***	-3.34***
	2	7.259***	-0.0251	-0.012***	0.0020	1.986***	1.664***	-1.87***	-7.249***	-12.189***	-15.81***	-16.718***	-14.60***	-11.356***	-7.561***	-3.343***
Lake Victoria	1	30.24***	0.01	-.01*	-.01*	1.49**	1.35**	-1.78**	-6.88***	-11.29***	-14.69***	-15.09***	-13.19***	-10.04***	-6.56***	-2.95***
	2	5.031***	-0.1412	-0.021*	0.0036	1.126**	1.32**	-1.19**	-5.157***	-8.647***	-11.164***	-11.646***	-10.09***	-7.621***	-4.98***	-2.118***
Leeton Met	1	29.79***	0.09*	-0.01*	0.01	1.63***	1.26***	-1.81***	-6.39***	-10.54***	-13.68***	-14.08***	-12.23***	-9.08***	-5.96***	-2.56***
	2	5.071***	-0.1412	-0.021*	0.0076	1.126***	1.32***	-1.191***	-5.157***	-8.647***	-11.168***	-11.646***	-10.099***	-7.621***	-4.98***	-2.118***
Mildura Airport	1	30.73***	0.15**	-0.02**	0.01*	1.58***	1.2***	-2.11***	-7.16***	-11.55***	-14.85***	-15.41***	-13.32***	-10.09***	-6.53***	-2.72
	3	6.3489	0.0117	-0.0160	0.0032	1.5535	1.1307	-2.1272	-7.1036	-11.5805	-14.8415	-15.4063	-13.3456	-10.1189	-6.5528	-2.7403
Murray Bridge	1	27.30***	-0.07	-0.01	00*	1.50**	2.06***	-0.85	-3.97***	-7.76***	-10.7	-11.14	-9.91	-7.6	-4.75	-2.02***
	2	4.187***	-0.211*	-0.0102	-0.0054	1.377***	1.82***	-0.7580	-3.568***	-6.925***	-9.638***	-10.119***	-9.031***	-6.906***	-4.284***	-1.781***
Adelaide Airport	1	35.57***	0.12	-0.01	0.01	2.05*	3.03*	2.59*	0.19	-4.76*	-10.82*	-15.08*	-16.65*	-13.31*	-8.52*	-3.81*
	2	5.138***	-0.0897	-0.0108	-0.0018	2.067***	3.838***	2.648***	0.253***	-4.651***	-10.763***	-15.013***	-16.583***	-13.273***	-8.536***	-3.83***
Canberra Airport	1	34.41***	0.05	-.05***	.02**	1.36***	-0.02	-3.05***	-8.47***	-13.85***	-18.24***	-19.12***	-16.36***	-11.86***	-7.51***	-3.11***
	2	8.35***	-0.0334	-0.052***	0.014*	1.36***	-0.0261	-3.04***	-8.45***	-13.816***	-18.22***	-19.104***	-16.23***	-11.845***	-7.502***	-3.113***
Melbourne Airport	1	36.20***	-0.02	-.04***	0.01	2.41***	1.73**	-1.62**	-8.02***	-13.56***	-18.59***	-19.43***	-16.81***	-12.88***	-7.45***	-3.17***
	2	8.119***	-0.1822	-0.041***	-0.0002	2.412***	1.704**	-1.613**	-8.017***	-13.49***	-18.58***	-19.35***	-16.73***	-12.83***	-7.444***	-3.193***
Sydney Obs. hill	1	21.72***	0.16	-.03**	0.002	-0.12	2.45***	6.54***	10.26***	11.80***	13.39***	13.53***	12.12***	10.64***	7.38***	3.56***
	2	7.588***	0.0539	-0.008***	0.0011	-0.1201	2.4536	6.545***	10.281***	11.82***	13.403***	13.576***	12.117***	10.604***	7.365***	3.545***

"1" defined as regression model, "2" defined as local weighted robust regression model

*coefficients are statistically significant at the 5% level

**coefficients are statistically significant at the 1% level

***coefficients are statistically significant at the 0.1% level

b. Temperature series

Rainfall Model		Constant	PDO	SOI	PDO*SOI	Jan	Feb	Mar	April	May	June	July	Aug	Sept	Oct	Nov
Co-efficient		β_0	β_1	β_2	β_3	β_4	β_5	β_6	β_7	β_8	β_9	β_{10}	β_{11}	β_{12}	β_{13}	β_{14}
Broken Hil	1	24.27***	-0.1300	.70***	-.348***	9.2800	-5.6000	-5.1100	-5.7100	0.7300	-8.1000	-3.1800	-5.6300	-2.1900	2.7000	-4.4390
	2	8.5047*	-0.2132	0.663***	-0.31**	9.3000	-5.4643	-4.9579	-5.5973	0.7404	-8.1166	-3.1708	-5.5432	-2.0992	2.7445	-4.4074
Hun Dum	1	46.92***	1.4300	1.03***	-0.188*	-3.7400	-9.2100	-2.2700	1.8100	13.69**	24.37***	28.84***	27.54***	15.98**	21.68***	1.9530
	2	-3.804	2.467*	1.042***	-0.1469	-3.6891	-9.0385	-2.2347	1.7492	13.506**	24.298***	28.729***	27.714***	16.161***	21.871***	2.0739
Lake Victoria	1	18.15***	0.0600	.47***	-.19***	0.3500	-0.7000	-5.7100	-0.2500	5.4200	4.4800	6.68*	5.5100	6.0800	9.12**	3.3700
	2	0.73505	0.4825	0.474***	-0.186***	0.3363	-0.6638	-5.7343	-0.5211	5.3211	4.4178	6.6187	5.5141	6.1099	9.1511	3.4308
Lorton Met	1	16.96***	0.3700	.42***	-.21***	-0.0300	3.5100	-2.8500	-0.7000	9.24**	8.67**	9.05**	10.36***	10.22***	10.56***	3.3600
	2	-1.76829	0.6410	0.409***	-0.195***	-0.0660	3.0264	-2.7521	-0.7034	8.5490	8.0438	8.4869	9.8272	9.4865	9.6867	2.9809
Mildura Airport	1	20.05***	-0.3500	.45***	-.21***	-0.2600	-0.8800	-2.9500	-3.4900	5.90*	4.6600	4.0300	5.7900	5.9000	7.91**	1.3800
	2	1.4920	-0.0836	0.447***	-0.202***	-0.245	-0.848	-2.9477	-3.5158	3.8531	4.6373	3.9980	3.8218	3.9430	7.9520	1.4080
Murray Bridge	1	25.67***	1.2400	.32**	-0.1100	-7.8800	-6.6600	-5.8100	2.2100	6.47**	13.07*	10.57**	13.87*	11.93*	11.6600	1.0400
	2	-1.26444	1.3303	0.298**	-0.0872	-7.8714	-6.5702	-5.7554	2.2386	6.4924	13.1340	10.5359	13.8935	11.9597	11.7403	1.1122
Adelaide Airport	1	23.49***	0.3600	.42***	-.24**	-6.17**	-6.4500	-3.8500	10.52*	30.17***	32.06***	35.48***	25.13***	22.07***	14.76**	1.3800
	2	-10.534**	1.3719	0.4087	-0.187***	-6.2061	-6.3643	-3.9366	10.431*	29.89***	31.92***	35.33***	24.97***	21.97***	14.79**	1.4354
Canberra Airport	1	51.92***	0.4600	.97***	-0.2200	6.96*	2.6600	-2.0600	-5.5900	-6.6300	-11.0000	-10.7700	-5.5200	0.1600	10.6100	11.6200
	2	6.37371	1.4980	0.933***	-0.21*	6.9204	2.5875	-2.1707	-5.7969	-6.9400	-11.2029	-10.9639	-5.7298	0.0956	10.6184	11.7972
Melbourne Airport	1	47.48***	0.3300	.34*	-0.0700	-5.1300	-4.6300	-11.5300	-2.3400	-6.1000	-8.8400	-10.9500	-1.0200	-1.0000	7.5100	11.3600
	2	8.20535	0.2349	0.353**	-0.0501	-5.1155	-4.4917	-11.5215	-2.0894	-5.9319	-8.6500	-10.8018	-1.0275	-1.0443	7.4978	11.3395
Sydney Obs hil	1	81.19***	-.58*	.640*	-.57*	23.5000	27.64*	46.67***	39.45**	36.25**	42.29***	11.7900	-0.6000	-16.8700	-4.9300	2.4500
	2	1.7884	-4.6991	0.668**	-0.536*	23.6242	27.821*	46.72***	39.412**	36.10**	42.218***	11.7676	-0.3798	-16.6370	-4.6838	2.6134

"1" defined as regression model, "2" defined as local weighted robust regression model

* coefficients are statistically significant at the 5% level

** coefficients are statistically significant at the 1% level

*** coefficients are statistically significant at the 0.1% level